

**ACIDIC DEPOSITION EMANATING FROM THE SOUTH  
AFRICAN HIGHVELD – A CRITICAL LEVELS AND  
CRITICAL LOADS ASSESSMENT**

**Miroslav (Micky) Josipovic**

The logo of the University of Johannesburg, featuring two stylized birds facing each other with a sunburst above them, and the text 'UNIVERSITY OF JOHANNESBURG' in a light grey font.

Department of Geography, Environmental Management and Energy Studies,  
Faculty of Science, University of Johannesburg

Supervisor:  
Professor H. J. Annegarn

A thesis submitted to the Faculty of Science,  
University of Johannesburg, in fulfilment of the requirements for the degree of  
Doctor of Philosophy in Environmental Science

Revised 22 July 2009



## Affidavit

To Whom It May Concern

This serves to confirm that I, Miroslav (Micky) Josipovic, ID Number: 6011045975084, Student number: 200517775 enrolled for the degree Philosophiae Doctor (Environmental Science), Faculty of Science, University of Johannesburg herewith declare that my academic work is in line with the Plagiarism Policy of the University of Johannesburg with which I am familiar.

I further declare that the work presented in this thesis: *Acid Deposition Emanating from the South African Highveld – a Critical Levels and Critical Loads Assessment*, is authentic and original unless clearly indicated otherwise and in such instances full reference to the source is acknowledged and I do not pretend to receive any credit for such acknowledged quotations, and that there is no copyright infringement in my work. I declare that no unethical research practices were used or material gained through dishonesty. I understand that plagiarism is a serious offence and that should I contravene the Plagiarism Policy, notwithstanding signing this affidavit, I may be found guilty of a serious criminal offence (perjury) that would amongst other consequences compel the University of Johannesburg to inform all other tertiary institutions of the offence and to issue a corresponding certificate of reprehensible academic conduct to whomever request such a certificate from the institution.

Signed at \_\_\_\_\_ on this \_\_\_\_ day of \_\_\_\_\_ 2009

Signature \_\_\_\_\_

Miroslav (Micky) Josipovic

**STAMP COMMISSIONER OF OATHS**  
**Affidavit certified by a Commissioner of Oaths**

This affidavit conforms to the requirements of the JUSTICES OF THE PEACE AND COMMISSIONERS OF OATHS ACT 16 OF 1963 and the applicable Regulations published in the GG GNR 1258 of 21 July 1972; GN 903 of 10 July 1998; GN 109 of 2 February 2001 as amended.



## Dedication

This work is dedicated to *my family*





## Acknowledgments

I would like to acknowledge and thank the following people who and institutions or organisations, which have aided me in the completion of this study:

First and foremost my supervisor Professor Harold Annegarn, for his more than standard supervisor–student time and effort sacrifices. This includes besides his academic guidance, complete scientist development and an unreserved access to his office and home. Words are not enough to describe the gratitude for his involvement in my life. In a similar way I am thankful to Professor’s senior research assistant, Mrs Melanie Kneen for her full support of my research which extended into a friendship between both our families.

Hereby I express my sincere gratitude to the academics, scientists and professionals who in one way or another contributed to my scientific growth: Prof. Stuart Piketh of Climatology Research Group (CRG); Prof. Kobus Pienaar, Dr Kobus Martins and Dr Pieter van Zyl of the Atmospheric Chemistry Research Group-North-West University (ACRG); Prof. Mary Scholes of Wits University; Dr Mark Zunckel of u-Moya-Nilu; Dr June Meeuwis of University of Johannesburg, Ms Fatima Ferraz of Anglo American-Geosciences Resources Group; Dr Kristy Ross of Eskom-Resources and Strategy Division; and Ms Mieke van Tienhoven of National Association of Clean Air (NACA).

Especial thanks go to the forty volunteers out there in my study-field region, who participated with me willingly and for a long period on my research project by being my field eyes and hands. This section is too short to mention all their names. However, without them my research could not be performed successfully. With regard to the field tasks, I must thank to my fellow student colleagues who contributed importantly – Mr Stephen Broccardo, Mr Simangele Dlamini, Mr Michael Weston, and Mr Thomas Bigala of CRG, Wits University. On the UJ side these individuals were Mr Allan Cochran and Dr Philip Goyns, and Ms Jennifer Jones of University of Virginia (UVA). I also thank my undergraduate assistant Miss Faith Magagula, for her input on the operational side of my research, who eased physical pressures of my research and dealt with administrative tasks. Special thanks go to Mrs Lisanne Frewin of the CRG, Wits University, for her efficient and always friendly administrative and logistics support. Ms Beverley Terry of the EnerKey Programme is greatly acknowledged for her support with many additional administrative details placed on me throughout my study. Valuable support to my study literature access by the subject librarian, Mrs. Pavlinka Kovatcheva is highly appreciated.

In addition, my special thanks go to Dr Kevin Hicks of Stockholm Environment Institute – York (SEI-Y) for the frequent advice and supply of relevant internal reports. On South African side, I thank to South African Weather Service (SAWS) for the prompt provision of ancillary (weather) data for my research and I have to single out Ms Coleen de Villiers in this. Also thanks to Mr Warren Carter of the CSIR for extraction of information from the CAPIA database and advice on models, as well as Dr Gerhard Fourie of Sasol for sharing all his air dispersion modelling results.



Their openness and collaboration meant so much in such periods when dependence on external involvement was crucial.

Sincere thanks must be extended to all people who and institutions that enriched my work with their inputs into my research through both data and personal knowledge sharing. Particularly, Dr Jos van Geffen from Belgian Institute for Space Aeronomy (BIRA-IASB), Dr Steffen Beirle from MPI-Ch (Mainz) to Dr Jerry Ziemke of NASA's Goddard Space Flight Center (GSFC). Dr Christian von Savigny of Institute for Environmental Physics (IUP), University of Bremen; Dr Sven Kuehl of Max Plank Institute for Chemistry (MPI) in Mainz; and Dr Frank Baier of German Space Agency (DLR) are thanked for prompt email exchanges to clarify challenging points in interpretation of remote sensing images.

My thanks go also to all employees of my Department for encouragement and interest, for treating me more as a colleague than a postgraduate student. Especially thanks to Mrs Esme Enslin for her technical support and Mrs Thea Schoeman for improvement of images in the thesis. Thanks to all my fellow postgraduate students, in Professor Annegarn's postgraduate group, for their occasional academic and specialist advice, and on-going friendship. Here I must specifically thank to Mr Matthew Ojelede and Ms Bhavika Bhika for access to their prior research, which I used in my thesis (Ojelede *et al.*, 2008; Bhika, 2008).

The following institutions are greatly acknowledged for their financial support:

- Anglo-American Corporation for initiating and financing the first stage of the study.
- Eskom (and Sasol) for funding the continuation of the study through their joint Acidic Deposition Research Consortium grant No. PRJ06-00658800-3078, as well as partial financial support towards my bursary.
- Oppenheimer Memorial Trust (OMT) for three years of study grants (OMT Ref. 16068).
- South African National Research Foundation, for support through a Focus Area Grant to Prof. H. Annegarn – *Sustainability Studies Using GIS & Remote Sensing (FA2005040600018)* and an associated grant-holder doctoral bursary.

Last, and far from the least, I hereby thank my family and friends for the sacrifices they have made for me as well as their support throughout the duration of my study.



## Abstract

A number of studies to detect effects of atmospheric acidic deposition on regional environments have been conducted in South Africa in the past, without finding any clear evidence of adverse effects. Despite these studies, scepticism remained that acidic deposition could accumulate on the decadal scale and reach a point where the natural buffering capacities of soils and water bodies would be exceeded. Against this background, this study was conceived to make direct measurements of atmospheric concentrations of the acidifying gases, over as an extensive area as possible, to provide an objective basis to the question of whether or not acidic deposition pose immediate or long-term threats to regional ecosystems. As an integral study, the research strategy was designed to address the question as to whether ozone, as a secondary pollutant, would exceed the tolerance of the same ecosystems.

A passive monitoring network was devised to measure monthly mean atmospheric concentrations of three trace gas species,  $\text{SO}_2$ ,  $\text{NO}_2$  and  $\text{O}_3$ . The network comprised of 37 monitoring sites at remote locations over the northern and eastern portions of South Africa, at  $1^\circ$  grid intervals ( $0.5^\circ$  for several sites). Trace gases were sampled monthly over two complete annual cycles at each site, using passive diffusive samplers exposed for approximately 30 days. Samples were chemically analysed at an internationally accredited laboratory (Atmospheric Chemistry Research Group, North-West University) and mean monthly results were recorded.

The collated database of trace gas concentrations enabled assessment in terms of standards, time and spatial distributions. Concentrations were evaluated in a *critical levels assessment against* several sets of South African and international standards and guidelines. The dry deposition rates were calculated from measured ambient trace gas concentrations, using an inferential model. For estimates of wet deposition, long-term acidic rainfall measurements were multiplied by the cumulative precipitation within the sampling period amount for each project site. These total dry and wet deposition estimates (for sulphur and nitrogen compounds), and concentrations of ozone were compared with results from two regional-scale studies of modelled concentration and deposition. The *total acidic deposition* estimates were adjusted with mitigating base cation deposition estimates, dry and wet, and the derived net acidity loads were subtracted from soils acid buffering (sensitivity) capacity loads to determine *critical loads exceedance*.

Two ancillary tasks were undertaken, which contribute to the central aim. The first accessed the most recent measured regional lightning strokes data and adjusted it for intra/inter-cloud strokes to estimate the *lightning produced  $\text{NO}_x$  ( $\text{LNO}_x$ )* budget. High and a low lightning  $\text{NO}_x$  budget estimates were then compared with three relevant anthropogenic emission inventories compiled for the Highveld region. The second task obtained regional  *$\text{SO}_2$ ,  $\text{NO}_2$  and  $\text{O}_3$  remote sensing* information and compared them with ground level concentrations from the passive sampling network. Remote sensing total column densities were converted and partitioned through atmospheric pressure averaging equations to derive tropospheric boundary concentrations appropriate for comparisons.



The main findings were:

- Concentration distributions for acidic gases  $\text{SO}_2$  and  $\text{NO}_2$  show prevailing high concentrations over the industrial Highveld. The areas downwind show substantially decreased concentrations, while remote areas show very low concentrations. Ozone concentrations are spatially uniform, with slightly increased concentrations located away from the central Highveld pollution source area, both north and south. However, ozone distributions and origins could not be directly related to the Highveld industrial emissions. No health-based exceedance (of long-term standards) was recorded for  $\text{SO}_2$ ,  $\text{NO}_2$  or  $\text{O}_3$ . Three areas of critical exceedances were found for  $\text{SO}_2$ , one in the industrial Highveld for sensitive lichen and semi-natural and forest vegetation; and two downwind, for sensitive lichen only. No ecosystem exceedance was established of  $\text{NO}_2$  and  $\text{O}_3$  critical levels.
- Acidic deposition distributions showed a direct relationship to high atmospheric concentration distributions, with exceptions for those areas which had high annual rainfall, and for coastal and escarpment areas where wet deposition prevailed. No concurrent regional modelling had been performed by other parties. Two non-concurrent regional modelling studies were selected for comparison of measured and modelling results. Substantial disparities were identified between the respective results and, although general patterns were followed, the modelling for dry and wet acidic compounds swayed from overestimates to underestimates for sulphur and nitrogen species. In contrast, modelling of ozone mainly overestimated measured concentrations. In terms of spatial distributions, ozone modelling matched a wide band of elevated concentrations in northern area of South Africa (Limpopo Province).
- Derived net acidic deposition loads were matched to critical loads from soil types in the region. This revealed areas with high deposition and highly sensitive local soils within the greater industrial Highveld with critical load exceedance. An area north-west of the central Highveld showed exceedance of the highest critical load, while several smaller areas downwind to the south-east showed exceedances of lower critical loads only.
- The lightning  $\text{NO}_x$  budget estimation showed that lightning  $\text{NO}_x$  is a significant contributor to overall regional  $\text{NO}_x$  budget and a major natural contributor. Depending on lightning count assumptions applied, annual  $\text{LNO}_x$  production varied from a 1/10<sup>th</sup> to 1/3<sup>rd</sup> of the  $\text{NO}_x$  anthropogenic trace gases emissions, taken from the most comprehensive of three recent inventories. However, when seasonal lightning budgets were examined, no distinct seasonal increases in ground-level  $\text{NO}_x$  were found in areas of high lightning frequency, suggesting that much of  $\text{LNO}_x$  is generated and transported above the boundary layer.
- Comparisons of remote sensing concentrations results for  $\text{SO}_2$  and  $\text{O}_3$  have not revealed very good spatial and temporal agreement, although both showed agreement within an order of magnitude between measured and remotely sensed concentrations.  $\text{NO}_2$  agreement was much better in both spatial and temporal comparisons. The mean ratio of remotely sensed to measured  $\text{NO}_x$  is 0.77, an encouraging result given the broad assumptions made in deriving the comparison. Disparities in the horizontal distributions between ground level and satellite products for  $\text{NO}_x$  indicate a need for better information on the vertical distributions of  $\text{NO}_x$



and other trace gases – the assumption of a uniformly mixed boundary layer is not robust enough for such comparisons.

From findings of all individual studies an overall answer to the central question is reached that pollution from acidic gases and their compounds is not a current or medium term threat to regional ecosystems (beyond the central pollution source area), at current rates of emission. Results from the control site, positioned specifically within the well-researched industrial Highveld, confirmed the known situation in this sub-region, while serving well to put in perspective the entire region. Ozone distributions indicate uniform regional distributions, with most monthly means below 30 ppb, and highest single month 43 ppb. Now that this project has established a detailed measured set of acidic trace gas concentrations, limiting factors in determining critical loads are (i) more detailed maps of soil sensitivity (acidic buffering capacity); and (ii) base cation deposition measurements, including dry deposition of dust, and wet deposition, both at more sites and over similar periods used in the current study for the acid components.







## Table of Contents

Affidavit .....	i
Dedication .....	ii
Acknowledgments .....	iii
Abstract .....	v
Table of Contents.....	viii
List of Figures.....	xii
List of Tables.....	xvii
List of Abbreviations and Acronyms.....	xix
<b>1. Introduction</b> .....	<b>1</b>
1.1 Acidic Deposition and Ecological Damage .....	1
1.1.1 Global context.....	1
1.1.2 South African context .....	4
1.1.3 Emissions, transportation and deposition of atmospheric pollutants in South Africa .....	5
1.1.4 Motivation for the study.....	9
1.2 Aim and Objectives .....	10
1.2.1 Aim .....	10
1.2.2 Objectives .....	12
1.3 Structure of Thesis.....	12
<b>2. Concentrations, Distributions and Critical Levels Assessment of Regional SO<sub>2</sub>, NO<sub>2</sub> and O<sub>3</sub></b> .....	<b>15</b>
2.1 Introduction .....	15
2.2 Derivations of Critical Levels as Assessment of Atmospheric Pollution.....	16
2.2.1 Critical levels .....	16
2.2.2 Critical levels for vegetation .....	17
2.2.3 Impacts of air pollution on vegetation in South Africa .....	18
2.3 Method .....	21
2.3.1 Study design.....	21
2.3.2 Passive sampling.....	23
2.3.3 The passive sampling monitoring network .....	27
2.3.4 Different ambient air quality standards and guidelines applied as critical levels .....	29
2.3.5 Quality Assurance and Quality Control .....	31
2.4 Results.....	32
2.5 Passive Sampler Campaign Results.....	32
2.5.1 SO <sub>2</sub> Concentrations and regional distribution .....	32
2.5.2 NO <sub>2</sub> concentrations and regional distribution .....	36
2.5.3 O <sub>3</sub> concentrations and regional distribution .....	40
2.6 Critical (Concentration) Levels Exceedance Assessment.....	43
2.6.1 Critical levels exceedance assessment for SO <sub>2</sub> .....	43
2.6.2 Critical levels exceedance assessment for NO <sub>2</sub> .....	46
2.6.3 Critical levels exceedance assessment for O <sub>3</sub> .....	48
2.7 Conclusions .....	51
2.7.1 Summary .....	52
2.7.2 Comments .....	53



<b>3. Dry and Wet Deposition of SO<sub>2</sub> and NO<sub>2</sub> and Comparison of Meso-scale Air Pollution Dispersion Modelling of SO<sub>2</sub>, NO<sub>2</sub> and O<sub>3</sub></b>	<b>55</b>
3.1 Introduction .....	55
3.2 From concentration to depositions for comprehensive modelling comparison .....	56
3.2.1 Deposition .....	56
3.2.2 Dry deposition .....	56
3.2.3 Wet deposition .....	59
3.2.4 Atmospheric dispersion models available .....	60
3.3 Methods .....	61
3.3.1 Dry deposition determination .....	61
3.3.2 Wet and total acidic deposition .....	63
3.3.3 Measured and modelled comparison method .....	66
3.4 Results .....	66
3.4.1 Dry deposition .....	66
3.4.2 Total wet deposition comparison .....	70
3.4.3 Sulphate wet deposition .....	73
3.4.4 Nitrate wet deposition .....	74
3.4.5 Ammonium wet deposition .....	75
3.4.6 Total (dry and wet) deposition inter-annual comparison .....	76
3.5 Comparison between measured and modelled results .....	78
3.6 Results of modelled and measured comparison .....	79
3.6.1 Sulphur .....	79
3.6.2 Nitrogen .....	89
3.6.3 Ozone modelled and measured comparison .....	96
3.7 Conclusions .....	102
3.7.1 Summary .....	103
3.7.2 Comments .....	104
<b>4. Regional Scale Critical Loads Assessment of Acidic Deposition from SO<sub>2</sub>, NO<sub>2</sub> Emissions from the Highveld</b>	<b>105</b>
4.1 Introduction .....	105
4.2 Cumulative Acidity Assessment as an Indicator of Ecological Risk .....	106
4.2.1 Ecosystem acidification and critical loads concept .....	106
4.2.2 Determining critical loads of acidity through mapping of soil sensitivity .....	109
4.2.3 Critical loads assessment method .....	110
4.2.4 Critical loads assessments in South Africa .....	114
4.3 Methods .....	116
4.3.1 Procedural steps .....	116
4.3.2 Base cation deposition .....	117
4.3.3 Soil data .....	120
4.3.4 Determining critical loads from soil sensitivity classes .....	121
4.4 Results .....	121
4.4.1 Deposition of acidic compounds over the study region .....	121
4.4.2 Soil sensitivity .....	124
4.4.3 Acidification risk in the study region .....	125
4.4.4 Exceedance of buffering capacity: exceedance of critical loads .....	125
4.5 Discussion .....	127
4.6 Conclusions .....	128
4.6.1 Summary .....	129
4.6.2 Comments .....	130



<b>5.</b>	<b>Comparison of Remote Sensing Tropospheric Trace Gas Measurements with Regional-scale SO<sub>2</sub>, NO<sub>2</sub> and O<sub>3</sub> Ground-level Measurements</b>	<b>131</b>
5.1	Comparison of Tropospheric Boundary Layer Concentrations to Ground-level Pollutant Concentrations.....	131
5.2	Measurements of Tropospheric Gases from Space .....	132
5.2.1	NO <sub>2</sub> remote sensing .....	133
5.2.2	SO <sub>2</sub> remote sensing .....	135
5.2.3	O <sub>3</sub> remote sensing .....	136
5.2.4	Validation of satellite remote sensing results.....	138
5.3	Methods.....	140
5.3.1	Ground-level measurements by passive diffusive sampling .....	140
5.3.2	Remote sensing of tropospheric gases and instruments used.....	140
5.3.3	Comparison of passive sampling with satellite remotely sensed data.....	143
5.4	Results.....	147
5.4.1	SO <sub>2</sub> passive sampling with remote sensing results .....	147
5.4.2	NO <sub>2</sub> passive sampling with remote sensing results.....	151
5.4.3	O <sub>3</sub> passive sampling with remote sensing results.....	156
5.5	Discussion .....	159
5.5.1	SO <sub>2</sub> by PS and RS comparison.....	159
5.5.2	NO <sub>2</sub> by PS and RS comparison.....	159
5.5.3	O <sub>3</sub> by PS and RS comparison.....	160
5.6	Conclusions .....	160
5.6.1	Summary.....	161
5.6.2	Comments .....	161
<b>6.</b>	<b>Comparison of Measured Ground-level NO<sub>x</sub> and Lightning-generated NO<sub>x</sub> (LNO<sub>x</sub>) Estimates in the Regional NO<sub>x</sub> Budget</b>	<b>163</b>
6.1	LNO <sub>x</sub> as a Component of the Southern African Regional Tropospheric Budget.....	163
6.2	Lightning and NO <sub>x</sub> generation .....	164
6.2.1	Lightning-produced nitrogen oxides budget .....	167
6.2.2	Intra-cloud and inter-cloud (IC) to cloud-to-ground (CG) lightning ratios.....	168
6.2.3	Soils and vegetation N emissions.....	168
6.3	Methods.....	169
6.3.1	Procedural steps .....	169
6.3.2	Lightning emission factor and stroke multiplicity .....	170
6.3.3	Lightning counts Data.....	172
6.3.4	Adjusted SAWS LDN lightning flash statistics .....	173
6.3.5	IC lightning ratios and LNO <sub>x</sub> generation strengths .....	175
6.3.6	The emission inventories extraction.....	177
6.3.7	NO <sub>x</sub> budget estimation based on passive sampling measurements .....	179
6.3.8	NO <sub>x</sub> budget on the basis of remote sensing measurements for the study region.....	181
6.4	Results.....	183
6.4.1	Lower LNO <sub>x</sub> estimate .....	183
6.4.2	Higher LNO <sub>x</sub> estimate.....	183
6.4.3	LNO <sub>x</sub> and anthropogenic NO <sub>x</sub> budget comparison .....	184
6.5	Discussion .....	186
6.6	Conclusions .....	190
6.6.1	Summary.....	191
6.6.2	Comments .....	191



<b>7. Conclusion</b>	<b>193</b>
7.1 Summary of Findings.....	193
7.2 Conclusions.....	199
7.3 Original Contributions and Significance.....	201
7.4 Future Research.....	203
<b>References</b>	<b>205</b>
<b>Appendix A: Example of Dry and Wet Deposition Calculations for a Site</b>	<b>222</b>
<b>Appendix B: Acidity Loads and Base Cation Deposition</b>	<b>226</b>
<b>Appendix C: Remote Sensing Sample Data and Conversion Examples</b>	<b>229</b>
<b>Appendix D: Publications, Technical Reports and Presentations</b>	<b>232</b>





## List of Figures

Figure 1.1:	Extent of the Mpumalanga Highveld (inner box) indicating the location of coal-fired power stations and various large industries (Source: Scorgie <i>et al.</i> , 2004a).....	6
Figure 1.2:	The main air transport pathways out of the Highveld (Source: Freiman and Piketh, 2003).....	7
Figure 2.1:	Extent of the study area within South and sub-Saharan Africa (map insert) with several pivotal sites marked.....	22
Figure 2.2:	A passive sampling monitor in position (Sampling site no. 17, Elandsfontein).....	24
Figure 2.3:	IDAF passive sampler design (Source: IDAF, 2005).....	25
Figure 2.4:	The passive diffusive sampling network distribution ■ [with locations of wet chemistry deposition sites ♦ (green lettering) in relation to this study sites (black and green lettering)].....	28
Figure 2.5:	Two-year SO <sub>2</sub> concentration comparison of mean, standard deviation, maximum and minimum (Sep05-Aug07).....	35
Figure 2.6:	Regional distributions of mean annual SO <sub>2</sub> concentrations: a) Sep05-Aug06; b) Sep06-Aug07.....	36
Figure 2.7:	Two-year NO <sub>2</sub> concentration comparison of mean, standard deviation, maximum and minimum (Sep05-Aug07).....	39
Figure 2.8:	Regional distributions of mean annual NO <sub>2</sub> concentrations: a) Sep05-Aug06; b) Sep06-Aug07.....	40
Figure 2.9:	Mean, standard deviation, maximum and minimum O <sub>3</sub> monthly concentrations for the period Sep05-Aug07.....	42
Figure 2.10:	Regional distributions of mean annual O <sub>3</sub> concentrations: a) Sep05-Aug06; b) Sep06-Aug07.....	43
Figure 2.11:	Annual mean SO <sub>2</sub> concentrations for two annual cycles (Sep05-Aug06 and Sep06-Aug07) compared to various annual SO <sub>2</sub> critical levels.....	44
Figure 2.12:	Moving-3-monthly SO <sub>2</sub> means over two annual cycles (Sep05-Aug06, and Sep06-Aug07) for three different categories of sites.....	45
Figure 2.13:	Mean winter SO <sub>2</sub> concentrations for winter half-years (2006 & 2007) compared to SO <sub>2</sub> vegetation winter (half-year) critical levels.....	46
Figure 2.14:	Mean annual NO <sub>2</sub> concentrations for two annual cycles (Sep05-Aug06 and Sep06-Aug07) compared to annual critical levels.....	47
Figure 2.15:	Three-month moving average NO <sub>2</sub> concentrations over two annual cycles (Sep05-Aug06 and Sep06-Aug07) for three different site categories.....	48
Figure 2.16:	Mean annual O <sub>3</sub> concentrations for two annual cycles (Sep05-Aug06 and Sep06-Aug07) compared to O <sub>3</sub> annual average critical levels. The error bars set as 25% (Martins, personal communication, 2007).....	48
Figure 2.17:	Three-month moving average O <sub>3</sub> over two annual cycles (Sep05-Aug06 and Sep06-Aug07) for three different site categories.....	49
Figure 2.18:	Growing season mean O <sub>3</sub> concentrations (Oct-Apr for two years) for all sites compared to ozone critical levels. The error bars set as 25% (Martins, personal communication, 2007).....	50
Figure 2.19:	Time-sequence of monthly mean O <sub>3</sub> concentrations (Oct-Apr for two seasons) compared to ozone critical levels for three representative sites.....	51
Figure 3.1:	Resistance analogy for the deposition of atmospheric pollutants (Source: UNECE CLTRAP mapping and modelling manual, 2004).....	58



Figure 3.2:	Modelled mean ambient SO <sub>2</sub> concentrations (µg m <sup>-3</sup> ) for the 2000 winter season based on the EDGAR 32FT2000 emission database (Source: Fourie, 2006).....	61
Figure 3.3:	SO <sub>2</sub> comparison of modelled (2000) and measured concentrations (Jan05-Sep07) for three sites. ....	80
Figure 3.4:	Comparison of SO <sub>2</sub> seasonal modelled and measured mean concentrations for Amersfoort (site 2).....	81
Figure 3.5:	Comparison of SO <sub>2</sub> seasonal modelled and measured mean concentrations for Elandsfontein (site 17).....	81
Figure 3.6:	Comparison of SO <sub>2</sub> seasonal modelled and measured mean concentrations for Louis Trichardt (site 36). ....	82
Figure 3.7:	Comparison of measured and modelled dry gaseous sulphur deposition: V <sub>d</sub> for modelled (Fourie, 2006); V <sub>d</sub> for measured (Mphepya, 2002) (Table 3.13). ....	83
Figure 3.8:	Seasonal rainfall comparison for three representative sites. ....	86
Figure 3.9:	Comparison of modelled (Fourie, 2006) and measured annual cumulative wet sulphate deposition. ....	86
Figure 3.10:	Seasonal rainfall comparison (2000 – 2006/7) for site 36, Louis Trichardt. ....	88
Figure 3.11:	NO <sub>2</sub> comparison of modelled (Fourie, 2006) concentration (2000) and measured concentration (Sep05-Aug07).....	89
Figure 3.12:	NO <sub>2</sub> comparison of monthly mean modelled (Jan00-Dec00) and monthly mean measured concentrations (Sep05-Aug07) for Amersfoort (site 2).....	90
Figure 3.13:	NO <sub>2</sub> comparison of monthly mean modelled (Jan00-Dec00) to monthly mean measured concentrations (Sep05-Aug07) for Elandsfontein (site 17).....	90
Figure 3.14:	NO <sub>2</sub> comparison of monthly mean modelled (Jan00-Dec00) to monthly mean measured concentrations (Sep05-Aug07) for Louis Trichardt (site 36). ....	91
Figure 3.15:	Comparison of modelled (Fourie, 2006) and measured cumulative dry gaseous nitrogen species deposition.....	92
Figure 3.16:	Comparison of average annual nitrogen wet modelled (Fourie, 2006) and measured deposition rates for three sites. ....	94
Figure 3.17:	Comparison of ozone (a) modelled concentrations (January 2000) Zunckel <i>et al.</i> , 2006, with (b) measured concentrations (January 2006).....	96
Figure 3.18:	Comparison of ozone concentrations modelled for the growing season (Oct00-Apr01) to measured concentrations, averaged for the two growing seasons (Oct05-Apr06 & Oct06-Apr07), for all monitored sites.....	97
Figure 3.19:	Comparison of modelled ozone for growing season (Oct00-Apr01) and measured ozone, mean of two growing seasons (Oct05-Apr06 & Oct06-Apr07) for Amersfoort (site 2). ....	99
Figure 3.20:	Comparison of modelled ozone for growing season (Oct00-Apr01) and measured ozone, mean of two growing seasons (Oct05-Apr06 & Oct06-Apr07) for Elandsfontein (site 17). ....	99
Figure 3.21:	Comparison of modelled ozone for growing season (Oct00-Apr01) and measured ozone, mean of two growing seasons (Oct05-Apr06 & Oct06-Apr07) for Louis Trichardt (site 36). ....	100
Figure 3.22:	Modelled and monitored surface ozone at Cape Point during the period October 2000 to April 2001 (Zunckel <i>et al.</i> , 2006).....	101
Figure 3.23:	Generalised atmospheric transport over southern Africa (Source: Tyson and Preston-Whyte, 2000). ....	104
Figure 4.1:	Methodology for assessing the risk of ecosystem acidification and associated impacts from acidifying deposition by Kuylenstierna <i>et al.</i> (2001a). ....	110
Figure 4.2:	Method used to allocate soil types to relative sensitivity classes by Kuylenstierna <i>et al.</i> (2001a, b). ....	111



Figure 4.3:	Compilation of weathering rates, based on literature reviews for matching the sensitivity classes, by Kuylenstierna <i>et al.</i> (2001a, b).....	112
Figure 4.4:	Critical load ranges assigned to relative sensitivity classes by Kuylenstierna <i>et al.</i> (2001a, b).....	113
Figure 4.5:	An overlay of relative soil sensitivity onto the map of sulphate deposition loads to identify areas of overlap between high deposition loads and high soil sensitivity (Source: Olbrich <i>et al.</i> , 1994).....	115
Figure 4.6:	Base cation deposition extracted from modelled dust deposition and based on depositions of soil dust alone, with assumed 10% Ca content (meq m <sup>-2</sup> yr <sup>-1</sup> ) (Source: Kuylenstierna <i>et al.</i> , 2001a).....	118
Figure 4.7:	Total (dry and wet) lower BC estimated deposition (meq m <sup>-2</sup> yr <sup>-1</sup> ).....	119
Figure 4.8:	Total (dry and wet) higher BC estimated deposition (meq m <sup>-2</sup> yr <sup>-1</sup> ).....	120
Figure 4.9:	Acidic deposition (total dry and wet) (meq m <sup>-2</sup> yr <sup>-1</sup> ).....	122
Figure 4.10:	The lower net acidic deposition (Net Level 1) for the study region ( <i>higher</i> base cation estimate) (meq m <sup>-2</sup> yr <sup>-1</sup> ).....	123
Figure 4.11:	The higher net acidic deposition (Net Level 2) for the study region ( <i>lower</i> base cation estimate) (meq m <sup>-2</sup> yr <sup>-1</sup> ).....	124
Figure 4.12:	Sensitivity classes of the soils based on soil attributes, with Class 1 being the most sensitive. (Source: ISRIC, 2003; Kuylenstierna <i>et al.</i> , 2001a).....	125
Figure 4.13:	Exceedance of critical loads, using case of the Net Level 2 acidic deposition and the more critical, lower level of soil sensitivity.....	126
Figure 4.14:	Exceedance of critical loads, using case of the Net Level 2 acidic deposition and the less critical, higher level of soil sensitivity.....	127
Figure 4.15	Coarse map of veld types of South Africa (Source: DEAT, 2008).....	129
Figure 5.1:	Annual tropospheric NO <sub>2</sub> observed by GOME instrument (Source: Wenig <i>et al.</i> , 2003).....	132
Figure 5.2:	NO <sub>2</sub> tropospheric VCD mean for May 2006 (Source: TEMIS, 2008: KNMI/IASB/ESA).....	134
Figure 5.3:	Ground level measured NO <sub>2</sub> concentration contours for May 2006.....	134
Figure 5.4:	A 32-month average of SCIAMACHY SO <sub>2</sub> for a part of the globe. (Source: IUP, University of Bremen, 2008).....	135
Figure 5.5:	Comparison of a) PS ground-level SO <sub>2</sub> measured (June 2007); and b) RS (SCIAMACHY) VCD at 1 km height over the study region (June 2007) (Source: (a) this work; (b) van Geffen, personal communication, 2008).....	136
Figure 5.6:	Monthly averaged OMI/MLS Tropospheric Column Ozone (DU) for September–November 2004 (Source: Ziemke <i>et al.</i> , 2006).....	137
Figure 5.7:	Ground-level O <sub>3</sub> measured by passive diffusive sampling and GIS-interpolated for Sep05.....	137
Figure 5.8:	Sample of a vertical profile comparison [Comparison of O <sub>3</sub> profiles inferred from SCIAMACHY limb observations with correlative balloon-borne measurements (Source: Pfeilsticker <i>et al.</i> , 2007)].....	138
Figure 5.9:	Vertical NO <sub>2</sub> column densities [10 <sup>15</sup> molec cm <sup>2</sup> ] observed by SCIAMACHY and AMAXDOAS on 10 March 2003 (Source: Heue <i>et al.</i> , 2004).....	139
Figure 5.10:	SCIAMACHY ozone profile plotted versus altitude and coincident ozone sonde profile (O3S) measured at the NDACC/Alpine station of Payerne. Corresponding correlative profile smoothed to the SCIAMACHY vertical perception using averaging kernel matrix and a priori information (Source: De Clercq <i>et al.</i> , 2006).....	140
Figure 5.11:	Spectral windows for the various species measured by GOME (Source: IUP, University of Heidelberg, 2008).....	141



Figure 5.12:	The DU and pressure-averaged mixing ratio (Source: Ziemke, personal communication, 2008; Ziemke <i>et al.</i> , 2006).....	144
Figure 5.13:	Spatial comparison of SO <sub>2</sub> concentrations by PS and RS measurements for all sites as the means over entire passive sampling period. The systematic error bars for PS are 25% and for RS are 50%.....	148
Figure 5.14:	Comparison of SO <sub>2</sub> concentrations by PS and RS at a site in the major pollution emission source-area (Site 17). The systematic error bars for PS are 25% and for RS are 50%. ....	149
Figure 5.15:	Spatial comparison of SO <sub>2</sub> concentrations by PS and RS for a site downwind from the major pollution emission source-area (Site 2). The systematic error bars for PS are 25% and for RS are 50%.....	149
Figure 5.16:	Spatial comparison of SO <sub>2</sub> concentrations by PS and RS for a site remote from the major pollution emission source-area (site 36). The systematic error bars for PS are 25% and for RS are 50%. ....	150
Figure 5.17:	Combined time series comparison of SO <sub>2</sub> concentrations measured by PS and RS for three different site categories (Site 2 – downwind; Site 17 – polluted; Site 36 – remote).....	150
Figure 5.18:	Spatial comparison of NO <sub>2</sub> concentrations by PS and RS for all sites for January 2006 (50% systematic error bars for RS data).....	151
Figure 5.19:	Comparison of a) ground-level NO <sub>2</sub> measured for October 2007 monthly averaged and b) RS (SCIAMACHY) VCD over the same region for October 2007. (Sources: (a) this work; (b) Beirle, personal communication, 2008).....	152
Figure 5.20:	Comparison of NO <sub>2</sub> concentrations by PS and RS for site 2 (Amersfoort, a site down-wind from the major pollution emission source-area). PS systematic error bars at 10% and RS at 50%. ....	153
Figure 5.21:	Time series comparison of NO <sub>2</sub> concentrations by PS and RS for site 17 (Elandsfontein, a site in the major pollution emission source-area). PS systematic error bars at 10%, RS at 50%.....	153
Figure 5.22:	Time series comparison of NO <sub>2</sub> concentrations by PS and RS for site 36 (Louis Trichardt, a remote rural site off the major wind axis from the major pollution emission source-area). PS systematic error bars at 10% and the RS at 50%.....	154
Figure 5.23:	Comparison of three categories of sites for NO <sub>2</sub> measured by PS and RS. NO <sub>2</sub> mean concentrations and standard deviations at sites DW-remote downwind site, IH – industrial Highveld site, RM – remote rural site). ....	155
Figure 5.24:	Spatial comparison of O <sub>3</sub> by PS and RS for all study sites during September 2006 (Systematic error bars for RS data are 50% and for PS 25%). ....	157
Figure 5.25:	Time series comparison of O <sub>3</sub> by PS and RS at site 2 (Amersfoort) over the period Sep05-Sep06. The systematic error bars for RS data are 50% and for PS are 25%. ....	157
Figure 5.26:	Time series comparison of O <sub>3</sub> by PS and RS at site 17 (Elandsfontein) over the period Sep05-Sep06. The systematic error bars for RS data are 50% and for PS are 25%. ....	158
Figure 5.27:	Time series comparison of O <sub>3</sub> by PS and RS at site 36 (remote rural) over the period Sep05-Sep06. The systematic error bars for RS data are 50% and for PS are 25%. ....	158
Figure 5.28:	Combined times series comparison of O <sub>3</sub> measured by PS and RS for three site categories.....	159
Figure 6.1:	Co-location of enhanced tropospheric NO <sub>x</sub> and lightning events over Gulf of Mexico: a) GOME tropospheric NO <sub>2</sub> slant column density (10 <sup>15</sup> molec cm <sup>-2</sup> ); b) cloud fraction; c) National (USA) Lightning Detection Network flashes (time of last lightning event) (Source: Beirle <i>et al.</i> , 2005). ....	164





Figure 6.2:	OTD Global map of total lightning activity from 1995-2000 (Source: Christian <i>et al.</i> , 2003).....	166
Figure 6.3:	LPATS chosen stroke count area with the Vaisala reported detection efficiency (Source: Ojelede <i>et al.</i> , 2008).....	171
Figure 6.4:	Location of SAWS lightning detection network sensors in South Africa. (Source: SAWS, as quoted in Bhika, 2008). ....	172
Figure 6.5:	Distribution of groundstroke lightning density for summer 2006/7 (Source: Bhika, 2008).....	174
Figure 6.6:	Individual (smoothed) 0.5 ° grid estimates of IC: CG ratio overlaid on prior observations (Source: Boccippio <i>et al.</i> , 2000).....	175
Figure 6.7:	4D extract of Fleming and van der Merwe emission database for NO <sub>2</sub> . ....	178
Figure 6.8:	NO <sub>2</sub> mean concentrations measured by passive sampling (Sep05-Aug07). Red marking is 4D square. ....	180
Figure 6.9:	NO <sub>2</sub> mean RS 4-year (2003 to 2007) tropospheric vertical column density (10 <sup>15</sup> molec cm <sup>-2</sup> ) by SCIAMACHY for the study area (Source: Beirle, personal communication, 2008). The red square represents 4D compared area. ....	182
Figure 6.10:	A NO <sub>2</sub> seasonal concentration means (Sep05-Aug07). ....	186
Figure 6.11:	Schematic illustration of a gaseous species mass budget calculation in a predefined volume (Source: Panitz and Nester, 2002). ....	187
Figure 6.12:	Sequence of distributions of tropospheric NO <sub>2</sub> columns from the GOME instrument east of SA in May 1998 (left column). Corresponding NO <sub>x</sub> tracer column densities (centre column) and vertical sections of the NO <sub>x</sub> tracer concentrations only for industrial emissions (Wenig <i>et al.</i> , 2003). ....	190





## List of Tables

Table 1.1:	Scheduled emissions from South Africa and the industrial Highveld region, metric tonnes per year (1993).....	6
Table 1.2:	Comparison of annual emissions from combustion sources for two nitrogen gaseous species in South Africa^.....	7
Table 2.1:	Chemical reactions used in passive sampling for NO <sub>2</sub> , SO <sub>2</sub> and O <sub>3</sub> *.....	23
Table 2.2:	Formulations of the coating solutions for trace gas passive samplers #.....	25
Table 2.3:	Detection limits for the various species for sampling and analysis.....	26
Table 2.4:	Atmospheric critical levels for trace gas species SO <sub>2</sub> , NO <sub>2</sub> and O <sub>3</sub> .....	30
Table 2.5:	Percentage of validated passive diffusive samplers (successful exposures) for each of annual cycles and overall over two cycles.....	32
Table 2.6:	SO <sub>2</sub> annual mean concentrations and inter-annual means comparison.....	33
Table 2.7:	Comparison of NO <sub>2</sub> inter-annual means.....	37
Table 2.8:	O <sub>3</sub> inter-annual concentration means comparison.....	41
Table 3.1:	Calculation of seasonal inferred deposition velocities of SO <sub>2</sub> and NO <sub>2</sub> in cm s <sup>-1</sup> for this study based on prior determined velocities*.....	62
Table 3.2:	The 10 year period volume weighted mean precipitation ion concentrations (µeq l <sup>-1</sup> ) extract*.....	63
Table 3.3:	Allocation of historical wet deposition anion concentrations* to monitoring sites used in this study. (Colour used to indicate the wet chemistry sites.).....	65
Table 3.4:	SO <sub>2</sub> dry deposition inter-annual means comparison.....	67
Table 3.5:	NO <sub>2</sub> dry deposition inter-annual means comparison.....	68
Table 3.6:	Total wet deposition rates of S and N acidifying (inorganic) species and their inter-annual comparison.....	70
Table 3.7:	The rainfall and total wet deposition inter-annual comparison.....	71
Table 3.8:	Wet deposition of SO <sub>4</sub> <sup>2-</sup> for two annual cycles and comparison.....	73
Table 3.9:	Wet deposition rates of NO <sub>3</sub> <sup>-</sup> as N (kg ha <sup>-1</sup> yr <sup>-1</sup> ) for two annual cycles and comparison.....	74
Table 3.10:	Wet deposition rates of NH <sub>4</sub> <sup>+</sup> for two annual cycles and comparison.....	75
Table 3.11:	Total cumulative (wet and dry) deposition rate inter-annual comparison.....	77
Table 3.12:	SO <sub>2</sub> mean annual concentration comparison for all three sites.....	80
Table 3.13:	Sulphur dry deposition modelled (SO <sub>2</sub> and SO <sub>4</sub> <sup>2-</sup> ) and measured (SO <sub>2</sub> ) comparison.....	83
Table 3.14:	Comparison of the deposition velocities (V <sub>d</sub> ) of SO <sub>2</sub> and NO <sub>2</sub> for this study and for the compared modelling results.....	84
Table 3.15:	SO <sub>2</sub> seasonal dry deposition comparison for site Amersfoort (AF).....	84
Table 3.16:	SO <sub>2</sub> seasonal dry deposition comparison for site Elandsfontein (EF).....	85
Table 3.17:	SO <sub>2</sub> seasonal dry deposition comparison for site Louis Trichardt (LT).....	85
Table 3.18:	Wet sulphate deposition comparison for three sites (Sep06-Aug07).....	87
Table 3.19:	SO <sub>4</sub> <sup>2-</sup> wet deposition comparison for site Amersfoort (AF).....	87
Table 3.20:	SO <sub>4</sub> <sup>2-</sup> wet deposition comparison for site Elandsfontein (EF).....	87
Table 3.21:	SO <sub>4</sub> <sup>2-</sup> wet deposition comparison for site Louis Trichardt (LT).....	87
Table 3.22:	The seasonal precipitation comparison for site Louis Trichardt (LT).....	88
Table 3.23:	NO <sub>2</sub> mean annual concentration comparison for all three sites.....	89



Table 3.24:	NO <sub>2</sub> modelled and measured dry deposition comparison.....	92
Table 3.25:	Nitrogen seasonal dry deposition for site Amersfoort (AF). .....	93
Table 3.26:	NO <sub>2</sub> seasonal dry deposition comparison for site Elandsfontein (EF). .....	93
Table 3.27:	NO <sub>2</sub> seasonal dry deposition comparison for site Louis Trichardt (LT). .....	93
Table 3.28:	Nitrogen cumulative wet deposition for all three sites. ....	94
Table 3.29:	Seasonal nitrogen wet deposition (NO <sub>3</sub> <sup>-</sup> only) comparison for Amersfoort (AF).....	95
Table 3.30:	Seasonal nitrogen wet deposition (NO <sub>3</sub> <sup>-</sup> only) comparison for Elandsfontein (EF).....	95
Table 3.31:	Seasonal nitrogen wet deposition (NO <sub>3</sub> <sup>-</sup> only) comparison for Louis Trichardt (LT).....	95
Table 3.32:	Comparison of the modelled to measured O <sub>3</sub> concentration averages for growing season for all monitored sites. ....	97
Table 3.33:	Comparison of modelled and measured O <sub>3</sub> concentrations for Amersfoort. ....	100
Table 3.34:	Comparison of modelled and measured O <sub>3</sub> concentrations for Elandsfontein. ....	100
Table 3.35:	Comparison of modelled and measured O <sub>3</sub> concentrations for Louis Trichardt.....	101
Table 4.1:	Synthesis of approaches and calculations adopted in applying the critical loads approach in South Africa (Source: van Tienhoven <i>et al.</i> , 1995). ....	116
Table 4.2:	The measured base cation concentrations used for the wet deposition of base cation estimates*.....	118
Table 4.3:	Allocated sensitivity classes against critical loads of acidity for use with the regional sensitivity map.....	121
Table 4.4:	The mean and standard deviations of chemical deposition rates for all options used.....	122
Table 5.1:	Annual and seasonal mean of <i>Total Ozone Column</i> (DU) and corresponding short-term trends (%/year) for the entire troposphere and for the boundary layer (BL, 0–2 km altitude), mid troposphere (MT, 2–8 km altitude) and upper troposphere (UT, 8 km altitude to the dynamical tropopause DT) over New York, Paris, Frankfurt and Japan (Source: Zbinden <i>et al.</i> , 2006). ....	147
Table 5.2:	Ratios and standard deviations of ratios between remote sensing and passive sampling measurements for all months. ....	156
Table 6.1:	Determination of lightning flashes from SAWS LDN* by using stroke multiplicity rates** for the compared study square (4D). ....	175
Table 6.2:	Major sources of NO <sub>x</sub> emissions in SA from the EDGAR emission database converted to NO <sub>x</sub> as N (Source: EDGAR, 2008: 32FT2000).....	177
Table 6.3:	Emission inventory extract from the FRIDGE study (t NO <sub>2</sub> yr <sup>-1</sup> )* .....	179
Table 6.4:	Passive sampling (PS) concentration data based estimate of NO <sub>2</sub> mean budget in the study region. ....	180
Table 6.5:	NO <sub>x</sub> budget within the VCD measured by SCIAMACHY and averaged for 2003-2007 <sup>#</sup> over 4D region. ....	182
Table 6.6:	LNO <sub>x</sub> budget based on flashes detected by the SAWS Lightning Detection Network <sup>#</sup> , adjusted with IC flashes (less energetic option). ....	183
Table 6.7:	LNO <sub>x</sub> budget based on flashes detected by the SAWS Lightning Detection Network <sup>#</sup> , adjusted with IC flashes (equally energetic option). ....	184
Table 6.8:	Comparison of NO <sub>x</sub> emissions (kt N yr <sup>-1</sup> ) from the major inventories applicable to the Highveld. ....	185
Table 6.9:	NO <sub>2</sub> budget over the 4D volume by passive sampling and by remote sensing. ....	188



## List of Abbreviations and Acronyms

ACCENT	Atmospheric Composition Change the European Network of Excellence
ADRAS	Acid Deposition Risk Advisory System
AMAXDOAS	Airborne Multi Axis DOAS
AOT	Accumulated Over Threshold
APINA	Air Pollution Information Network for Africa
AQA	Air Quality Act
ARC-ISCW	Agricultural Research Council – Institute for Soil, Climate and Agriculture
ASCII	American Standard Code for Information Interchange
asl	Above sea level
BAPMoN	Background Monitoring Network
BC	Base Cation
BIBLE	Burning and Lightning Experiment
BIRA-IASB	Belgian Institute for Space Aeronomy
BL	Boundary Layer
BS	Base Saturation
CAAP	Composition and Acidity of Asian Precipitation
CAD	Composition of Asian Deposition
CAMx	Comprehensive Air Quality Model with Extensions
CAPIA	Cross Border Air Pollution Impact Assessment Project
CEC	Cation Exchange Capacity
CG	Cloud to Ground
CLRTAP	Convention on Long Range Trans-boundary Air Pollution
CSIR	Council for Scientific and Industrial Research
DEAT	Department of Environmental Affairs and Tourism
DEBITS	Deposition of Biogeochemically Important Trace Species
DLR	German Aerospace Centre
DOAS	Differential Optical Absorption Spectroscopy
DT	Dynamical Tropopause
DU	Dobson Unit
EDGAR	Emission Database for Global Atmospheric Research
EMEP	Cooperative Programme for Monitoring and Evaluation of the Long-Range Transmission of Air Pollutants in Europe
ENSO	<i>El Niño</i> Southern Oscillation
ENVIRON	ENVIRON Holdings
ENVISAT	Environmental Satellite
ESA	European Space Agency
EULINOX	European Lightning Nitrogen Oxide Project
FAO	Food and Agriculture Organization
FRIDGE	Fund for Research into Industrial Development Growth and Equity
FTIR	Fourier Transform Infrared Spectrometer



GEMS	Global Environment Monitoring System
GMES	Global Monitoring for Environment and Security
GOME	Global Ozone Monitoring Experiment
GSFC	Goddard Space Flight Center
IC	Intra/inter-Cloud
ICP	International Cooperative Programme
IDAF	IGBP/IGAC/DEBITS' in AFRICA
IDL	Interactive Data Language
IGAC	International Global Atmospheric Chemistry
IGBP	International Geosphere Biosphere Programme
IPCC	Intergovernmental Panel on Climate Change
ISRIC	International Soil Reference and Information Centre
ITCZ	Inter-Tropical Convergence Zone
IUP	Institute for Environmental Physics
IUSS	International Union of Soil Science
LBA	Large-scale Biosphere-Atmosphere Experiment in Amazonia
LDN	Lightning Detection Network
LED	Lagrangian-Eulerian Diffusion Model
LF	Low frequency
LINOX	Lightning produced NO <sub>x</sub> (project)
LNO <sub>x</sub>	Lightning produced NO <sub>x</sub> (term)
LPATS	Lightning Positioning and Tracking System
MDF	Magnetic Direction Finder
MLS	Microwave Limb Sounder
MT	Mid Troposphere
NAPAP	National Acid Precipitation Program
NASA	National Aeronautics and Space Administration
NDACC	International Network for the Detection of Atmospheric Composition Change
NEMA	National Environmental Management Act
NLDN	National Lightning Detection Network (USA)
OMI	Ozone Monitoring Instrument
OTD	Optical Transient Detector
ppb	parts per billion
ppm	parts per million
PROMOTE	Protocol Monitoring for the GMES Service
PS	Passive Sampling
R <sub>a</sub>	Aerodynamic Resistance
RAINS	Regional Air pollution Information and Simulation
RAPIDC	Regional Air Pollution in Developing Countries
R <sub>b</sub>	Boundary Layer Resistance
R <sub>c</sub>	Surface Resistance
RS	Remote Sensing
RSD	Relative Standard Deviation



SAEON	South African Environmental Observation Network
SANS	South African National Standards
SASOTER	South African SOTER
SAWS	South African Weather Service
SCD	Slant Column Density
SCIAMACHY	Scanning Imaging Absorption Spectrometer for Atmospheric Cartography
SEI	Stockholm Environment Institute
SONEX	Subsonic Assessment Ozone and Nitrogen Oxide Experiment
SOTER	Soil and Terrain Digital Database
SOTERSAF	Soil and Terrain Digital Database for Southern Africa
TEMIS	Tropospheric Emission Monitoring Internet Service
TOC	Total ozone Column
TOMS	Total Ozone Monitoring Spectrometer
TroCCiNO <sub>x</sub>	Tropical Convection Cirrus and Lightning Nitrogen Oxide Experiment
TROPOSAT	Use and Usability of Satellite Data for Tropospheric Research
UN WHO	United Nations World Health Organization
UNECE	United Nations Economic Commission for Europe
UNEP	UN Environment Programme
UNESCO	United Nations Educational, Scientific and Cultural Organization
UT	Upper Troposphere
VCD	Vertical Column Density
V <sub>d</sub>	Deposition Velocity
VMR	Volume Mixing Ratio
VOC	Volatile Organic Compound
WGE	Working Group on Effects
WHO	World Health Organization
WISE	World Inventory of Soil Emission Potentials
WMO	World Meteorological Organization

UNIVERSITY  
OF  
JOHANNESBURG

# CHAPTER ONE

*This chapter opens the thesis with a review of the history of acid pollution as an environmental problem. It presents the South African situation in context of high emissions and introduces the overall aim and specific objectives. A layout of the thesis structure in a form of synopses for each of the chapters is given.*

## **1. Introduction**

### **1.1 Acidic Deposition and Ecological Damage**

#### **1.1.1 Global context**

Forest dieback and irreversible acidification of lakes linked to serious loss of fish stocks and other sensitive aquatic species in Scandinavia in the middle of the 20<sup>th</sup> century were attributed to deposition of acidic species (acid rain) originating from the United Kingdom (Oden, 1968). Ever since these experiences became known there have been global and local concerns that such ecological damage due to acid rain in other regions downwind of large coal fired power plants and industries are and could be repeated (Kuylenstierna and Hicks, 2002; Kuylenstierna *et al.*, 2001a; Whelpdale and Kaiser, 1996; Kuylenstierna *et al.*, 1995, 1989; Wesely and Hicks, 1977).

First isolated instances of acidification damage from atmospheric pollution were reported in the late 19<sup>th</sup> and early 20<sup>th</sup> centuries in parts of Europe and North America (McCormick, 1997). Further research in the 1950s confirmed the existence of problems of air pollution crossing local, regional and international boundaries. A number of Swedish scientists – Rossby, Eriksson and Oden – brought together then existing knowledge about acid precipitation in the fields of limnology, agriculture and atmospheric chemistry and argued for a link between industrial emissions and observed environmental damage (Oden, 1968, McCormick, 1997). Oden argued that precipitation over Scandinavia was becoming increasingly acidic, and that the large quantities of sulphur compounds causing acidification came from British and central European industrial emissions. Soon after, further studies showed that sulphur pollutants could be carried 1 000 km or more. Numerous Scandinavian studies (Almer *et al.*, 1978. Henriksen, 1980; Bernhard, 1983; Hörnström *et al.*, 1984; Lydén and Gratin, 1985; Nihlgard, 1985; Morling and Pejler,



1990) caught the public attention and prompted research elsewhere (Cowling 1982; Scütt and Cowling, 1985; Pearce, 1986; Linzon, 1986; Hinrichsen, 1988; Smith et al., 1988) predominantly in Europe and North America. This eventually led to the signing of the United Nations Economic Commission for Europe Long-range Transboundary Air pollution (UNECE LRTAP) Convention in 1979. Later, in 1999 the Multi-effect ("Gothenburg") Protocol as a multi-pollutant protocol was designed to reduce acidification, eutrophication and ground-level ozone by setting emissions ceilings for sulphur dioxide, nitrogen oxides, volatile organic compounds and ammonia to be met by 2010 (UNECE, 2009).

In response, countries in Western Europe and North America responded to air pollution problems and through policies and coordinated measures managed to reduce substantially the emissions of SO<sub>2</sub>, the primary acidic precursor, although NO<sub>x</sub> emissions still remain a problem. In the meantime, later research has shown that pollutants such as Volatile Organic Compounds (VOC) and ammonia are also involved in processes that lead to acidification (McCormick, 1997).

The science and knowledge on acid pollution has made rapid progress, especially in countries of Western Europe and North America. Most of industrialised countries operate their own local and countrywide atmospheric monitoring programmes. At the global level, the World Meteorological Organisation (Miller, 1992, Georgii, 1982) has been operating a Background Monitoring Network (BAPMoN), and the UN Environment Programme (UNEP, 2008) coordinates global and regional monitoring through its Global Environment Monitoring System (GEMS). In Europe, monitoring is done under the Cooperative Programme for Monitoring and Evaluation of the Long-Range Transmission of Air Pollutants in Europe (EMEP, 2008) under the UNECE (UNECE, 2008). Research on emissions has been also performed by the International Institute for Applied Systems Analysis, which has developed an interactive computer simulation called RAINS (Regional Air Pollution Information and Simulation). There are several monitoring networks in the USA, such as the National Atmospheric Deposition Program, which collects data from nearly 200 sites across the USA. A major project, called the National Acid Precipitation Program (NAPAP), was launched in 1980 to study the causes and potential effects of acid deposition in and around the United States. The final report was issued in 1990, raising more question than it answered (McCormick, 1997).





In contrast to declining SO<sub>2</sub> emissions in Europe and North America in response to stringent government regulation, emissions are rising in many developing nations across the world (McCormick, 1997, Held *et al.*, 1996, Galloway, 1995). There is an opportunity for policy-makers in developing countries to take into account the potential acidification impacts associated with increasing emissions so that they can avoid some of the costly mistakes that have been made during industrial development in Europe and North America. The knowledge obtained in these regions with regard to acidic deposition and the effects of the acidification can be used and adopted to local conditions for this purpose.

Previous experience shows that in order to manage acid deposition, emissions of the acidifying precursor species need to be controlled. The acidification of soil and surface water has indirect effects, including the cumulative impacts of both wet and dry sulphur (S) and nitrogen (N) deposition. Reducing emissions cannot result in the immediate recovery of affected ecosystems (Bishop and Hultberg, 1995) and the major risks of the cumulative effects of acidification in developing countries lie in the future as emissions increase (Kuylenstierna *et al.*, 2001a). Therefore, the establishment of quantifiable estimates of acidification of the environment in developing regions still requires attention.

In newly industrialised countries of Asia, South America and Africa efforts are being made to monitor acidic pollution and influence policy changes through the efforts of international organisations, notably through the International Geosphere Biosphere Programme (IGBP) and its International Global Atmospheric Chemistry (IGAC) commission. The acid deposition activities of IGAC are managed through the research programme *Deposition of Biogeochemically Important Trace Species* (DEBITS) and its regional subsidiaries, such as the *Composition of Asian Deposition* (CAAP/CAD) in Asia, *IGBP/IGAC/DEBITS in AFRICA* (IDAF) and *Large-scale Biosphere-Atmosphere Experiment in Amazonia* (LBA) in South America.

The formation of bodies for international pollution control cooperation and knowledge transfer through specialised institutions such as the Swedish International Development Cooperation Agency (SIDA) coordinated by the Stockholm Environment Institute (SEI, 2008) and their programmes such as *Regional Air Pollution in Developing Countries* (RAPIDC, 2008) is notable. This has led to the formation of air pollution information and capacity building collaboration dedicated organisations such as *Air Pollution Information*



*Network for Africa* (APINA, 2008) based in southern Africa, but with activities extending to the rest of Africa.

### **1.1.2 South African context**

Industries on the South African Mpumalanga Highveld emit large quantities of NO<sub>x</sub>, SO<sub>2</sub> and other gas species from power generation, petro-chemical and metallurgical processes (Wells *et al.*, 1996; Held *et al.*, 1996, Scorgie *et al.*, 2004a, b, and c). Similarly, petrochemical industries emit these gas species from petrochemical and coal liquefaction processes. Ore smelting and processing and coal mining with cases of spontaneous combustion contribute further to the overall emission quantities emanating from the central industrial and mining region. Some of these emissions such as NO<sub>x</sub> and VOCs are associated also with the subsequent production of ozone (O<sub>3</sub>).

While the transport of atmospheric pollutants from the Highveld has been measured and confirmed (Freiman and Piketh, 2003; Piketh 2000; Galpin and Turner, 1999; Zunckel *et al.*, 1999; Turner *et al.*, 1996; Bluff *et al.*, 1991; Snyman, 1991), implications of these pollutants and regional integration of their impacts have not yet been adequately addressed. The effects of gaseous pollution are exacerbated by the region-specific low dispersion and circulatory climatology returning air pollution to its epicentre, while depositing it also on adjacent areas. The current stage of domestic energy consumption, characterised by expanding electrical energy demands, is likely to lead to increasing emissions of pollutant trace gases. Furthermore, due to cost constraints and the current shortage of electrical power generating capacity, it is not clear that flue-gas desulphurisation will be enforced on this new generation of coal-fired power plants. Besides anthropogenic pollution, natural emissions such as natural fires and lightning contribute significantly to trace gas budgets and effects.

In view of the large industrial emission and substantial natural sources, concerns have been expressed about both short-term and cumulative impacts of trace gases emitted from industrial activities on the receiving environment (Emberson *et al.*, 2003; Tienhoven *et al.*, 2003; Emberson *et al.*, 2001; van Rensburg 1993; Tyson *et al.*, 1988; Engelbrecht 1987). Particular concerns have been expressed on the potential impacts on the natural forests and commercial plantations of the Drakensberg Escarpment and northern Natal by acidic deposition and ozone.



Measurements of trace substances in the atmosphere on the central Highveld are well characterised. Previous studies have investigated intensively areas close to the point sources of the emissions and the Highveld region itself (Turner *et al.*, 1996, Rorich and Galpin, 1998). In situ studies on the escarpment forestry region have failed to find evidence of leaf damage attributable to deposition of acidic gases or particles (Olbrich, 1993, 1990). Other studies have been conducted to detect effects of acidic deposition on soil (Van Tienhoven *et al.*, 2004, 1995; Olbrich, 1994); acidification of catchments (Skoroszewski, 1995); rates of dry and wet deposition (Fourie, 2006, Mphepya, 2002, Zunckel *et al.*, 2000); transport pathways of the trace gases using dispersion modelling (Held *et al.*, 1996) or trajectory modelling (Freiman & Piketh, 2003); and measurement campaigns to detect these trace gases along anticipated pathways (Piketh 2000, Zunckel *et al.*, 1999, Zunckel, 1999, Garstang & Tyson, 1997). Despite these studies, scepticism remained that acid deposition might accumulate on the decadal scale and reach a point where the natural buffering capacities of soils and water bodies would be exceeded (R. Scholes, personal communication).

However, among the questions that remain unanswered are the trace gases concentrations and deposition rates in areas further from the “epicentre” of South African trace gas pollution. Against this background, this study was conceived to make direct measurements of atmospheric concentrations of the acidifying gases, over as an extensive area as possible, to provide an objective basis on which to address the question of *whether or not acidic deposition poses an immediate or long-term threat to ecosystems in the region*. Prior monitoring of the acidic precursor gases has been largely confined to the vicinity of power plants (Held *et al.*, 1996, Annegarn *et al.*, 1996b) and monitoring at locations away from the source of emissions only has been carried out as part of short term field campaigns, (Swap *et al.*, 2003, Piketh, 2000), or at single/isolated locations (Mphepya *et al.*, 2004; Pienaar *et al.*, 2003).

### **1.1.3 Emissions, transportation and deposition of atmospheric pollutants in South Africa**

#### *Generation of trace gas pollution*

South Africa has one of the largest industrialised economies in the southern hemisphere and is the only industrialised regional energy producer on the African continent (Sivertsen *et al.*, 1995; Rorich and Galpin 1998). A large proportion (~75%) of the industrial infrastructure is concentrated on the Highveld plateau (Figure 1.1).

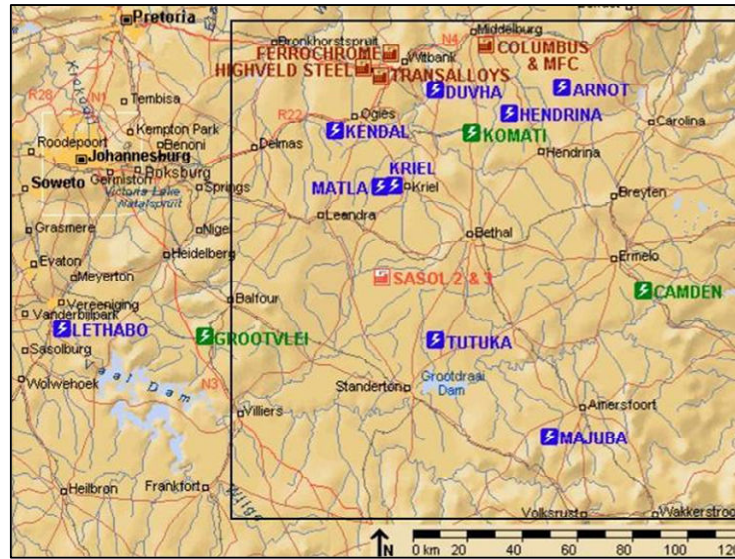


**Figure 1.1:** Extent of the Mpumalanga Highveld (inner box) indicating the location of coal-fired power stations and various large industries (Source: Scorgie *et al.*, 2004a).

The industrial Highveld plateau (~1 700 m asl, ~30 000 km<sup>2</sup>) accounts for approximately 90% of South Africa's scheduled emissions of industrial dust, SO<sub>2</sub> and NO<sub>x</sub> (Table 1.1) (Wells *et al.*, 1996). In addition to primary pollutants, a major secondary pollutant, O<sub>3</sub>, is formed from naturally occurring and anthropogenic chemical precursors, including NO<sub>x</sub> and VOCs that can be emitted from by industry.

**Table 1.1:** Scheduled emissions from South Africa and the industrial Highveld region, metric tonnes per year (1993).

	<b>South Africa</b>	<b>Industrial Highveld Region</b>	<b>% of total</b>
<b>Particulates</b>	331 399	285 405	86
<b>SO<sub>2</sub></b>	2 120 452	1 986 193	94
<b>NO<sub>x</sub></b>	1 004 716	913 486	91

Source: Wells *et al.*, 1996

The role of biomass burning emissions in contributing to the tropospheric trace gases load cannot be underestimated. South Africa (as is the case for the whole of Africa) is prone to large-scale veld and bush fires during dry seasons. In addition, firewood forms the basis of the domestic energy economy for a large number of South African rural populations (Helas and Pienaar, 1996), while a large percentage of urbanised lower income population burn domestic coal fires. All of these sources contribute to the overall load of trace gas pollution in the region (Table 1.2).



**Table 1.2: Comparison of annual emissions from combustion sources for two nitrogen gaseous species in South Africa<sup>^</sup>.**

<i>Activity</i>	<i>NO<sub>x</sub> (Gg)</i>
Industrial coal use	1 359
Domestic coal fires	13,1
Domestic wood fires	49,3
All types of vehicles	519
Veld and bush fires <sup>#</sup>	30,9
*Veld and bush fires <sup>#</sup>	122
⊕Veld and bush fires <sup>#</sup>	38 <sup>⊕</sup>
Sugar cane burning	1,88

? = value not known;

# based on an estimated total of 44.3 Tg dry mass burnt per annum;

\* using averaged emission ratios as reported by [Helas and Pienaar \(1995\)](#);

⊕ for emission ratios measured during SAFARI'92 ([Helas and Pienaar, 1995](#))

<sup>^</sup> Extracted from [Helas and Pienaar, 1996](#).

### *Air pollution transport*

In addition to substantial air pollution generation, it is important to note the role of air pollution transport. The prevailing synoptic conditions include recirculation associated with the stable anti-cyclonic circulation systems that dominate this region. These also govern the accumulation of atmospheric pollutants over the whole sub-continent (Figure 1.2).

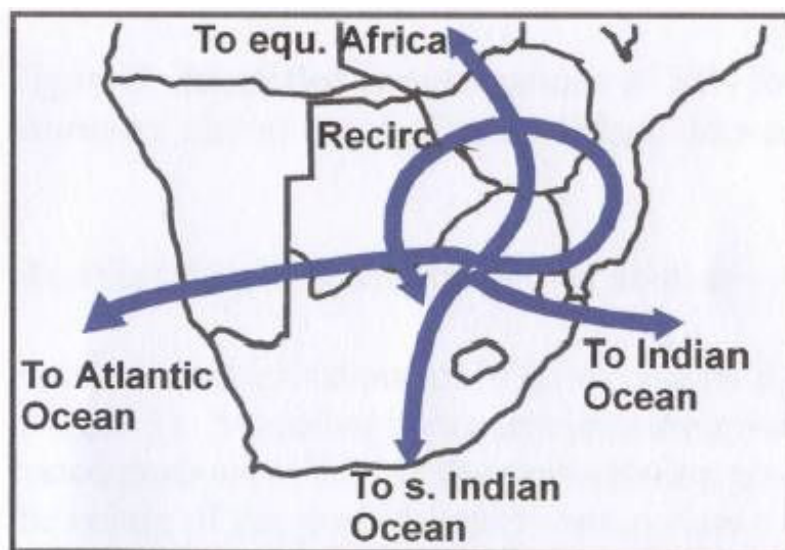


**Figure 1.2: The main air transport pathways out of the Highveld (Source: [Freiman and Piketh, 2003](#)).**

There are two main transport modes of air masses containing aerosols and trace gases out of the industrial Highveld region. The first is direct transport, in which material is advected



directly with little delay in different directions. The second is re-circulated transport, in which material re-circulates towards the point of origin over the subcontinent on a regional or sub-continental scale before exiting the region (Held *et al.*, 1994; Annegarn *et al.*, 1993). There is evidence of large-scale transport and distribution of anthropogenic trace gas pollution over southern Africa and recirculation over the Indian Ocean (Annegarn, 1993). The long-range atmospheric transport and recirculation of anthropogenic trace gases over southern Africa affects the photochemistry and biochemistry (and the radiative balance) of the whole region (Freiman and Piketh, 2003). Inversion layers also restrict vertical mixing of the atmosphere and this influences the concentrations of gaseous pollutants (Annegarn *et al.*, 1996a, 1996b). Given the relatively high emissions of pollutant trace gases from the source region and the inhibiting dispersion climatology, it is important to quantify the deposition of these pollutants on a regional scale in order to address their effects on the environment.

#### *Air quality legal environment*

In year 2004 a new air quality act [National Environmental Management Act: Air Quality Act 39 of 2004, (NEMA: AQA 39, 2004)] was promulgated, repealing the outdated Air Pollution Prevention Act 45 of 1965. This Act signifies a paradigm shift in air quality regulation. A shift from end-of-pipe air pollution control measures to effects-based air quality management using proactive, more flexible, varied and fairer measures that are supported by the new Act. The key aspects of the new legislation are as follows (Annegarn and Scorgie, personal communication 2005):

- A shift to a receiving environment approach
- Decentralisation (which affects responsibilities right down to the levels of provincial and local government)
- Baseline air quality characterisation (identification of pollutants, sources and priority areas)
- All sources to be addressed
- A range of emission reduction measures (command and control, market incentives, voluntary reduction)
- Standardisation (monitoring, quality assurance, quality control, information management, voluntary reductions) and
- Public participation and access to information.

New obligations and responsibilities for authorities, industries and civil society are irreversibly changed with the introduction of this Act. However, numerous activities are



needed to regulate fully air pollution issues (such as declaration of priority areas, licensing of listed activities and establishment of national and provincial standards).

Although the Act came into the force one year after promulgation (beginning of 2005) and the period for full implementation is set over five years, all affected sectors are expected to prepare to fulfil obligations imposed by the Act. There are many challenges for all parties involved when it comes to implementation and compliance to the new law, including capacity building, the formulation of air quality management plans, the establishment of air quality monitoring systems and concrete measures to improve air quality. Notably, the measurement of ambient air quality including the identification and quantification of air quality impacts are integral tasks of new legislative measures.

Even before the AQA (Act 39 of 2004) suggestions had been made to apply an effect-based methodology to assess the air pollution impacts. Comprehensive data and better understanding can influence policymaking; more importantly, they can protect the environment. The critical loads (and levels) approach, developed under the LRTAP Convention in Europe incorporated into a wider system to define air pollution policies (and quality management programmes) should be tested at an extended level. This system is believed to be the most cost effective solution in terms of quantifying and assessing air quality and air pollution affects ([van Tienhoven \*et al.\*, 1995](#)).

#### **1.1.4 Motivation for the study**

Although there is widespread awareness of the potential ecological risks associated with NO<sub>x</sub> and SO<sub>x</sub> emissions, the above discussion has established that there are many remaining uncertainties and unanswered questions. This research aims to address several of these related issues, by determining exceedance of critical levels of SO<sub>2</sub>, NO<sub>2</sub> and O<sub>3</sub> and critical loads for acidic deposition in areas surrounding and downwind of the industrial Highveld. The need is identified for an empirical, spatially comprehensive survey, with high quality measurements of a year or longer, to establish spatial, seasonal and inter-annual patterns of trace gases from anthropogenic sources. Such concentration measurements and deposition estimates will allow assessment of exceedance of concentration levels and deposition loads of pollutants in terms of the sensitivity of local and regional ecosystems.



In addition to the quest to measure concentrations and possible exceedance of damage thresholds, it was appropriate to address another closely related matter, namely validation of air dispersion modelling. Modelling is a widely used tool for air quality estimation and control so this was a very good opportunity to validate the medium-scale regional modelling outputs with the measured concentrations results and inferred dry and wet depositions (Scorgie *et al.*, 2004a, b and c).

Another question closely related to any measurements of NO<sub>x</sub> ambient concentrations is the issue of the NO<sub>x</sub> generation by lightning (Ojelede *et al.*, 2008). The regional scale of the NO<sub>2</sub> measurements is well suited for comparison of lightning NO<sub>2</sub> budgets as a major natural source, especially as its seasonality over the study region is indicative of relative ratio against essentially steady anthropogenic (mainly industrial) budget contribution to overall NO<sub>x</sub> budget in the study region.

Satellite-borne remote sensing constantly shows the study region as one of the world hotspots of SO<sub>2</sub> and particularly of NO<sub>2</sub> pollution (IUP, University of Heidelberg, 2008; IUP University of Bremen, 2008; TEMIS, 2008; PROMOTE, 2008; Accent-Troposat-2, 2008). Thus, an attempt to validate satellite-borne remote sensing observations for the studied region became a desirable and important additional task of this research. The ground-level concentration fields with the spatially enlarged and highly concentrated pollutant units remotely sensed over and above the central industrial area needed to be compared with the measurements over a regional-scale spatial and concurrent temporal domain.

## **1.2 Aim and Objectives**

### **1.2.1 Aim**

The aim of this study is to address a perennial problem, to which there has so far been no satisfactory answer in the Southern African context, namely:

*Will the emissions of acidifying trace gases (sulphur and nitrogen oxides) from coal-fired power plants and industries on the industrial Highveld of Mpumalanga result in exceedance of critical loads for acidic deposition and critical levels of acidic air pollutants SO<sub>2</sub>, NO<sub>2</sub>, that will exceed the carrying capacity of the natural environment?*





While monitoring of trace gas species has been carried out on the Highveld over extended periods by the largest emitters using active trace gas monitoring stations, these stations have largely been concentrated close to the source region – within a 50 km radius of the sources. Background trace gas monitoring sites, using passive diffusive monitors, have been established in South Africa as part of the international **IDAF (IGBP/IGAC/DEBITS' in AFRICA)** network. The IDAF programme is an initiative of **International Geosphere Biosphere Programme/International Global Atmospheric Chemistry/Deposition of Biogeochemically Important Trace Species in Africa** to determine atmospheric depositions (IDAF, 2005). These sites aim to establish natural levels of these gases at truly remote locations, such as Cape Point, Etosha Pan, Louis Trichardt (Makhado). The latter site is a point close to the northernmost border of South Africa and along the inflow path of the main rain-bearing air masses into the interior. One additional monitoring site was included in this network downwind from the Highveld power plant region, at Amersfoort (~60 km south-east of Witbank), to represent concentrations directly downwind of the points of emission.

A programme of monitoring was thus devised and executed to challenge the hypothesis that at current rates of emissions, acid deposition from sulphur and nitrogen species does not pose a threat to the environment. This passive monitoring study was devised to measure exposures at locations distant from the Mpumalanga Highveld industrial region to assess potential longer-term impacts on environments in areas within the dispersion footprint and thereby provide a credible answer to persistent questions on *regional acid deposition*. Thus, the field area for this study was set to be larger than previous studies, extending into Mpumalanga Lowveld, northwards into Limpopo Province, southwards to encompass a large part of Free State and northern Kwa-Zulu Natal provinces and westwards to the Botswana border. (The scope of the study was limited to be within the political borders of South Africa because of logistical and cost constraints). A closely related NO<sub>2</sub> pollution issue is in relation to regional ozone concentrations fields. It was possible to use the planned network for SO<sub>2</sub> and NO<sub>2</sub>, to deploy also monitors for O<sub>3</sub>. Accordingly, a secondary aim could be addressed, namely:

*Do anthropogenic precursors from urban/industrial regions of the Highveld contribute substantially to secondary pollutant, ozone, exceeding defined levels of tolerance?*

To address these aims the following objectives were formulated.



### **1.2.2 Objectives**

The tasks and objectives of this study are:

- Monitoring of concentrations and distribution of SO<sub>2</sub>, NO<sub>2</sub> and O<sub>3</sub> over a two-year period and determining whether critical concentration levels are exceeded
- Estimating dry and wet deposition of SO<sub>2</sub>, NO<sub>2</sub> and comparing of dispersion modelling results within the study region
- Determining critical deposition loads for SO<sub>2</sub> and NO<sub>2</sub> and assessing deposition loads exceedance of regional soils buffering capacities
- Comparison and analysis of ground-level measured NO<sub>x</sub> versus lightning-generated NO<sub>x</sub> in the overall regional NO<sub>x</sub> budget
- Comparison of regional SO<sub>2</sub>, NO<sub>2</sub> and O<sub>3</sub> remote sensing information with ground level concentrations from the passive sampling network.

### **1.3 Structure of Thesis**

The body of the thesis has been constructed as a series of autonomous but interrelated sub-studies, each chapter addressing one or two of the main objectives. Each of these chapters follows the general structure of an academic report. After an introductory section, follows a chapter-relevant literature review, methods, results, discussion and conclusion. The final chapter draws together the findings of the sub-studies and places them in the context of the overarching question relating to concentration critical levels and acidic deposition loads in South Africa. The remainder of this section will give an outline of how the individual chapters address the themes of the thesis.

#### *Chapter Two*

This chapter deals with the group of the objectives, entitled “*Concentrations, distributions and critical levels assessment of regional SO<sub>2</sub>, NO<sub>2</sub> and O<sub>3</sub>*”. The concentrations and spatial distributions for three gaseous species, SO<sub>2</sub>, NO<sub>2</sub> and O<sub>3</sub> were measured. Concentrations at upwind, downwind and remote sites are tested against the vegetation critical levels for SO<sub>2</sub>, NO<sub>2</sub> and O<sub>3</sub> and the results are presented.

#### *Chapter Three*

This chapter deals with two study objectives grouped as: “*Dry and wet deposition determination of SO<sub>2</sub> and NO<sub>2</sub> and comparison of meso-scale air pollution dispersion modelling of SO<sub>2</sub>, NO<sub>2</sub> and O<sub>3</sub> using regional-scale monitoring results*”. Dry deposition rates are computed for SO<sub>2</sub> and NO<sub>2</sub> as annual averages. Estimates of wet deposition rates,



based on historical rain chemistry data, are computed. This enables a combined estimate of total dry and wet acidic deposition to be calculated as a basis for the assessment of the total acidic load. Templates are created and all computations performed for both years of sampling and presented as inter-annual comparisons. The concentrations, dry and wet acidic depositions are then compared with two model outputs that deal with the regional-scale air pollution dispersion results, including dry and wet deposition for acidic species.

#### *Chapter Four*

This chapter deals with the group of the objectives entitled: “*Regional Scale Critical Loads Assessment of Acidic Deposition from SO<sub>2</sub>, NO<sub>2</sub> Emissions from the Highveld*”. The measured concentrations of acidic species enable computation of deposition loads for the entire study area. These loads are then assessed against ability of the local soils to buffer acidification and so determine estimated critical loads exceedances over the study area.

#### *Chapter Five*

This chapter deals with a single objective entitled: “*Comparison of Remote Sensing Tropospheric Trace Gas Measurements with Regional-scale SO<sub>2</sub>, NO<sub>2</sub> and O<sub>3</sub> Ground-level Measurement*”. Remote sensing (satellite-borne) concentration measurements for the study region and for a concurrent period of the tropospheric trace gas species are checked for their suitability to support results obtained by the ground-level measurements and vice-versa. For this study, a set of remote sensing data was obtained from different remote sensing institutions that retrieve and utilise RS (satellite-borne) data. These data are then further processed to enable comparability with the ground-level measurements.

#### *Chapter Six*

This chapter deals with a single objective entitled: “*Comparison of Measured Ground-level NO<sub>x</sub> and Lightning-generated NO<sub>x</sub> (LNO<sub>x</sub>) Estimates in the Regional NO<sub>x</sub> Budget*”. This section compares the different lightning NO<sub>2</sub> budgets, based on prior measurements of lightning strokes, with three relevant emission inventories and analysed the differences between them. This chapter adjusts and updates previous lightning counts to estimate contributions of lightning NO<sub>2</sub> relative to the anthropogenic NO<sub>x</sub> budget extracted from existing emission inventories.

#### *Chapter Seven*

The concluding chapter gathers the findings from Chapters Two to Six, integrating the entire study of related sub-studies that are connected through a common thread of the



general topic of primary acidifying pollution, their secondary compounds and dealing with the central environmental question of impacts of trace gas species on regional ecosystems. In addition, original contributions of this thesis are emphasised. Recommendations for the future research are discussed, arising from identified shortcomings or information gaps identified in the course of this work. This chapter thus serves to integrate the overall argument of the thesis in the classical mode, with a central message summarising conclusions and findings on the status of atmospheric acid deposition threat in South Africa.





## CHAPTER TWO

*The study described in this chapter constitutes the foundation for the subsequent studies. Here the design for experimental data collection is introduced and methods of data analysis explained. This chapter addresses two of the objectives, namely empirical determination of trace gas concentration distributions and assessment of any exceedance of relevant air quality and ecological limits.*

### **2. Concentrations, Distributions and Critical Levels Assessment of Regional SO<sub>2</sub>, NO<sub>2</sub> and O<sub>3</sub>**

#### **2.1 Introduction**

The purpose of this chapter was to fulfil the first and basic goal of the entire study, namely to determine the concentrations of SO<sub>2</sub>, NO<sub>2</sub> and O<sub>3</sub>, their spatial distributions and assess possible exceedance of damage thresholds. The question is posed in this context, whether the industrial emissions are influencing the concentrations away from their sources and what is level of those and their spatial distribution if taken into account the specific regional synoptic and general air mass movement over the subcontinent.

The scope of this study was relatively simple in its design although extensive in its spatial and temporal extent. It involved setting up a network of monitoring sites over the entire north-east sector of South Africa and collating concentration data samplers for over two annual cycles. This was necessary as to obtain a two annual cycle averages in addition to annual and seasonal data around and away from the industrial source emission centre.

The procedure was designed with the intension to capture effectively the region in which the influence of the industrial pollution could be measured, avoiding the local influences. The data was subsequently numerically assessed and graphically presented for its absolute and relative relationship between sites in terms of maxima, minima, means and standard deviations. Related to the spatial distribution of the concentrations were analyses performed to determine direction and magnitude of the industrial emissions influence within the entire study domain. The final procedural step of this study was to assess exceedance of the international and local air pollution standards for vegetation.



## 2.2 Derivations of Critical Levels as Assessment of Atmospheric Pollution

The atmosphere is an effective medium for the delivery of acidic materials and their precursors to terrestrial ecosystems. Atmospheric constituents follow a series of processes from the time of their release into the atmosphere until their eventual removal from it. The main processes that comprise the atmospheric pathway are emissions, transformation, transport and deposition (WMO, 1996). These determine the resident times, distribution and ambient concentrations of atmospheric pollutants. To understand the origin of the chemical species and their ultimate fate one needs a comprehensive knowledge of the emissions atmospheric transport, chemical transformation and removal processes of local, regional and global scale. Emissions have been directly measured at point sources as well in ambient environment. In addition, large-scale regional and national emissions have been estimated by empirical and inferential techniques. However, up-to-date information on emission rates, their ambient concentrations and geographical distributions is essential if we are to understand better movements and effects of acidifying species. Atmospheric concentrations must be correctly quantified in order to estimate accurate deposition values. Although not always easily measured, atmospheric concentrations of pollutants to which sensitive ecosystems are exposed can and are often measured.

Thus if one's goal is to assess impact to a specific area, one should locate concentration monitoring devices at specific locations spread within an area. Measurements of concentrations of pollutants can then be used to validate modelling studies, determine critical levels exceedance and to determine the dry deposition component of total deposition.

### 2.2.1 *Critical levels*

The term “**critical levels**” is often used in relation to gaseous pollutants. The concept of critical levels is part of an effect-based approach that has been used for defining emission reductions aimed at protecting ecosystems and other receptors. In the UNECE region critical levels have been defined as: “[t]he concentrations of pollutants in the atmosphere above which direct adverse effects on receptors, such as plants, ecosystems or materials, may occur, according to present knowledge” (UNECE, 1988).

During the 1970s it was recognised that transboundary air pollution has ecological and economic consequences as a result of air pollutants that cause acidification. In response, the countries of the United Nations Economic Commission for Europe (UNECE)



developed a legal, organisational and scientific framework to deal with air pollution problems associated with acidification.

The UNECE Convention (LRTAP) was the first international legally binding instrument to deal with problems of air pollution on a broad regional basis. Critical levels/loads provided a fixed reference point against which pollution levels could be compared. They were used for calculating emission ceilings with respect to acceptable air pollution levels in UNECE countries ([Manual on Methodologies and Criteria for Mapping Critical Loads/Levels, 2004](#)).

As well as critical levels there is also the concept of critical load. The CLRTAP established a Working Group on Effects (WGE), which is supported by a number of International Cooperative Programmes (ICP). A work programme under the Nordic Council of Ministers ([Nilsson, 1986](#)) agreed upon scientific definitions of critical loads for sulphur and nitrogen only. This provided a base for further Convention work. The following two workshops evaluated critical loads and introduced the concept of critical levels. The Bad Harzburg workshop in Germany dealt with critical levels for the direct effects of air pollutants on forests, crops, materials and natural vegetation [[Report on the Initial ECE Mapping Workshop \(1989\) in Manual on Methodologies and Criteria for Mapping Critical Loads/Levels \(2004\)](#)]. It discussed the possible use of critical levels/loads maps for determining areas at risk of air pollution acidification for the first time. This concept can be applied in South Africa and this thesis presents such an assessment.

### ***2.2.2 Critical levels for vegetation***

Excessive exposure to atmospheric pollutants has harmful effects on several different types of vegetation. Critical levels for vegetation are described in different ways for different pollutants. They can be expressed as mean concentrations, cumulative exposures, or fluxes through plant stomata. The effects considered significant can vary between receptor and pollutant and include growth changes, yield losses, visible injury and reduced seed production. The pollutant receptors are generally divided into five categories: agricultural crops, horticultural crops, semi-natural vegetation, natural vegetation and forest trees [[Manual on Methodologies and Criteria for Mapping Critical Loads/Levels \(2004\)](#)].

The same source [[Manual on Methodologies and Criteria for Mapping Critical Loads/Levels \(2004\)](#)] states that the critical levels for vegetation are defined as the “**concentration**, cumulative exposure or cumulative stomatal flux of atmospheric



pollutants above which direct adverse effects on sensitive vegetation may occur according to present knowledge”. Critical level exceedance can thus show the difference between the critical level and the monitored or modelled air pollutant **concentration**, cumulative exposure or cumulative flux.

In this study critical levels were assessed based on measured monthly mean **pollutant concentration** only. Important to emphasise here is that the monthly means do not allow for the calculation of the accumulated hours above the 40 ppb threshold – which is the basis for O<sub>3</sub> AOT40 approach. For this study a simplified approach was adopted of using values, 30 ppb and 40 ppb, as threshold limit values with which to compare the monthly mean O<sub>3</sub> values.

### **2.2.3 Impacts of air pollution on vegetation in South Africa**

Very few studies have been undertaken in South Africa on the impacts of gaseous pollutant species on non-commercial vegetation species (Emberson *et al.*, 2001, Emberson *et al.*, 2003, Tienhoven *et al.*, 2003). More such studies need to be performed in order to determine critical levels with confidence (G.H.J. Kruger and M. Scholes, *personal communication*, 2007).

No confident pollutant gaseous concentration level values could be used for vegetation in South Africa to compare the levels measured in this thesis. However, South African ambient air quality standards still have a role in this type of assessment when it comes to human and animal health.

However, it is debatable whether using critical limits established to suit northern hemisphere species for vegetation in South Africa is advisable because of the different environmental factors involved. The responses of plants to air pollution in hotter and drier climates are influenced by water availability and temperature stress. For example, stomata close in response to severe water stress to reduce the loss of water by transpiration. In this way, the intake of air pollutants is reduced and therefore damage to plants is decreased (Schenone, 1993; Levitt 1980). Therefore critical limits accepted under different conditions elsewhere should be tested in South Africa.

A review of locally established impact levels evaluated their suitability as critical levels for comparison with measured concentrations. For this reason a review of most documents pertinent to the past and on-going research on the impact of air pollution on South African





vegetation was undertaken. The past research explored the effects of air pollution on natural vegetation (grassland, Fynbos, Acacia), commercial forests (Eucalyptus, pines species) and agricultural crops (maize, sunflowers, dry beans, potatoes, tomato and tobacco).

The results from past studies were inconclusive ([van Tienhoven and Scholes, 2003](#), [Emberson \*et al.\*, 2003](#)). There were many different reasons for this, including the use of mean exposure values while not recording high spikes; insufficient replicates; the non-inclusion of parallel/synergistic measurements; the failure to address other factors such as fungal pathogens, viruses and insects; and different ranges of exposure levels and exposure times for experimental studies. The results of a recent bio-monitoring study at the North-West University, Potchefstroom, were not published at the time of compilation of this thesis.

#### *Field evidence*

The symptoms and responses of vegetation to air pollution impacts in different floral regions of South Africa and among different plant species were investigated through field evidence.

#### *Indigenous vegetation*

With respect to indigenous vegetation, Breytenbach (as cited in [van Rensburg, 1993](#)) compared the floristic composition of grassland sites on the industrial Highveld to those of the same sites sampled 50 years earlier. The vegetation changes were determined to be greatest close to the pollution source. On a broad scale, a gradient was found in which site vegetation deterioration corresponded to distance downwind of the pollution source. However, the limited number of sample sites and variation in conditions and practices were thought to have a greater influence than air pollution impacts ([van Tienhoven and Scholes, 2003](#)).

#### *Commercial forestry species*

Several studies were focused on commercial forestry species such as pines and Eucalyptus. The existing literature on the responses of forestry species to atmospheric pollution was reviewed by [Tyson \*et al.\* \(1988\)](#). The species of Eucalyptus were found to be sensitive to SO<sub>2</sub> (40 to 100 ppb). Foliar symptoms in *Pinus patula* (a pine species) which corresponded to a gradient of pollution concentration impacts were surveyed in five forestry regions in Mpumalanga and Kwa-Zulu Natal provinces. It was found that ‘*broad bending*’ appeared



to be correlated with pollution. Further monitoring of this symptom failed to reveal any obvious causes (Olbrich, 1993); although a number of potential factors were not addressed at the time. A study to determine the risk posed by ambient ozone to the commercial forests of Mpumalanga Province was conducted by Carlson (1994). Records of concentrations were analysed to determine the frequency with which potentially phytotoxic events occurred. At the Palmer monitoring station, the cumulative dose over 40 ppb (AOT 40) exceeded 10 000 ppb h for every year of the study. O<sub>3</sub> concentrations were found to be relatively high with frequent potentially phytotoxic events.

#### *Commercial agricultural crops*

There are a number of commercial agricultural crops grown in South Africa, many of which are known to be sensitive to air pollution. Maize is relatively tolerant to SO<sub>2</sub> and NO<sub>x</sub>, but is sensitive to O<sub>3</sub>; sunflower is relatively sensitive to SO<sub>2</sub> and NO<sub>x</sub>, but is tolerant of O<sub>3</sub>, whereas dry beans are sensitive to all three pollutants (Tyson *et al.*, 1988). Also the different cultivars of same species can show different sensitivities. It has been suggested that crops are also at risk from O<sub>3</sub>, but over a greater area than they are sensitive to SO<sub>2</sub> (Marshall *et al.*, 1998) In addition, potato, tomato and tobacco might be sensitive to high O<sub>3</sub> levels. It is important to note that plants generally respond to episodes of high concentrations of pollutant gas even if they are infrequent (van Rensburg, 1992) so annual means will not indicate the complete risk of potential impact.

#### *Experimental studies*

Several experimental studies on the effects of air pollution on vegetation have been carried out locally. One of earliest such studies in South Africa attempted to determine the responses of three **commercially important forest species** of pine and *Eucalyptus* to pollutants, although results were inconclusive. Impact studies of **South African crops** as bio-indicators of SO<sub>2</sub> and O<sub>3</sub> air pollution have also been undertaken. The bean cultivar was tested as an indicator for SO<sub>2</sub> and O<sub>3</sub> pollution (Botha *et al.*, 1990.) and again, results were inconclusive. A variety of tobacco (Bel-W-3) was used for a ground-level O<sub>3</sub> impact study (Blair, 1998) and leaf injury was observed at O<sub>3</sub> concentrations below the 40 ppb threshold. In an earlier study (Engelbrecht, 1987), bean varieties (*Phaseolus*) were exposed to different SO<sub>2</sub> ranges (50 – 100 ppb) and exposure times (30 – 120 minutes). The responses were inconclusive (van Tienhoven and Scholes, 2003).

A recent bio-monitoring study under the auspices of the Air Pollution Information Network for Africa (APINA/RAPIDC) during the period from January to April 2006 “for



monitoring the impact of tropospheric ozone on white clover” has been undertaken by the School of Environmental Sciences, North-West University (Potchefstroom). One growing season’s data have been analysed and indicated that the ozone-sensitive clone was affected by the ambient ozone concentration at the site. However, experimental weaknesses and the small sample size meant that the results could not be taken as a confident measure of ozone impact and further study is required (Hicks, personal communication, 2008).

## 2.3 Method

### 2.3.1 Study design

The air pollutant concentration network for this research was designed for the measurement of trace gas species SO<sub>2</sub> and NO<sub>2</sub>, originating from coal fired power plants on the industrial Highveld, at sites within the dispersion modelling footprint (van der Merwe, 1998) (but constrained to lie within the political boundary of South Africa). Geographically, the industrial Highveld is centred on the Mpumalanga Highveld. Areas upwind and downwind of the source zone also required monitoring. Geometrically, the area of concern can be presented as a square centred on Witbank, Mpumalanga and a gridded network was chosen to cover the monitoring sites. This study was unique because it required an empirical survey of a large (~600 x 600 km) array to generate a regional scale dispersion field of key pollutants (Figure 2.1). Therefore, the task posed several challenges in its design, specifically its estimated spatial and planned temporal domain. Besides seasonal trends and patterns the study needed to obtain the annual means and two annual cycle averages. These challenges required a suitable yet manageable solution in its design, operational handling and anticipated outputs.

Thus, the size of the study area coupled with the requirement for a simple power and maintenance-free precise and reliable monitoring system influenced the choice of passive sampling as the methodology for concentration measurements. There are many advantages of passive diffusive sampling in the field, such as the fact that there is no need for calibration or power supply, they have good detection limits and the samplers are small, light, re-usable, cost-effective and soundless.

It was necessary to avoid effects on the study sites from significant local air pollution sources. Thus care was taken to position the sites away from urban centres, industrial areas and local point sources and the sites chosen were mostly in rural farmland, forestry and natural reserves, sparsely inhabited and often non-electrified.



However, a reference site was chosen at the approximate centre of the industrial Highveld. This site was at the Eskom Air Quality Station, Elandsfontein (site 17), which is within visual sight line of several of the Mpumalanga-located coal-fired power stations. In the same region are located major ore smelters, several surface coal mines, a major coal liquefaction and petro-chemical complex. This central source site served for use in all comparisons of the sites, both in proximity and downwind the central source region as well as background and upwind located sites.

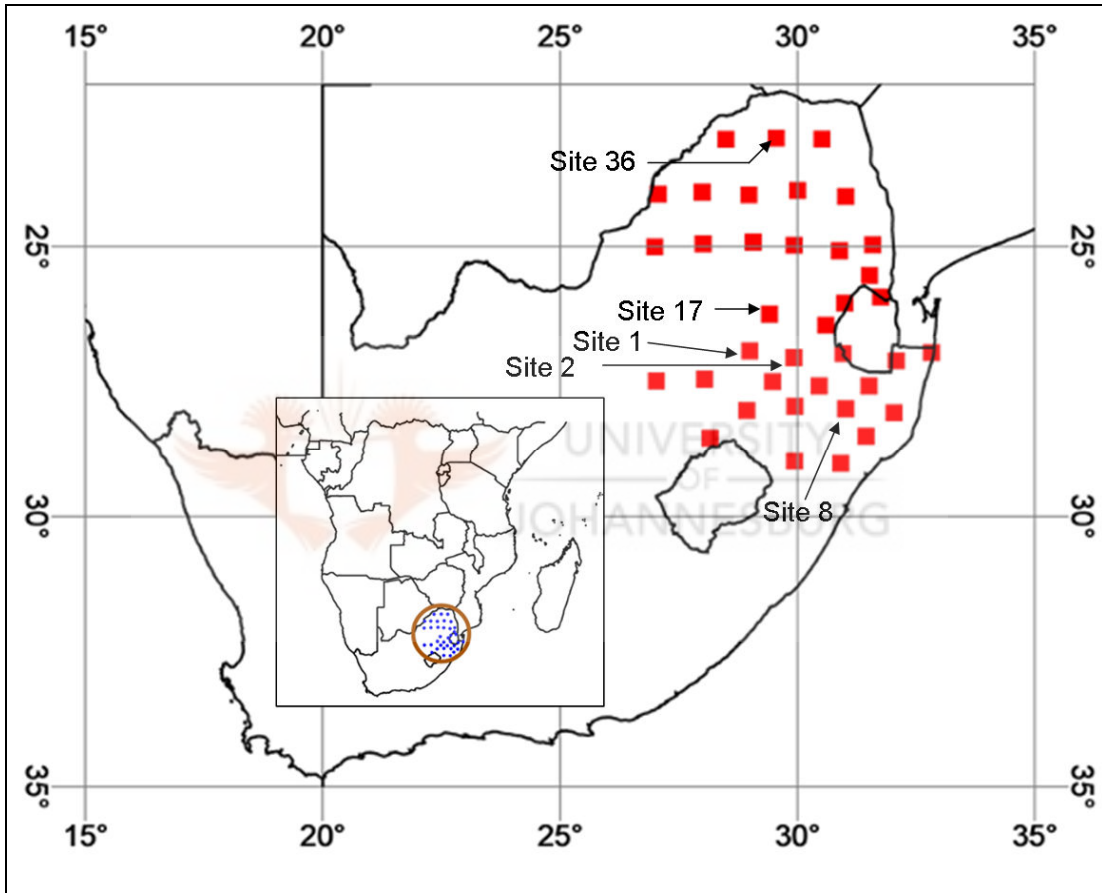


**Figure 2.1:** Extent of the study area within South and sub-Saharan Africa (map insert) with several pivotal sites marked.

While passive monitors have been used in South Africa in previous studies, these have either been used in truly remote areas with only a small number of samplers (typically at four to six sites), or in intense urban surveys (Zunckel *et al.*, 2006, Kuylenstierna and Hicks, 2002).



### 2.3.2 *Passive sampling*

This study uses the passive sampling technology applied for the IDAF network. The IDAF programme is an initiative of IGBP/IGAC/DEBITS in Africa to determine atmospheric depositions. For the IDAF project, a set of passive samplers was developed at the “Laboratoire d’Aérodologie” in Toulouse, France. These samplers have been developed according to the DEBITS procedures based on the work of Ferm (1991, 1994). Passive samplers have been tested and validated since the beginning of 1998 in the IDAF network at six African stations (Al Ourabi and Lacaux, 1999; Lacaux, 1999). This technique has also been tested in different tropical and subtropical regions (Ferm and Rodhe, 1997). Such measurements are based on the property of molecular diffusion of gases and species-specific collection on an impregnated filter specific to each pollutant measured (Table 2.1).

**Table 2.1: Chemical reactions used in passive sampling for NO<sub>2</sub>, SO<sub>2</sub> and O<sub>3</sub> \***

<i>Sampler</i>	<i>Gas</i>	<i>Chemical reaction on the filter</i>
<i>Grey Sampler</i>	NO <sub>2</sub>	$2 \text{NO}_2(\text{g}) + 3 \text{I}^- > 2 \text{NO}_2^- + \text{I}_3^-$
<i>Black sampler</i>	SO <sub>2</sub>	$2 \text{SO}_2(\text{g}) + 4 \text{OH}^- + \text{O}_2 > 2 \text{SO}_4^{2-} + 2 \text{H}_2\text{O}$
<i>Grey and Black sampler</i>	O <sub>3</sub>	$\text{O}_3(\text{g}) + \text{NO}_2^- > \text{NO}_3^- + \text{O}_2$

\* Source: Dhammapala, 1996.

All the samplers are exposed in pairs to ensure reproducibility results and to reduce data loss if a sampler suffers interference. At the monitoring sites, samplers are installed mesh-side down in the underside of a metal rain shelter, which is screwed or welded to the top of a metal pole and left in position for one month (Figure 2.2).



**Figure 2.2:** A passive sampling monitor in position (Sampling site no. 17, Elandsfontein).

In the IDAF network three kinds of samplers are used, which differ only by their colour (which is important for the exposed samplers processing) and their coating solutions. The design of the IDAF passive sampler is presented below (Figure 2.3).

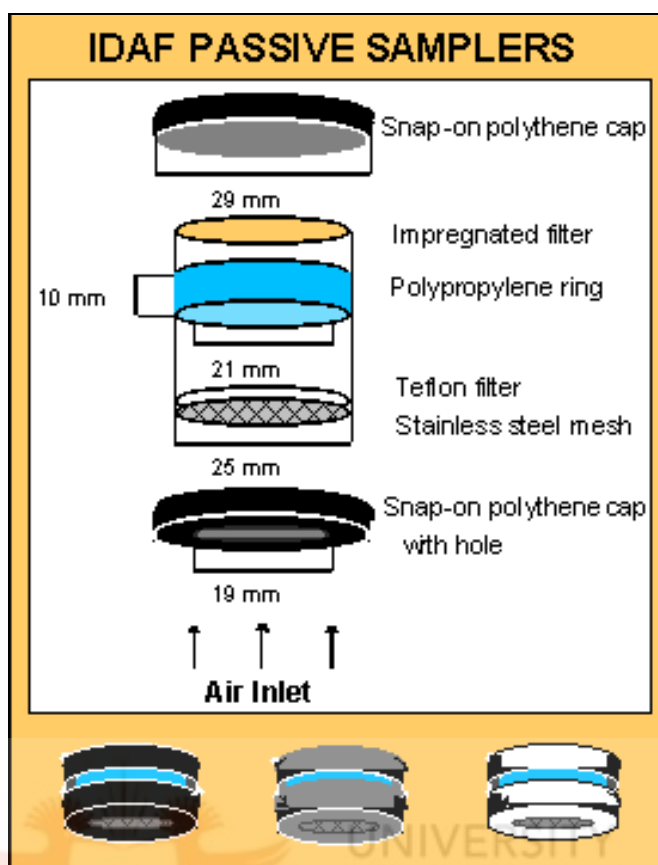


**Figure 2.3:** IDAF passive sampler design (Source: IDAF, 2005).

The different parts are assembled under a laminar flow clean hood. In both cases, 50 µl of coating solution are added by pipette to a paper filter, which is dried and placed into a sampler body (Table 2.2).

**Table 2.2:** Formulations of the coating solutions for trace gas passive samplers #.

<i>Colour of the sampler</i>	<i>Sampled species</i>	<i>Coating solution</i>
<b>Black</b>	<b>SO<sub>2</sub></b>	0.5 g NaOH in 50 ml methanol (pH>12)
<b>Grey</b>	<b>NO<sub>2</sub></b>	0.44 g KOH + 3.95 g NaI in 50 ml methanol (pH>12)
<b>Grey + black</b>	<b>O<sub>3</sub></b>	0.25g NaNO <sub>2</sub> + 0.25g K <sub>2</sub> CO <sub>3</sub> + 0.5 ml redistilled glycerol in 50 ml water

# Source: IDAF, 2005.

The Laboratory of the Atmospheric Chemistry Research Group, School for Chemistry and Biochemistry, North-West University (NWU) (Potchefstroom Campus) prepared and analysed the passive samplers for this research. The passive sampler was supplied ready for use in a sealed container loaded with a filter treated for a nominated pollutant gas. It



was sent to the station with a technical sheet requiring the input of dates of insertion/removal, temperatures, rainfall and local fires during exposition. Upon receipt of an exposed sampler, the impregnated filter was removed and analysed for pollutant concentration in the laboratory using ion chromatography (in the case of SO<sub>2</sub> and O<sub>3</sub>) and spectrophotometry (for NO<sub>x</sub>). The sampler was reloaded with a fresh impregnated filter, re-sealed ready for re-use and returned by mail to the user. The reproducibility and the detection limits for each of the observed species (IDAF, 2005) is given in Table 2.3.

**Table 2.3: Detection limits for the various species for sampling and analysis.**

<b>Gas</b>	<b>Reproducibility (%) *</b>	<b>Detection Limit (ppbv) *</b>
<b>NO<sub>2</sub></b>	3.7%	0.3
<b>SO<sub>2</sub></b>	17.4%	0.1
<b>O<sub>3</sub></b>	7.9%	0.1

\* Source: IDAF, 2005.

In the work of Dhammapala (1996) the results of an experiment where the performance of diffusive samplers of Atmospheric Chemistry Research Group (the same laboratory for this study) was compared against that of calibrated active (continuous) samplers were presented. This comparison demonstrated that the results obtained by diffusive samplers are comparable to those of active samplers over longer sampling periods. In Ayers *et al.* (1998), precision of the samplers, expressed as mean percentage difference between duplicates, was in the range 5–10% for NO<sub>2</sub> and 25–10% for SO<sub>2</sub>. Also, in Cruz *et al.* (2004), it is stated that method precision as relative standard deviation for three simultaneously applied SO<sub>2</sub> passive samplers was within 10% and when compared to active monitoring methods under real conditions, used in urban and industrial areas, showed an overall accuracy of 15%.

Recently an international inter-laboratory comparison of passive samplers was undertaken under the auspices of SEI-RAPIDC and as a part of “Male Declaration” (*on Control and Prevention of Air Pollution and its Likely Transboundary Effect for South Asia*) activities, mainly undertaken at the University of Singapore. It is supportive of the concentration data used in this study. The report states that acceptable intra-lab and inter-lab **Relative Standard Deviations (RSD %)** value were obtained for NO<sub>2</sub> and SO<sub>2</sub> in NWU samplers”. Compared to active sampling are accurate to approximately 20% of each other (He and Bala, personal communication, 2008).





### ***2.3.3 The passive sampling monitoring network***

The positioning of air quality monitoring sites is typically done so that the gathered data provide information to address specific air quality related questions. This is to determine either background air quality, to monitor air quality in a specific area, or to estimate the influence of a particular source or activity on air quality. Air quality monitoring stations are therefore positioned according to the specific monitoring purpose.

As introduced earlier, the rationale for air quality monitoring in this study concerns industrial air pollution emanating from the industrial Highveld and the resultant concentrations in the ambient environment within and downwind from this epicentre of South African air pollution. Therefore, the air pollutant monitoring network for this research was designed for measuring background pollution, away from the main pollution centre on the industrial Highveld. However, a control site positioned in the heart of the industrial Highveld was necessary in order to determine differences measured at this site with sites in vicinity as well as in remote areas down and upwind from the central pollution source area. For this a suitable location (existing continuous monitoring station enclosure of Eskom) was chosen.

Geographically the industrial Highveld is centred on the Mpumalanga Highveld. Areas upwind and downwind of the source also required monitoring. These include most of Limpopo Province to the north, Kwa-Zulu Natal Province in the south and east, the eastern Free State Province in the south and a part of the north-eastern Northwest Province in the north-west (Figure 2.4).

Geometrically, the area of concern could be presented as a square and a gridded network was chosen to cover the monitoring sites. The meridians and parallels crossing within the study square were chosen to determine the geo-position of most of the monitoring sites. The distance between each site within the grid was half or one degree. It was necessary to avoid effects on the study measurements by major local air pollution sources and thus care was taken to position the sites out of urban centres, industrial areas and close local point sources. Leeway for setting sites in the field was maximised at 10' longitude latitude away from the nominal geo-position.

This study for the first time has explored the effects of pollutant trace gases on a large regional scale measured over an extended period. By implementing a two-year long programme of passive monitoring at 37 sites, distributed on a one-degree grid from the



Highveld to the Indian Ocean coast, Mozambique, Zimbabwe and Botswana borders, the study obtained a unique data set for the region. Although the running of the monitoring sites was simple and results reliable compared to more laborious and expensive active monitoring stations, there were several constraints that are inherent to the design of the network.

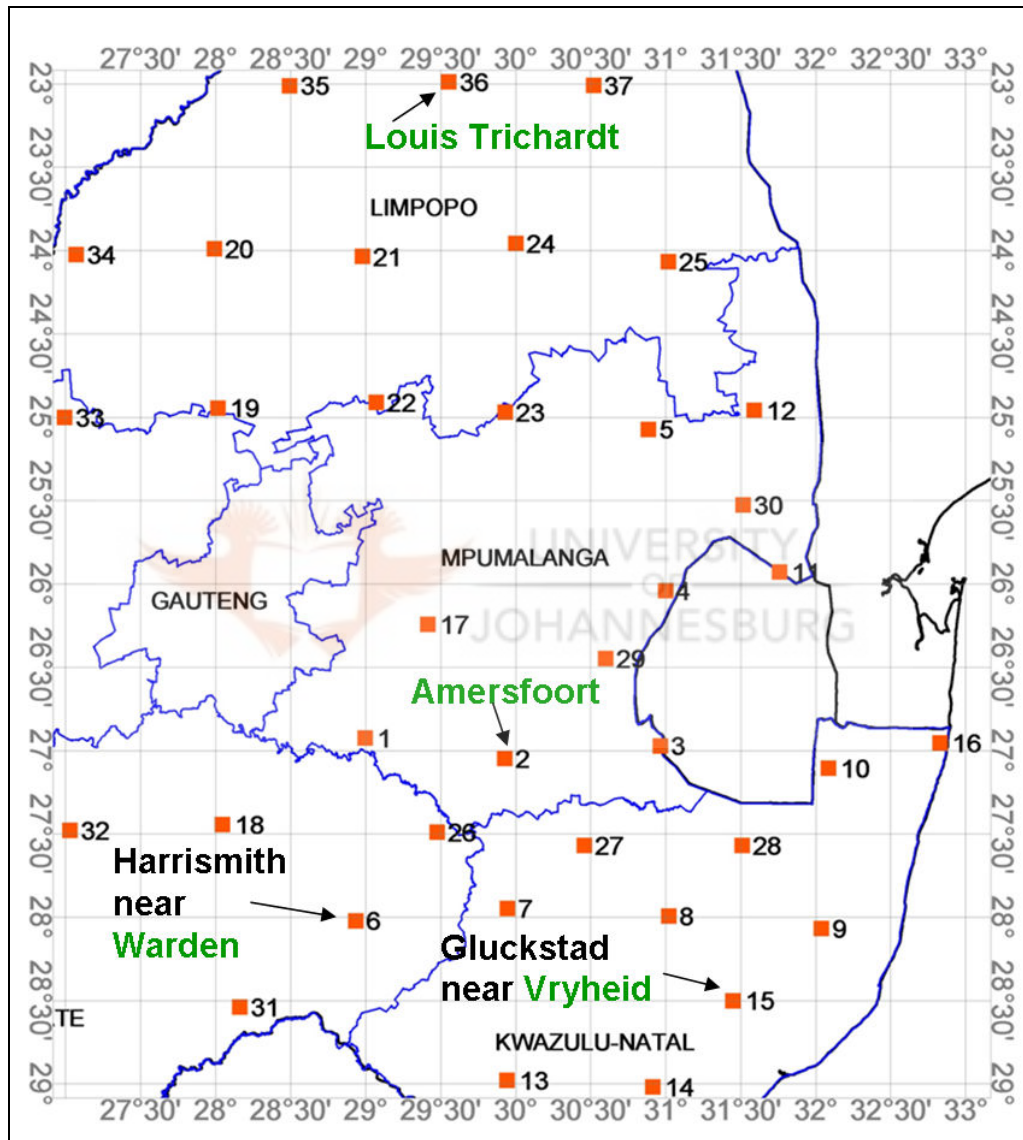


Figure 2.4: The passive diffusive sampling network distribution ■ [with locations of wet chemistry deposition sites ◆ (green lettering) in relation to this study sites (black and green lettering)].

Operation of the monitoring stations involved a partnership with field volunteers and was dependant on the performance of volunteers and the every-day running arrangement of the network operation. The supply of unexposed samplers as well as return of the exposed



ones was done through the South African post and a commercial courier network and this increased costs, while the security of the sampler delivery was not guaranteed.

Another limitation involved the cross-border extension of monitoring. Air pollution crosses national borders, thus it made sense to include parts of southern Zimbabwe, south-east Botswana and southern Mozambique in the study. However, financial and logistical constraints prevented the extension of the measurement network out of the South African borders.

This initial monitoring of SO<sub>2</sub> was extended for NO<sub>x</sub> and O<sub>3</sub> for a period of a two annual cycles. The results of two concurrent years of monitoring for each monitored species (September 2005 to August 2007) have been used in this thesis.

#### **2.3.4 Different ambient air quality standards and guidelines applied as critical levels**

In this study several sets of pre-determined levels were compared to measured ambient pollutant concentrations. Critical levels have been defined as “... **the concentrations of pollutants in the atmosphere above which direct adverse effects on receptors, such as plants, ecosystems or materials, may occur, according to present knowledge**” (UNECE, 1988). The critical levels assessment involves comparison of measured concentrations with a selected set of relevant atmospheric standards, guideline values and thresholds. The critical levels selected are:

- Pre-2004 South African guidelines/standards, set out in Schedule 2 of the NEMA Air Quality Act (NEMA AQA, 2004);
- The current Standards South African air quality standards (SANS 1929, 2004);
- United Nations Economic Commission for Europe (UNECE) Convention on Long Range Trans-boundary Air Pollution Limits (UNECE CLRTAP, 2004);
- World Health Organisation (WHO) guidelines (UN WHO, 2005); and
- Ozone monthly concentration thresholds: cut-off concentrations for the *Accumulated over Threshold* (AOT) levels applied in UNECE CLRTAP and adopted in the UN WHO: *Air Quality Guidelines for Europe* (2000).

As the monitoring intervals are monthly, only critical levels for averaging periods monthly or longer have been extracted from the above standards documents (Table 2.4). Exceedance of a critical level occurs when the measured mean concentration is greater than the critical level concentration.



The first two sets of standards (NEMA and SANS) are concerned with human (and animal) health protection, while the third is concerned with limits for vegetation. Past research on the effects of air pollution on vegetation in South Africa was assessed to trace limits specific to South Africa. The reviewed literature did not contain a conclusive impact value for use as a confident critical level. In addition, vegetation-specific guidelines or standards for South African vegetation have not yet been legislated. Thus, the widely used the concentration thresholds of 40 ppb and 30 ppb were used in this study. Although there is an on-going research on the impact of ozone on vegetation in South Africa, no results have been published at the time of finishing this thesis.

**Table 2.4: Atmospheric critical levels for trace gas species SO<sub>2</sub>, NO<sub>2</sub> and O<sub>3</sub>.**

<b>Sources</b>	<b>Averaging period</b>	<b>Applicability</b>	<b>Units</b>	<b>SO<sub>2</sub></b>	<b>NO<sub>2</sub></b>	<b>O<sub>3</sub></b>
<b>SA NEMA: AQA 39, 2004 and SANS: 1929, 2004)</b>	Annual mean	Human (and animal) health	ppm	0.019	0.05	n/a
			µg m <sup>-3</sup>	50 (50)**	95.5* (40)**	n/a
<b>UN - WHO 2000/2005 AQ Guidelines</b>	Annual mean	Human (and animal health)	ppb	n/a	n/a	n/a
			µg m <sup>-3</sup>	50 <sup>^</sup> (10-30) <sup>^^</sup>	40 (40)**	n/a
<b>UNECE - CLRTAP (for SO<sub>2</sub> and NO<sub>2</sub>)</b>	Annual mean and half-year (winter) mean for (semi)-natural and agricultural vegetation	Agricultural crops	µg m <sup>-3</sup>	30		n/a
		(Semi-) natural vegetation	µg m <sup>-3</sup>	20	30	n/a
		Forest ecosystems	µg m <sup>-3</sup>	20		n/a
		Lichen	µg m <sup>-3</sup>	10		n/a
<b>Ozone monthly thresholds (cut-off concentration for the AOT 30 and 40 critical levels)</b>	Annual and growing season	Vegetation	ppb	n/a	n/a	30 and 40 <sup>^^^</sup>

\* Re-calculated from NEMA standard = 0.05 ppm and \*\* (SANS standard).

<sup>^</sup> WHO Guidelines for the protection of human health (UN WHO).

<sup>^^</sup> The critical level of eco-toxic effects (issued by WHO for Europe); a range is given to account for different sensitivities of vegetation types (UN WHO).

<sup>^^^</sup> Cut-off concentration for the AOT 30 and 40 critical levels, UN WHO: Air Quality Guidelines for Europe (2000)



### 2.3.5 *Quality Assurance and Quality Control*

The use of an accredited atmospheric chemistry laboratory with its own quality assurance and control measures was of paramount importance. The atmospheric chemistry laboratory of the Atmospheric Chemistry Research Group, of Northwest University, Potchefstroom Campus was thus chosen for the laboratory related work. The samplers were marked with an identification number, sealed and packed. Samplers were transported to each monitoring site by either registered mail or courier services, in sealed parcels marked as fragile.

Throughout the sampling campaign, measures were undertaken for field quality assurance. These ranged from duplicate sampling, seasonal site visits with monitors and procedures inspection as set on the outset of the monitoring campaign.

During the return phase after 4-week (one calendar month) exposures the samplers were retrieved and stored for transport as per pre-arranged and communicated protocol explained to the site operators, volunteers in the field as simple set of steps. The samplers were enclosed in separate plastic vials (distinct colour for each gaseous species), sealed, and stored in dry, cool pre-packaging for postal and courier service. Any samplers damaged in transit and that arrived late were marked as such for the laboratory. As a result, the laboratory established a relatively small number of *not exposed*, *overexposed* and *beyond detection limit* samplers and those were dealt as per standard laboratory procedures. Furthermore certain loss of samplers was suffered during the sampler transport, these were sometimes replaced if notified on time or treated as non-exposures. The results were reported for each duplicate and final results were reported as the mean of two values. Overall, the number of acceptable results laboratory validated was over 70% for the entire sampling period and this was considered sufficient for a viable data analysis.

For internal quality control purposes, comparisons were made of monthly, seasonal trends and annual means between year one to year two and time trends for each site checked as each batch of samplers was returned from the field. In addition, at the time of data analysis finding and checking the extreme concentrations prompted the scientific flagging out of the outliers (greater than two standard deviations) for all sets during the data analyses. All sites with concentration values and (subsequently deposition values) beyond three standard deviations above the mean were excluded from further analyses. In addition, for readings which exceeded two standard deviations above the mean, the entire chain of sampling, chemical analysis reports and data processing were re-inspected.



## 2.4 Results

### 2.5 Passive Sampler Campaign Results

Although the sampling of SO<sub>2</sub> started on January 2005, the results presented are based on data obtained from the start of the period for which all three species were monitored, September 2005. The results were divided into two annual cycles, September to August, based on the onset of the spring and the start of a new rainy season, rather than on calendar years. Overall statistics of samples remaining after exposure, return, analysis and validation are presented in Table 2.5. Rate of valid sample return for the first annual cycle was below 60% and insufficient to meet quality control criteria. For the second annual cycle, the data return was above 80%, which is an adequate return rate on which to derive statistical results.

**Table 2.5: Percentage of validated passive diffusive samplers (successful exposures) for each of annual cycles and overall over two cycles.**

<i>Period</i>	<i>Percentage of valid samples per species (%)</i>			<i>Average percentage valid samples for all species (%)</i>
	<i>SO<sub>2</sub></i>	<i>NO<sub>2</sub></i>	<i>O<sub>3</sub></i>	
<b><i>Sep05-Aug06</i></b>	62.6	56.5	56.5	58.5
<b><i>Sep06-Aug07</i></b>	82.2	83.3	82.7	82.7
<b><i>2-year mean</i></b>	72.4	69.9	69.6	70.6

Calculated annual mean concentrations of three measured species – SO<sub>2</sub>, NO<sub>2</sub> and O<sub>3</sub> – are presented in summary tables and as spatial contour plots. Further interpretation evaluated measured concentrations in relation to critical levels. Computations were performed separately for each of the two annual cycles to facilitate inter-annual comparisons. Results for two annual cycles are reported. For ozone, a comparison over the growing season could be reported only.

In this section results are presented, compared and commented on for the period during which all three trace gas species were monitored (September 2005 to August 2007). These data on regional SO<sub>2</sub>, NO<sub>2</sub> and O<sub>3</sub> ground-level concentrations are used to address the specific study objectives.

#### 2.5.1 *SO<sub>2</sub> Concentrations and regional distribution*

Annual average SO<sub>2</sub> concentrations for the two annual cycles (September to August) are presented in Table 2.6. Differences between the two years are presented as absolute and



relative values. *Box and whisker* plots of the SO<sub>2</sub> medium-term (two-year) mean concentrations are presented in Figure 2.5.

When inter-annual differences were checked, the results did not diverge substantially from one sampling annual cycle to another (Table 2.6). Differences ranged from -1.7 to +1.3 µg m<sup>-3</sup> in absolute terms and -32% to +42% in relative terms.

**Table 2.6: SO<sub>2</sub> annual mean concentrations and inter-annual means comparison.**

Site No.	Nearest geographic location	AveSep05-Aug06 SO <sub>2</sub> (µg m <sup>-3</sup> )	AveSep06-Aug07 SO <sub>2</sub> (µg m <sup>-3</sup> )	Absolute difference SO <sub>2</sub> (µg m <sup>-3</sup> )	Relative variation from 2-year mean (%)
1	Standerton	12.5	11.6	-0.9	-7%
2	Amersfoort	13.0	13.2	0.2	1%
3	Piet Retief	8.6	8.5	-0.1	-1%
4	Badplaas	4.4	3.9	-0.6	-14%
5	Sabie	2.4	3.7	1.3	42%
6	Harrismith	4.0	3.3	-0.7	-19%
7	Newcastle	4.4	4.1	-0.3	-6%
8	Gluckstad	3.1	4.3	1.2	33%
9	Hluhluwe	2.8	2.2	-0.6	-25%
10	Ingwavuma	1.7	2.0	0.3	14%
11	Masibikela	2.0	2.3	0.3	13%
12	Skukuza	2.0	2.5	0.6	25%
13	Escourt	1.8	2.5	0.7	31%
14	Kranskop	2.6	2.3	-0.3	-12%
15	Melmoth	3.8	2.7	-1.0	-32%
16	Kosi Bay	1.4	1.2	-0.2	-16%
17	Kriel	28.7	27.7	-1.1	-4%
18	Heilbron	6.1	6.4	0.3	5%
19	Warmbaths	3.4	3.6	0.1	4%
20	Vaalwater	2.5	3.2	0.8	26%
21	Potgietersrus	7.3	5.6	-1.7	-27%
22	Marble Hall	3.9	3.9	0.0	0%
23	Steelpoort	3.9	3.8	-0.1	-2%
24	Haenertsburg	2.2	2.4	0.2	9%
25	Phalaborwa	3.3	2.6	-0.7	-24%
26	Memel	6.2	5.3	-0.9	-15%
27	Utrecht	5.7	5.1	-0.5	-10%
28	Louwsburg	3.1	2.4	-0.7	-26%
29	Amsterdam	5.1	6.3	1.2	21%
30	Malelane	5.0	3.8	-1.2	-27%
31	Fouriesburg	3.4	3.7	0.3	7%
32	Kroonstad	3.5	3.4	-0.2	-5%



<b>Site No.</b>	<b>Nearest geographic location</b>	<b>AveSep05-Aug06 SO<sub>2</sub> (µg m<sup>-3</sup>)</b>	<b>AveSep06-Aug07 SO<sub>2</sub> (µg m<sup>-3</sup>)</b>	<b>Absolute difference SO<sub>2</sub> (µg m<sup>-3</sup>)</b>	<b>Relative variation from 2-year mean (%)</b>
33	Pillansberg	4.7	4.8	0.1	2%
34	Thabazimbi	6.5	4.8	-1.7	-29%
35	Tolwe	3.0	3.5	0.4	13%
36	Louis Trichardt	2.4	2.0	-0.4	-20%
37	Thohoyandou	1.6	1.6	0.0	-1%

Box-and-whisker plots are used to illustrate the means, one standard deviation and extreme maximum and minimum concentrations for each site. The box-and-whisker plot for SO<sub>2</sub> shows that Elandsfontein (Site 17), located in the centre of the industrial Highveld, has mean and maximum much greater than any of the other sites, as expected (Figure 2.5). The means of all other sites are distinctly different and only one site (Site 1, Standerton) has an overlap of the one standard deviation boxes. This observation confirms that the sites chosen were appropriately remote from direct influences from the main emission points on the industrial Highveld, or from other local strong emission sources.

Site 1 (Standerton), Site 2 (Amersfoort) and Site 3 (Piet Retief) are downwind from the industrial Highveld and have the 2<sup>nd</sup>, 3<sup>rd</sup> and 4<sup>th</sup> highest mean concentrations and maximum values. The extent of the standard deviation boxes indicates occasional higher concentrations of those sites.



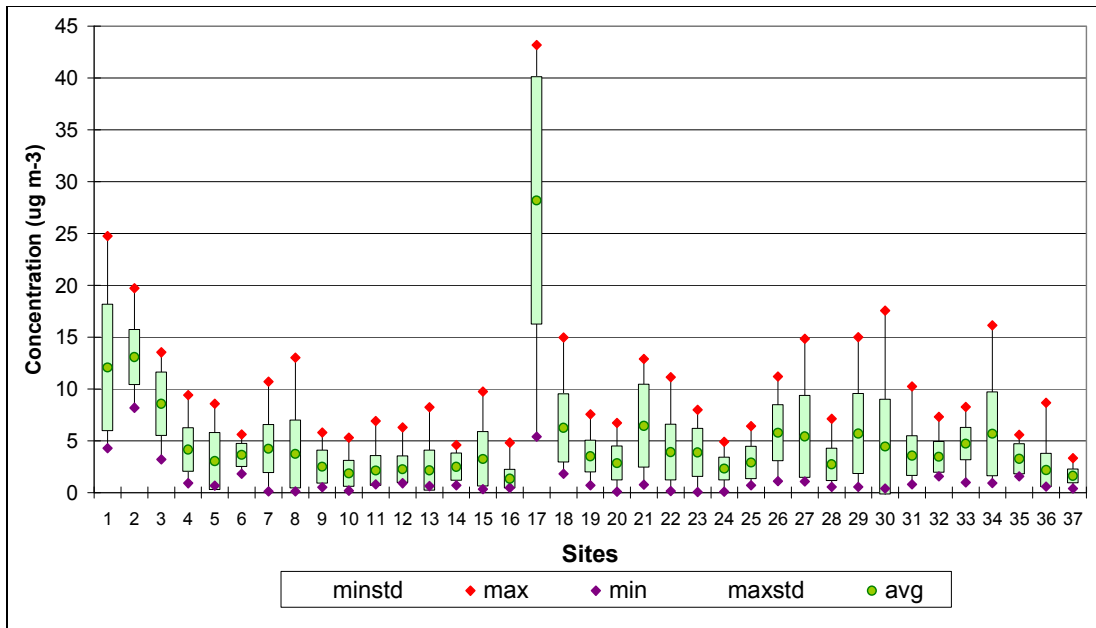


**Figure 2.5: Two-year SO<sub>2</sub> concentration comparison of mean, standard deviation, maximum and minimum (Sep05-Aug07).**

The mean concentrations at the remaining sites were below  $6 \mu\text{g m}^{-3}$ , with standard deviations below  $10.5 \mu\text{g m}^{-3}$ . Those sites with higher variations (height of the boxes in Figure 2.5) are downwind of the source areas, influenced by air mass movements from source to receptor throughout the sampling period, e.g. at sites: 1, 3, 8, 27, 29 and 30. Site 21 has a broad standard deviation. Although lies to the north (upwind) of the industrial Highveld. Site 34 (Thabazimbi) is downwind of the Matimba power plant near Ellisras (Lephalale) near the Botswana-Limpopo border and also has a broad standard deviation, for no obvious reason. This sampling site is  $\sim 50$  km northwest of the Thabazimbi iron ore mine and smelter, in an upwind direction. The standard deviations were rather small for the remainder of the sites. Further investigations at those sites could better characterise these fluctuations.

The spatial distributions of the concentrations for the two annual cycles (Sep05-Aug06 and Sep06-Aug07) of monitoring are presented in Figure 2.6. The SO<sub>2</sub> concentrations were highest at the centre of the Mpumalanga industrial Highveld, dominated by the influence of site 17 (Elandsfontein, near Kriel). The concentration gradient is a near concentric tear drop shape, with the point towards the south east, indicating the transport of SO<sub>2</sub> under influence of prevalent north-westerly mid-tropospheric winds. Sites positioned downwind and further away, but still on the Highveld plateau, (site 1, near Standerton and site 2, near Amersfoort) show mean concentrations lower than Elandsfontein, but enhanced over the



values over the rest of the study region. With the exception of site 21 (NW of Potgietersrus/Mokopane), the further sites have much lower concentrations in both years, while the furthest sites have the lowest concentrations. Site 21 has two possible influences for slightly higher mean and maximum concentrations. Matimba power station lies ~150 km upwind and 8 km to the west is Mokopane Platinum mine, although it does not appear that this mine has a smelter on site.

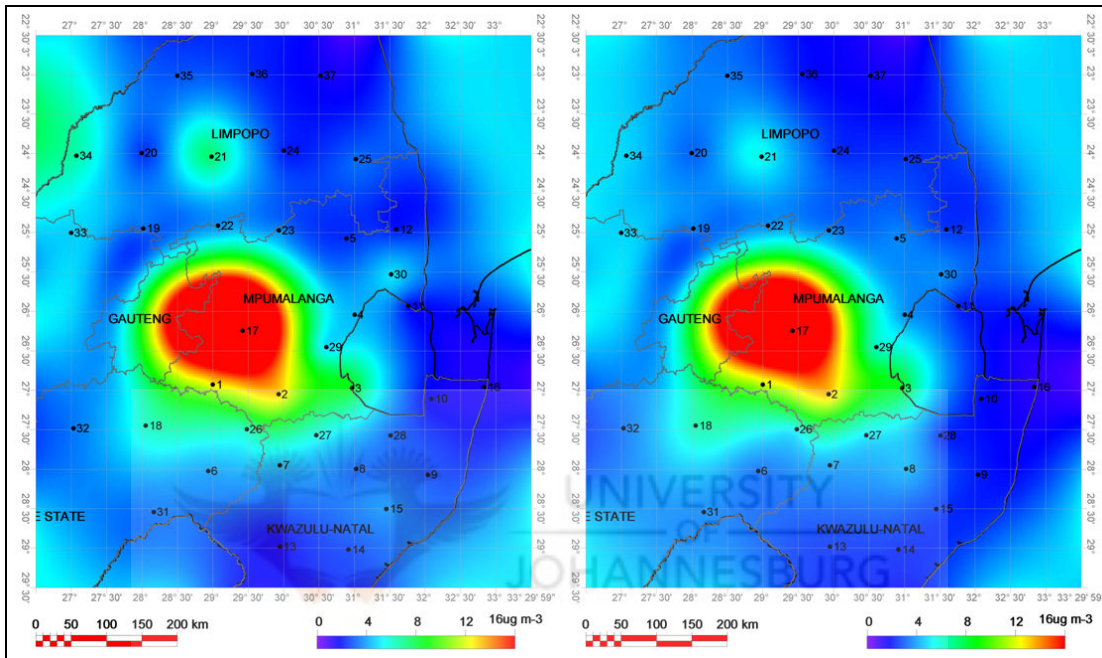


**Figure 2.6:** Regional distributions of mean annual SO<sub>2</sub> concentrations: a) Sep05-Aug06; b) Sep06-Aug07.

Overall observation of SO<sub>2</sub> concentrations for each year, their amplitudes, variations and the ground-level distributions behave as expected from known source locations and prevalent synoptic meteorology and confirm the conclusions from prior studies based on dispersion modelling.

### 2.5.2 NO<sub>2</sub> concentrations and regional distribution

Annual average NO<sub>2</sub> concentrations for the two annual cycles (September to August) are presented in Table 2.7. Differences between the two annual cycles are presented as absolute and relative values. *Box-and-whisker* plots of the NO<sub>2</sub> medium-term (two-year) mean concentrations are presented in Figure 2.7.



An evaluation of the inter-annual differences for NO<sub>2</sub> (Table 2.7) shows that concentrations did not diverge substantially from one another, with differences ranging from -0.6 to +0.8 µg m<sup>-3</sup> (-10% to +52% from two-year mean) (Table 2.7).

**Table 2.7: Comparison of NO<sub>2</sub> inter-annual means.**

Site No.	Nearest geographic location	Sep05-Aug06* NO <sub>2</sub> (µg m <sup>-3</sup> )	Sep06-Aug07* NO <sub>2</sub> (µg m <sup>-3</sup> )	Difference** NO <sub>2</sub> (µg m <sup>-3</sup> )	Variation from 2-year mean value (%)
1	Standerton	6.5	5.9	-0.6	-9%
2	Amersfoort	3.7	4.3	0.6	15%
3	Piet Retief	3.1	3.3	0.1	5%
4	Badplaas	1.7	1.6	-0.1	-7%
5	Sabie	1.3	1.9	0.6	35%
6	Harrismith	2.7	3.1	0.5	15%
7	Newcastle	2.6	3.2	0.6	20%
8	Gluckstad	1.7	2.3	0.6	30%
9	Hluhluwe	1.4	1.6	0.2	11%
10	Ingwavuma	2.4	2.4	0.0	0%
11	Masibikela	3.0	3.0	0.0	1%
12	Skukuza	1.0	1.5	0.5	38%
13	Escourt	2.2	2.6	0.4	16%
14	Kranskop	2.4	2.3	-0.1	-4%
15	Melmoth	2.0	2.5	0.5	23%
16	Kosi Bay	1.5	1.9	0.4	23%
17	Kriel	6.6	6.7	0.2	2%
18	Heilbron	2.8	3.5	0.7	22%
19	Warmbaths	2.4	2.8	0.4	17%
20	Vaalwater	2.5	2.5	0.0	-1%
21	Potgietersrus	2.6	2.6	0.0	-1%
22	Marble Hall	2.6	2.9	0.3	10%
23	Steelpoort	3.8	3.9	0.1	4%
24	Haenertsburg	2.3	2.8	0.4	17%
25	Phalaborwa	2.2	2.0	-0.2	-10%
26	Memel	2.8	2.8	0.0	0%
27	Utrecht	2.0	2.1	0.1	5%
28	Louwsburg	1.1	1.9	0.8	52%
29	Amsterdam	2.5	3.2	0.8	26%
30	Malelane	3.2	3.6	0.4	12%
31	Fouriesburg	2.1	2.7	0.5	22%
32	Kroonstad	3.8	3.8	0.0	-1%



Site No.	Nearest geographic location	Sep05-Aug06* $NO_2$ ( $\mu g m^{-3}$ )	Sep06-Aug07* $NO_2$ ( $\mu g m^{-3}$ )	Difference** $NO_2$ ( $\mu g m^{-3}$ )	Variation from 2-year mean value (%)
33	Pillansberg	2.4	3.2	0.8	28%
34	Thabazimbi	2.4	2.6	0.2	7%
35	Tolwe	1.7	1.8	0.1	8%
36	Louis Trichardt	1.8	1.8	0.0	-1%
37	Thohoyandou	4.2	3.9	-0.3	-7%

\* Mean for the annual cycle; \*\* Difference later year to earlier one

Box-and-whisker plots are used to illustrate the means, one standard deviation and extreme maximum and minimum concentrations for each site. The box-and-whisker plot for  $NO_2$  shows that Elandsfontein (Site 17), located in the centre of the industrial Highveld, has mean and maximum much greater than any of the other sites, as expected (Figure 2.7).

The sites with higher concentrations were positioned either within the industrial Highveld source area (sites 1, 2, 17) or were downwind of the source area (sites 3, 6, 7, 8). The maximum  $NO_2$  concentration at Site 17 (Elandsfontein) was only 2.5 times greater than the mean  $NO_2$  at all other sites, whereas for  $SO_2$  concentrations, Site 17 was 6.5 times greater than the background mean. For the majority of the remaining sites, mean concentrations were between 2 to 3  $\mu g m^{-3}$ , except sites 23 (Steelpoort) and 37 (Thohoyandou) which recorded concentrations  $\sim 4 \mu g m^{-3}$ . There are chrome-manganese smelters within the Steelpoort valley, which may account for the high  $NO_x$  at site 23. There are no known large industries near Thohoyandou and the traffic emissions from a small town such as this should not generate elevated  $NO_x$  at a site  $\sim 10$  km distant.

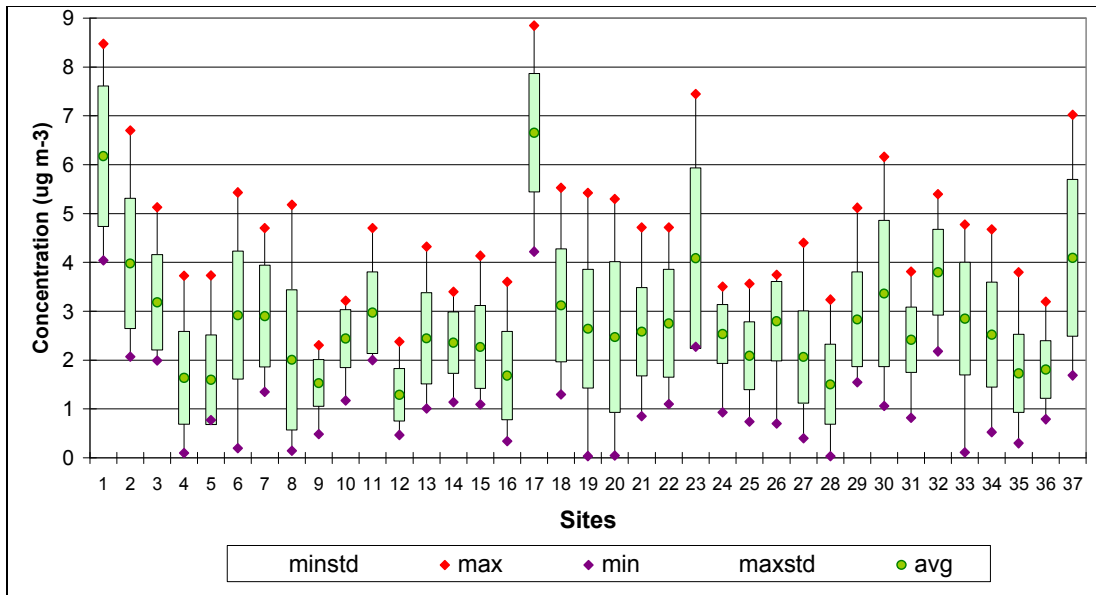


**Figure 2.7: Two-year NO<sub>2</sub> concentration comparison of mean, standard deviation, maximum and minimum (Sep05-Aug07).**

These observations confirm that the sites chosen were appropriately remote from direct influences from the main emission points on the industrial Highveld or from other local strong emission sources of NO<sub>x</sub>, with the two exceptions noted.

The lowest mean NO<sub>2</sub> (1.3 µg m<sup>-3</sup>) was recorded at site 12 (Skukuza) on the Mpumalanga Lowveld. Other low mean NO<sub>2</sub> values, below 2 µg m<sup>-3</sup>, occurred at sites 9, 16 and 28, all on the northern KwaZulu-Natal coastal plain, presumably well ventilated by clean marine air.

For the annual mean NO<sub>2</sub> concentrations, spatial concentrations contours for both annual cycles are compared (Figure 2.8). The highest NO<sub>2</sub> concentrations at sites on the industrial Highveld close to coal-fired power plants leads to the contours plots having a *fried egg* appearance, with the central red/yellow almost circular distribution, surrounded by otherwise relatively uniformly low background field. Contours for the two sampling cycles are similar. The higher concentrations north of site 37 (Thohoyandou) on the edge of the plot should be disregarded as an edge effect.

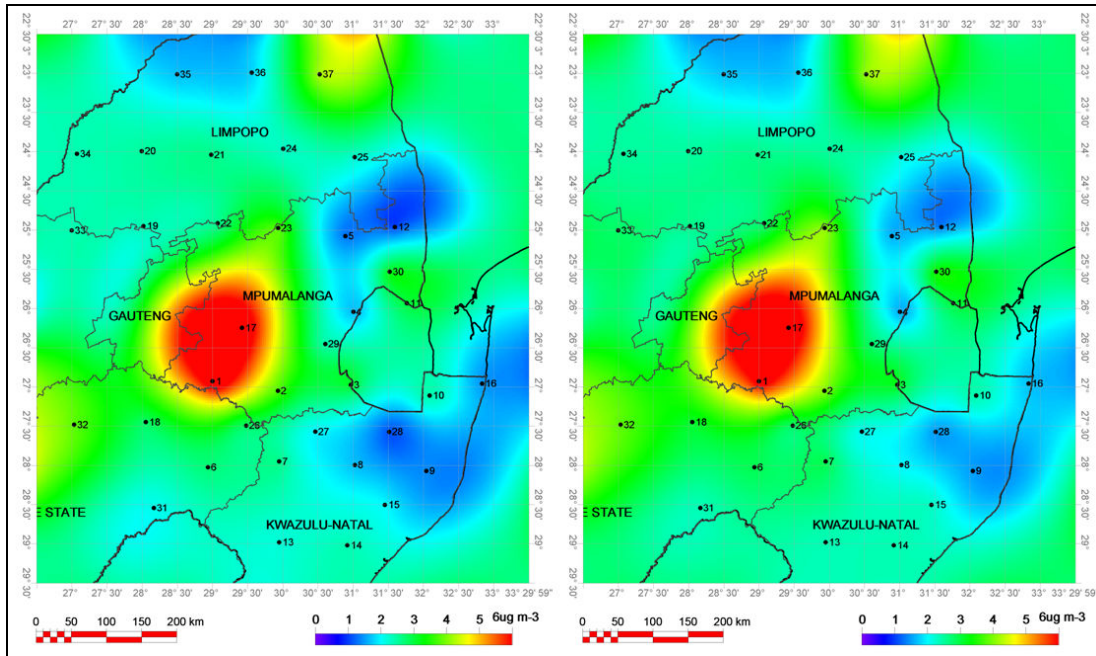


**Figure 2.8: Regional distributions of mean annual NO<sub>2</sub> concentrations: a) Sep05-Aug06; b) Sep06-Aug07.**

The industrial Highveld has been clearly delineated as a zone of elevated NO<sub>2</sub> concentrations. The areas surrounding it show the rapidly decreasing concentrations. For the sites positioned southwest and northwest and to a lesser extent, southeast slightly elevated concentrations are detectable. The overall observation of NO<sub>2</sub> concentrations, their amplitudes, variations and distributions confirm expectations based on known transport and dispersion patterns and on regional scale dispersion models (Scorgie *et al.*, 2004b, c).

### 2.5.3 O<sub>3</sub> concentrations and regional distribution

Annual average O<sub>3</sub> concentrations for the two annual cycles (September to August) are presented in Table 2.7. Differences between the two annual cycles are presented as absolute and relative values. *Box-and-whisker* plot of the O<sub>3</sub> medium-term (two-year) mean concentrations is presented in Figure 2.9.

An evaluation of the inter-annual differences for O<sub>3</sub> show that concentrations diverged more from one annual cycle to the next than for the other concentrations analysed. Changes ranged between -6.7 to +2.4 ppb in absolute terms and between -30% to +14% changes from the bi-annual mean in relative terms (Table 2.8).



**Table 2.8: O<sub>3</sub> inter-annual concentration means comparison.**

<b>Site No.</b>	<b>Nearest geographic location</b>	<b>Sep05-Aug06* (ppb)</b>	<b>Sep06-Aug07* (ppb)</b>	<b>Difference** (ppb)</b>	<b>Below or above 2-year mean (%)</b>
1	Standerton	25.6	18.9	-6.7	-30%
2	Amersfoort	20.6	19.6	-1.0	-5%
3	Piet Retief	19.7	18.2	-1.5	-8%
4	Badplaas	18.1	17.1	-1.0	-6%
5	Sabie	21.9	21.2	-0.8	-4%
6	Harrismith	20.5	18.6	-1.9	-10%
7	Newcastle	19.1	16.9	-2.2	-12%
8	Gluckstad	24.1	22.1	-1.9	-8%
9	Hluhluwe	21.5	19.2	-2.3	-11%
10	Ingwavuma	16.9	14.5	-2.3	-15%
11	Masibikela	16.5	15.8	-0.6	-4%
12	Skukuza	18.7	16.8	-2.0	-11%
13	Escourt	16.2	16.0	-0.2	-1%
14	Kranskop	23.2	19.6	-3.5	-16%
15	Melmoth	17.3	15.5	-1.8	-11%
16	Kosi Bay	15.9	13.4	-2.5	-17%
17	Kriel	22.5	21.3	-1.2	-5%
18	Heilbron	21.3	22.4	1.1	5%
19	Warmbaths	17.0	16.0	-1.1	-7%
20	Vaalwater	18.0	18.8	0.8	4%
21	Potgietersrus	20.0	18.5	-1.5	-8%
22	Marble Hall	13.8	15.8	2.0	14%
23	Steelpoort	19.5	15.9	-3.7	-21%
24	Haenertsburg	20.5	16.5	-4.1	-22%
25	Phalaborwa	18.4	17.7	-0.7	-4%
26	Memel	22.1	24.4	2.4	10%
27	Utrecht	18.5	15.8	-2.7	-16%
28	Louwsburg	21.3	21.4	0.1	0%
29	Amsterdam	16.7	16.0	-0.7	-4%
30	Malelane	15.3	15.1	-0.2	-1%
31	Fouriesburg	17.5	20.0	2.5	13%
32	Kroonstad	14.7	14.3	-0.5	-3%
33	Pillansberg	18.9	16.5	-2.4	-14%
34	Thabazimbi	17.4	17.2	-0.2	-1%
35	Tolwe	23.0	24.2	1.3	5%
36	Louis Trichardt	25.2	24.4	-0.8	-3%
37	Thohoyandou	23.5	19.9	-3.6	-17%

\* Mean for the annual cycle; \*\* Difference later year to earlier one



A box-and-whisker plot for O<sub>3</sub> monthly concentrations at all sites is shown in Figure 2.9. In contrast to wide variations in the mean concentrations at different sites for SO<sub>2</sub> and NO<sub>2</sub>, O<sub>3</sub> mean concentrations lie in a narrow band (between 14 and 23 ppb). For a majority of the sites, the mean measured concentrations were around 20 ppb. The maximum monthly mean concentration was 43 ppb, recorded at site 34 (near Thabazimbi). Lowest O<sub>3</sub> values were less than 5 ppb, but still well above the detection limit of 0.1 ppb.

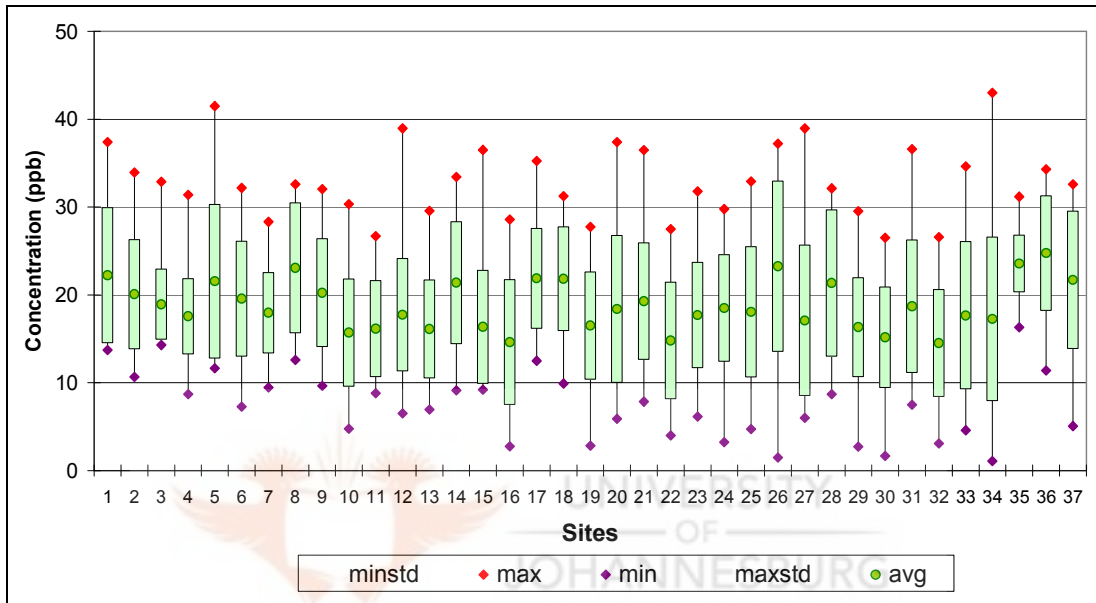


**Figure 2.9:** Mean, standard deviation, maximum and minimum O<sub>3</sub> monthly concentrations for the period Sep05-Aug07.

The spatial distributions of the mean annual O<sub>3</sub> concentrations for the two annual cycles are presented in Figure 2.10. Ozone concentrations were *not* enhanced in the central industrial region, as was the case for SO<sub>2</sub> and NO<sub>2</sub>. This is expected as ozone is a secondary pollutant and the conversion of the ozone precursors happens during air transport from source regions. There is no evidence in the medium term averages of enhanced ozone downwind from the Gauteng conurbation. A marginally enhanced concentration at Standerton (26 ppb) in 05/06 did not recur the following annual cycle 06/07.

The slightly higher concentrations in the northernmost sites (35, 36 and 37) may be a real effect. The averages are consistently higher and the standard deviations lower. These observations will be discussed further in terms of similar trends from photochemical dispersion modelling (Section 3.7.3).



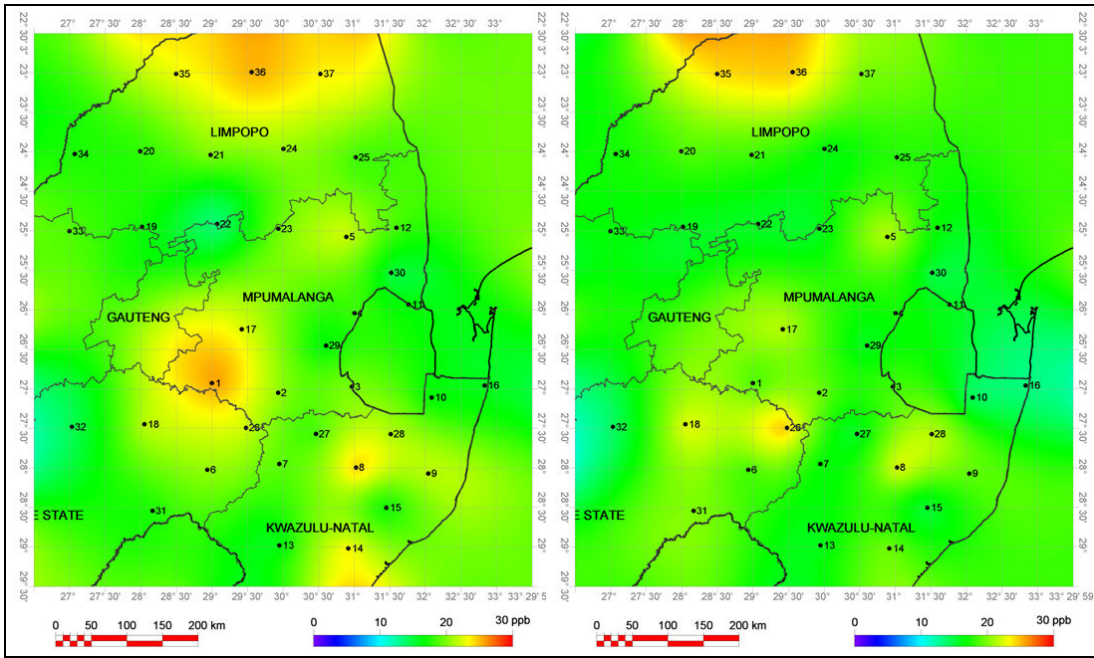


**Figure 2.10: Regional distributions of mean annual O<sub>3</sub> concentrations: a) Sep05-Aug06; b) Sep06-Aug07.**

## 2.6 Critical (Concentration) Levels Exceedance Assessment

In the following section, exceedance assessments of annual mean levels against annual mean concentrations of SO<sub>2</sub>, NO<sub>2</sub> and O<sub>3</sub> measurements are presented.

### 2.6.1 Critical levels exceedance assessment for SO<sub>2</sub>

Comparisons between SO<sub>2</sub> *annual* mean values for each site and critical levels are shown in Figure 2.11. Overall, three sites exceeded one or other critical level. The most stringent critical level is for lichen, exceeded at sites 17 (Elandsfontein), 1 (Standerton) and 2 (Amersfoort). At only one site (site no. 17) in the heart of the industrial Highveld was the CLRTAP critical level for forest and (semi)-natural vegetation were exceeded. In addition, SO<sub>2</sub> concentration at this site approached the CLRTAP critical level for agricultural vegetation.

South Africa is distinguished by exceptionally variable climates. The study region is no different. In general, morphologically and climatologically this region can be divided in several sub-regions (Schulze, 1965). The first, Highveld, inland plateau is typified by hot summers with afternoon showers and cold, dry winters with strong thermal stratification near ground. The second, the Drakensberg Mountains form a steep escarpment 200-300 km inland from the eastern seaboard. Summer showers are common and fogs occur with high frequency throughout the year. The Lowveld region at the base of the escarpment is



relatively flat and summers are hot and humid. Rainfall occurs mostly as summer showers. The winters are dry, but mild. The SA eastern coast and its coastal plateau are well ventilated and rainfall occurs throughout the year. Summers are hot and humid while winters are cool and less humid.

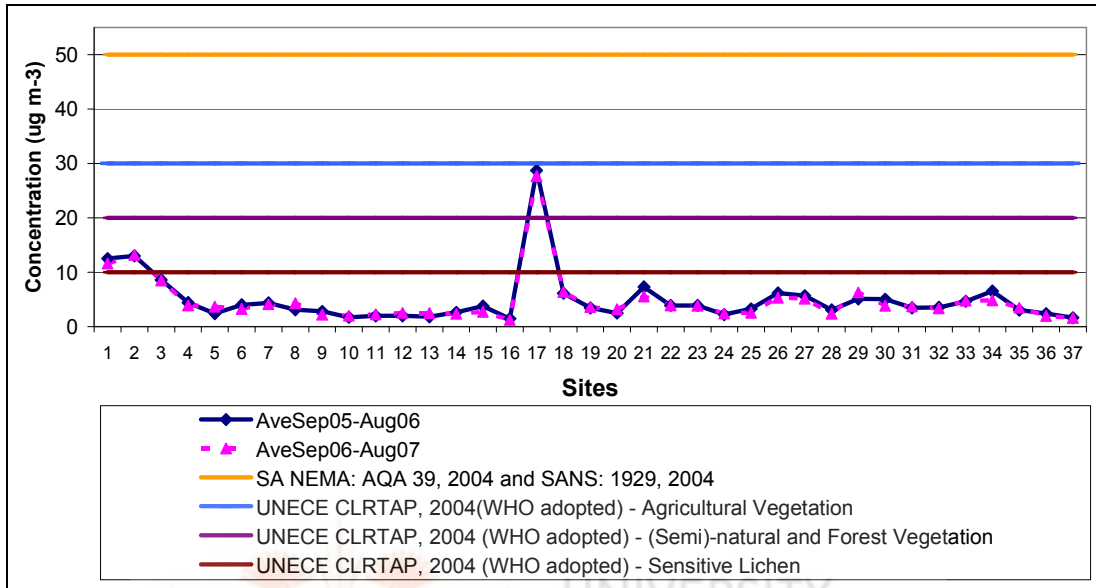


**Figure 2.11: Annual mean SO<sub>2</sub> concentrations for two annual cycles (Sep05-Aug06 and Sep06-Aug07) compared to various annual SO<sub>2</sub> critical levels.**

The prevailing winter meteorology is dictated by a lower dispersion potential, so winter months should have higher trace gas concentrations than in summer, for constant emission rates. This general observation is supported by the seasonal concentrations from five representative sites, chosen in the industrial Highveld, downwind from the industrial Highveld and at remote sites. Graphs of seasonal trends for these three categories are shown in Figure 2.12. The selected categories of different sites are:

- Remote sites (one far north - site no. 36 - near Louis Trichardt and a site southeast of the industrial Highveld, site no. 8 near Gluckstad)
- One site in the centre of the industrial Highveld; no. 17 (near Kriel)
- The sites downwind from the industrial Highveld site no. 1 (near Standerton) and site no. 2 (near Amersfoort).

To highlight the seasonal trends, monthly concentrations have been averaged by zone and by three-month moving averages. The summer means are lowest and mid-winter means highest. The factor from lowest to highest ranges from ~2 to ~3.5 – seasonal differences



are strongest in the industrial Highveld zone, close to the source areas and less marked at remote zones (Figure 2.12).

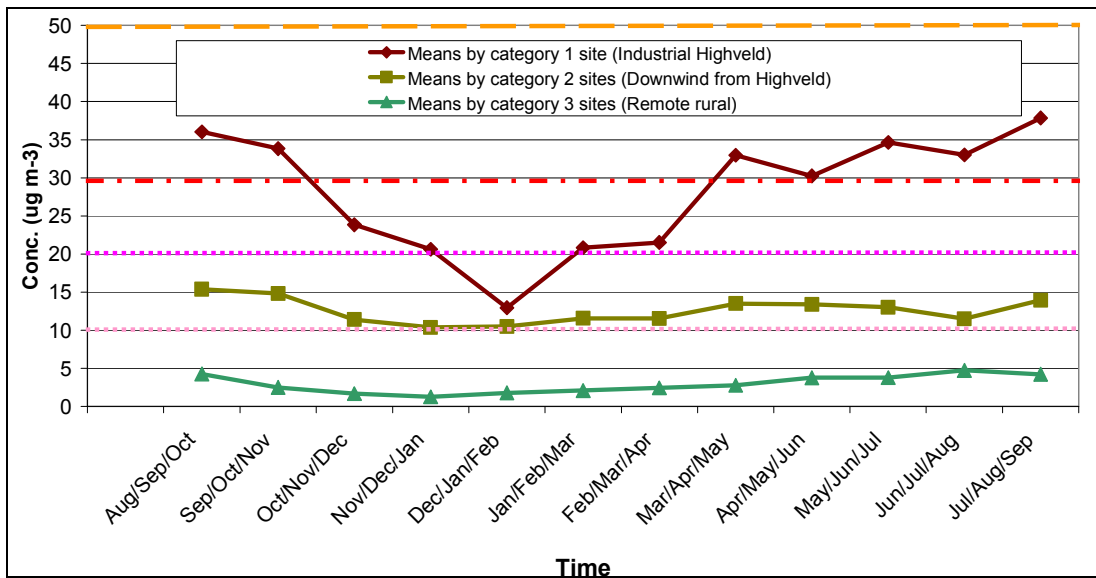


**Figure 2.12: Moving-3-monthly SO<sub>2</sub> means over two annual cycles (Sep05-Aug06, and Sep06-Aug07) for three different categories of sites.**

The SO<sub>2</sub> half-year (winter) critical level was set by CLTRAP on the basis that there is greater impact of SO<sub>2</sub> under winter conditions. In its original form, the winter half-year in the boreal climate was taken to be the period from October to March. This level is set for three vegetation types, (semi)-natural, forests and agricultural vegetation.

It is recommended that this value should not be exceeded as a mean concentration for the winter months in view of the abundant evidence for increased sensitivity of crops growing slowly under winter conditions. A lower air quality guideline of 20 µg m<sup>-3</sup> is recommended for forests and natural vegetation, as both an annual and winter mean concentration. New data have confirmed concerns over low-temperature stress contributing to greater sulphur dioxide sensitivity in forests. In its original form, UN ECE set this critical level for areas where the accumulated temperature sum above +5°C is less than 1000°C-days a year (UN WHO: Air Quality Guidelines for Europe, 2000). This is based on new evidence of periods of high sensitivity of conifers during needle elongation and the longevity of many of the species concerned as well as their being unmanaged or minimally managed, which renders them more sensitive to pollution stress. This lower concentration is now recommended as a WHO air quality guideline for regions below this threshold temperature sum (UN WHO: Air Quality Guidelines for Europe, 2000).



Although the study region is not assessed for the above temperature dependent condition, the SO<sub>2</sub> winter half-year exceedance level as per CLRTAP was still assessed against the winter half-year concentration means for each of the sampling years (Figure 2.13). The winter half-year was taken to comprise of the period from April through September.

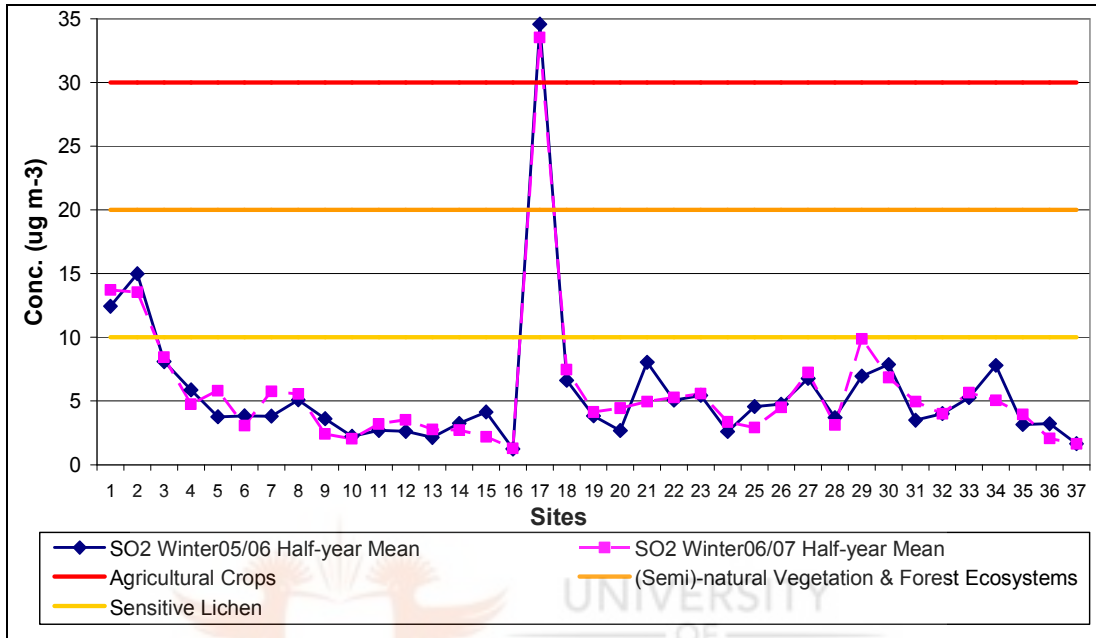


**Figure 2.13: Mean winter SO<sub>2</sub> concentrations for winter half-years (2006 & 2007) compared to SO<sub>2</sub> vegetation winter (half-year) critical levels.**

The result is almost identical to the annual exceedance assessment graph. The site in centre of the industrial Highveld (site 17, Elandsfontein) exceeded all three (winter) critical levels. The sites located downwind (sites 1, Standerton and 2, Amersfoort) have exceeded one critical level only, for lichen, while only one remote locality, site 29 near Amsterdam, reached the most sensitive level in one annual cycle only. Overall, there is no evident impact of sulphur in regions away from the industrial Highveld, either upwind or further downwind.

### 2.6.2 Critical levels exceedance assessment for NO<sub>2</sub>

There was no exceedance for NO<sub>2</sub> at any given level against mean annual results. The mean annual values of NO<sub>2</sub> for each site were much lower than all the specified critical levels (Figure 2.14).

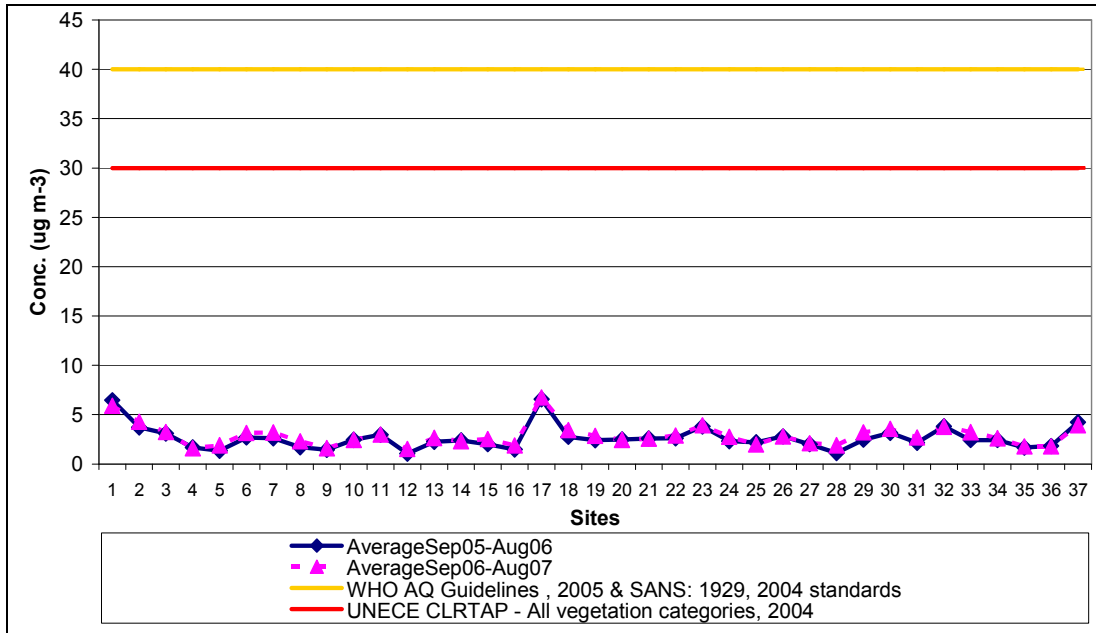


**Figure 2.14: Mean annual NO<sub>2</sub> concentrations for two annual cycles (Sep05-Aug06 and Sep06-Aug07) compared to annual critical levels.**

This general observation is supported by the seasonal (three-month moving mean) concentrations from five representative sites, chosen in the industrial Highveld, downwind from the industrial Highveld and at remote sites. Graphs of seasonal trends for these three locality categories are shown in Figure 2.15. There is little seasonal variation of NO<sub>2</sub> at any of the sites. Once again, the gradient with spatial reduction from the highest in the Highveld centre to the remote rural background is evident.

For the industrial Highveld, NO<sub>2</sub> shows elevated concentrations by ~25% of the minimum during summer and is constant for the remainder of the year. For the downwind sites, NO<sub>2</sub> shows no distinct seasonal variation. For remote sites, there is a variation from minimum to maximum of ~80%, with a slight enhancement during summer months. These relatively constant mean NO<sub>2</sub> concentrations show no trends that would indicate strong influences from lightning produced NO<sub>x</sub> (LNO<sub>x</sub>). Ojelede has shown that LNO<sub>x</sub> peaks strongly in summer over the Highveld and is less than 1% of peak production during winter. Total LNO<sub>x</sub> production on the Highveld was estimated to be ~10% of power plant production (Ojelede *et al.*, 2008).

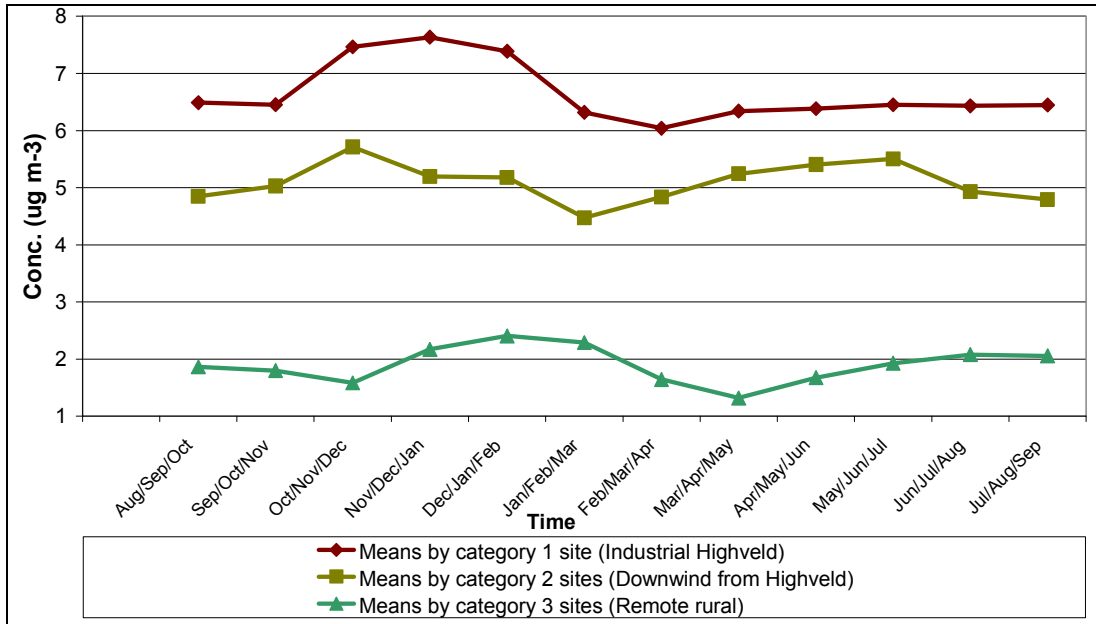


**Figure 2.15: Three-month moving average NO<sub>2</sub> concentrations over two annual cycles (Sep05-Aug06 and Sep06-Aug07) for three different site categories.**

### 2.6.3 Critical levels exceedance assessment for O<sub>3</sub>

The following diagram presents the results of O<sub>3</sub> annual mean measured values exceedance assessment of the annual critical levels for all the sites (Figure 2.16).

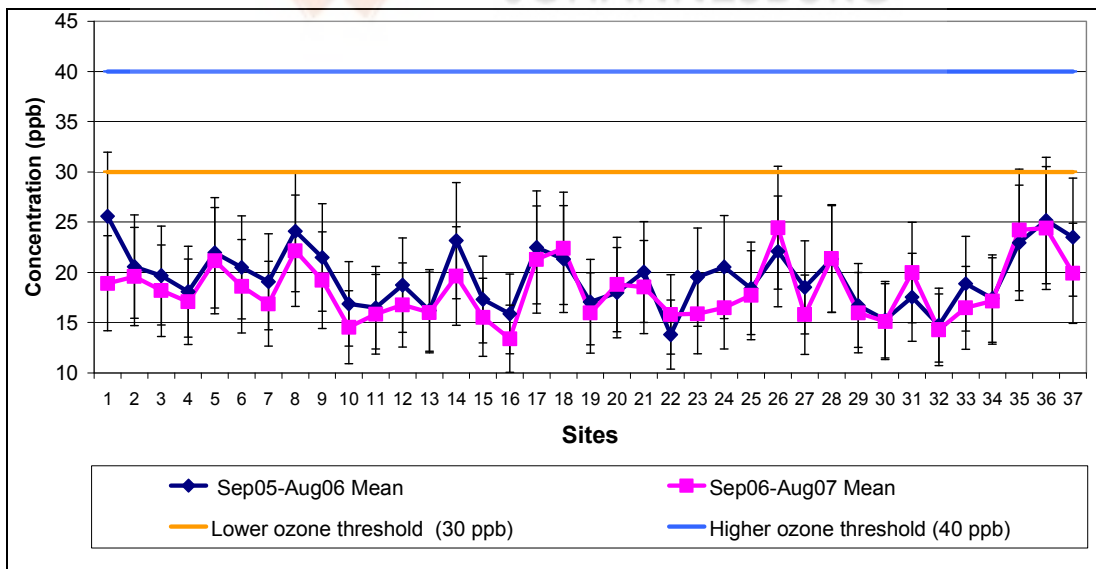


**Figure 2.16: Mean annual O<sub>3</sub> concentrations for two annual cycles (Sep05-Aug06 and Sep06-Aug07) compared to O<sub>3</sub> annual average critical levels. The error bars set as 25% (Martins, personal communication, 2007).**

In the case of ozone, no exceedance of the measured annual mean was found for either of 40 ppb or 30 ppb concentration thresholds in either of the two annual cycles, although concentrations at several sites were relatively close to the 30 ppb threshold level (sites 1, 8,



14, 26, 35 and 36). If the error margins are taken into account then a few sites could reach or exceed only the lower 30 ppb threshold in cases of positive error margin being adjusted (sites 1, 8, 26, 35 and 36).

Seasonal trends at the industrial Highveld, downwind and remote sites are shown in Figure 2.17. All three sites show lowest concentrations during winter. The remote sites show the strongest summer enhancement of ozone concentration. In contrast, the pattern for the industrial Highveld appears erratic and does not follow the common understanding that ozone production in the troposphere is highest during summer due to greater solar radiation. The mean for remote sites and slightly less for the sites downwind from industrial Highveld show the highest records for spring months and secondarily for late winter. However, the industrial Highveld category site shows the highest records for Mid-summer months.

Increasing ozone concentrations are observed in late winter and early spring. This pattern is logical, as this season has increased pyrogenic ozone precursors from wild fires to the north and within South Africa (Swap *et al.*, 2003) and together with increased sunlight and daytime results in higher readings for remote sites.

Overall, the Figure 2.17 shows highly variable regional ozone generation and distribution. Certain temporal and spatial regional trends can be recognised. However, both monthly and long-term averages are below the critical levels.

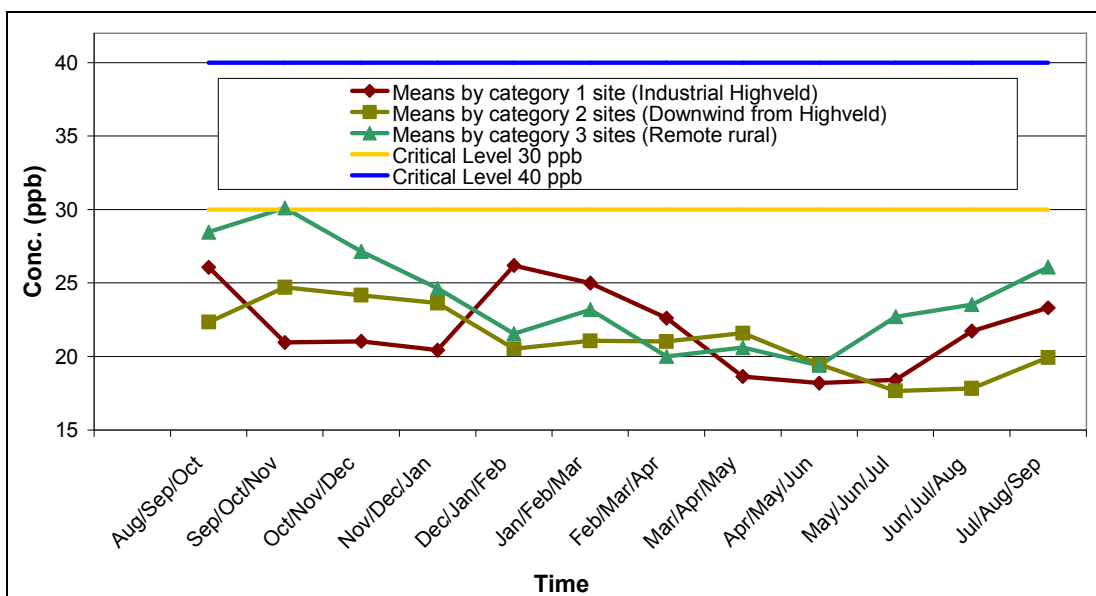
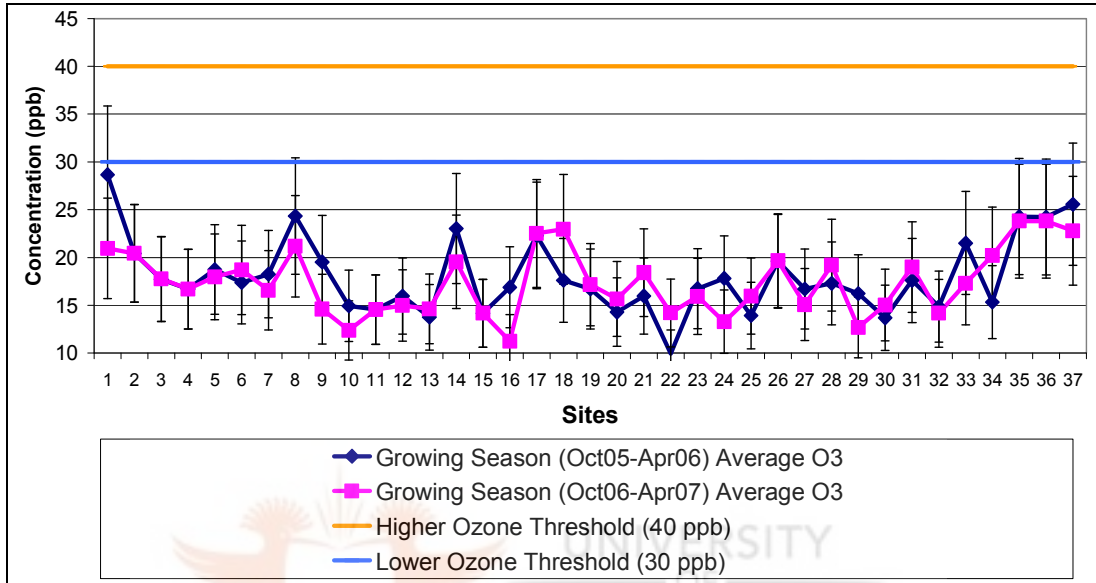


Figure 2.17: Three-month moving average O<sub>3</sub> over two annual cycles (Sep05-Aug06 and Sep06-Aug07) for three different site categories.



Ozone is taken into the plant through stomata. As all plants have increased activity during the growth season, this is an important period for plant exposure. The growing season for South African climates is considered to be from October to April. The average concentration for the growing seasons in both annual cycles (Oct05-Apr06 and Oct06-Apr07) were compared to two ozone critical levels for all sites (Figure 2.18).



**Figure 2.18: Growing season mean O<sub>3</sub> concentrations (Oct-Apr for two years) for all sites compared to ozone critical levels. The error bars set as 25% (Martins, personal communication, 2007).**

The seasonal diagram shows that no site exceeded either higher (40 ppb) or lower ozone critical level (30 ppb) in any of the sampling periods. Certain sites (1, 8, 14, 17, 18, 34, 35 and 37) came relatively close to 30 ppb threshold for one year only, while only one site (1) almost reached the lower 30 ppb threshold. If the error margins are taken into account then a few sites could reach or exceed only the lower 30 ppb threshold in cases of positive error margin being adjusted (sites 1, 8, 35, 36 and 37).

Figure 2.19 shows the time-sequence of monthly mean O<sub>3</sub> concentrations, over the summer growing season October to April for two successive years, compared to ozone critical concentration levels for three representative sites. The site category 1 (central industrial Highveld) reached the lower threshold level once in late summer, while sites of category 2 (downwind industrial Highveld) reached it once in late spring only. The category 3 (remote rural) exceeded slightly the lower threshold once in late spring. This temporal trend and the spatial pattern coincide with the annual observance and the conclusions on the annual trends and patterns confirm ozone assessment findings (Figure 2.10).



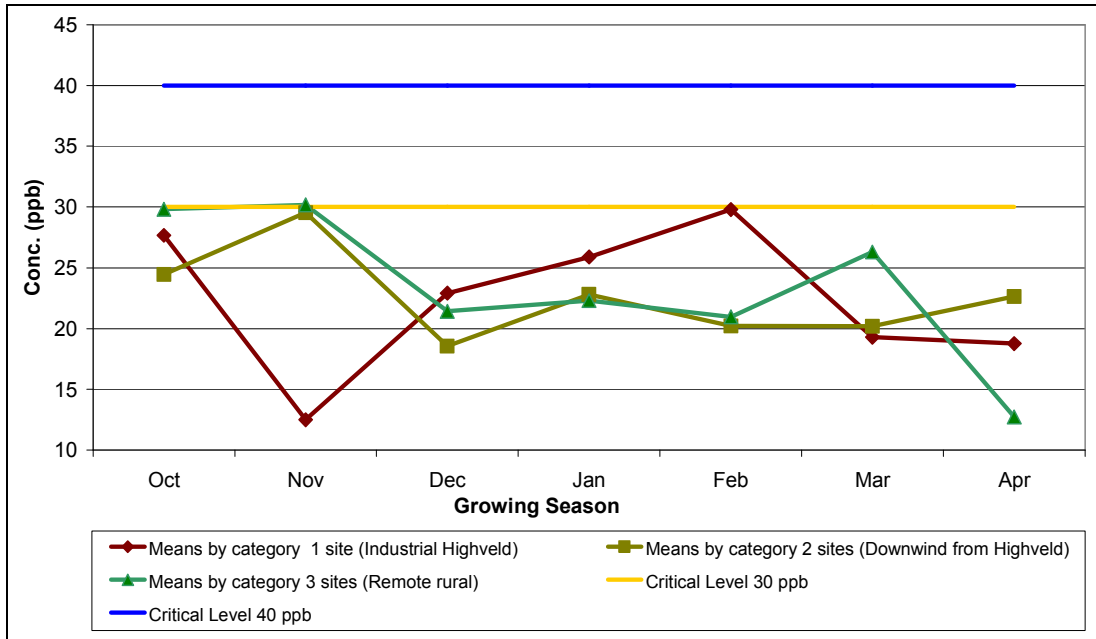


**Figure 2.19: Time-sequence of monthly mean O<sub>3</sub> concentrations (Oct-Apr for two seasons) compared to ozone critical levels for three representative sites.**

## 2.7 Conclusions

The assessment of exceedance for the observed SO<sub>2</sub>, NO<sub>2</sub> and O<sub>3</sub> concentrations resulted in the following conclusions. Several critical levels were exceeded for SO<sub>2</sub> in the Highveld industrial source area. Only the lowest critical level was exceeded for the sites located in downwind vicinity. SO<sub>2</sub> critical levels were not exceeded at the remote locations stations either downwind or upwind from the source. The sites downwind and closer to the industrial Highveld are influenced by its SO<sub>2</sub> emissions, while remote sites do not show evident influence of SO<sub>2</sub> impacts.

NO<sub>2</sub> did not exceed any critical level at any site. However, NO<sub>2</sub> concentrations were higher at sites within and downwind of the industrial Highveld source area, compared to remote sites. Although far below the critical levels, a simple temporal trend is recognizable, indicating relative increases during the summer. Observed seasonal trends of NO<sub>2</sub> do not reflect the known pattern of lightning produced NO<sub>x</sub> (strong summer production, close to zero winter production), thus LNO<sub>x</sub> is not expected to be a strong contributor to the observed concentrations. Nevertheless, further investigations of the contribution of LNO<sub>x</sub> to the near-surface budget of NO<sub>2</sub> are recommended.

Ozone exceedance of the lower concentration critical level occurred at several sites. Exceedances occurred for remote sites located both north and southeast off the industrial



Highveld. No exceedance of the higher critical level was measured. Ozone exceedance for the growing season shows a similar pattern. The different categories of representative sites assessed and their means showed that a slight maximum during late winter and early spring. The distribution of ozone is uniform on a regional basis, without a localised maximum on the industrial Highveld that was characteristic of SO<sub>2</sub> and NO<sub>2</sub>, confirming the mixed origin of ozone precursors and the regional nature of ozone.

### **2.7.1 Summary**

Critical levels for the measured gases were not often exceeded. Exceedance occurs occasionally at a few sites. This finding indicates that the concentrations for the measured gas species over the study region (background and downwind pollution from the epicentre of industrial gaseous pollution) have not reached or exceeded the existing (legislated and regulated) limits. Here it must be repeated that the vegetation critical levels used are European limits and sensitivity of the South African vegetation might be quite different.

In case of ozone, experimental evidence shows that exposures with the same mean but larger frequency of high concentrations have a greater biological effect. Plants generally respond to episodes of high concentrations of pollutant gas even if the episodes are infrequent. The past, on-going and future empirical testing of trace gas limits for Southern African biomes/ecosystems (e.g. “O<sub>3</sub> bio-monitoring study in North-West University quantifying the impact of tropospheric ozone on crops using protective chemicals”) may help with the ozone limits at least.

Another way to gain more confidence with regard to critical levels determination for South African vegetation is to determine a “flux-based pollutant rate intake” for South African plants. Specifically for O<sub>3</sub> plants respond to the stomatal gaseous flux, or internal doses, rather than ambient concentrations, so the biological response should be expressed in terms of a relevant flux-based parameter rather than an exposure index such as the AOT40 approach. However, although the flux-based approach is biologically more appropriate, it requires a considerable amount of data compared to both the cumulative (AOT40 and AOT30) index and concentration threshold (40 ppb and 30 ppb) and for the purposes of this study this was not considered. Hence it is necessary here to underline importance of future studies, which would determine the cumulative doses over a well researched threshold of ozone, be it either AOT30 ppb or AOT40 ppb if and for as long ozone fluxes are not viable to measure.



Concentrations and critical limits should be compared to the closely related *deposition values* of the pollutant gaseous compounds calculated on the basis of the measured concentrations. Critical levels and loads for pollution are inter-dependable values which must be examined together to gain higher confidence levels when assessing particular gaseous environmental pollution.

### **2.7.2 Comments**

This study determined that most of the concentration values presented do not reach or exceed Critical limits for the gases measured in the background of the major industrial/pollution source area. SO<sub>2</sub> is exceeded in the source area for several levels, while NO<sub>2</sub> levels were not exceeded even in the wider source area. It is possible that the design of the network – including measuring sites one degree apart (~111 km) – contributed to the low reading of the NO<sub>2</sub> in the source area. However, a conclusion can be reached concerning levels of NO<sub>2</sub> in the background areas with more confidence. These are low and unless measured at local sources and near major roads, are far from exceeding the levels used in this study. The measurement of the other gaseous acidifying nitrogen compounds (such as ammonia and nitric acid) could change the overall nitrogen acidifying potential, in which case all nitrogen species should be looked at in terms of their synergistic critical level.

The ozone exceedance assessment has shown limited exceedance of the 40 ppb concentration threshold. However, this particular level might not be the critical one for the most South African species of flora even if only the concentration-based mode is considered. In the case of the 30 ppb concentration threshold, the exceedance in background areas over the measured one year period is inconsistent. This supports the idea that ozone ground pollution is a regional pollutant, most likely of mixed origin ([van Tienhoven and Scholes, 2003](#); [Zunckel \*et al.\*, 2006](#)).

The establishment of specific ecosystem-relevant critical limits determined for local conditions on local species of both flora and fauna including water-living species, is required. These should be determined through both field and experimental research and should be undertaken in the short-, medium- and long-term. Future results of deposition studies for the gaseous species studied should be analysed on a cumulative basis over the corresponding period.



Flux experiments should be undertaken to determine the local air pollutant flux limits in local conditions for the local environment. The current uncertain situation is a challenge for the establishment of gaseous pollutant limits (critical levels) beyond the concern for human and commercial animal health and should be tackled when evaluating the effects of air quality on the wider natural environment.

Ideally, adverse effects on the weakest species should be taken as the most sensitive critical level because critical effects on the weakest species constitute impacts on the biodiversity of the affected ecosystem. The possible loss of certain species would mean that more species in the ecosystem chain could become critically impacted even if the species lost are the weakest parts of the chain. Therefore, all efforts towards controlling air pollution among the other environmental changes should strive towards reducing imbalances however small they appear. Gradual measures for the reduction of air pollution are better than no measures at all.





## CHAPTER THREE

*A short overview of acidic deposition theories is given, together with an introduction to air pollution dispersion modelling. The study specific methods used to estimate regional dry and wet deposition of trace gases are provided. The results address two objectives, dry and wet deposition computation; and comparison of these empirically based results with appropriate regional scale modelling results.*

### **3. Dry and Wet Deposition of SO<sub>2</sub> and NO<sub>2</sub> and Comparison of Meso-scale Air Pollution Dispersion Modelling of SO<sub>2</sub>, NO<sub>2</sub> and O<sub>3</sub>**

#### **3.1 Introduction**

Acidification is still a potential environmental problem for developing countries in the context of increasing emissions. Acidification effects are primarily associated with the atmospheric deposition of sulphur and nitrogen compounds. There are three pathways by which chemical species can be removed from the atmosphere: chemical transformation, wet deposition and dry deposition.

The purpose of this study was to derive both dry and wet depositions for the study area. The deposition determination is an important indicator of acidic pollution on its own and the secondary step to the task to follow, primarily assessment of critical loads of acidity exceedance for the study area. The regional size of the task enabled another important assessment of acidity potential for the region, namely to compare the deposition results mainly based on measurements (of ambient concentrations rain chemistry and precipitation) with the available regional scale air dispersion modelling results.

The scope of this study did not extend to direct measurements of the deposition either dry or wet. Also no concurrent regional scale modelling could be performed as it was out of the study scope.

The procedure chosen was to use inferential methods for both dry and wet deposition. The measured database for both acidic species of SO<sub>2</sub> and NO<sub>2</sub> together with prior measured deposition velocity in the same study area produced empirical set of the dry deposition results. The wet deposition computation used prior long term measurement of the precipitation chemistry essentially for the same region and in combination with the precipitation measurements concurrent with the monitoring produced regional estimate. In



addition to the deposition calculations the numerical comparisons were performed of dry and wet deposition together and the ambient concentrations against numerical results of the suitable existing regional scale air dispersion modelling.

### **3.2 From concentration to depositions for comprehensive modelling comparison**

#### **3.2.1 Deposition**

Wet deposition is the removal by precipitation scavenging of atmospheric pollutants and, to a lesser extent, impaction of fog or cloud droplets on vegetation. Dry deposition includes the direct adsorption or deposition of gases on the surface of particles and the settling and impaction of particles. On a global scale, precipitation scavenging and dry deposition are by far the most efficient methods. Fog and droplet deposition can be locally important, especially in cloudy, high elevation regions in South Africa (WMO, 1996).

Deposition may occur in the form of strong acids (sulphuric acid, nitric acid and infrequently hydrochloric acid) or compounds, which, after deposition, may be converted to strong acids (e.g. sulphur dioxide and nitrogen dioxide). In this context ammonia is also a potentially strong acid. In soils it may be converted to nitric acid and thus cause acidification. In tropical areas organic-acid deposition may contribute as much as 50% of the deposition of acids in precipitation. It is assumed, however, that these acids are absorbed or oxidized in soil and will not contribute to soil acidification (McDowell, 1988).

Acidic deposition has been of interest not only for its role in acidification but also for effects associated with the deposition of nitrogen as a nutrient (eutrophication). In addition, direct effects from sulphur dioxide and nitrogen oxides have sometimes been considered as acidification effects. In many areas of the world, concentrations of sulphur and nitrogen oxides exceed ambient air quality standards and considerable emission reductions are necessary to protect environment. Sulphur and nitrogen compounds may also affect physical and chemical properties of the atmosphere (Isaksen and Hov, 1987; Langner *et al.*, 1992).

#### **3.2.2 Dry deposition**

The dry-deposition process involves close interaction between the atmosphere and the surface in which the characteristics of individual underlying surfaces often determine the mass-transfer rates. The transport of gases and particles from the atmosphere to the vicinity of the receptor surface is governed by the level of atmospheric turbulence, generated by



both wind shear and buoyancy. The higher the level of atmospheric turbulence, the more efficiently gases and particles are transported to a given receptor surface. Depending on the characteristics of the surface, the ability to “capture” pollutants from the air may vary by more than an order of magnitude, causing highly varied dry-deposition rates even over small areas. Forests, especially coniferous forests, normally receive relatively high dry deposition of acidifying compounds, whereas lake surfaces receive much lower ones. Deposition extremes are often observed at forest edges or in forests on mountain slopes (Hicks *et al.*, 1987).

Around the source, dry deposition is determined primarily by the configuration of the sources, the type of sources and the mixing of the pollutant in the atmosphere. For high-level sources, the deposition near to the source is small and increases with downwind distance from it, until it reaches a maximum and decreases again. However, for ground-level sources, dry deposition takes place in the immediate vicinity of the source, where concentrations are highest and then gradually decreases downwind. At some distance, the influence of the source on the concentration gradient is decreased. At this point, the pollutant is mixed throughout the boundary layer and the concentration gradient is determined primarily by dry deposition processes (Erisman and Draaijers, 1995).

For gases, surface uptake is frequently controlled by the ability of the surface to adsorb the specific chemical species. In any circumstance dry-deposition rates are proportional to the concentrations of air immediately above (or surrounding) the receptor under consideration. The constant of proportionality is referred to as a *deposition velocity* ( $V_d$ ), which depends on factors mainly associated with turbulence and related to characteristics of the air near the surface, as well as the composition of the surface itself. Depending on the chemical in question, different factors assume important roles in determining the magnitude of  $V_d$ .

In practice, using a standardized deposition velocity in numerical estimations is an engineering approximation that is particularly attractive in relation to large-scale simulations because it combines the effects of many complex processes into a single term (Wesely and Hicks, 1977).

Dry deposition can be estimated from concentration measurements. Dry deposition is inferred by multiplying the concentration with the deposition velocity of the component of interest (Hicks *et al.*, 1993). The latter is calculated using a resistance model in which the



transport to and absorption or uptake of the component by the surface is described (Figure 3.1).

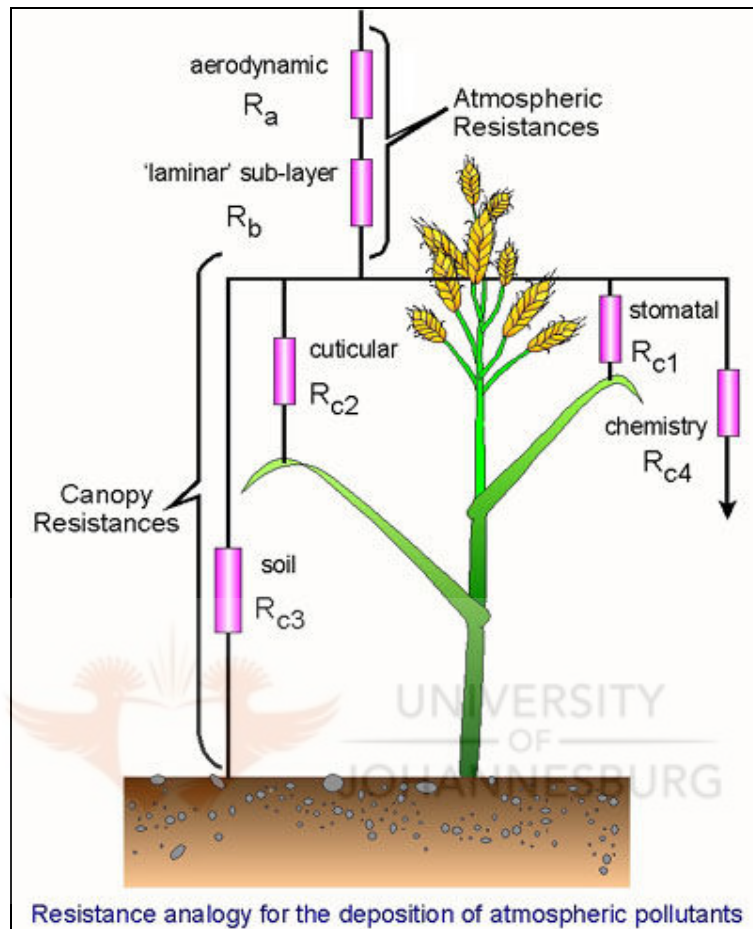


**Figure 3.1:** Resistance analogy for the deposition of atmospheric pollutants (Source: [UNECE CLTRAP mapping and modelling manual, 2004](#)).

The stages in the dry deposition process analogous to the flow of electrical current through a network of resistances (Garland, 1978). In this analogy, the aerodynamic resistance ( $R_a$ ) refers to turbulent transport from the free atmosphere down to the receptor surface. The boundary layer resistance ( $R_b$ ) applies to transport across the quasi-laminar layer near the receptor surface and the canopy or surface resistance ( $R_c$ ) refers to the interaction of the gas with the surface. An advantage of the resistance analogy is that processes are separated and related to ‘measurable’ quantities. The inverse of the total resistance is known as the *dry deposition velocity* ( $V_d$ ):

$$V_d = 1 / (R_a + R_b + R_{n...}) \quad (3.1)$$





### 3.2.3 *Wet deposition*

Wet deposition is defined as the natural process by which atmospheric pollutants are attached to or dissolved in cloud and precipitation droplets (or particles) and subsequently deposited on the Earth's surface (Erisman and Draaijers, 1995). Precipitation removal is an effective mechanism for removing soluble trace gases and small particles from the troposphere.

The gases and particles are incorporated into cloud droplets and falling rain drops in several ways. Those trace particles in the atmosphere that act as ice-forming nuclei or condensation nuclei can be incorporated into hydrometeors during the nucleation process itself. This is the process that generates cloud droplets from which raindrops form. In many parts of the world, sulphate particles are the most commonly found condensation nuclei in the atmosphere (Whelpdale and Kaiser, 1996). The cloud droplets that are generated continue to scavenge gases and particles in cloud as they grow in size. As they grow, the droplets fall faster until they leave the cloud base and are deposited as rain, carrying all of the scavenged pollutants with them. It is not only particulate sulphate that is scavenged in this way. Gaseous sulphur dioxide can also be dissolved in cloud droplets, where it can be oxidized to sulphate by means of aqueous-phase chemical reactions (Summers, 1992).

The complexity of wet deposition removal processes led early investigators to attempt a quantification of the relationship between airborne species concentrations, meteorological conditions and wet deposition rates by grouping the effects of these processes into a few parameters.

In many regions the day-to-day variation in wet-chemical deposition is controlled more by the precipitation amount than by trace-chemical concentrations (Barrie, 1988). The wet-deposition flux is given by the product of the measured concentration of the species of interest in the rain and the precipitation rate:

$$F = C * P \quad (3.2)$$

Where **F** = wet flux ( $\text{mol m}^{-2} \text{yr}^{-1}$ ), **C** = measured concentration in precipitation ( $\text{mol m}^{-3}$ ), **P** = precipitation rate ( $\text{mm yr}^{-1}$ ).

One overwhelming characteristic of wet deposition is how much the total wet deposition of one chemical species can vary from one event to another. In addition, precipitation itself varies for a given trace with several centimetres from one event to the next; the



concentration of a chemical species can vary by an order of magnitude. The largest difference between events occurs on the periphery of industrial regions where emission rates are high. There, depending on air-mass trajectories, the air can be clean or heavily polluted. Within regions with high emissions and in remote areas, the concentrations vary less.

#### **3.2.4 Atmospheric dispersion models available**

Atmospheric dispersion models play a major part in extrapolating and predicting pollutant concentration and deposition fields. Monitoring provides data needed for use and evaluation of atmospheric models. Evaluation of models often points out gaps in our understanding, leading to more laboratory and field measurements and further modelling development (Seinfeld and Pandis, 1998).

Such models have not yet been validated against direct observations in southern Africa on the scale of several hundred kilometres. Relevant modelling studies, such as Zunckel *et al.*, 2000, focussed on quantifying the dispersion and deposition of sulphur and nitrogen. The recent CAPIA project (van Tienhoven and Zunckel, 2004, Zunckel *et al.*, 2006) modelled ozone concentrations. Without validation by direct measurements, the validity and usefulness of air dispersion model outputs is questionable. Confidence in the modelling results will only be achieved by comparison between predictions and measurements. This research obtained a unique data set that can serve to compare and validate (to a certain extent) the current (CAMx and LED) and future models results such as one sample presented in Figure 3.2. Modelled SO<sub>2</sub> and NO<sub>2</sub> concentrations and depositions were derived from “Modelling the Long-range Transport and Transformation of Air Pollutants over the Southern African Region”, the doctoral thesis of Fourie (2006). A long-range air pollution transport and diffusion model with atmospheric chemistry was developed, using a combined Lagrangian-Eulerian approach (LED). Fourie run his modelling for the period January to December 2000.

The measured ozone concentrations for South African growing season were compared with the ozone modelling concentrations from the Cross Border Air Pollution Impact Assessment Project (CAPIA) (Zunckel and Carter, personal communication 2007). The Comprehensive Air Quality Model with extensions (CAMx), version 4.00 (ENVIRON, 2003), was used by the CAPIA modellers.

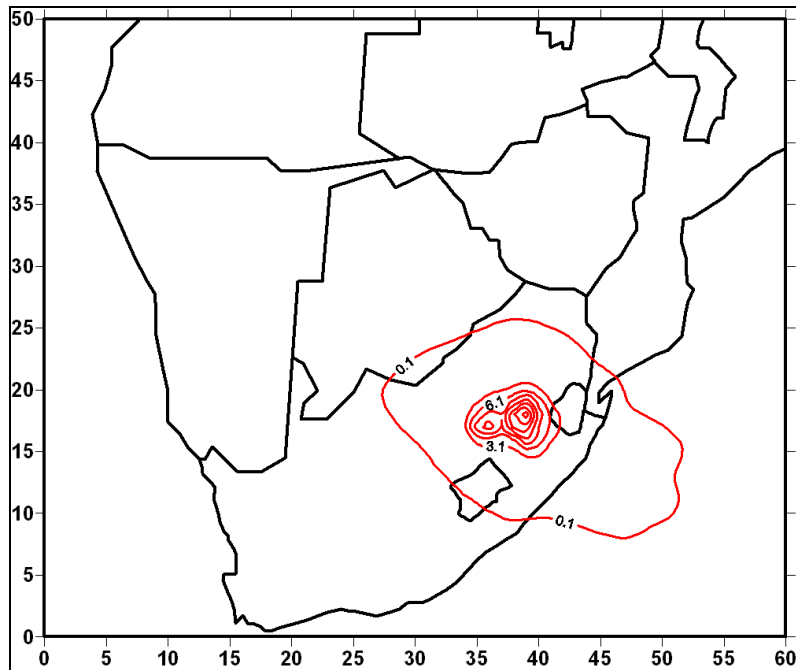


**Figure 3.2:** Modelled mean ambient SO<sub>2</sub> concentrations (µg m<sup>-3</sup>) for the 2000 winter season based on the EDGAR 32FT2000 emission database (Source: [Fourie, 2006](#)).

### 3.3 Methods

The measured gaseous species fields provided a unique data set to validate recently available regional scale dispersion models that incorporate complex topography and varied land-use categories. This has been done electronically using GIS and by comparison of tabular and spatial data. The differences and divergence of the results were recorded and characterised.

#### 3.3.1 Dry deposition determination

One year of data from September 2006 to August 2007 was used for the calculations of **dry acidic deposition** over a year. The dry deposition rates were calculated from the measured ambient concentration (this study) and dry deposition velocity for the species using an inferential model ([Hicks \*et al.\*, 1987](#), [Hicks \*et al.\*, 1991](#)). The dry deposition rate, **F** is found as follows:

$$F = -V_d * C \quad (3.3)$$

where **C** is the atmospheric concentration and **V<sub>d</sub>** is the deposition velocity (downward flux). For an inferential model a number of meteorological parameters are required. Those parameters have been measured and included into an inferential model in a deposition calculation presented by [Mphepya \(2002\)](#).



For this study, a set of the deposition velocities were taken from [Mphepya \(2002\)](#). His work, based on a set of three years of monitored data (1996-1998), was used to calculate the deposition velocities for two particular sites – Elandsfontein and Palmer. A mix of 66% grass and 34% maize was considered to be representative of the Elandsfontein site, while a mix of 85% grass and 15% forest was considered for Palmer and this was based on field observation and GIS land cover analysis ([Mphepya, 2002](#)). Such surface vegetation mixes were considered to be well representative for the sites of this study and thus both set of data were suitable for this study. Differentiated deposition velocities for day and night were given for each different annual season ([Mphepya, 2002](#)) in each calendar year of observation as well as the three-year means. Those three-year means (per day/night and season) for both Elandsfontein and Palmer were then averaged and the Elandsfontein-Palmer averages applied to each site in the dry deposition calculations of this study (Table 3.1).

**Table 3.1: Calculation of seasonal inferred deposition velocities of SO<sub>2</sub> and NO<sub>2</sub> in cm s<sup>-1</sup> for this study based on prior determined velocities\*.**

SO <sub>2</sub>	Autumn		Winter		Spring		Summer	
	Day time	Night time	Day time	Night time	Day time	Night time	Day time	Night time
<i>Palmer average (1996-1998)</i>	0.26	0.12	0.14	0.1	0.24	0.12	0.37	0.15
<i>Elandsfontein average (1996-1998)</i>	0.26	0.12	0.15	0.1	0.22	0.11	0.35	0.15
<i>Mean between Palmer and Elandsfontein (1996-1998)</i>	<b>0.260</b>	<b>0.120</b>	<b>0.145</b>	<b>0.100</b>	<b>0.230</b>	<b>0.115</b>	<b>0.360</b>	<b>0.150</b>
NO <sub>2</sub>	Autumn		Winter		Spring		Summer	
	Day time	Night time	Day time	Night time	Day time	Night time	Day time	Night time
<i>Palmer average (1996-1998)</i>	0.13	0.04	0.05	0.04	0.11	0.04	0.24	0.08
<i>Elandsfontein average (1996-1998)</i>	0.14	0.1	0.05	0.04	0.12	0.05	0.26	0.08
<i>Mean between Palmer and Elandsfontein (1996-1998)</i>	<b>0.135</b>	<b>0.070</b>	<b>0.050</b>	<b>0.040</b>	<b>0.115</b>	<b>0.045</b>	<b>0.250</b>	<b>0.080</b>

\* Source: [Mphepya, 2002](#).



Another step taken in this calculation was to record daylight and darkness time. This was calculated exactly for different months and specific sites, based on the exact geo-position of each sampling site for the exact sampling period (US Navy Office, [Astronomical Information Center, Data Service, 2007](#)).

The deposition values were calculated for each month of both sampling years and summed for different seasons within the year by combining three months in each specific season.

### 3.3.2 *Wet and total acidic deposition*

In most cases, the long-term spatial variation in wet deposition is determined more by variations in the amount of precipitation amount and less by variations in concentrations in rain. The complexity of wet deposition led to the simplification of a few parameters. The wet deposition flux is given by calculating the measured concentration of the species of interest in the rain and the precipitation rate (Mphepya, 2002). The amount of precipitation is available from the dense meteorological network of the South African Weather Service (SAWS). The rain chemistry data used came from an extensive network of precipitation monitoring for the study region (Eskom).

In order to compile the study-specific estimate on the cumulative acidic deposition a **wet deposition** was estimated by using Eskom-researched 10 year chemical precipitation data (Turner and de Beer, 1996). Only the ion concentrations for the compounds of interest were extracted for this study wet deposition calculation (Table 3.2).

**Table 3.2: The 10 year period volume weighted mean precipitation ion concentrations ( $\mu\text{eq l}^{-1}$ ) extract\*.**

<i>Long-term precipitation chemistry measurement sites</i>	<i>Louis Trichardt</i>	<i>Amersfoort</i>	<i>Warden</i>	<i>Vryheid</i>
<i>Cations of importance</i>	<i>Cation Concentrations</i>			
<i>NH<sub>4</sub><sup>+</sup></i>	11.3	25.0	23.1	21.1
<i>Anions of importance</i>	<i>Anion Concentrations</i>			
<i>SO<sub>4</sub><sup>2-</sup></i>	15.3	57.2	46.8	40.5
<i>NO<sub>3</sub><sup>-</sup></i>	7.9	24.6	23.1	18.4

\* Source: [Turner and de Beer, 1996](#)

For the wet deposition estimate a simple inferential process was followed where the concentration of the chemical compound of interest (ten-year mean) was multiplied by the



cumulative (monthly and seasonal) precipitation amount for this study sampling time-frame.

$$F = C * P \quad (3.4)$$

In this equation **F** is wet flux ( $\text{mol m}^{-2} \text{yr}^{-1}$ ), **C** is measured concentration in precipitation ( $\text{mol m}^{-3}$ ) and **P** is precipitation rate ( $\text{mm yr}^{-1}$ ). For this study sulphate, nitrate and ammonium (in addition) were considered to obtain the overall in-organic sulphur and nitrogen deposition loads. The examples of the wet deposition calculation are provided in the Appendix A. Both the dry and wet deposition results were combined in order to derive a study-specific **total acidic deposition** estimate from sulphur and nitrogen (excluding organic acids). All the results (dry S and N deposition, wet S and N deposition and S and N acidic cumulative totals) were then compared with the available prior deposition estimated values for the comparably located sites (Amersfoort, Elandsfontein and Louis Trichardt).

Having four long-term precipitation chemistry sets for the four different geographic regions where the long-term precipitation chemistry was monitored enabled the use of varied sets differently suitable for the monitoring sites of this study. The deciding factor on which set of chemical precipitation concentration to use for which of the study sites depended on several factors such as geographical proximity, closeness to the pollution source region and distance from the background site (Table 3.3 and Figure 2.4).



**Table 3.3: Allocation of historical wet deposition anion concentrations\* to monitoring sites used in this study. (Colour used to indicate the wet chemistry sites.)**

<i>Site Number</i>	<i>Nearby Town</i>	<i>The pivot sites - basis for the others</i>	<i>10-year volume weighted mean (<math>\mu\text{eq.l}^{-1}</math>) for the pivot sites</i>
1	Standerton	Amersfoort	57.2
2	Amersfoort	Amersfoort	57.2
3	Piet Retief	Louis Trichardt	15.3
4	Badplaas	Louis Trichardt	15.3
5	Sabie	Louis Trichardt	15.3
6	Harrismith	Warden	46.8
7	Newcastle	Vryheid	40.5
8	Gluckstadt	Vryheid	40.5
9	Hluhluwe	Vryheid	40.5
10	Igwavuma	Vryheid	40.5
11	Masibikela	Louis Trichardt	15.3
12	Skukuza	Louis Trichardt	15.3
13	Escourt	Vryheid	40.5
14	Kranskop	Vryheid	40.5
15	Melmoth	Vryheid	40.5
16	Kwangwanase	Vryheid	40.5
17	Kriel	Amersfoort	57.2
18	Heilbron	Warden	46.8
19	Warmbaths	Louis Trichardt	15.3
20	Vaalwater	Louis Trichardt	15.3
21	Potgietersrus	Louis Trichardt	15.3
22	Marble Hall	Louis Trichardt	15.3
23	Steelpoort	Louis Trichardt	15.3
24	Haenertsburg	Louis Trichardt	15.3
25	Phalaborwa	Louis Trichardt	15.3
26	Memel	Warden	46.8
27	Utrecht	Vryheid	40.5
28	Pongola	Vryheid	40.5
29	Amsterdam	Louis Trichardt	15.3
30	Malelane	Louis Trichardt	15.3
31	Fourisburg	Warden	46.8



<b>Site Number</b>	<b>Nearby Town</b>	<b>The pivot sites - basis for the others</b>	<b>10-year volume weighted mean (<math>\mu\text{eq.l}^{-1}</math>) for the pivot sites</b>
<b>32</b>	Kroonstad	Warden	46.8
<b>33</b>	Northam	Louis Trichardt	15.3
<b>34</b>	Thabazimbi	Louis Trichardt	15.3
<b>35</b>	Tolwe	Louis Trichardt	15.3
<b>36</b>	Louis Trichardt	Louis Trichardt	15.3
<b>37</b>	Thohoyandou	Louis Trichardt	15.3

\*Turner and de Beer, 1996

### 3.3.3 *Measured and modelled comparison method*

Tables and diagrams were compared numerically, while plots were compared visually. This sub-task was limited to comparable sites, for which dry and wet deposition was modelled on a regional scale (Fourie, 2006). These were compared for concentrations of SO<sub>2</sub>, NO<sub>2</sub> and O<sub>3</sub> and dry and wet depositions for SO<sub>2</sub> and NO<sub>2</sub> over annual and seasonal cycles.



## 3.4 Results

### 3.4.1 *Dry deposition*

Dry deposition calculations are linearly dependant on concentration results, so similar observations for the spatial and temporal trends of dry deposition of SO<sub>2</sub> and NO<sub>2</sub> are expected to those expressed for the SO<sub>2</sub> and NO<sub>2</sub> concentrations respectively. As different deposition rates are applicable for day and night, total deposition rates are dependent on the changes of season and latitude. Calculations of deposition make use of publically accessible tables of daylight time at specified localities and by month (US Navy Office, Astronomical Information Center, Data Service, 2007).

#### *SO<sub>2</sub> dry deposition*

Annual average SO<sub>2</sub> dry depositions rates for the two annual cycles with the overall mean rate (September to August) are presented in Table 3.4.





**Table 3.4: SO<sub>2</sub> dry deposition inter-annual means comparison.**

<b>Site No.</b>	<b>Nearest geographic location</b>	<b>Sep05-Aug06 SO<sub>2</sub> as S (kg ha<sup>-1</sup> yr<sup>-1</sup>)</b>	<b>Sep06-Aug07 SO<sub>2</sub> as S (kg ha<sup>-1</sup> yr<sup>-1</sup>)</b>	<b>Mean rate SO<sub>2</sub> as S (kg ha<sup>-1</sup> yr<sup>-1</sup>)</b>	<b>Difference SO<sub>2</sub> as S (kg ha<sup>-1</sup> yr<sup>-1</sup>)</b>
1	Standerton	3.81	3.27	3.54	-0.54
2	Amersfoort	3.65	3.48	3.57	-0.17
3	Piet Retief	2.51	2.41	2.46	-0.10
4	Badplaas	1.23	1.08	1.16	-0.15
5	Sabie	0.57	0.93	0.75	0.36
6	Harrismith	1.12	0.86	0.99	-0.26
7	Newcastle	1.24	1.11	1.18	-0.14
8	Gluckstad	0.75	1.16	0.96	0.41
9	Hluhluwe	0.73	0.59	0.66	-0.15
10	Ingwavuma	0.46	0.55	0.51	0.09
11	Masibikela	0.56	0.62	0.59	0.06
12	Skukuza	0.52	0.68	0.60	0.15
13	Escourt	0.51	0.78	0.65	0.27
14	Kranskop	0.72	0.59	0.66	-0.13
15	Melmoth	1.09	0.86	0.98	-0.22
16	Kosi Bay	0.48	0.36	0.42	-0.11
17	Kriel	7.90	7.40	7.65	-0.50
18	Heilbron	1.77	1.78	1.78	0.01
19	Warmbaths	0.94	1.00	0.97	0.06
20	Vaalwater	0.73	0.88	0.81	0.14
21	Potgietersrus	1.95	1.61	1.78	-0.33
22	Marble Hall	1.05	1.03	1.04	-0.02
23	Steelpoort	1.08	0.95	1.02	-0.13
24	Haenertsburg	0.62	0.66	0.64	0.04
25	Phalaborwa	0.87	0.72	0.80	-0.15
26	Memel	1.89	1.42	1.66	-0.47
27	Utrecht	1.60	1.40	1.50	-0.20
28	Louwsburg	0.76	0.63	0.70	-0.13
29	Amsterdam	1.35	1.53	1.44	0.18
30	Malelane	1.19	1.02	1.11	-0.17
31	Fouriesburg	0.87	0.90	0.89	0.03
32	Kroonstad	0.99	0.94	0.97	-0.05
33	Pillansberg	1.37	1.37	1.37	0.01
34	Thabazimbi	1.92	1.37	1.65	-0.55
35	Tolwe	0.86	0.99	0.93	0.13
36	Louis Trichardt	0.63	0.57	0.60	-0.06
37	Thohoyandou	0.49	0.48	0.49	0.00



Site No.	Nearest geographic location	Sep05-Aug06 SO <sub>2</sub> as S (kg ha <sup>-1</sup> yr <sup>-1</sup> )	Sep06-Aug07 SO <sub>2</sub> as S (kg ha <sup>-1</sup> yr <sup>-1</sup> )	Mean rate SO <sub>2</sub> as S (kg ha <sup>-1</sup> yr <sup>-1</sup> )	Difference SO <sub>2</sub> as S (kg ha <sup>-1</sup> yr <sup>-1</sup> )
----------	-----------------------------	--	--	--	---

The highest annual mean SO<sub>2</sub> dry deposition rate (7.9 kg ha<sup>-1</sup> yr<sup>-1</sup> first year and 7.4 kg ha<sup>-1</sup> yr<sup>-1</sup> for the second year) occurred for the site in the centre of industrial source zone (site 17), followed by downwind sites (sites 1 and 2). The lowest SO<sub>2</sub> dry deposition (0.48 kg ha<sup>-1</sup> yr<sup>-1</sup> first year and 0.36 kg ha<sup>-1</sup> yr<sup>-1</sup> second year) occurred at the remote Kwa-Zulu Natal north coast (site 16). The combined record indicates an initially steep concentration gradient, spreading from high deposition at the epicentre of the industrial pollution over medium-distance remote to far-distant remote sites.

When deposition rates at all sites were compared year on year, the results for the two years differed, but no major difference was determined. Differences between rates varied up to 0.54 kg ha<sup>-1</sup> yr<sup>-1</sup> of SO<sub>2</sub> (Table 3.4).

#### *NO<sub>2</sub> dry deposition*

Annual average NO<sub>2</sub> deposition rates for the two annual cycles with the overall mean rate (September to August) are presented in Table 3.5.

**Table 3.5: NO<sub>2</sub> dry deposition inter-annual means comparison.**

Site no.	Nearest geographic location	Sep05-Aug06 NO <sub>2</sub> as N (kg ha <sup>-1</sup> yr <sup>-1</sup> )	Sep06-Aug07 NO <sub>2</sub> as N (kg ha <sup>-1</sup> yr <sup>-1</sup> )	Mean rate NO <sub>2</sub> as N (kg ha <sup>-1</sup> yr <sup>-1</sup> )	Difference NO <sub>2</sub> as N (kg ha <sup>-1</sup> yr <sup>-1</sup> )
1	Standerton	0.63	0.56	0.59	-0.07
2	Amersfoort	0.37	0.37	0.37	0.00
3	Piet Retief	0.23	0.24	0.24	0.00
4	Badplaas	0.15	0.14	0.14	-0.01
5	Sabie	0.10	0.15	0.12	0.04
6	Harrismith	0.28	0.33	0.31	0.05
7	Newcastle	0.23	0.29	0.26	0.06
8	Gluckstad	0.18	0.20	0.19	0.02
9	Hluhluwe	0.14	0.15	0.14	0.01
10	Ingwavuma	0.23	0.22	0.22	0.00
11	Masibikela	0.28	0.28	0.28	0.00
12	Skukuza	0.09	0.14	0.11	0.05
13	Escourt	0.20	0.23	0.22	0.03
14	Kranskop	0.23	0.22	0.23	-0.02
15	Melmoth	0.19	0.21	0.20	0.02
16	Kosi Bay	0.16	0.18	0.17	0.02



Site no.	Nearest geographic location	Sep05-Aug06 NO <sub>2</sub> as N (kg ha <sup>-1</sup> yr <sup>-1</sup> )	Sep06-Aug07 NO <sub>2</sub> as N (kg ha <sup>-1</sup> yr <sup>-1</sup> )	Mean rate NO <sub>2</sub> as N (kg ha <sup>-1</sup> yr <sup>-1</sup> )	Difference NO <sub>2</sub> as N (kg ha <sup>-1</sup> yr <sup>-1</sup> )
17	Kriel	0.66	0.64	0.65	-0.02
18	Heilbron	0.24	0.35	0.29	0.11
19	Warmbaths	0.22	0.27	0.25	0.05
20	Vaalwater	0.23	0.23	0.23	0.00
21	Potgietersrus	0.24	0.24	0.24	0.00
22	Marble Hall	0.26	0.28	0.27	0.03
23	Steelpoort	0.33	0.38	0.36	0.05
24	Haenertsburg	0.23	0.25	0.24	0.03
25	Phalaborwa	0.21	0.19	0.20	-0.02
26	Memel	0.25	0.25	0.25	0.00
27	Utrecht	0.17	0.18	0.18	0.00
28	Louwsburg	0.08	0.16	0.12	0.08
29	Amsterdam	0.21	0.29	0.25	0.08
30	Malelane	0.26	0.30	0.28	0.04
31	Fouriesburg	0.20	0.27	0.23	0.07
32	Kroonstad	0.36	0.36	0.36	0.00
33	Pillansberg	0.20	0.31	0.26	0.11
34	Thabazimbi	0.24	0.27	0.25	0.03
35	Tolwe	0.17	0.17	0.17	0.00
36	Louis Trichardt	0.18	0.18	0.18	0.00
37	Thohoyandou	0.44	0.41	0.43	-0.03

The highest record, 0.66 kg ha<sup>-1</sup> yr<sup>-1</sup> of NO<sub>2</sub> as N, occurred for the site downwind from the centre of industrial source pollution for the first year (site 1) and 0.64 kg ha<sup>-1</sup> yr<sup>-1</sup> of NO<sub>2</sub> as N in the centre of the industrial Highveld for the second year (site 17). The sites positioned downwind also show higher depositions (sites 1, Standerton and 2, Amersfoort). The lowest records 0.08 and 0.14 kg ha<sup>-1</sup> yr<sup>-1</sup> of NO<sub>2</sub> as N resulted for remote sites (site 28, Louwsburg in first annual cycle) and sites 4, Badplaas and 12, Skukuza (for the second annual cycle) respectively. Similar to the SO<sub>2</sub> conclusion, these results indicate a concentration gradient from high in the industrial Highveld over medium-distance sites towards the remote sites.

When deposition rates at all sites were compared year to year, the results for the two years differed by minor amounts. Differences in the rates varied up to 0.11 kg ha<sup>-1</sup> yr<sup>-1</sup> of NO<sub>2</sub> as N (Table 3.5).



### 3.4.2 Total wet deposition comparison

The wet deposition estimates are strongly dependant on the precipitation and greater inter-annual differences can be explained mostly by differences in inter-annual rainfall. It was chosen to present first the total deposition as potentially the most interesting (Table 3.6). Depositions for the separate acidic species follow (Table 3.8 - Table 3.10).

**Table 3.6: Total wet deposition rates of S and N acidifying (inorganic) species and their inter-annual comparison.**

Site No.	Nearest geographic location	Sep05-Aug06* (kg ha <sup>-1</sup> yr <sup>-1</sup> )	Sep06-Aug07* (kg ha <sup>-1</sup> yr <sup>-1</sup> )	Mean rate* (kg ha <sup>-1</sup> yr <sup>-1</sup> )	Difference 1 <sup>st</sup> year to 2 <sup>nd</sup> (kg ha <sup>-1</sup> yr <sup>-1</sup> )
1	Standerton	10.74	7.56	9.15	3.18
2	Amersfoort	15.03	6.59	10.81	8.44
3	Piet Retief	7.52	4.06	5.79	3.46
4	Badplaas	4.58	4.62	4.60	-0.04
5	Sabie	7.62	4.46	6.04	3.16
6	Harrismith	9.04	6.91	7.98	2.13
7	Newcastle	12.82	8.92	10.87	3.90
8	Gluckstad	6.14	7.09	6.62	-0.95
9	Hluhluwe	9.49	10.71	10.10	-1.22
10	Ingwavuma	10.04	10.78	10.41	-0.74
11	Masibikela	7.94	6.18	7.06	1.76
12	Skukuza	4.44	2.74	3.59	1.69
13	Escourt	10.93	8.16	9.55	2.76
14	Kranskop	10.95	9.26	10.11	1.68
15	Melmoth	8.09	7.97	8.03	0.13
16	Kosi Bay	10.31	13.12	11.72	-2.82
17	Kriel	14.65	7.74	11.20	6.92
18	Heilbron	10.94	4.95	7.95	6.00
19	Warmbaths	3.08	1.99	2.54	1.09
20	Vaalwater	4.17	2.64	3.41	1.53
21	Potgietersrus	2.79	2.81	2.80	-0.02
22	Marble Hall	3.54	2.95	3.25	0.59
23	Steelpoort	3.74	3.60	3.67	0.13
24	Haenertsburg	3.19	2.66	2.93	0.53
25	Phalaborwa	2.03	1.95	1.99	0.09
26	Memel	12.33	6.24	9.29	6.09
27	Utrecht	8.60	8.07	8.34	0.53
28	Louwsburg	4.02	5.56	4.79	-1.54
29	Amsterdam	4.49	4.95	4.72	-0.46
30	Malelane	7.94	3.58	5.76	4.36
31	Fouriesburg	13.03	8.25	10.64	4.78
32	Kroonstad	7.94	2.21	5.08	5.72
33	Pillansberg	3.77	3.62	3.70	0.15



34	Thabazimbi	4.73	2.10	3.42	2.64
35	Tolwe	2.46	2.17	2.32	0.28
36	Louis Trichardt	3.22	2.92	3.07	0.31
37	Thohoyandou	4.85	3.61	4.23	1.24

\* Wet deposition of  $\text{SO}_4^{2-}$  as S,  $\text{NO}_3^-$  and  $\text{NH}_4^+$  as N;

As to be expected, the highest total wet deposition estimates were for sites in and near the industrial Highveld source area (site 2, Amersfoort,  $15.0 \text{ kg ha}^{-1} \text{ yr}^{-1}$  of  $\text{SO}_4^{2-}$  as S,  $\text{NO}_3^-$  and  $\text{NH}_4^+$  as N); and site 17, Elandsfontein,  $14.7 \text{ kg ha}^{-1} \text{ yr}^{-1}$ ) for the first year. However, second year results show the limitation of generalising, as the highest total wet deposition ( $13.1 \text{ kg ha}^{-1} \text{ yr}^{-1}$ ) was for a far-background location, site 16 at Kosi Bay, which recorded the third highest annual precipitation for the second year. The lowest wet deposition estimates of  $2.03$  and  $1.95 \text{ kg ha}^{-1} \text{ yr}^{-1}$  were for site 25, Phalaborwa, which also had the lowest precipitation records for both years.

When the total wet deposition rates for all sites were compared year to year, the results for two years differed substantially, varying by up to  $8.44 \text{ kg ha}^{-1} \text{ yr}^{-1}$  ( $\text{SO}_4^{2-}$  as S,  $\text{NO}_3^-$  and  $\text{NH}_4^+$  as N) (Table 3.6).

The extent of the precipitation differences and their relationship with the wet depositions thus needed to be compared. The absolute difference between the two years of precipitation records varied and in almost similar range to the wet deposition results (Table 3.7).

**Table 3.7: The rainfall and total wet deposition inter-annual comparison.**

<i>Site No.</i>	<i>Nearest geographic location</i>	<i>Rainfall Sep05 - Aug06 (mm)</i>	<i>Rainfall Sep06 - Aug07 (mm)</i>	<i>Difference 1<sup>st</sup> to 2<sup>nd</sup> yr rainfall (mm)</i>	<i>Difference from 2-year rainfall mean (%)</i>	<i>Differences from 2-year mean wet deposition (%)</i>	<i>Difference between two last columns (%)</i>
1	Standerton	668	470	198	9%	9%	0%
2	Amersfoort	934	410	525	35%	35%	0%
3	Piet Retief	1465	543	922	78%	78%	0%
4	Badplaas	892	619	273	92%	60%	32%
5	Sabie	1485	598	887	36%	-1%	37%
6	Harrismith	648	488	160	85%	52%	33%
7	Newcastle	1068	693	375	28%	27%	1%
8	Gluckstad	512	551	-39	43%	36%	7%
9	Hluhluwe	790	832	-42	-7%	-14%	7%



<b>Sit e No.</b>	<b>Nearest geographic location</b>	<b>Rainfall Sep05 - Aug06 (mm)</b>	<b>Rainfall Sep06 - Aug07 (mm)</b>	<b>Difference 1<sup>st</sup> to 2<sup>nd</sup> yr rainfall (mm)</b>	<b>Difference from 2-year rainfall mean (%)</b>	<b>Differences from 2-year mean wet deposition (%)</b>	<b>Differenc e between two last columns (%)</b>
10	Ingwavuma	836	838	-1	-5%	-12%	7%
11	Masibikela	1547	827	720	0%	-7%	7%
12	Skukuza	865	367	497	61%	25%	36%
13	Escourt	910	634	276	81%	47%	34%
14	Kranskop	912	719	192	36%	29%	7%
15	Melmoth	674	619	55	24%	17%	7%
16	Kosi Bay	858	1019	-161	9%	2%	7%
17	Kriel	911	481	430	-17%	-24%	7%
18	Heilbron	784	349	435	62%	62%	0%
19	Warmbaths	600	266	334	77%	75%	1%
20	Vaalwater	813	354	459	77%	43%	34%
21	Potgietersrus	544	376	168	79%	45%	34%
22	Marble Hall	690	396	295	36%	-1%	37%
23	Steelpoort	728	483	245	54%	18%	36%
24	Haenertsburg	621	357	265	41%	4%	37%
25	Phalaborwa	396	260	135	54%	18%	36%
26	Memel	884	440	444	41%	4%	37%
27	Utrecht	717	627	90	67%	66%	1%
28	Louwsburg	335	432	-97	13%	6%	7%
29	Amsterdam	875	663	212	-25%	-32%	7%
30	Malelane	1547	480	1067	28%	-10%	37%
31	Fouriesburg	934	583	351.1	105%	76%	30%
32	Kroonstad	668	470	198	46%	45%	1%
33	Pillansberg	934	410	525	114%	113%	1%
34	Thabazimbi	1465	543	922	41%	4%	37%
35	Tolwe	892	619	273	107%	77%	29%
36	Louis Trichardt	1485	598	887	49%	12%	37%
37	Thohoyandou	648	488	160	47%	10%	37%

In terms of individual sulphur and nitrogen acidifying compounds wet deposition comparisons the following sections contain the tables and highlights for each of those compounds.



### 3.4.3 Sulphate wet deposition

The estimation for this compound followed the general wet deposition trends, similar to the total wet deposition (Table 3.8).

**Table 3.8: Wet deposition of  $\text{SO}_4^{2-}$  for two annual cycles and comparison.**

Site No.	Nearest geographic location	Sep05-Aug06 $\text{SO}_4^{2-}$ as S ( $\text{kg ha}^{-1} \text{yr}^{-1}$ )	Sep06-Aug07 $\text{SO}_4^{2-}$ as S ( $\text{kg ha}^{-1} \text{yr}^{-1}$ )	Mean rate ( $\text{kg ha}^{-1} \text{yr}^{-1}$ )	Difference 1st to 2nd year ( $\text{kg ha}^{-1} \text{yr}^{-1}$ )
1	Standerton	6.11	4.30	5.21	1.81
2	Amersfoort	8.55	3.75	6.15	4.80
3	Piet Retief	3.59	1.33	2.46	2.26
4	Badplaas	2.18	1.51	1.85	0.67
5	Sabie	3.63	1.46	2.55	2.17
6	Harrismith	4.85	3.65	4.25	1.20
7	Newcastle	6.92	4.49	5.71	2.43
8	Gluckstad	3.31	3.57	3.44	-0.26
9	Hluhluwe	5.12	5.39	5.26	-0.27
10	Ingwavuma	5.42	5.43	5.43	-0.01
11	Masibikela	3.79	2.03	2.91	1.76
12	Skukuza	2.12	0.90	1.51	1.22
13	Escourt	5.90	4.11	5.01	1.79
14	Kranskop	5.91	4.66	5.29	1.25
15	Melmoth	4.37	4.01	4.19	0.36
16	Kosi Bay	5.56	6.61	6.09	-1.04
17	Kriel	8.33	4.40	6.37	3.93
18	Heilbron	5.87	2.61	4.24	3.26
19	Warmbaths	1.47	0.65	1.06	0.82
20	Vaalwater	1.99	0.87	1.43	1.12
21	Potgietersrus	1.33	0.92	1.13	0.41
22	Marble Hall	1.69	0.97	1.33	0.72
23	Steelpoort	1.78	1.18	1.48	0.60
24	Haenertsburg	1.52	0.87	1.20	0.65
25	Phalaborwa	0.97	0.64	0.81	0.33
26	Memel	6.62	3.30	4.96	3.32
27	Utrecht	4.64	4.06	4.35	0.58
28	Louwsburg	2.17	2.80	2.49	-0.63
29	Amsterdam	2.14	1.62	1.88	0.52
30	Malelane	3.79	1.17	2.48	2.61
31	Fouriesburg	6.99	4.36	5.68	2.63
32	Kroonstad	4.26	1.17	2.72	3.09



33	Pillansberg	1.80	1.19	1.50	0.61
34	Thabazimbi	2.26	0.69	1.48	1.57
35	Tolwe	1.17	0.71	0.94	0.46
36	Louis Trichardt	1.54	0.96	1.25	0.58
37	Thohoyandou	2.31	1.18	1.75	1.13

When sulphate wet deposition rates for all sites were compared year to year, the results for two years differed. Values varied up to  $4.80 \text{ kg ha}^{-1} \text{ yr}^{-1}$  ( $\text{SO}_4^{2-}$  as S) for the later year in comparison with the earlier one in absolute terms

### 3.4.4 Nitrate wet deposition

The estimation for this compound followed the general wet deposition trend and the same can be said as for the total wet deposition (Table 3.9).

**Table 3.9: Wet deposition rates of  $\text{NO}_3^-$  as N ( $\text{kg ha}^{-1} \text{ yr}^{-1}$ ) for two annual cycles and comparison.**

Site No.	Nearest geographic location	Sep05-Aug06* ( $\text{kg ha}^{-1} \text{ yr}^{-1}$ )	Sep06-Aug07 ( $\text{kg ha}^{-1} \text{ yr}^{-1}$ )	Mean deposition* ( $\text{kg ha}^{-1} \text{ yr}^{-1}$ )	Difference * ( $\text{kg ha}^{-1} \text{ yr}^{-1}$ )
1	Standerton	2.30	1.62	1.96	0.68
2	Amersfoort	3.22	1.41	2.32	1.81
3	Piet Retief	1.62	1.87	1.75	-0.25
4	Badplaas	0.99	2.13	1.56	-1.14
5	Sabie	1.64	2.06	1.85	-0.42
6	Harrismith	2.10	1.68	1.89	0.42
7	Newcastle	2.75	2.38	2.57	0.36
8	Gluckstad	1.32	1.90	1.61	-0.58
9	Hluhluwe	2.04	2.86	2.45	-0.83
10	Ingwavuma	2.15	2.88	2.52	-0.73
11	Masibikela	1.71	2.85	2.28	-1.14
12	Skukuza	0.96	1.27	1.12	-0.31
13	Escourt	2.34	2.18	2.26	0.16
14	Kranskop	2.35	2.48	2.42	-0.13
15	Melmoth	1.74	2.13	1.94	-0.39
16	Kosi Bay	2.21	3.51	2.86	-1.30
17	Kriel	3.14	1.66	2.40	1.48
18	Heilbron	2.54	1.20	1.87	1.33
19	Warmbaths	0.66	0.92	0.79	-0.25
20	Vaalwater	0.90	1.22	1.06	-0.32
21	Potgietersrus	0.60	1.30	0.95	-0.69





Site No.	Nearest geographic location	Sep05-Aug06* (kg ha <sup>-1</sup> yr <sup>-1</sup> )	Sep06-Aug07 (kg ha <sup>-1</sup> yr <sup>-1</sup> )	Mean deposition* (kg ha <sup>-1</sup> yr <sup>-1</sup> )	Difference * (kg ha <sup>-1</sup> yr <sup>-1</sup> )
22	Marble Hall	0.76	1.36	1.06	-0.60
23	Steelpoort	0.80	1.66	1.23	-0.86
24	Haenertsburg	0.69	1.23	0.96	-0.54
25	Phalaborwa	0.44	0.90	0.67	-0.46
26	Memel	2.86	1.52	2.19	1.34
27	Utrecht	1.85	2.16	2.01	-0.31
28	Louwsburg	0.86	1.49	1.18	-0.63
29	Amsterdam	0.97	2.28	1.63	-1.31
30	Malelane	1.71	1.65	1.68	0.06
31	Fouriesburg	3.02	2.01	2.52	1.01
32	Kroonstad	1.84	0.54	1.19	1.30
33	Pillansberg	0.81	1.67	1.24	-0.86
34	Thabazimbi	1.02	0.97	1.00	0.05
35	Tolwe	0.53	1.00	0.77	-0.47
36	Louis Trichardt	0.69	1.34	1.02	-0.65
37	Thohoyandou	1.04	1.66	1.35	-0.62

\* Wet deposition rates of NO<sub>3</sub><sup>-</sup> as N

When all sites results were compared year to year, the results for two years differed. No major difference was determined and values varied up to 1.81 kg ha<sup>-1</sup> yr<sup>-1</sup> (NO<sub>3</sub><sup>-</sup> as N) for the later year in comparison with the earlier one in absolute term.

### 3.4.5 Ammonium wet deposition

The estimation for this compound followed the general wet deposition trend and the same can be said as for the total wet deposition (Table 3.10).

**Table 3.10: Wet deposition rates of NH<sub>4</sub><sup>+</sup> for two annual cycles and comparison.**

Site	Nearest geographic location	Sep05-Aug06* (kg ha <sup>-1</sup> yr <sup>-1</sup> )	Sep06-Aug07* (kg ha <sup>-1</sup> yr <sup>-1</sup> )	Mean rate * (kg ha <sup>-1</sup> yr <sup>-1</sup> )	Difference 1 <sup>st</sup> year to 2 <sup>nd</sup> (kg ha <sup>-1</sup> yr <sup>-1</sup> )
1	Standerton	2.33	1.64	1.99	0.69
2	Amersfoort	3.27	1.43	2.35	1.83
3	Piet Retief	2.31	0.86	1.59	1.46
4	Badplaas	1.41	0.98	1.20	0.43
5	Sabie	2.35	0.94	1.65	1.40
6	Harrismith	2.09	1.58	1.84	0.52
7	Newcastle	3.15	2.04	2.60	1.11
8	Gluckstad	1.51	1.63	1.57	-0.12



Site	Nearest geographic location	Sep05-Aug06* (kg ha <sup>-1</sup> yr <sup>-1</sup> )	Sep06-Aug07* (kg ha <sup>-1</sup> yr <sup>-1</sup> )	Mean rate * (kg ha <sup>-1</sup> yr <sup>-1</sup> )	Difference 1 <sup>st</sup> year to 2 <sup>nd</sup> (kg ha <sup>-1</sup> yr <sup>-1</sup> )
9	Hluhluwe	2.33	2.45	2.39	-0.12
10	Ingwavuma	2.47	2.47	2.47	0.00
11	Masibikela	2.44	1.31	1.88	1.14
12	Skukuza	1.37	0.58	0.98	0.79
13	Escourt	2.69	1.87	2.28	0.81
14	Kranskop	2.69	2.12	2.41	0.57
15	Melmoth	1.99	1.83	1.91	0.16
16	Kosi Bay	2.53	3.01	2.77	-0.47
17	Kriel	3.18	1.68	2.43	1.50
18	Heilbron	2.53	1.13	1.83	1.41
19	Warmbaths	0.95	0.42	0.69	0.53
20	Vaalwater	1.28	0.56	0.92	0.73
21	Potgietersrus	0.86	0.59	0.73	0.26
22	Marble Hall	1.09	0.62	0.86	0.47
23	Steelpoort	1.15	0.76	0.96	0.39
24	Haenertsburg	0.98	0.56	0.77	0.42
25	Phalaborwa	0.63	0.41	0.52	0.21
26	Memel	2.86	1.42	2.14	1.43
27	Utrecht	2.11	1.85	1.98	0.26
28	Louwsburg	0.99	1.27	1.13	-0.29
29	Amsterdam	1.38	1.05	1.22	0.33
30	Malelane	2.44	0.76	1.60	1.69
31	Fouriesburg	3.02	1.88	2.45	1.13
32	Kroonstad	1.84	0.51	1.18	1.33
33	Pillansberg	1.16	0.77	0.97	0.39
34	Thabazimbi	1.46	0.44	0.95	1.01
35	Tolwe	0.76	0.46	0.61	0.30
36	Louis Trichardt	0.99	0.62	0.81	0.38
37	Thohoyandou	1.49	0.76	1.13	0.73

\* Wet deposition rates of NH<sub>4</sub><sup>+</sup> as N

When all depositions were compared year to year, the results for two years differed. No major difference was determined and values varied up to 1.83 kg ha<sup>-1</sup> yr<sup>-1</sup> (NH<sub>4</sub><sup>+</sup> as N) in absolute terms.

### 3.4.6 Total (dry and wet) deposition inter-annual comparison

Dry deposition calculations were directly dependant on concentration results. Thus, similar trends to those expressed for the SO<sub>2</sub> and NO<sub>2</sub> concentrations were found to be valid for



the dry deposition of SO<sub>2</sub> and NO<sub>2</sub>. Wet deposition was dependant on the sampling period precipitation, thus the wetter year had higher deposition rates than the dryer year. The precipitation difference between years was substantial for many sites and that reflected in the wet deposition differences from one year to the next. These variable wet deposition estimates thus influenced the cumulative (total dry & wet) deposition results (Table 3.11). It is important to note here that the total deposition calculated in this study did not include dry particulate deposition but included only the gaseous dry deposition and wet deposition.

**Table 3.11: Total cumulative (wet and dry) deposition rate inter-annual comparison.**

Site No.	Nearest geographic location	Sep05-Aug06 (kg ha <sup>-1</sup> yr <sup>-1</sup> )*	Sep6-Aug07 (kg ha <sup>-1</sup> yr <sup>-1</sup> )*	Mean rate (kg ha <sup>-1</sup> yr <sup>-1</sup> )*	Difference 1 <sup>st</sup> year to 2 <sup>nd</sup> (kg ha <sup>-1</sup> yr <sup>-1</sup> )*
1	Standerton	15.20	11.40	13.30	3.80
2	Amersfoort	19.00	10.40	14.70	8.60
3	Piet Retief	10.30	6.70	8.50	3.60
4	Badplaas	6.00	5.80	5.90	0.10
5	Sabie	8.30	5.50	6.90	2.80
6	Harrismith	10.40	8.10	9.25	2.30
7	Newcastle	14.30	10.30	12.30	4.00
8	Gluckstad	7.10	8.50	7.80	-1.40
9	Hluhluwe	10.40	11.40	10.90	-1.10
10	Ingwavuma	10.70	11.60	11.15	-0.80
11	Masibikela	8.80	7.10	7.95	1.70
12	Skukuza	5.10	3.60	4.35	1.50
13	Escourt	11.60	9.20	10.40	2.50
14	Kranskop	11.90	10.10	11.00	1.80
15	Melmoth	9.40	9.00	9.20	0.30
16	Kosi Bay	10.90	13.70	12.30	-2.70
17	Kriel	23.20	15.80	19.50	7.40
18	Heilbron	13.00	7.10	10.05	5.90
19	Warmbaths	4.20	3.30	3.75	1.00
20	Vaalwater	5.10	3.80	4.45	1.40
21	Potgietersrus	5.00	4.70	4.85	0.30
22	Marble Hall	4.80	4.30	4.55	0.60
23	Steelpoort	5.10	4.90	5.00	0.20
24	Haenertsburg	4.00	3.60	3.80	0.50
25	Phalaborwa	3.10	2.90	3.00	0.30
26	Memel	14.50	7.90	11.20	6.60
27	Utrecht	10.40	9.60	10.00	0.70
28	Louwsburg	4.90	6.40	5.65	-1.50
29	Amsterdam	6.00	6.80	6.40	-0.70
30	Malelane	9.40	4.90	7.15	4.50



Site No.	Nearest geographic location	Sep05-Aug06 (kg ha <sup>-1</sup> yr <sup>-1</sup> )*	Sep6-Aug07 (kg ha <sup>-1</sup> yr <sup>-1</sup> )*	Mean rate (kg ha <sup>-1</sup> yr <sup>-1</sup> )*	Difference 1 <sup>st</sup> year to 2 <sup>nd</sup> year (kg ha <sup>-1</sup> yr <sup>-1</sup> )*
31	Fouriesburg	14.10	9.40	11.75	4.70
32	Kroonstad	9.30	3.50	6.40	5.80
33	Pillansberg	5.30	5.30	5.30	0.00
34	Thabazimbi	6.90	3.70	5.30	3.20
35	Tolwe	3.50	3.30	3.40	0.10
36	Louis Trichardt	4.00	3.70	3.85	0.40
37	Thohoyandou	5.80	4.50	5.15	1.30

\*Wet deposition includes: SO<sub>4</sub><sup>2-</sup> and SO<sub>2</sub> as S, NO<sub>3</sub><sup>-</sup>, NO<sub>2</sub> and NH<sub>4</sub><sup>+</sup> as N.

As expected total deposition estimates are highest for the site with high dry deposition and relatively high wet deposition. The site 17, Elandsfontein at the centre of the industrial Highveld was expected to be the highest with overall total acidic deposition 23.2 kg ha<sup>-1</sup> yr<sup>-1</sup> for the first year and 15.8 kg ha<sup>-1</sup> yr<sup>-1</sup> for the second year. The sites downwind of the industrial Highveld (site 1, Standerton and site 2, Amersfoort) had second highest cumulative deposition results for both annual cycles. The lowest total acidic deposition estimate was recorded for the site 25 near Phalaborwa, which had low dry and wet deposition, markedly with low precipitation affecting the wet deposition; 3.1 kg ha<sup>-1</sup> yr<sup>-1</sup> first year and 2.9 kg ha<sup>-1</sup> yr<sup>-1</sup> second year.

When the results for all the sites were compared year to year, the results differed substantially for certain sites as the difference range varied up to 8.6 kg ha<sup>-1</sup> yr<sup>-1</sup> for the later year in comparison with the earlier one in absolute terms (Table 3.11).

### 3.5 Comparison between measured and modelled results

The measured concentration data derived from this study, with derived computations of dry and wet deposition, provided results for a comparison with two suitable regional scale sets of modelled concentration and deposition results. Comparisons of the measured sulphur and nitrogen compounds are presented for two annual cycles and for seasonal periods for concentrations and for dry and wet depositions. A regional scale ozone comparison was carried out of modelled versus measured study data, for two growing seasons, as the modelling data did not extend to a full annual cycle (Zunckel *et al.*, 2006).



### 3.6 Results of modelled and measured comparison

#### 3.6.1 Sulphur

The next sections presents a comparison of measured results averaged over the period 2005 to 2007, to modelled results using meteorological data for 2000 and emission inventories from two sources from circa 1995 and 2000. Methodologically such a comparison could be challenged. Thus, some of the assumptions are stated here in advance of the presentation:

- It is assumed that the source activity has not changed significantly between the modelled and measured years – a reasonable assumption, as there have been no new large power plants commissioned or decommissioned.
- As the averaging periods used are monthly, obvious daily variations in meteorology are averaged out. However, it is assumed that there are no significant inter-annual variations in synoptic meteorology. This is a weak assumption, as significant changes in air transport patterns occur depending on the phase of the ENSO cycle, as recently shown by [Kanyanga \(2008\)](#).

Acknowledging these possible weaknesses, the comparison is made as a first step towards validating the most recent available regional modelling estimates against the only available set of comprehensive regional measured concentrations.

Tabulated modelled concentrations and depositions were available at three locations corresponding to measured sites for this study – Amersfoort (site 2), Elandsfontein (site 17, near Kriel) and Louis Trichardt (site 36).

##### *Comparison of annual average SO<sub>2</sub> airborne concentrations*

Annual average measured concentrations are compared to the modelled concentrations in Figure 3.3.

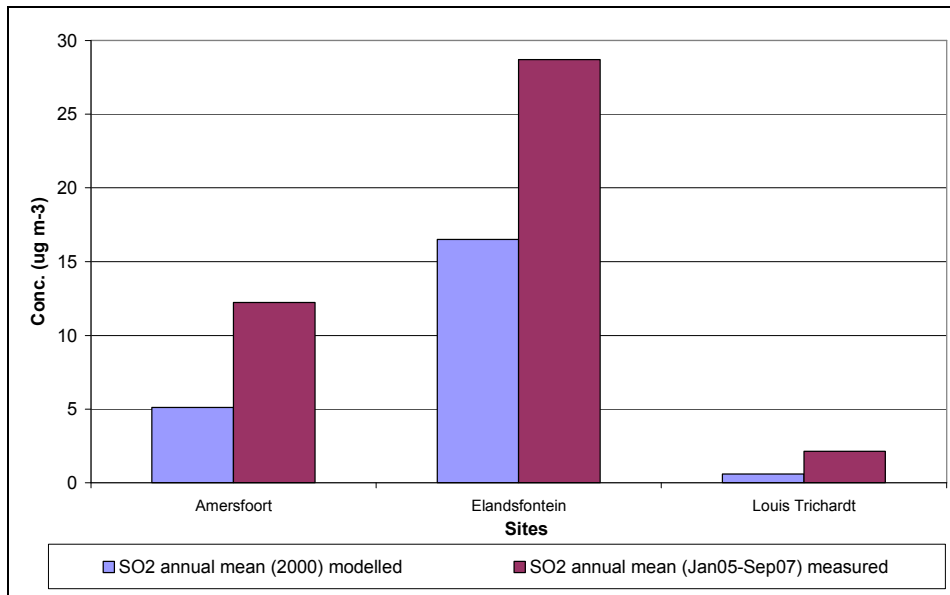


**Figure 3.3: SO<sub>2</sub> comparison of modelled (2000) and measured concentrations (Jan05-Sep07) for three sites.**

The model under-predicts the concentrations significantly at these locations. This could be due to the coarse resolution of the modelling domain leading to smoothing of the peak plume impacts. Alternatively, the differences may be due to inter-annual synoptic meteorological differences, which affect the transport and fate of the pollutants.

In terms of absolute and relevant number differences (the annual concentration means), they are given in Table 3.12.

**Table 3.12: SO<sub>2</sub> mean annual concentration comparison for all three sites.**

Site	SO <sub>2</sub> annual mean (2000) modelled (µg m <sup>-3</sup> )	SO <sub>2</sub> annual mean (Jan05-Sep07) measured (µg m <sup>-3</sup> )	Relative difference (modelled – measured) / measured (%)
<b>Amersfoort</b>	5.1	12	-58%
<b>Elandsfontein</b>	17	29	-41%
<b>Louis Trichardt</b>	0.6	2.1	-71%

*Comparison of seasonal SO<sub>2</sub> airborne concentrations*

Comparisons of monthly mean measured and modelled SO<sub>2</sub> concentrations for each site are made in Figure 3.4 to Figure 3.6.

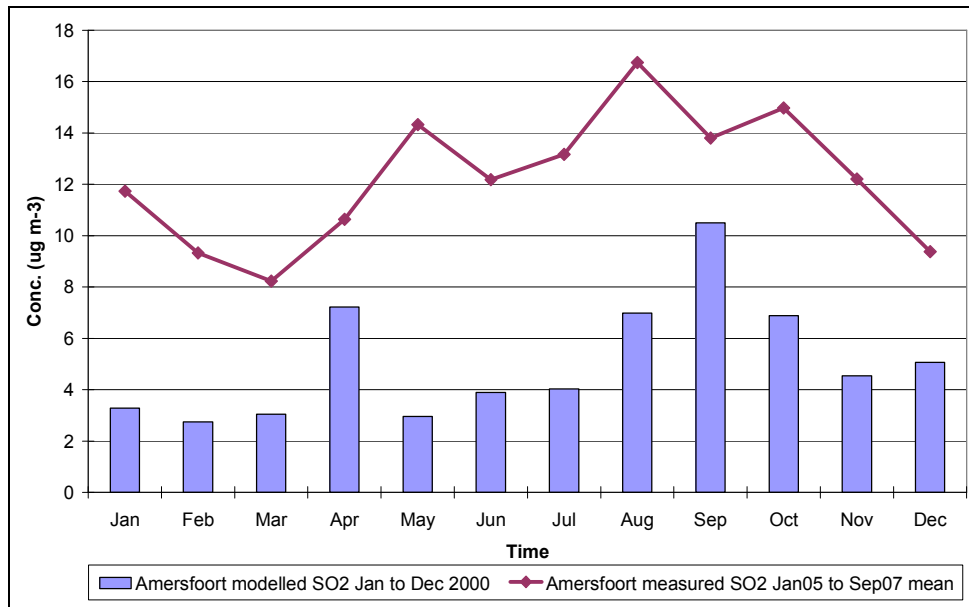


**Figure 3.4:** Comparison of SO<sub>2</sub> seasonal modelled and measured mean concentrations for Amersfoort (site 2).

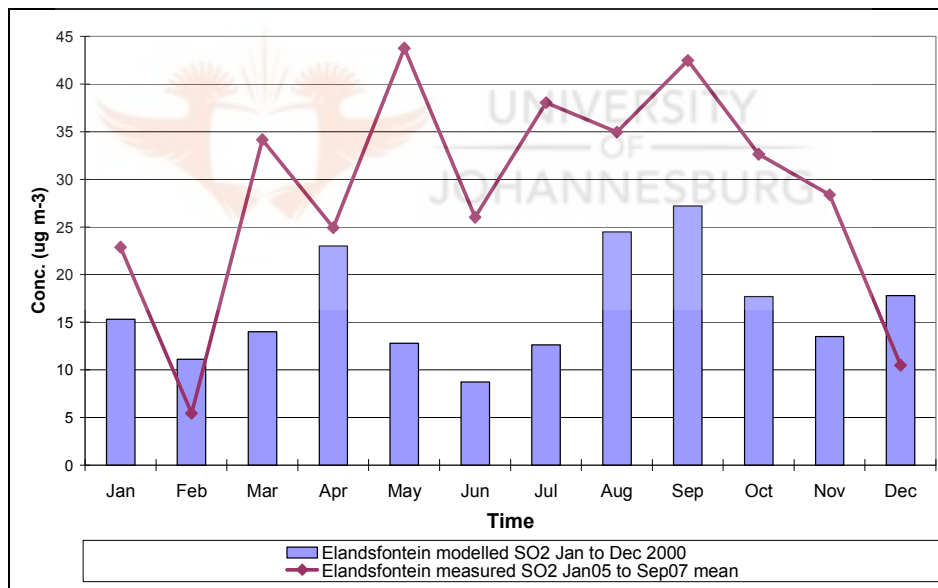


**Figure 3.5:** Comparison of SO<sub>2</sub> seasonal modelled and measured mean concentrations for Elandsfontein (site 17).

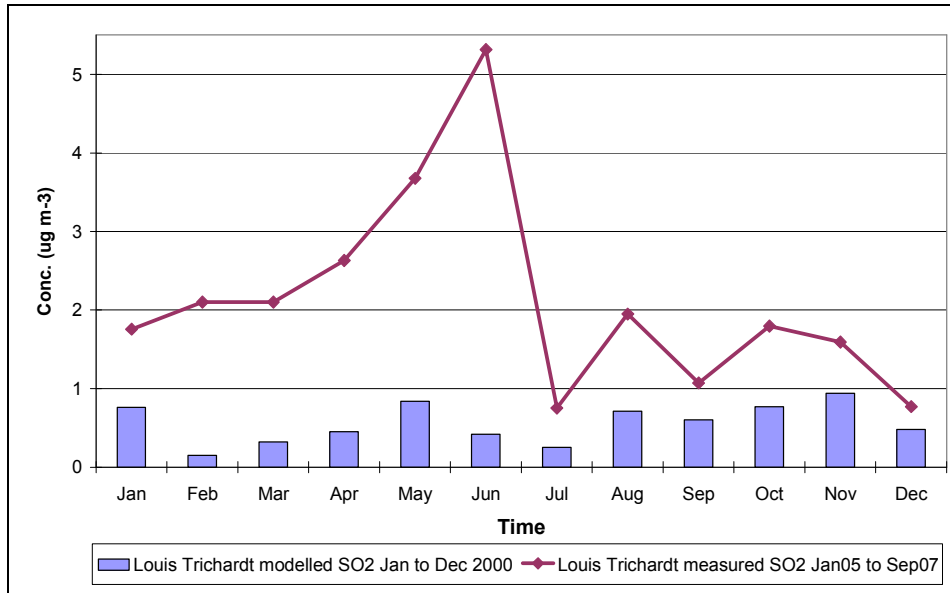


**Figure 3.6: Comparison of SO<sub>2</sub> seasonal modelled and measured mean concentrations for Louis Trichardt (site 36).**

The modelling and monitoring concentrations match within a broad range and the seasonal variations do not show high correlation. Thus no further statistical analysis was performed. A need for a dedicated modelling, which would match the time span and the species monitored for this study, is suggested for a proper modelling validation.

#### *Comparison of annual sulphur dry deposition rates*

The sulphur dry deposition results were compared in a similar way. However, for this comparison the resulting values were for the period from September 2005 to August 2006 (one annual cycle) while the modelled data compared were for the time period from January to December 2000 (one annual cycle).

Although the dry S deposition results are directly dependent on the concentration data, the comparison for the modelled data set shows a close match. Considering all uncertainties of modelling the modelling dry deposition rates are almost identical to the S dry deposition rates based on the measured results (Figure 3.7).



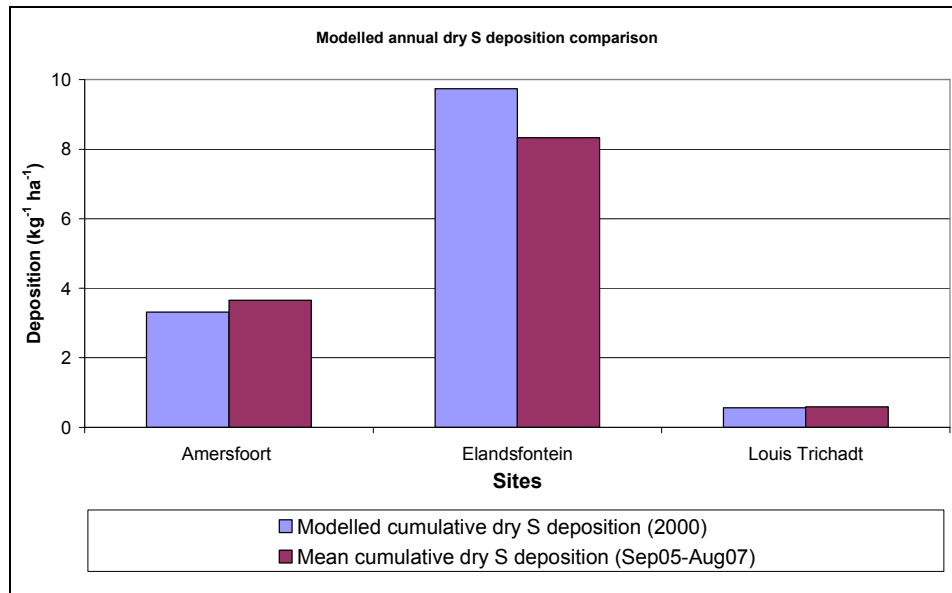


**Figure 3.7: Comparison of measured and modelled dry gaseous sulphur deposition:  $V_d$  for modelled (Fourie, 2006);  $V_d$  for measured (Mphepya, 2002) (Table 3.13).**

In terms of absolute and relative difference, the following table presents the numerical comparison (Table 3.13).

**Table 3.13: Sulphur dry deposition modelled ( $\text{SO}_2$  and  $\text{SO}_4^{2-}$ ) and measured ( $\text{SO}_2$ ) comparison.**

Site	Modelled dry S deposition (2000) (kg ha <sup>-1</sup> yr <sup>-1</sup> )	Measured dry S deposition (Sep06-Aug07) (kg ha <sup>-1</sup> yr <sup>-1</sup> )	Relative difference (modelled – measured) / measured (%)
<b>Amersfoort</b>	3.3	3.7	-2%
<b>Elandsfontein</b>	9.7	8.3	16%
<b>Louis Trichardt</b>	0.56	0.60	-1%

The strong influence of different deposition velocity rates,  $V_d$ , for modelling and to convert measured concentrations from this work (applied to both S and N species) seems to be the reason, which resulted in the modelling depositions being closer to measurements than for the comparison of modelling and measured concentration data (Table 3.14). The  $V_d$  values used by Fourie (2006) from which the modelling results are derived are higher than the  $V_d$  values chosen from Mphepya (2002). If the same  $V_d$  values were chosen, the modelled and measured deposition rates would differ by a factor of two.



**Table 3.14: Comparison of the deposition velocities ( $V_d$ ) of  $SO_2$  and  $NO_2$  for this study and for the compared modelling results.**

<b>Season</b>	<b>Day split</b>	<b>Measured mean* <math>V_d</math> for <math>SO_2</math> (<math>cm\ s^{-1}</math>)</b>	<b>Modelled** <math>V_d</math> for <math>SO_2</math> (<math>cm\ s^{-1}</math>)</b>	<b>Measured mean* <math>V_d</math> for <math>NO_2</math> (<math>cm\ s^{-1}</math>)</b>	<b>Modelled** <math>V_d</math> for <math>NO_2</math> (<math>cm\ s^{-1}</math>)</b>
<b>Autumn</b>	<b>daytime</b>	0.260	0.650	0.135	0.200
	<b>night-time</b>	0.120	0.070	0.070	0.070
<b>Winter</b>	<b>daytime</b>	0.145	0.650	0.050	0.200
	<b>night-time</b>	0.100	0.070	0.040	0.070
<b>Spring</b>	<b>daytime</b>	0.230	0.650	0.115	0.200
	<b>night-time</b>	0.115	0.070	0.045	0.070
<b>Summer</b>	<b>daytime</b>	0.360	0.650	0.250	0.200
	<b>night-time</b>	0.150	0.070	0.080	0.070
<b>Overall average</b>		<b>0.185</b>	<b>0.360</b>	<b>0.098</b>	<b>0.135</b>

Source: \* Mphepya, (2002); \*\* Fourie, (2006).

*Comparison of seasonal sulphur dry deposition rates*

In terms of seasonal dry sulphur deposition comparison for the representative sites, the results are presented in Table 3.15 to Table 3.17.

**Table 3.15:  $SO_2$  seasonal dry deposition comparison for site Amersfoort (AF).**

<b>Season</b>		<b>Spring</b>	<b>Summer</b>	<b>Autumn</b>	<b>Winter</b>
<b>Modelled</b>	<b>AF 2000 <math>SO_2</math> as S (<math>kg\ ha^{-1}\ yr^{-1}</math>)</b>	0.8	0.51	0.52	0.56
<b>Measured</b>	<b>AF 2006/7 <math>SO_2</math> as S (<math>kg\ ha^{-1}\ yr^{-1}</math>)</b>	0.93	1.26	0.66	0.64
<b>(Modelled – measured) /measured (%)</b>		-14%	-60%	-21%	-12%



**Table 3.16: SO<sub>2</sub> seasonal dry deposition comparison for site Elandsfontein (EF).**

Season		Spring	Summer	Autumn	Winter
<b>Modelled</b>	<b>EF 2000 SO<sub>2</sub> as S (kg ha<sup>-1</sup> yr<sup>-1</sup>)</b>	2	2	2.2	1.7
<b>Measured</b>	<b>EF 2006/7 SO<sub>2</sub> as S (kg ha<sup>-1</sup> yr<sup>-1</sup>)</b>	2.27	1.36	2.04	1.73
	<b>(Modelled – measured) /measured (%)</b>	-12%	47%	8%	-2%

**Table 3.17: SO<sub>2</sub> seasonal dry deposition comparison for site Louis Trichardt (LT).**

Season		Spring	Summer	Autumn	Winter
<b>Modelled</b>	<b>LT 2000 SO<sub>2</sub> as S (kg ha<sup>-1</sup> yr<sup>-1</sup>)</b>	0.10	0.10	0.10	0.10
<b>Measured</b>	<b>LT 2006/7 SO<sub>2</sub> as S (kg ha<sup>-1</sup> yr<sup>-1</sup>)</b>	0.12	0.16	0.21	0.08
	<b>(Modelled – measured) /measured (%)</b>	-16%	-39%	-51%	27%

The seasonal dry deposition comparison reveals that the modelling *underestimated* the concentration for remote rural sites although the measured and modelling results are both low. The SO<sub>2</sub> concentrations for the site in the centre of industrial Highveld were *overestimated* by modelling substantially. The Elandsfontein (site 17) modelling overestimation is the highest for autumn and then winter, while summer result diverged least. The concentrations for the site just downwind off the industrial Highveld are essentially very close. There is a reasonable agreement between monitored and modelled seasonal concentrations for the sites.

*Comparison of sulphur annual wet deposition rates*

The measured wet deposition results are derived from the measured concentration of the species of interest in the rain and multiplied by the precipitation rate. The rain chemistry data used came from an extensive Eskom network of precipitation monitoring for the study region (Turner and de Beer, 1996) (as discussed in Section 2.3.2). As the wet deposition is highly dependant on rainfall that varies considerably between years, comparisons of wet deposition rates show much more variability. Both sulphur and nitrogen wet deposition species should show a strong correlation with annual differences, and particularly seasonality of rainfall (Figure 3.8).

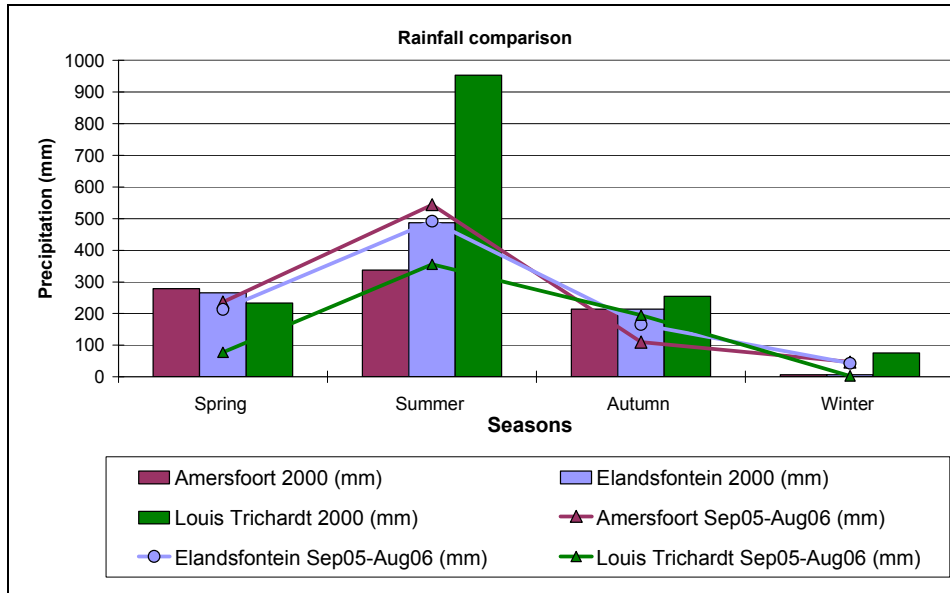


**Figure 3.8: Seasonal rainfall comparison for three representative sites.**

Comparison of the absolute and relative differences between modelled and measured sulphate wet deposition rates are presented in Figure 3.9 and Table 3.18.

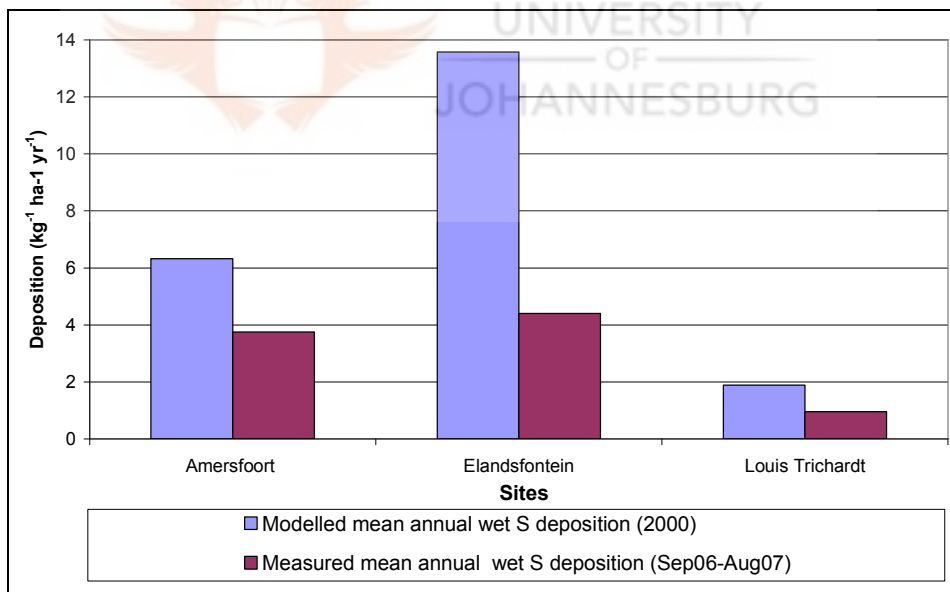


**Figure 3.9: Comparison of modelled (Fourie, 2006) and measured annual cumulative wet sulphate deposition.**

In this case, Elandsfontein and Louis Trichardt are *over-predicted* by the modelling while Amersfoort is *under-predicted*. In terms of absolute and relative difference, the following table presents the numerical comparison (Table 3.18).



**Table 3.18: Wet sulphate deposition comparison for three sites (Sep06-Aug07).**

Site	Modelled mean annual $SO_4^{-2}$ ( $kg\ ha^{-1}\ yr^{-1}$ )	Measured mean annual $SO_4^{-2}$ ( $kg\ ha^{-1}\ yr^{-1}$ )	(modelled – measured) / measured (%)
Amersfoort	6.3	3.7	69%
Elandsfontein	14	4.4	208%
Louis Trichardt	1.9	1.0	98%

*Comparison of seasonal sulphur wet deposition rates*

Seasonal wet sulphur (sulphate) deposition site comparisons are presented in Table 3.19 to Table 3.21.

**Table 3.19:  $SO_4^{2-}$  wet deposition comparison for site Amersfoort (AF).**

Season		Spring	Summer	Autumn	Winter
Modelled	AF 2000 $SO_4^{-2}$ ( $kg\ ha^{-1}\ yr^{-1}$ )	1.6	1.8	1.5	1.4
Measured	AF 2006/7 $SO_4^{-2}$ ( $kg\ ha^{-1}\ yr^{-1}$ )	1.41	1.73	0.45	0.16
(Modelled – measured) / measured (%)		13%	4%	234%	774%

**Table 3.20:  $SO_4^{2-}$  wet deposition comparison for site Elandsfontein (EF).**

Season		Spring	Summer	Autumn	Winter
Modelled	EF 2000 $SO_4^{-2}$ ( $kg\ ha^{-1}\ yr^{-1}$ )	2.8	4.3	3.6	2.9
Measured	EF 2006/7 $SO_4^{-2}$ ( $kg\ ha^{-1}\ yr^{-1}$ )	0.51	2.88	0.74	0.27
(Modelled – measured) / measured (%)		450%	49%	388%	974%

**Table 3.21:  $SO_4^{2-}$  wet deposition comparison for site Louis Trichardt (LT).**

Season		Spring	Summer	Autumn	Winter
Modelled	LT 2000 $SO_4^{-2}$ ( $kg\ ha^{-1}\ yr^{-1}$ )	0.46	0.58	0.43	0.42
Measured	LT 2006/7 $SO_4^{-2}$ ( $kg\ ha^{-1}\ yr^{-1}$ )	0.35	0.23	0.26	0.11
(Modelled – measured) / measured (%)		31%	149%	63%	295%

The modelling *underestimated* the measurements in spring and summer. Louis Trichardt site was also *underestimated* for autumn. The above tables reveal that modelling



overestimated the measurement for all three sites in winter and for two during autumn. The remote site (Louis Trichardt) is *overestimated* by 40 times but this is not significant as changes in the precipitation measured during the monitoring and modelling periods explain these differences. Figure 3.10 shows the precipitation measured for Louis Trichardt for four seasons over the annual cycles used for modelling and monitoring. The nearly zero precipitation during winter in 2006 caused the disparity between two compared years (Table 3.22).

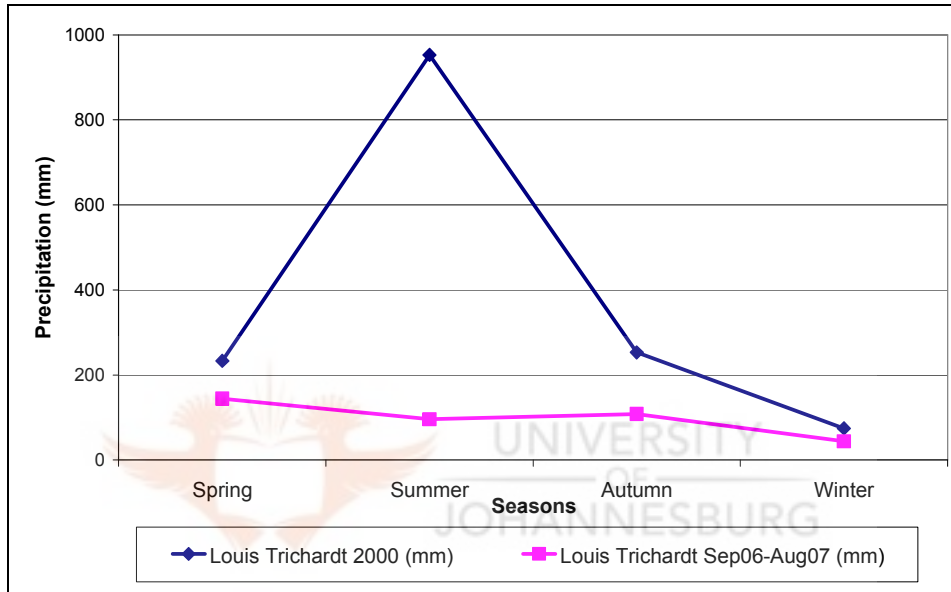


**Figure 3.10: Seasonal rainfall comparison (2000 – 2006/7) for site 36, Louis Trichardt.**

Table 3.22, which indicates absolute and relative precipitation differences for this site for all seasons, supports this.

**Table 3.22: The seasonal precipitation comparison for site Louis Trichardt (LT).**

Season	Spring	Summer	Autumn	Winter
<b>LT 2000 (mm)</b>	233	953	253	74
<b>LT Sep06-Aug07 (mm)</b>	143.9	95.2	107.7	43.4
<b>Difference (%)</b>	62%	901%	135%	71%

However, the substantial difference between the relative difference in wet sulphate deposition and relative difference in the rainfall data does not fully support a near-levelled sulphate deposition in winter with the rest of the seasons either for the Louis Trichardt site or for the other two sites.



### 3.6.2 Nitrogen

#### *Comparison of annual average NO<sub>2</sub> concentrations*

In a similar way, measured concentrations (averaged September 2005 to August 2007) are compared to annual modelled concentrations (Figure 3.11).

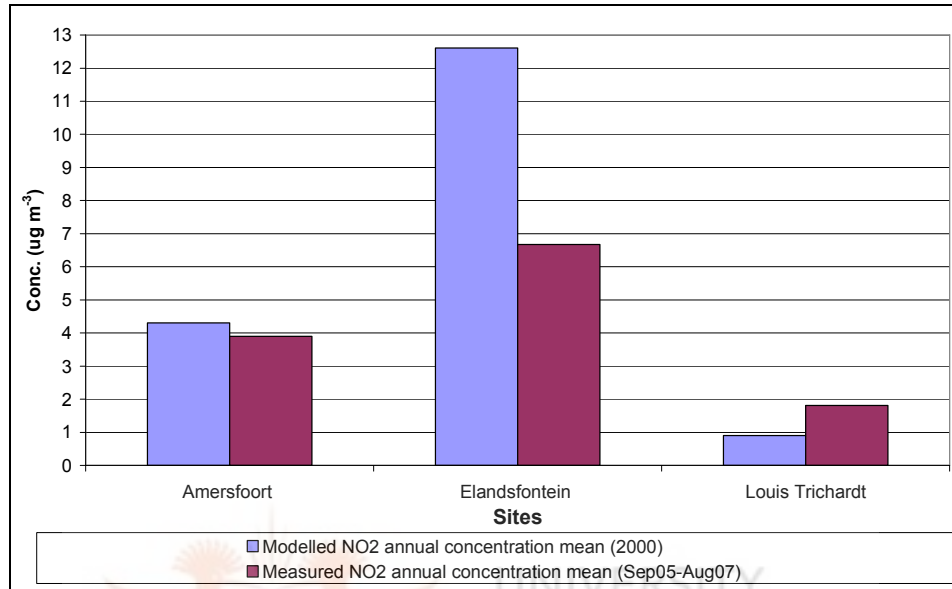


**Figure 3.11: NO<sub>2</sub> comparison of modelled (Fourie, 2006) concentration (2000) and measured concentration (Sep05-Aug07).**

The annual mean of the modelled concentrations is substantially higher than the measured value for Elandsfontein (industrial Highveld), while the opposite is the case for Louis Trichardt (remote rural). The difference for Amersfoort (downwind off industrial Highveld) is small. Absolute and relative annual mean concentrations are provided in Table 3.23.

**Table 3.23: NO<sub>2</sub> mean annual concentration comparison for all three sites.**

Site	Modelled NO <sub>2</sub> annual mean (Sep05-Aug07) (µg m <sup>-3</sup> )	Measured NO <sub>2</sub> annual mean (2000) (µg m <sup>-3</sup> )	(Modelled – measured) / measured (%)
Amersfoort	4.3	3.9	10%
Elandsfontein	13	6.7	88%
Louis Trichardt	0.90	1.8	-50%



### Comparison of seasonal NO<sub>2</sub> concentrations

The NO<sub>2</sub> concentrations derived from modelling and measurements from this campaign are compared on a seasonal basis (Figure 3.12 to Figure 3.14), using the period from September 2005 to September 2007 (averaged each month over two observational years) for measured data and January to December 2000 for modelled data (Fourie, 2006).

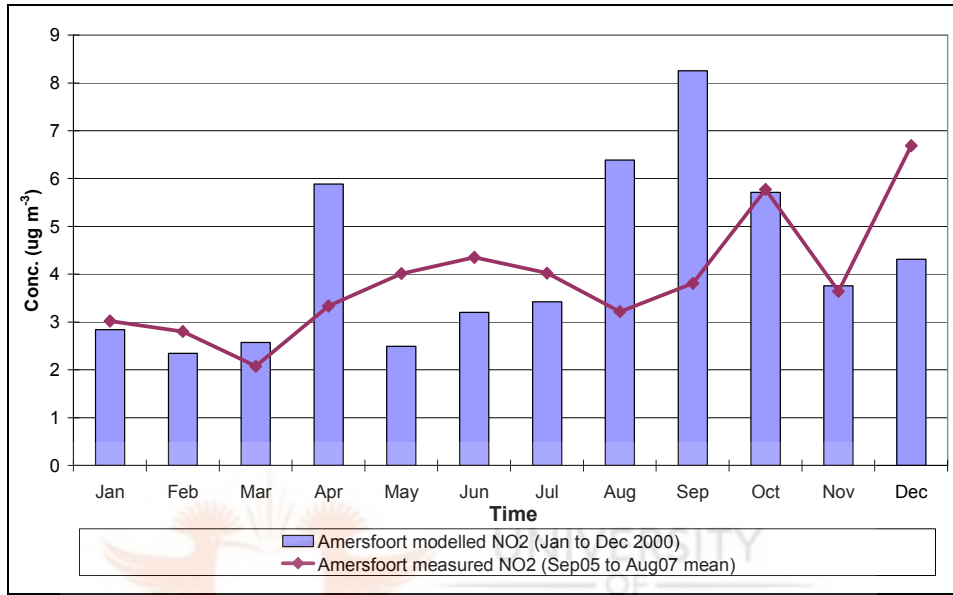


Figure 3.12: NO<sub>2</sub> comparison of monthly mean modelled (Jan00-Dec00) and monthly mean measured concentrations (Sep05-Aug07) for Amersfoort (site 2).

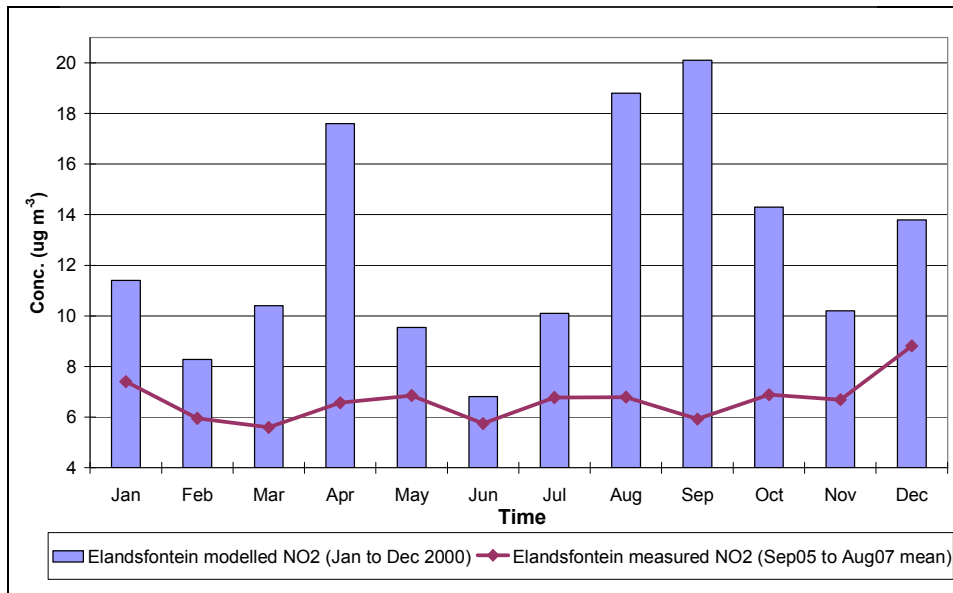
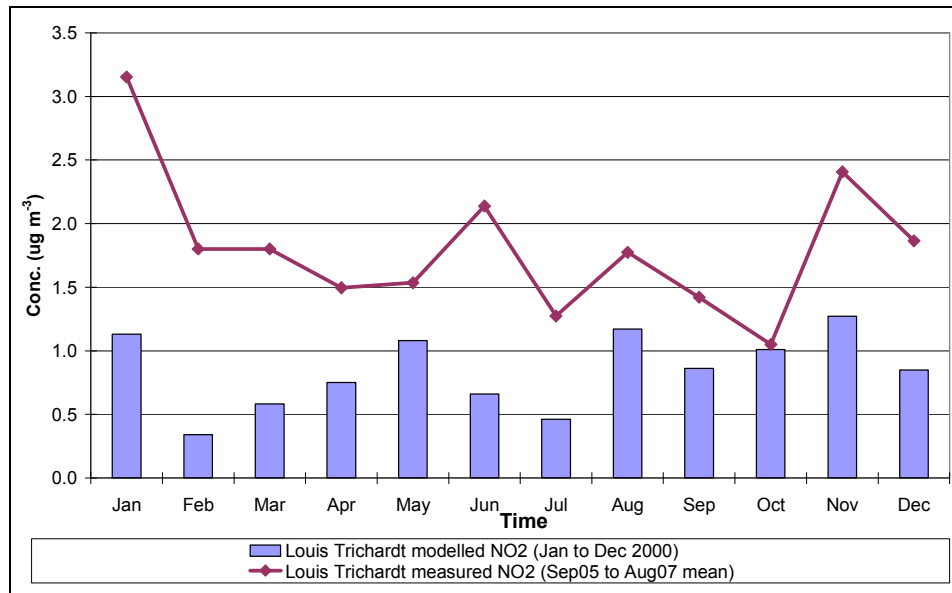


Figure 3.13: NO<sub>2</sub> comparison of monthly mean modelled (Jan00-Dec00) to monthly mean measured concentrations (Sep05-Aug07) for Elandsfontein (site 17).





**Figure 3.14: NO<sub>2</sub> comparison of monthly mean modelled (Jan00-Dec00) to monthly mean measured concentrations (Sep05-Aug07) for Louis Trichardt (site 36).**

The modelling *underestimates* the NO<sub>2</sub> concentrations at downwind (site 2, Amersfoort) and remote (site 36, Louis Trichardt) sites and *overestimates* NO<sub>2</sub> concentrations in the centre of industrial Highveld (site 17, Elandsfontein). Although the seasonal patterns are similar, no regular correlation is evident. In addition, there are no clear seasonal trends in the measured NO<sub>2</sub> concentrations.

#### *Comparison of annual nitrogen dry deposition rates*

The nitrogen dry deposition rates were compared. Deposition results based on measurements span the period from September 2005 to August 2006 (one annual cycle), while the modelled deposition results cover the period from January to December 2000 (Figure 3.15).

The nitrogen dry deposition rates (which directly depend on the atmospheric concentrations for their inferential results) have similar relative patterns to the concentration annual comparison (Figure 3.11, Table 3.23). The large modelling *overestimation* relative to measurements for Elandsfontein sites is stark contrast to the moderate *underestimation* at the Louis Trichardt site and almost matching for the Amersfoort (Figure 3.15). A possible cause could be that in the modelled dry nitrogen deposition, nitrous oxide (NO) deposition was included in the calculation as a separate species, which amounted to a substantial portion of total N deposition. For the measured dry deposition calculation, only NO<sub>2</sub> concentrations were available. Close to the source



region, the emissions might be anticipated to have still a high fraction of unprocessed NO present. The site in the central industrial Highveld (site Elandsfontein, 17) has much higher modelled values (88%) while the values for remote site (where there would be little unconverted NO) is under-matched by ~50%.

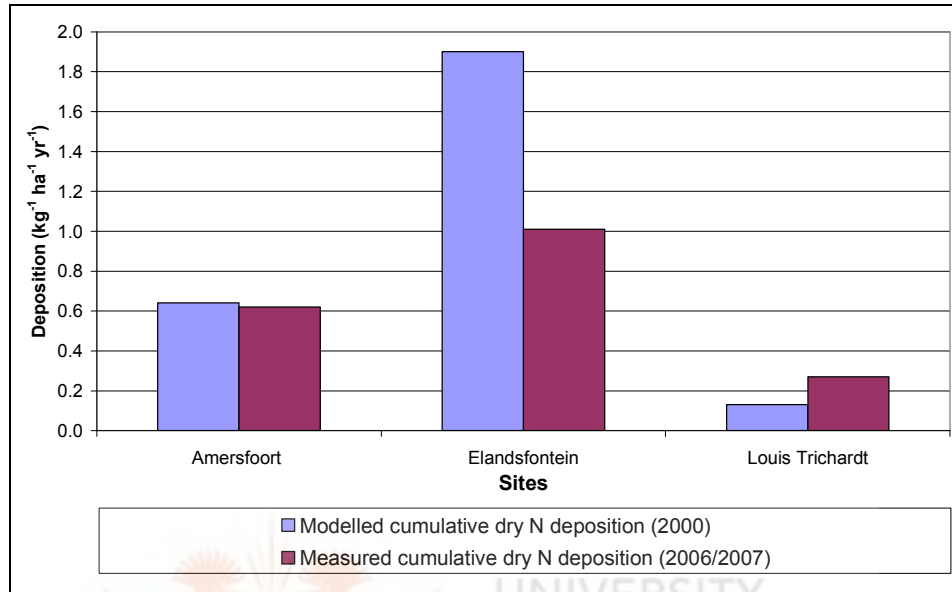


**Figure 3.15: Comparison of modelled (Fourie, 2006) and measured cumulative dry gaseous nitrogen species deposition.**

When the graphical comparison is presented as relative differences, then the following numerical differences are found (Table 3.24).

**Table 3.24: NO<sub>2</sub> modelled and measured dry deposition comparison.**

Site	Modelled cumulative N dry deposition (2000) (kg ha <sup>-1</sup> yr <sup>-1</sup> )	Measured cumulative N dry deposition (2006/2007) (kg ha <sup>-1</sup> yr <sup>-1</sup> )	(Modelled – measured) /measured (%)
<b>Amersfoort</b>	0.64	0.62	3%
<b>Elandsfontein</b>	1.9	1.01	88%
<b>Louis Trichardt</b>	0.13	0.27	-52%

*Comparison of seasonal nitrogen dry deposition rates*

In terms of seasonal dry nitrogen deposition comparison, results are presented in Table 3.25 to Table 3.27. As the atmospheric concentration seasonal plots showed distinct seasonal trends, further seasonal trends have been averaged over seasonal quarters.



**Table 3.25: Nitrogen seasonal dry deposition for site Amersfoort (AF).**

Season		Spring	Summer	Autumn	Winter
<b>Modelled</b>	<b>AF 2000, NO<sub>2</sub> as N (kg ha<sup>-1</sup> yr<sup>-1</sup>)</b>	0.17	0.10	0.11	0.13
<b>Measured</b>	<b>AF 2006/2007, NO<sub>2</sub> as N (kg ha<sup>-1</sup> yr<sup>-1</sup>)</b>	0.35	0.15	0.08	0.05
<b>(Modelled – measured) / measured (%)</b>		-51%	-34%	46%	168%

**Table 3.26: NO<sub>2</sub> seasonal dry deposition comparison for site Elandsfontein (EF).**

Season		Spring	Summer	Autumn	Winter
<b>Modelled</b>	<b>EF 2000, NO<sub>2</sub> as N (kg ha<sup>-1</sup> yr<sup>-1</sup>)</b>	0.41	0.36	0.40	0.35
<b>Measured</b>	<b>EF 2006/2007, NO<sub>2</sub> as N (kg ha<sup>-1</sup> yr<sup>-1</sup>)</b>	0.50	0.27	0.16	0.08
<b>(Modelled – measured) / measured (%)</b>		-18%	33%	153%	350%

**Table 3.27: NO<sub>2</sub> seasonal dry deposition comparison for site Louis Trichardt (LT).**

Season		Spring	Summer	Autumn	Winter
<b>Modelled</b>	<b>LT 2000, NO<sub>2</sub> as N (kg ha<sup>-1</sup> yr<sup>-1</sup>)</b>	0.03	0.02	0.03	0.02
<b>Measured</b>	<b>LT 2006/2007 NO<sub>2</sub> as N (kg ha<sup>-1</sup> yr<sup>-1</sup>)</b>	0.13	0.08	0.05	0.02
<b>(Modelled – measured) / measured (%)</b>		-76%	-74%	-35%	13%

The comparison for winter season for the site in the industrial Highveld and downwind show the highest discrepancies (350% and 168% respectively) followed by spring and then by autumn concentrations. However, this is not a case with the remote site as higher disparities are found for spring and summer. Both modelled and measured concentrations at Louis Trichardt are very low throughout the year and can be considered equal.

*Comparison of average annual nitrogen wet deposition rates*

The nitrogen *wet deposition* pattern shows that the modelled results overestimate the measured results for all three compared sites (Figure 3.16).

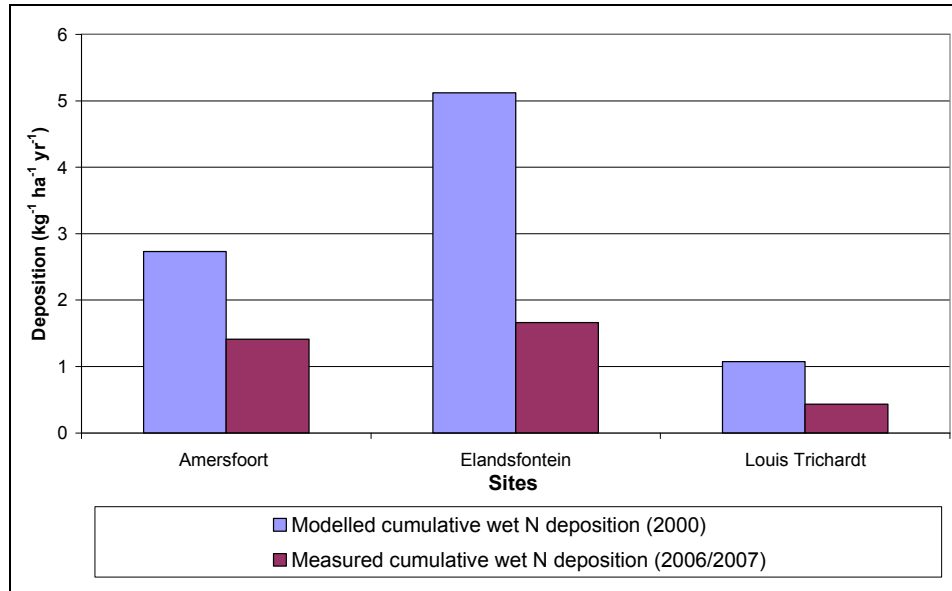


**Figure 3.16: Comparison of average annual nitrogen wet modelled (Fourie, 2006) and measured deposition rates for three sites.**

When the comparison in Figure 3.16 is presented as absolute and relative values, the following differences are found (Table 3.28).

**Table 3.28: Nitrogen cumulative wet deposition for all three sites.**

Site	Modelled N cumulative wet deposition (2000) (kg ha <sup>-1</sup> yr <sup>-1</sup> )	Measured N cumulative wet deposition (2006/2007) (kg ha <sup>-1</sup> yr <sup>-1</sup> )	(Modelled – Measured) / Measured (%)
<b>Amersfoort</b>	2.7	1.41	94%
<b>Elandsfontein</b>	5.1	1.66	208%
<b>Louis Trichardt</b>	1.1	0.43	149%

A comparison of precipitation data show that the precipitation for the modelled period is higher than the precipitation sum for the measured period for two of three sites (Elandsfontein and Louis Trichardt) (Table 3.22). Thus, *overestimation* of wet nitrogen deposition is greater than expected for Louis Trichardt, indicating possible systematic model overestimation for the distant site(s).

#### *Comparison of seasonal nitrogen wet deposition rates*

As discussed in the methodology (section 2.3.2) and for sulphur wet deposition (section 4.5.1), the major driving force for nitrogen wet deposition is the precipitation. This can be related particularly to differences in seasonal precipitation.



In terms of *seasonal* nitrogen wet deposition (comprising of nitrate and ammonium depositions for the measured results and nitrate deposition only for the modelled results) site comparison, results are presented in Table 3.29 to Table 3.31.

**Table 3.29: Seasonal nitrogen wet deposition (NO<sub>3</sub><sup>-</sup> only) comparison for Amersfoort (AF).**

<b>AF</b>	<b>Season</b>	<b>Spring</b>	<b>Summer</b>	<b>Autumn</b>	<b>Winter</b>
<b>Modelled (2000)</b>	<b>NO<sub>3</sub><sup>-</sup> (kg ha<sup>-1</sup> yr<sup>-1</sup>)</b>	0.64	0.81	0.69	0.59
<b>Measured (2006/2007)</b>	<b>NO<sub>3</sub><sup>-</sup> (kg ha<sup>-1</sup> yr<sup>-1</sup>)</b>	0.53	0.65	0.17	0.06
<b>(Modelled – measured) /measured (%)</b>		20%	25%	309%	879%

**Table 3.30: Seasonal nitrogen wet deposition (NO<sub>3</sub><sup>-</sup> only) comparison for Elandsfontein (EF).**

<b>EF</b>	<b>Season</b>	<b>Spring</b>	<b>Summer</b>	<b>Autumn</b>	<b>Winter</b>
<b>Modelled (2000)</b>	<b>NO<sub>3</sub><sup>-</sup> (kg ha<sup>-1</sup> yr<sup>-1</sup>)</b>	1.1	1.6	1.3	1.1
<b>Measured (2006/2007)</b>	<b>NO<sub>3</sub><sup>-</sup> (kg ha<sup>-1</sup> yr<sup>-1</sup>)</b>	0.19	1.09	0.28	0.10
<b>(Modelled – measured) /measured (%)</b>		459%	46%	383%	1022%

**Table 3.31: Seasonal nitrogen wet deposition (NO<sub>3</sub><sup>-</sup> only) comparison for Louis Trichardt (LT).**

<b>LT</b>	<b>Season</b>	<b>Spring</b>	<b>Summer</b>	<b>Autumn</b>	<b>Winter</b>
<b>Modelled (2000)</b>	<b>NO<sub>3</sub><sup>-</sup> (kg ha<sup>-1</sup> yr<sup>-1</sup>)</b>	0.24	0.36	0.24	0.24
<b>Measured (2006/2007)</b>	<b>NO<sub>3</sub><sup>-</sup> (kg ha<sup>-1</sup> yr<sup>-1</sup>)</b>	0.16	0.11	0.12	0.05
<b>(Modelled – measured) /measured (%)</b>		51%	242%	102%	400%

Seasonal differences resulting from the above comparisons, for wet deposition, show that the modelling *overestimated* the measured results for all seasons for all sites.

High variability in the meteorological data for different seasons is a contributing factor. Wet deposition for nitrogen diverged more than the dry deposition. Besides the precipitation difference, an anomaly with the modelling seasonal wet deposition is spotted for the wet nitrogen deposition (as it was for the wet sulphur deposition). The seasonality of the modelled wet deposition, both sulphur and nitrogen compounds is not as large as expected, given the evident seasonality of rainfall data as the main driving force (assuming nearly uniform emissions throughout the seasons). Further testing of the particular model



used for wet deposition computations are suggested to establish more accurately reasons for such internal rainfall versus wet deposition disparity.

### 3.6.3 Ozone modelled and measured comparison

The measured ozone concentrations for South African growing season were compared with the ozone modelling concentrations from the Cross Border Air Pollution Impact Assessment Project (CAPIA) (Zunckel and Carter, personal communication 2007). The Comprehensive Air Quality Model with extensions (CAMx), version 4.00 (ENVIRON, 2003), was used by the CAPIA modellers. A validation was not performed due to the different timeframes of two sets of results. However, the measured results were compared numerically and spatially. The CAPIA modelling results were supplied by the Natural Resources and the Environment Division of the CSIR (Zunckel and Carter, personal communication, 2007, Zunckel *et al.*, 2006, van Tienhoven *et al.*, 2006).

Nevertheless, comparisons were performed of comparable growing seasons October through April. CSIR ozone modelling results were available for October 2000 to April 2001; monitored results from the current study were extracted and averaged for two growing seasons (Oct05-Apr06 and Oct06-Apr07). Ozone contours for one selected month (January) are shown (Figure 3.17) as a sample of the spatial comparison performed for each month of the growing season.

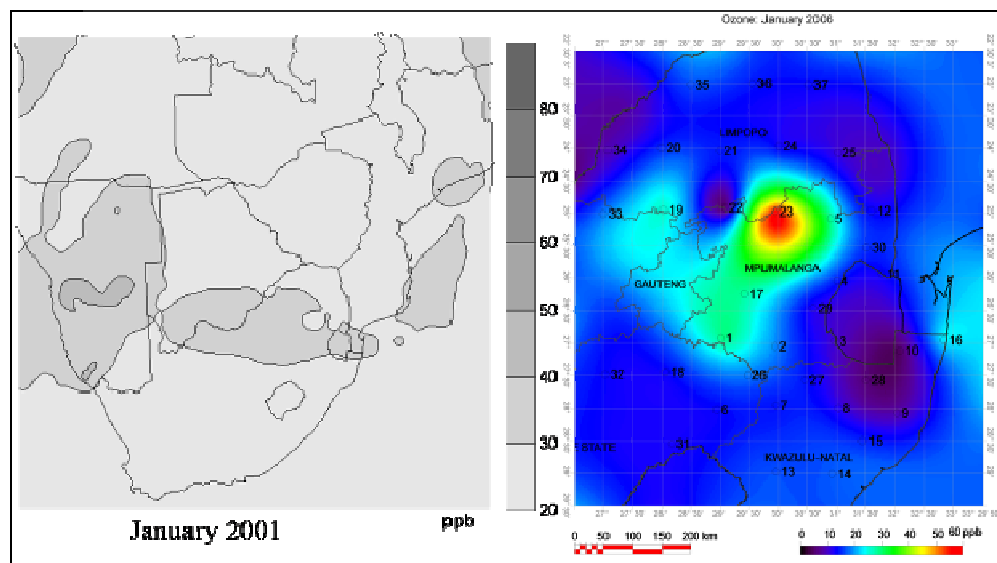
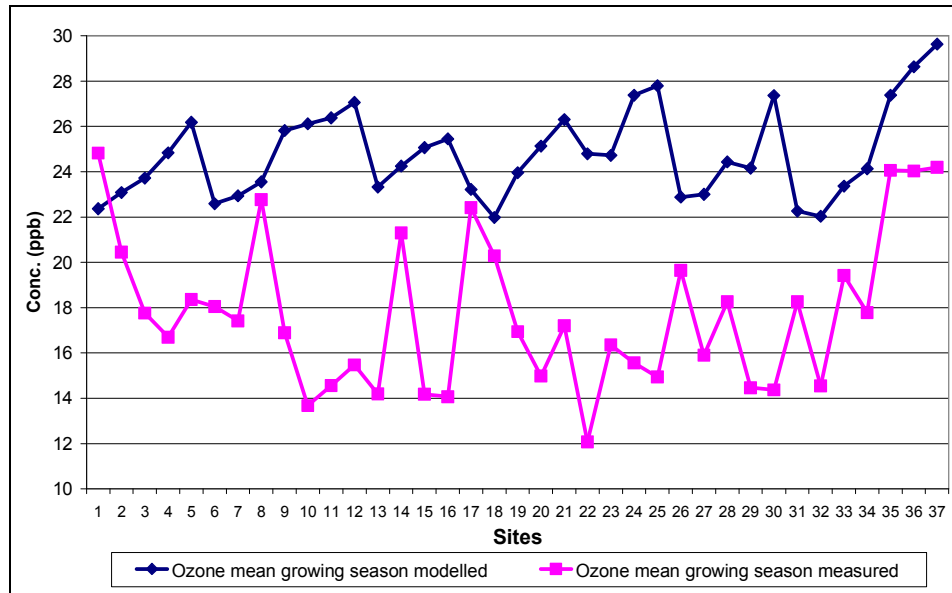


Figure 3.17: Comparison of ozone (a) modelled concentrations (January 2000) Zunckel *et al.*, 2006, with (b) measured concentrations (January 2006).



A comparison diagram for the comparable growing seasons shows disparity for the most of the sites (Figure 3.18).



**Figure 3.18: Comparison of ozone concentrations modelled for the growing season (Oct00-Apr01) to measured concentrations, averaged for the two growing seasons (Oct05-Apr06 & Oct06-Apr07), for all monitored sites.**

There is no satisfactory agreement between the monitored and modelled concentrations in either spatial contour for a particular month, or in the seasonal averages over all sites, although both measurement and modelling indicate a zone of elevated ozone concentrations for the northernmost sites (sites 35, 36 and 37, in northern Limpopo Province). The modelling overestimated the concentrations over the entire region, except for a single location (Site 1).

When a numerical comparison was carried out for all sites between the modelled and measured values, then the following absolute and relative differences were found (Table 3.32).

**Table 3.32: Comparison of the modelled to measured O<sub>3</sub> concentration averages for growing season for all monitored sites.**

Site No.	Nearest geographic location	Modelled O <sub>3</sub> mean (Oct00-Apr01) (ppb)	Measured O <sub>3</sub> mean (Oct05-Apr07) (ppb)	(Modelled-measured) / measured (%)
1	Standerton	22.4	24.8	-10%
2	Amersfoort	23.1	20.4	13%
3	Piet Retief	23.7	17.7	34%
4	Badplaas	24.8	16.7	49%



<b>Site No.</b>	<b>Nearest geographic location</b>	<b>Modelled O<sub>3</sub> mean (Oct00-Apr01) (ppb)</b>	<b>Measured O<sub>3</sub> mean (Oct05-Apr07) (ppb)</b>	<b>(Modelled-measured) / measured (%)</b>
5	Sabie	26.2	18.4	43%
6	Harrismith	22.6	18.0	25%
7	Newcastle	22.9	17.4	32%
8	Gluckstad	23.5	22.8	3%
9	Hluhluwe	25.8	16.9	53%
10	Ingwavuma	26.1	13.7	91%
11	Masibikela	26.4	14.6	81%
12	Skukuza	27.1	15.5	75%
13	Escourt	23.3	14.2	64%
14	Kranskop	24.2	21.3	14%
15	Melmoth	25.1	14.2	77%
16	Kosi Bay	25.4	14.1	81%
17	Kriel	23.2	22.4	4%
18	Heilbron	22	20.3	8%
19	Warmbaths	24	16.9	42%
20	Vaalwater	25.1	15.0	68%
21	Potgietersrus	26.3	17.2	53%
22	Marble Hall	24.8	12.1	106%
23	Steelpoort	24.7	16.3	51%
24	Haenertsburg	27.4	15.6	76%
25	Phalaborwa	27.8	14.9	86%
26	Memel	22.9	19.6	17%
27	Utrecht	23.0	15.9	45%
28	Louwsburg	24.4	18.2	34%
29	Amsterdam	24.2	14.5	67%
30	Malelane	27.4	14.4	91%
31	Fouriesburg	22.3	18.2	22%
32	Kroonstad	22.0	14.5	51%
33	Pillansberg	23.4	19.4	21%
34	Thabazimbi	24.1	17.8	36%
35	Tolwe	27.4	24.1	14%
36	Louis Trichardt	28.6	24.0	19%
37	Thohoyandou	29.6	24.2	22%
<b>Mean</b>		<b>24.8</b>	<b>17.7</b>	<b>33%</b>

The differences varied from site to site and ranged from -10% to +106% below or above the measurement mean. The mean variation between modelled and measured was 33% overestimation. However, the absolute and relative differences between the modelling and





measurements for ozone were of smaller amplitude in comparison with the differences established for sulphur and nitrogen concentrations.

If the measured modelled comparison is carried out over the entire growing season for the three sites for which sulphur and nitrogen comparisons were performed as well, then the growing seasonal ozone concentration trends are as shown in Figure 3.19 to Figure 3.21.

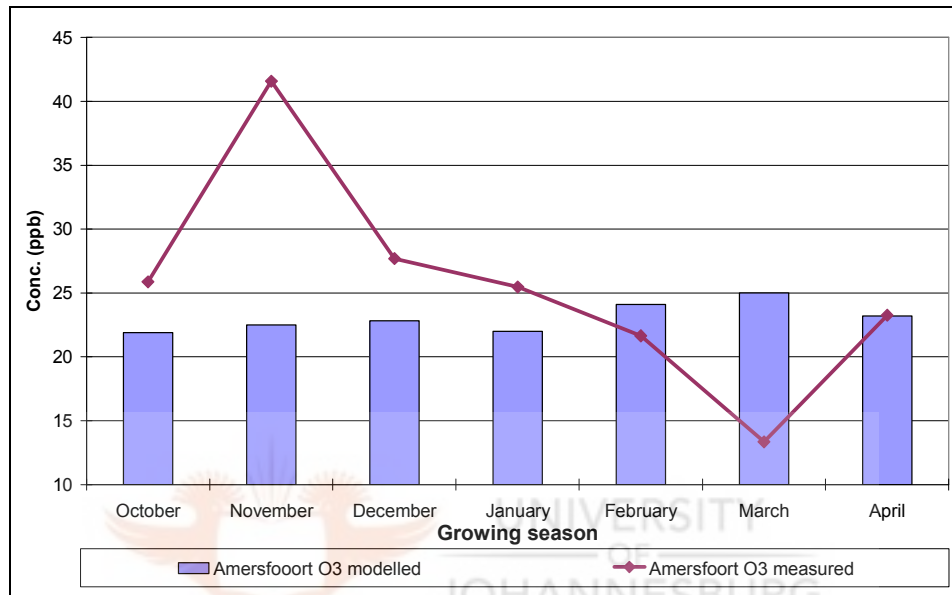


**Figure 3.19: Comparison of modelled ozone for growing season (Oct00-Apr01) and measured ozone, mean of two growing seasons (Oct05-Apr06 & Oct06-Apr07) for Amersfoort (site 2).**

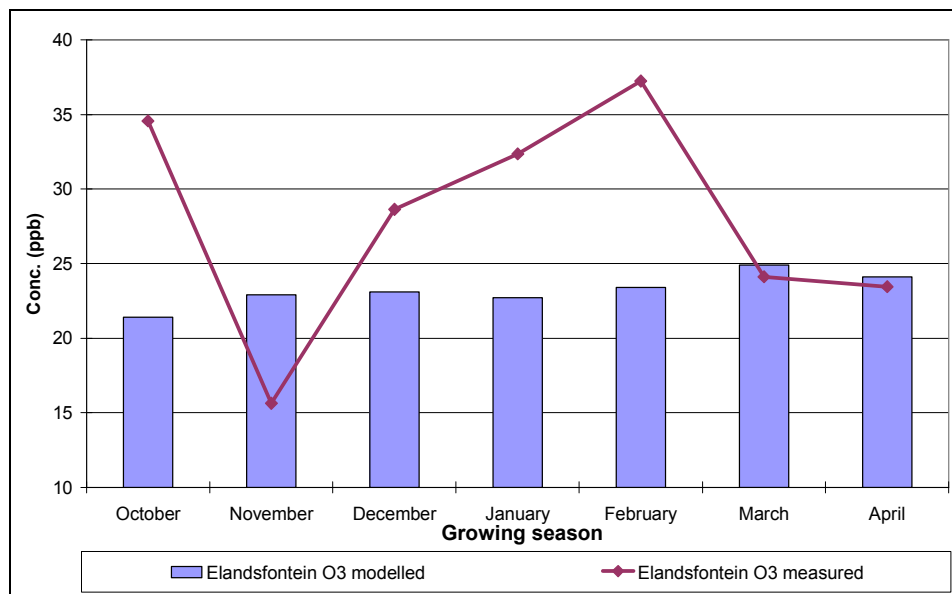


**Figure 3.20: Comparison of modelled ozone for growing season (Oct00-Apr01) and measured ozone, mean of two growing seasons (Oct05-Apr06 & Oct06-Apr07) for Elandsfontein (site 17).**

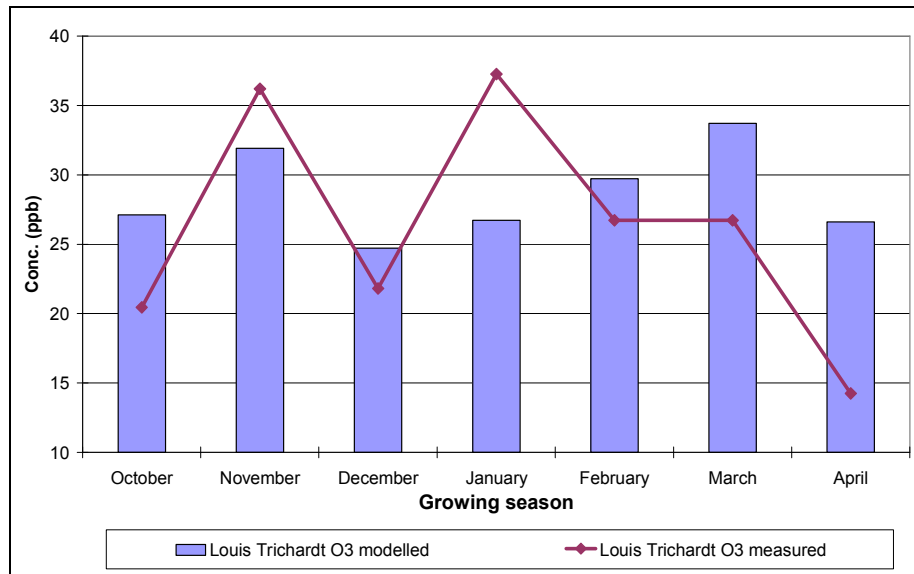


**Figure 3.21: Comparison of modelled ozone for growing season (Oct00-Apr01) and measured ozone, mean of two growing seasons (Oct05-Apr06 & Oct06-Apr07) for Louis Trichardt (site 36).**

In contrast to the ozone concentrations comparison for all study sites, the analysis of seasonal trends for three representative sites revealed different patterns. The modelled concentrations were generally uniform with time and no characteristic spring-early summer peaks were spotted for the sites at the centre of the industrial Highveld (Elandsfontein) or just downwind (Amersfoort). In addition, the relatively elevated ozone during summer season (anomalously) at the central, Elandsfontein site was not matched either in the modelling. However, for the remote rural site (Louis Trichardt), spring was well matched.

The absolute and relative differences between the modelled and measured data over the growing season for those three sites are found to be as follows (Table 3.33 to Table 3.35).

**Table 3.33: Comparison of modelled and measured O<sub>3</sub> concentrations for Amersfoort.**

<i>Period</i>	<i>Oct</i>	<i>Nov</i>	<i>Dec</i>	<i>Jan</i>	<i>Feb</i>	<i>Mar</i>	<i>Apr</i>
<b><i>Amersfoort modelled (ppb)</i></b>	21.9	22.5	22.8	22	24.1	25	23.2
<b><i>Amersfoort measured (ppb)</i></b>	20.7	33.3	22.1	20.4	17.3	10.7	18.6
<b><i>(Modelled – measured)/measured (%)</i></b>	6%	-32%	3%	8%	39%	134%	25%

**Table 3.34: Comparison of modelled and measured O<sub>3</sub> concentrations for Elandsfontein.**

<i>Period</i>	<i>Oct</i>	<i>Nov</i>	<i>Dec</i>	<i>Jan</i>	<i>Feb</i>	<i>Mar</i>	<i>Apr</i>
<b><i>Elandsfontein modelled (ppb)</i></b>	21.4	22.9	23.1	22.7	23.4	24.9	24.1
<b><i>Elandsfontein measured (ppb)</i></b>	27.7	12.5	22.9	25.9	29.8	19.3	18.8
<b><i>(Modelled – measured)/measured (%)</i></b>	-23%	83%	1%	-12%	-21%	29%	28%



**Table 3.35: Comparison of modelled and measured O<sub>3</sub> concentrations for Louis Trichardt.**

<i>Period</i>	<i>Oct</i>	<i>Nov</i>	<i>Dec</i>	<i>Jan</i>	<i>Feb</i>	<i>Mar</i>	<i>Apr</i>
<b><i>Louis Trichardt modelled (ppb)</i></b>	27.1	31.9	24.7	26.7	29.7	33.7	26.6
<b><i>Louis Trichardt measured (ppb)</i></b>	27.1	29	17.4	29.8	26.7	26.7	11.4
<b><i>(Modelled – measured)/measured (%)</i></b>	0%	10%	42%	-10%	11%	26%	134%

The numerical comparisons reinforce the findings from the diagram comparisons from Figure 3.19 to Figure 3.21, namely that modelling tends to overestimate the measured values. These findings confirm similar findings by the CAPIA authors, in which they compared the CAPIA CAMx data with Cape Point measured data (Figure 3.22) (Zunckel *et al.*, 2006).

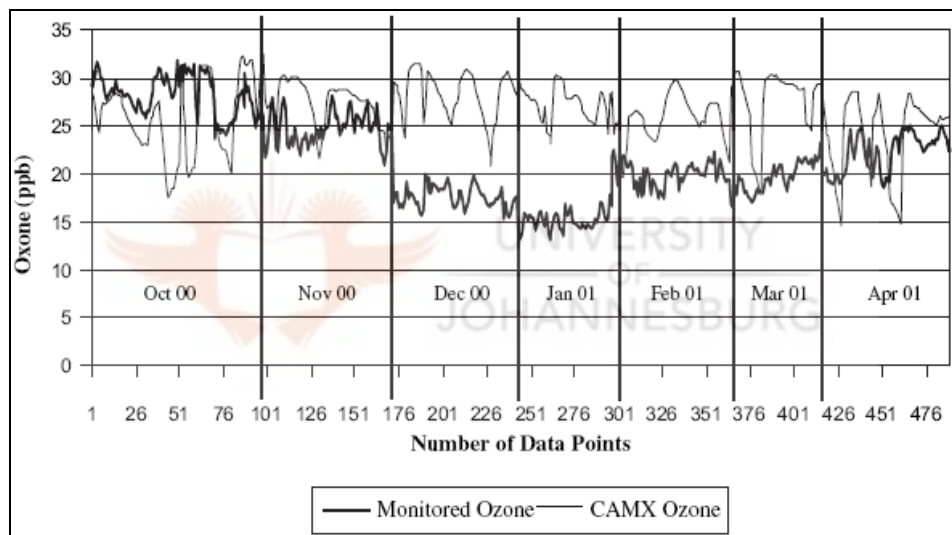


**Figure 3.22: Modelled and monitored surface ozone at Cape Point during the period October 2000 to April 2001 (Zunckel *et al.*, 2006).**

Despite a few outlying modelled concentrations, the differences between measured and modelled concentrations are generally less than 5 ppb. During the mid-summer months, December 2000 to March 2001, the modelled surface ozone concentrations are consistently higher than the measured values. This is possibly attributed to higher biogenic emissions during the summer resulting in higher modelled ozone (Zunckel *et al.*, 2006).

There are several factors that affected the comparison for ozone between the CAPIA project and ozone measured for this study.

The modelling took into account ten daylight hours per day for five days a month, extrapolated into a monthly mean average. As daylight ozone concentrations are inevitably



higher than night time values, this selection of daily modelling hours could already explain much of the discrepancy between modelled and measured values (mean 33% overestimation). While the measurements were taken from the monitoring stations positioned at 1.5 m above surface, the CAMx model provided an estimate of the concentrations in a grid block of 2 500 km<sup>2</sup> and a 70 m deep lower tropospheric layer. In addition, anthropogenic emissions used in CAPIA project did not include all emission sources. The biogenic emissions were limited to only three volatile organic compounds (VOC), while emissions from biomass burning sources were entirely excluded.

The influence of the air transport on oxidation of ozone precursors and other strong local (and regionally positioned) sources such as biogenic and pyrogenic are likely to influence ozone concentrations and distributions (at least for the sites positioned in the northern zone of the study area – Limpopo region) (van Tienhoven and Scholes, 2003, Zunckel *et al.*, 2006). Contrary to the modelling findings, the relatively elevated concentrations were also recorded in places south and southeast of the study area (comparable to the increased concentrations in the north of the study area of which the origins are well documented). Possible answers should be further investigated. One possibility under consideration includes the transport (and transformation) of ozone precursors from the central industrial area mixed with locally generated ozone precursors of mixed origin: anthropogenic, biogenic and pyrogenic. However, no clear evidence could be established through the results of this study.

Overall ozone observations confirm prior spatial modelling (although not its maxima) results. A broad area of increased concentrations in the far north of South Africa confirms existence of slightly elevated concentrations in comparison to the central study region. In addition, the modelled-measured matching for this sub-region confirms seasonality of ozone peaks and their different origin, as positioned far north, distant from the central anthropogenic pollution source region, but downwind of the main pyrogenic and on-path of the Highveld re-circulated air mass stream.

### **3.7 Conclusions**

This task in this section was to compare the trace chemical meso-scale monitoring concentrations and deposition with results from two regional (meso-scale) to sub-continental modelling studies. A direct validation of the monitored results with modelled results could not be carried out, as available modelling studies dealt with different years



from the measuring campaign. Nevertheless, comparisons were done for comparable annual and seasonal cycles. The measured modelled comparison of trace gas species and deposition of their non-organic acidic compounds was found to be useful, despite different years and seasons being compared.

Deviations between modelled and measured results may occur for a variety of reasons (model assumptions, errors and inaccuracies in input data, uncertainties in nature of atmospheric processes), also uncertainties and representativeness of both monitored and modelled data (Fourie, 2006). Despite these limitations, the above comparisons can contribute to an improved understanding of overall regional trace gas distribution.

The comparison produced mixed results. In most cases, for annual means the modelling for SO<sub>2</sub> concentrations underestimated the measured results. The S modelled dry deposition (SO<sub>2</sub> and SO<sub>4</sub><sup>2-</sup>) and was almost equal. The S wet deposition rate (SO<sub>4</sub><sup>2-</sup>) was mixed depending on site from underestimate to overestimate. The annual NO<sub>2</sub> was generally overestimated. The dry NO<sub>2</sub> deposition rates overestimated the measurements while wet modelled deposition rates (NO<sub>3</sub><sup>-</sup>) underestimated the study results (NO<sub>3</sub><sup>-</sup> and NH<sub>4</sub><sup>+</sup>). The seasonal trends are less well matched and both model results used were less in correlation with the evident measured seasonality for all three species. This was particularly well evident with the wet seasonal comparisons for sulphur and nitrogen compounds.

### **3.7.1 Summary**

The different air transport as well as differing annual meteorology influenced those differences. Long-term air mass movement research was taken into account (Figure 3.23).

However, strong links between the air mass movements from the central, industrial Highveld region with the ground level concentration of the studied trace gas species were not apparent. In contrast, rainfall differences were much more recognisable, more so in annual than seasonal modelled results.

During the design phase of this study attention was paid to the general synoptic and recirculation situation with respect to the transport and fate of the pollutant plumes. It is not within the scope of this study to analyse the relationships between the measurement results and the synoptic data in detail. The long averaging period of passive sampling (1 month) combined with the density of the data is not the ideal data set for this analysis. The results confirm the general trends and expectations based on synoptic work and this issue



was not pursued further. The results of this study confirm in general the detailed investigations performed by other researchers on this issue (Freiman and Piketh 2002; Piketh 2000; Tyson and Preston-Whyte, 2000; Garstang and Tyson, 1997).

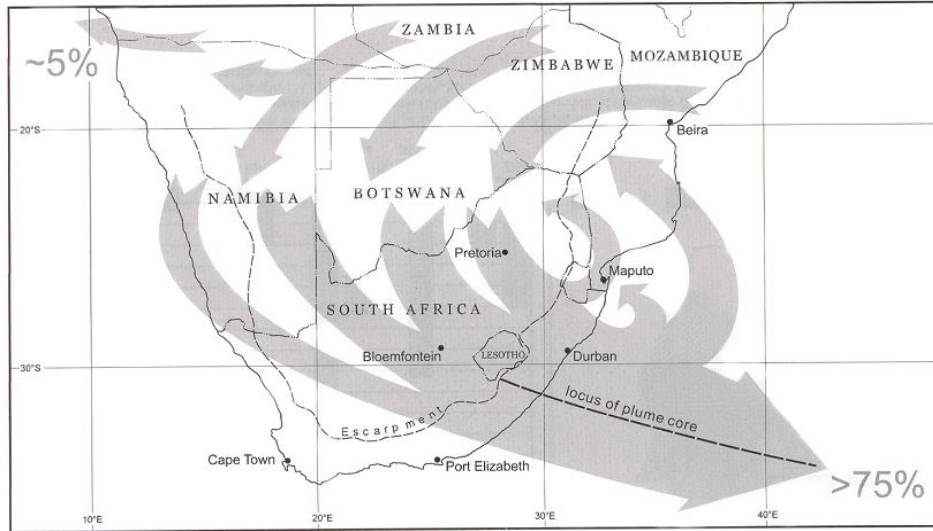


**Figure 3.23: Generalised atmospheric transport over southern Africa (Source: Tyson and Preston-Whyte, 2000).**

### 3.7.2 *Comments*

The uncertainty in the magnitude of the model inaccuracies as well as margin of error of the measured data remained. Ideally modelling should be repeated for times corresponding to the measuring period in order to give an accurate evaluation assessment. However, the general patterns predicted by the modelling are shown in the monitoring results confirm that the general understanding of the emissions and their fate is accurate.



## CHAPTER FOUR

*The concept of critical loads is presented in detail and recent literature on critical load research is reviewed. The method selected for use in this sub-study follows a method selected from one of the reviewed studies. The methods section elaborates on the variations to this chosen method that are applied in this chapter. The results provide one of the answers to the central question of the study. A discussion of the measurement and other uncertainties on the empirical measurements and subsequent processing steps is given.*

### **4. Regional Scale Critical Loads Assessment of Acidic Deposition from SO<sub>2</sub>, NO<sub>2</sub> Emissions from the Highveld**

#### **4.1 Introduction**

Acidification of soils and water bodies is a potential environmental problem for developing countries in the light of increasing emissions of acidic precursor gases. Critical loads and levels represent applicable and tested impact-based assessment tools in the context of protection of terrestrial environments from acidification. The purpose of this study was to determine the total acidic deposition load and subsequently to assess any current exceedance of the critical sensitivity thresholds of soils in terms of their buffering capacity.

The approach used in this study follows the procedure developed for critical loads assessment in developing countries (Kuylenstierna *et al.*, 2001a; 2001b). The critical loads exceedance concept was established after the severe acidification of Scandinavian forests and lakes and subsequent joint efforts for mitigation. However, countries of the European Union (and many other European countries) adopted more elaborated methods including direct measurements and critical loads exceedance determination (UNECE, 2004).

The procedure adopted for this study starts by obtaining the total acidic deposition loads based on measurements (instead of modelled results as in the original study), which are then adjusted to account for mitigation due to base cation deposition. Soil sensitivity categories are generated based on an empirical world soil database inventory (ISRIC, 2003). The soil chemical attributes, *Cation Exchange Capacity* (CEC) and *Base Saturation* (BS), are used to determine sensitivity categories (buffering capacity). The sensitivity categories are then linked to weathering rates (using available field studies from a limited



range of sites) representing the critical loads relevant to each sensitivity category. Finally these critical loads are then compared with acidic rates (usually  $\text{meq m}^{-2} \text{ yr}^{-1}$ ). Sensitivity soil maps are created based on these categories of soil buffering capacity. Exceedance maps are generated by overlaying the total acidic deposition layer onto the sensitivity map.

In carrying out this critical load assessment, use is made of existing soil inventories. The soil inventories were used only in this chapter while acidic deposition loads are derived from the results of preceding Chapters Two and Three, dealing with concentrations and subsequently derived depositions.

## 4.2 Cumulative Acidity Assessment as an Indicator of Ecological Risk

### 4.2.1 *Ecosystem acidification and critical loads concept*

The consequences of acidic deposition on the natural environment depend on the interactions between magnitude of deposition and sensitivity of the ecosystem. The sensitivity refers to the susceptibility of terrestrial ecosystem to changes in structure and function should the pH change significantly. This depends largely on buffering processes in the soil-plant system. Vegetation changes are assumed to occur because of alterations in soil water chemistry. Acidification of the soil results in reduction of pH, that leads to changes in nutrient and aluminium (potentially toxic to plant roots) bioavailability (Ulrich and Sumner, 1991; Jordan, 1985).

One effect of soil acidification is to impoverish the soil nutrient status, as base cations such as potassium ( $\text{K}^+$ ), calcium ( $\text{Ca}^{2+}$ ) and magnesium ( $\text{Mg}^{2+}$ ) are leached out more readily at low pH values. This may in turn result in nutrient deficiencies and imbalances and consequent decreases in growth rates. At even lower pH values, solubility of certain metals, specifically of aluminium (Al), is increased. This is important, as aluminium ions are toxic to plant roots (Ulrich, 1985). Under extreme conditions, Al toxicity can lead to changes in plant community composition or forest die back.

Terrestrial and aquatic ecosystems differ in their sensitivity to acidic deposition, depending on the buffering ability of the soils and parent rock material and the sensitivity of organisms to changes in the soil solution or surface-water chemistry. Critical loads in this sense represent quantitative estimates of *ecosystems sensitivity* (more than just the soil chemistry properties) (Kuylenstierna *et al.*, 2001a, b). In any effort to protect a given area





from acidification, the total acidic input must be combined with the sensitivity to that acidic input to identify troubled ecosystems.

The rationale for using soil characteristics in determining the sensitivity of entire terrestrial ecosystems needs to be explained here.

Acidification (change in pH) will be avoided if deposition is maintained at a level within the buffering capacity of the soil. Consequently, the major component influencing terrestrial ecosystem sensitivity can be determined by considering soil buffering alone. Well-buffered ecosystems are unlikely to acidify and therefore will be insensitive. Poorly buffered systems will acidify under continued acidic deposition, which will cause impacts on organisms according to their tolerance of acidic conditions. Even the yield of tolerant species decreases upon acidification of the soil and, for this reason, acidification of the soil is the primary concern. If acidification is avoided, impacts on living organisms will be prevented irrespective of the tolerance of species (Kuylenstierna *et al.*, 2001a, b).

The most important in-soil process that can buffer acidifying deposition is the chemical weathering of soil minerals. The weathering reaction between the minerals and hydrogen ions neutralises acidity. Minerals weather at different rates and therefore the overall buffering rate will depend on the proportion of various minerals in the soil.

Thus, as different soils are able to buffer to different degrees depending on soil chemical and physical properties, ecosystems will have different sensitivity to acidic deposition. Soils with a high proportion of fast weathering minerals will be well buffered in the long term. Soils with a high proportion of inert minerals will have low weathering rates and be more susceptible to acidification.

The buffering ability of soils and hence the sensitivity of terrestrial ecosystems to acidic deposition is based upon two parameters: **Base Saturation (BS)** and **Cation Exchange Capacity (CEC)**. The number of positively charged ions on soil particles is measured by the *Cation Exchange Capacity (CEC)*. The proportion of this filled by base cations, as opposed to acidic cations (hydrogen or aluminium), is called the *base saturation* (BS, usually expressed as a percentage). The total amount of exchangeable bases represents the capacity of the soil to buffer by means of cation exchange (Kuylenstierna *et al.*, 2001a, b).



### *Base saturation*

*In the absence of soil mineralogy data and other specific information, the soil buffering properties of different soil types have been assessed based on base saturation, which is generally measured in soil profile analyses. Base saturation is therefore the variable used in this assessment to identify those soils that have high weathering rate. Soils with high base saturation have either a high input rate or low loss rate of base cations. High weathering rate soils, with a high input rate of base cations to the soil exchange complex, will therefore tend to have high base saturation. In addition, high base saturation indicates those soils where base cations accumulate due to soil processes other than weathering such as net upward water flux and calcification (Kuylenstierna et al., 2001b).*

### *Cation exchange capacity*

*The sensitivity of a soil having a certain base saturation will be modified by the CEC. If there is a very large CEC then this will have the effect of dampening any fluctuations in pH from a given acid load. A combination of BS and CEC will be related to the ability of a soil to buffer acidic inputs by the process of cation exchange. Buffering by cation exchange can only occur for a finite period of time. If the CEC is high then the buffering by cation exchange may be considerable. Ecosystems with high CEC soils would then be considered to have a lowered sensitivity compared to soils with moderate CEC. In areas with very low CEC, episodic inputs of acidity may cause larger fluctuations in pH, even where weathering rates are reasonably high. Therefore, such areas might be considered to have slightly higher sensitivity (Kuylenstierna et al., 2001b).*

### *Base cation deposition*

In many regions of the World, there are substantial transfers and deposition of soil particles, emitted mainly from arid areas. This soil dust is mainly alkaline in nature and therefore contributes to the buffering cations of soils onto which it is deposited. The source areas of wind-blown dust are located primarily in arid areas of the World, which often have calcareous soils. When wind exceeds threshold speeds, soil particles become airborne, with the smallest particles potentially transported over large distances. The global emission, transfer and deposition of soil dust have been modelled by Tegen and Fung (1995).



#### 4.2.2 *Determining critical loads of acidity through mapping of soil sensitivity*

In 1988, the *Convention on Long-range Transboundary Air Pollution* (CLRTAP, UN ECE) adopted the *critical-load* concept – “**a quantitative estimate of an exposure to one or more pollutants below which significant harmful effects on specified sensitive elements of the environment do not occur according to present knowledge**”. The adoption of this concept then constituted a basis for the future development of international agreements concerning limitation of the emissions of air pollutants (Skeffington, 1999).

Mapping of soil sensitivity to acidification gives a relative measure of the susceptibility of ecosystems to such changes. The process of sensitivity mapping can increase confidence in acidity evaluation, in the assessment of sensitivity in regions that have not been studied intensively. Various methods to calculate and map critical loads to inputs of acidity have been developed (e.g. Sverdrup, 1989; de Vries and Henriksen, 1989).

Global, regional and national maps showing ecosystem sensitivity to acidic deposition have been produced for a number of years. Global assessments include Troedsson and Nykvist (1973) and Rodhe *et al.* (1988) who produced maps giving a broad overview of areas sensitive to acidic deposition. Kuylenstierna *et al.* (1995) produced a map using soil buffering, land cover and climatic variables that showed sensitivity of terrestrial ecosystems to acidic deposition.

Prior regional studies include: sensitivity distribution in Canada (Environment Canada, 1987); a surface water alkalinity maps for the USA (alkalinity of waters is highly correlated with soil and geological properties) by Omernik (1982); in China (Zhao *et al.*, 1994); in Japan (Wada *et al.*, 1983); and in Australia (Chartres *et al.*, 1996). In relation to other regional work, it is important to include the critical loads map from the RAINS-Asia activity (Hettelingh *et al.*, 1995).

Generally, mapping of soil sensitivity to acidification is consistent with previous global and regional approaches. The method used by Kuylenstierna *et al.* (2001a, b) followed the pattern of sensitivity mapping in the UK, Scandinavia and other countries in Europe (Kuylenstierna and Chadwick, 1989; Hornung and Skeffington, 1992; Downing *et al.*, 1993; Posch *et al.*, 1995).



#### 4.2.3 Critical loads assessment method

It is important here to review the method of critical loads assessment through soils sensitivity mapping used by [Kuylenstierna et al. \(2001a, b\)](#) as this is the basis of the procedures use in the current study:

Atmospheric transfer models were used to calculate transfer and deposition of sulphur (using emissions for year 1990 and a projection for year 2050) and alkaline soil dust. The simplest estimate of the critical load is to equate it to the buffering rate (weathering rate) of ecosystem soils. This assumes that soil buffering is the most important factor determining the response from entire ecosystem. A two-stage process of mapping relative scale sensitivity with a secondary application of critical loads was used (Figure 4.1).

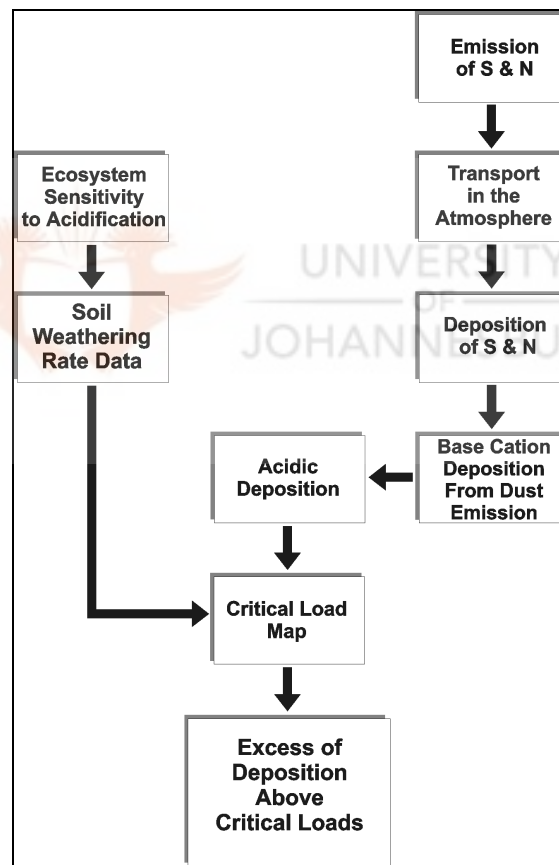


**Figure 4.1:** Methodology for assessing the risk of ecosystem acidification and associated impacts from acidifying deposition by [Kuylenstierna et al. \(2001a\)](#).

#### *Soil buffering parameters – determining soil sensitivity classes*

Cation Exchange Capacity has been used as a parameter for the estimation of soil sensitivity to acidic deposition by a number of authors ([McFee, 1980](#); [Lucas and Cowell, 1984](#)). They proposed three categories of CEC for mapping purposes and in the review of



Kuylenstierna *et al.* (2001a, b) method, the categories of Lucas and Cowell (1984) have been used: <10, 10-25 and >25 meq per 100 g soil.

The base saturation and cation exchange capacity were combined to give a ranking of soil buffering ability. Essentially soils with moderate CEC are ranked 1-5 to show increasing buffering ability according to base saturation categories. For low CEC soils, the buffering ranking is one class lower than for moderate CEC soils. Being already at the lowest rank, unit ranking cannot be decreased further. So, soils with high CEC have been ranked one class higher than those with moderate CEC. The higher number of base saturation classes reflects the higher importance given to the long-term buffering from mineral weathering. The CEC range is ranked from 1 (high sensitivity) to 5 (low sensitivity) across five classes of percentage of Base Saturation, incremented at 20% intervals. This particular method with a combination of three classes of CEC and five classes of BS then defines five relative classes of sensitivity (Kuylenstierna *et al.*, 2001a, b) (Figure 4.2).

**Table 1. Method used to allocate soil types to relative sensitivity classes. The sensitivity score (1, high sensitivity; 5, low sensitivity) is assigned to different combinations of base saturation and cation exchange capacity.**

		Base saturation (%)				
		0–20	20–40	40–60	60–80	80–100
CEC (meq 100g <sup>-1</sup> ) at field pH	< 10	1	1	2	3	5
	10–25	1	2	3	4	5
	> 25	2	3	4	5	5

**Figure 4.2: Method used to allocate soil types to relative sensitivity classes by Kuylenstierna *et al.* (2001a, b).**

Five categories of base saturation have been derived according to the following classes: 0-20%, 20-40%, 40-60%, 60-80% and 80-100%. These have been related to different soil buffer ranges characterised by buffering mechanisms related to the weathering of different minerals and to cation exchange. For example, it is assumed that soils in the range 80-100% will be in the carbonate buffer range; whereas soils with 60-80% will either have a low content of carbonate minerals or a high content of relatively high weathering rate minerals. Soils with a BS of 0-20% will be likely to exist in the aluminium buffer range and 20-40% either within or close to the aluminium buffer range (Kuylenstierna *et al.*, 2001a, b).



This represents a simple method for the combination of CEC and BS where the decreasing sensitivity is indicated by increasing buffering rate and vice-versa.

#### *Weathering rates determination*

Assuming critical loads derived for well-studied areas were applicable to ecosystems with the same sensitivity that are less well studied, damage thresholds might be assigned to new areas to be assessed. Data for critical loads from Europe and North America and estimates for weathering rates were compiled based on works from various sources (Eldar and Brydges, 1983; Nilsson and Grennfelt, 1988; Bain *et al.*, 1995a, 1995b; Hall *et al.*, 1995; Langan *et al.*, 1995a, 1995b; Xie *et al.*, 1995) (Figure 4.3).

**Table 2. Site specific data from the literature for base saturation (BS in %), Cation Exchange Capacity (CEC, units: meq 100 g<sup>-1</sup>) and estimated weathering rate (WR, units: meq m<sup>-2</sup> yr<sup>-1</sup> with method of estimation indicated) compared to sensitivity class (derived from the site BS and CEC)**

Site	% BS	CEC	Sensitivity class	WR	Method	Source
Nordmoen	10.7	2	1	28.1	MAGIC	(49)
Birkenes	9	4.6	1	31.5	MAGIC	(50)
Storgama	6.9	12.1	1	10.7	MAGIC	(50)
ausdal	18.3	6.2	1	41.2	MAGIC	(50)
Sogndal	26.4	3.7	1	11.7	MAGIC	(50)
Dalvatn	21.1	2.7	1	28.7	MAGIC	(51)
Llynn Brianne CL5i	5.3	4.4	1	51	MAGIC	(52)
Llynn Brianne CL5ii	23.1	16.53	2	51	MAGIC	(52)
Alit a'Marcaldh	10	38.9-48.2	1	50.2	MAGIC	(53)
"				10-80	9 methods	(54)
Solling spruce site	5.3	7.59	1	44	BC depletion	(55)
Solling beech site	6.3	7	1	29	BC depletion	(55)
La Castanya, Spain	56	10	3	125	MAGIC	(56)
"	53	5.1	2	73	PROFILE	(56)
Yellow soil, China	20	20	2	59	PROFILE	(57)
Chongqing	50	10	3	250	MAGIC	(58)
Guizhou	30	15	2	250	MAGIC	(58)
Sichuan	50	20	3	250	MAGIC	(58)
Guiyang (LCG)	15	7.8-12.6	1	28.4	MAGIC	(32,59)
Chongqing (TSP)	17	3.2-7.4	1	34.9	MAGIC	(32,59)
Guiyang	13.4 <sup>1</sup>	8.7 <sup>1</sup>	1	75.9 <sup>2</sup>	Column	(60)
Nanchang	10.8 <sup>1</sup>	2.3 <sup>1</sup>	1	24.9 <sup>2</sup>	Column	(60)

<sup>1</sup> depth weighted means      <sup>2</sup> average calculated from several experiments

**Figure 4.3: Compilation of weathering rates, based on literature reviews for matching the sensitivity classes, by Kuylenstierna *et al.* (2001a, b).**

#### *Critical load ranges*

Kuylenstierna *et al.* (2001a, b) derived and assigned two ranges of critical loads to the five sensitivity classes. These ranges were then used to assess the exceedance of critical loads of acidity on a global scale (Figure 4.4).



**Table 3. Preliminary critical load ranges assigned to relative sensitivity classes.**

Sensitivity class	Critical load range (units: meq m <sup>-2</sup> yr <sup>-1</sup> )	
	Low range	High range
1	0–25	25–50
2	25–50	50–100
3	50–100	100–200
4	100–200	200–400
5	> 200 (no critical load)	> 400 (no critical load)

Note: The higher value of each range has been used to map critical load exceedance

**Figure 4.4:** Critical load ranges assigned to relative sensitivity classes by [Kuylenstierna et al. \(2001a, b\)](#).

*Exceedance of critical loads: a measure of risk*

Using the methodology of Figure 4.1, it was possible to derive and map the degree to which net acidic deposition deriving from sulphur emissions (sulphur deposition minus the base cation deposition rate) exceeded critical loads. [Kuylenstierna et al. \(2001a, b\)](#) used the [Tegen and Fung \(1995\)](#) modelled deposition to calculate and plot the global base cation deposition and offset the sulphur acidic deposition. They also did not include the nitrogen compounds and thus their assessment was a partial assessment.

Critical loads are based on a steady-state concept. However, many ecosystems are not in equilibrium with present or projected depositions, since there are processes ('buffer mechanisms') at work, which delay the reaching of equilibrium (steady state) for years, decades or even centuries. Biogeochemical processes can delay the chemical response in soil, and biological processes can further delay the response of indicator organisms, such as damage to trees in forest ecosystems. Therefore dynamic modelling is needed to estimate the times involved in attaining a certain chemical state in response to deposition scenarios, e.g. the consequences of 'gap closures' in emission reduction. In addition to the delay in chemical recovery, there is likely to be a further delay before the 'original' biological state is reached, i.e. even if the chemical criterion is met ([Manual on Methodologies and Criteria for Mapping Critical Loads/Levels, 2004](#)). Thus it is important to bear in mind the uncertainty of the time dimension when the conclusions based on the steady state concept such as applied here are discussed.



#### 4.2.4 *Critical loads assessments in South Africa*

In South Africa two pilot critical loads assessment have been undertaken previously (Olbrich *al.*, 1994, van Tienhoven *et al.*, 1995). The first assessment investigated the potential of the critical loads approach as a key component of an Acid Deposition Risk Advisory System (ADRAS) for South Africa. A region “F” (as per Development Bank of Southern African regionalisation) was selected for a test study and a first attempt was made to define actual deposition loads and critical loads of soils and surface waters in the particular region. Terrestrial critical loads prediction had high uncertainty in a part of the region due to the lack of monitoring stations. A soil critical load map could not be constructed due to the lack of information on mineral weathering rates expected under the climatic conditions within the region F (Olbrich *et al.*, 1994). Instead, a map of relative sensitivity was constructed, based on bedrock lithology, annual rainfall, soil chemistry and land use. This map showed the most and least sensitive areas (Figure 4.5). The need for a refined classification of land-use and soil types was highlighted (Olbrich *al.*, 1994).

The second assessment used rain chemistry data and mean annual rainfall data to infer wet deposition results while dry deposition was not taken into account (van Tienhoven *et al.*, 1995). The estimates for soil critical loads were derived by producing a sensitivity map (using soil parameters such as pH, cation exchange capacity and base saturation). Then critical loads were assigned to the final sensitivity classes (Table 4.1). The report concludes that there was little threat of acidification through wet deposition and it was suggested to focus future investigations on more accurate quantification of the wet component of regional acidification (van Tienhoven *et al.*, 1995).



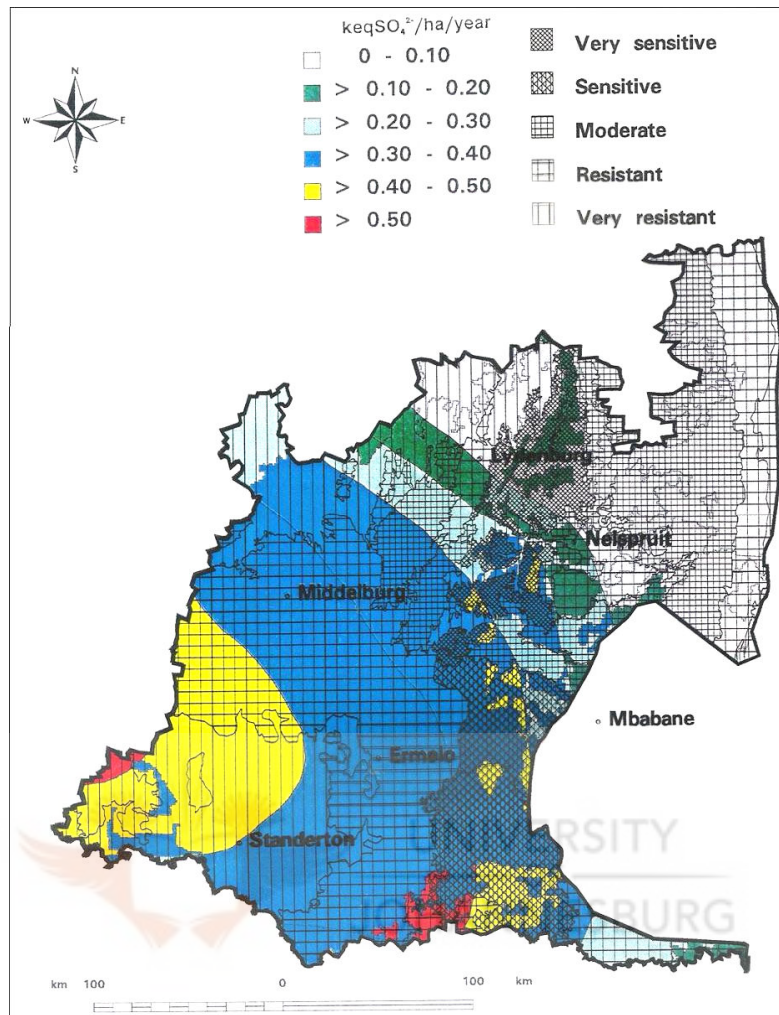


**Figure 4.5:** An overlay of relative soil sensitivity onto the map of sulphate deposition loads to identify areas of overlap between high deposition loads and high soil sensitivity (Source: Olbrich *et al.*, 1994).

This present study extends the two assessments discussed above, by determining dry acidic deposition distribution in addition to using wet deposition. Dry deposition values are based on measured ambient concentrations and then the net acidic (terrestrial) critical loads are assessed over a wider area, covering areas upwind, downwind and around of the major point sources on the Highveld.



**Table 4.1: Synthesis of approaches and calculations adopted in applying the critical loads approach in South Africa (Source: van Tienhoven *et al.*, 1995).**

Approach		Classes	Results
			Critical load
Actual deposition of sulphate	Product of mean annual rainfall and mean volume-weighted sulphate concentration	Actual deposition ranged from 0.1-0.7 keq $SO_4^{2-}$ /ha/yr	
Soil sensitivity	Derived from : Land cover (forestry, woodland, grassland, cultivated lands) Soil features (CEC, pH, base saturation) Lithology (eg granite, quartz, shale, etc)	1: sensitive 2 3 4 5: resistant	Estimated weathering rate of a sensitive site (class 1) to be the critical load for class 1 sites ie. 0.39-0.86 keq/ha/yr is the critical load for sensitive sites
Surface water critical loads	Critical load = (pre-acidification flux of base cations) - (base cation concentration in rainfall) - (alkalinity leaching)		<0.2 keq $H^+$ /ha/yr - Sensitive 0.2-0.5 0.5-1.0 1.0-2.0 >2.0 keq $H^+$ /ha/yr - Resistant

### 4.3 Methods

This section is based on the methodology as explained in “*Acidification in Developing Countries: Ecosystem Sensitivity and Critical Load Approach on a Global Scale*” (Kuylenstierna *et al.*, 2001a), reviewed in Section 4.2. Certain modifications, discussed below, were made to take into account updated soil data and procedures for base cation estimation. The soil data used were SOTERSAF from *ISRIC 2003 database* (ISRIC., 2003) an update of *ISRIC 1995 database* (ISRIC, 1995) used by Kuylenstierna study. The soil dust base cation content percentage (a lower 3% and a higher 20 % were applied contrary to the Kuylenstierna study where only 10 % was applied. In addition to soil-dust base cation deposition, a wet deposition of base cation was included to give a cumulative estimate of base cation deposition for this study.

#### 4.3.1 Procedural steps

Based on the above, the methodology steps for mapping regional sensitivity to acidification were set to be as following:

- Measured concentrations of sulphur and nitrogen were calculated to derive sulphur and nitrogen depositions.
- Net acidifying inputs to ecosystems were determined by estimating the neutralising effect of base cations derived from soil blown dust and wet cation deposition and subtracting the total of BC from the acidifying inputs of sulphur and nitrogen deposition.



- Determining and mapping the soil sensitivity based on the regional soil parameters obtained from the international soil information centre.
- Net acidic inputs were mapped.
- Different (empirical and modelled based) critical loads have been assigned to the relative sensitivity classes of the regional soils.
- Net acidic deposition maps (two levels of the higher option) were laid over soil-sensitivity-class maps (resulting in alternate maps incorporating two options of exceedance).

Several specific adjustments performed in order to prepare necessary input data for the assessment are explained in the following sub-sections.

#### **4.3.2 Base cation deposition**

For this study, two relative concentration values of carbonate compounds in the deposited soil-dust were used, taken from the literature. [Kuylenstierna \*et al.\* \(2001a, b\)](#) set the carbonate content in wind-blown dust at 10% ([Gomes and Gillette, 1993](#)). However, different percentages have been cited within the range 3% to 20% ([FAO-UNESCO, 1977](#); [Gomes and Gillette, 1993](#); [Avila \*et al.\*, 1996](#)). The latter range limits were taken for comparison in this study, being the lowest and highest percentages found. So the BC dry deposition was estimated to be in one instance 20% of the wind-blown and deposited soil dust, while the other was 3%. These carbonate depositions were then combined in the total (wet and dry) cation deposition, deduced from the total S and N cumulative deposition, to obtain the net acidic deposition for each monitoring site.

Two ranges of soil base cation deposition are applicable to the study region, 10-25 meq m<sup>-2</sup> yr<sup>-1</sup> and 25-50 meq m<sup>-2</sup> yr<sup>-1</sup> (Figure 4.6). The midpoint of each range was used to estimate a corresponding BC deposition from soil dust, using the provided estimate of 10% calcium carbonate content. This midpoint value was used as the basis (10%) for an adjusted range of carbonate content being 3% and 20% BC for the study area.

The relatively wide range and high uncertainty of the soil deposition data prompted a strategy for this work to test an upper and a lower estimate, to create a range within which the acidic loads would be evaluated against the soil/ecosystems sensitivity.

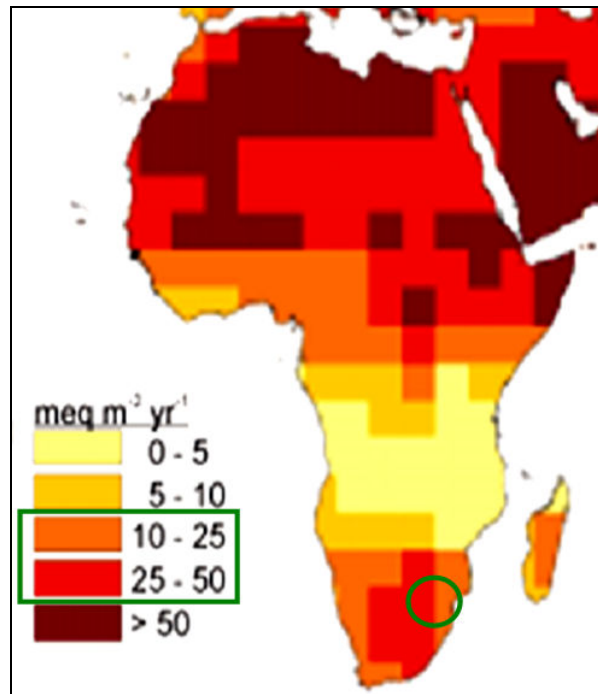


**Figure 4.6:** Base cation deposition extracted from modelled dust deposition and based on depositions of soil dust alone, with assumed 10% Ca content ( $\text{meq m}^{-2} \text{yr}^{-1}$ ) (Source: [Kuylenstierna et al., 2001a](#)).

In addition, an estimate for a wet deposition of BC using long-term measurements of rain chemistry base cations in the study region ([Turner and De Beer, 1996](#)) was added to infer a cumulative BC deposition and to improve the net acidic load estimate. For this calculation of the wet BC deposition, based on the long-term (10-year) rain chemistry measurements ([Turner and De Beer, 1996](#)), were used (Table 4.2).

**Table 4.2:** The measured base cation concentrations used for the wet deposition of base cation estimates\*.

<i>Long-term precipitation chemistry measurement sites</i>	Louis Trichardt	Amersfoort	Warden	Vryheid
<i>Cations of importance</i>	<b>Cation Concentrations (<math>\mu\text{eq l}^{-1}</math>)</b>			
<i>Ca<sup>2+</sup></i>	13.0	22.8	20.5	19.9
<i>Na<sup>+</sup></i>	12.1	9.7	11.5	16.6
<i>K<sup>+</sup></i>	3.9	4.2	8.3	14.0
<i>Mg<sup>2+</sup></i>	4.6	5.5	6.8	6.0
<i>Cumulative precipitation BC mean concentration</i>	<b>33.6</b>	<b>42.2</b>	<b>47.1</b>	<b>56.5</b>

\* Source: [Turner and De Beer, 1996](#).

Having four long-term precipitation chemistry sets for the four different geographic regions where the long-term precipitation chemistry was monitored, enabled the use of



these rain chemistry data sets as the rain chemistry concentration for all project sites. The matching of long-term rain chemistry sets with each project site depended on several spatial factors for each project site, such as geographical proximity to a matching rain chemistry measurement site, closeness to the pollution source region or relative remoteness in the background (Figure 2.4 and Table 3.3). The BC ions (not  $\text{NH}_4^+$ ) concentrations were summed and such concentrations were multiplied by the precipitation measurements (for each monitoring site) for each observed annual cycle. The annual results were then averaged and further used as the wet BC component. This BC component was not apportioned for the industrial and sea-source BC.

For this study, two cumulative BC (a lower and a higher) estimates (determined by soil-dust carbonate input) were taken into account when the net acidic deposition was calculated. First the lower cumulative base cation deposition was plotted and interpolated into isopleths through use of a GIS programme for a spatial distribution overview (Figure 4.7).

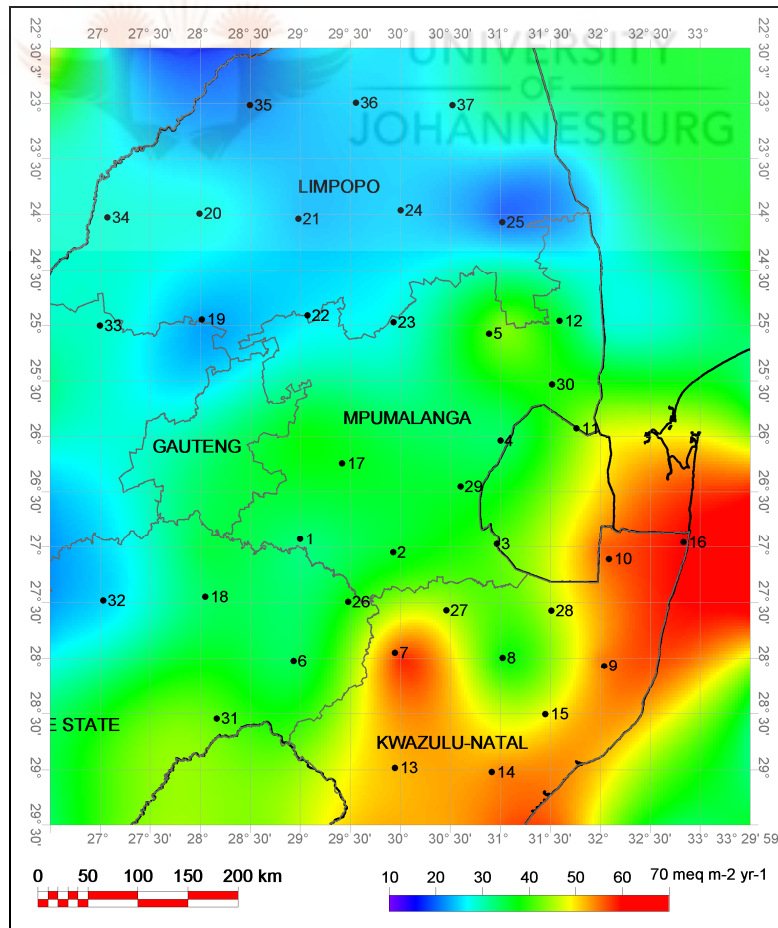


Figure 4.7: Total (dry and wet) lower BC estimated deposition ( $\text{meq m}^{-2} \text{yr}^{-1}$ ).



In addition, the higher cumulative base cation deposition was plotted and interpolated into isopleths through use of a GIS programme for a spatial distribution overview (Figure 4.8).

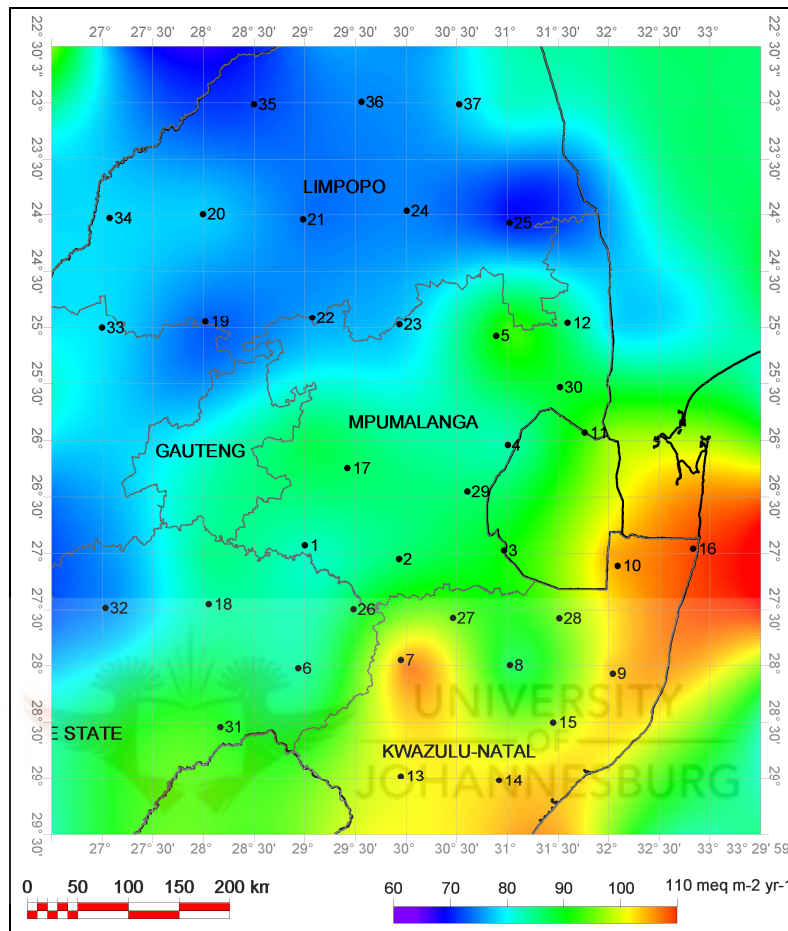


Figure 4.8: Total (dry and wet) higher BC estimated deposition ( $\text{meq m}^{-2} \text{yr}^{-1}$ ).

#### 4.3.3 Soil data

Soil types are described according to typical characteristics. Suitable soil maps and soil databases were searched that contain data with appropriate soil attributes. An international registry of soil information is updated and maintained by ISRIC, FAO and UNEP under the International Union of Soil Sciences (IUSS) in a compilation named *Soil and Terrain Digital Database* (SOTER). Each SOTER database is comprised of two main elements, a geographical component and an attribute component. For this study, the regional SOTER base for southern Africa was used, SOTERSAF (SOTER for Southern Africa) release 1.0 (FAO and ISRIC, 2003). The SOTER database part for South Africa (SASOTER) was originally compiled by the Agricultural Research Council – Institute for Soil, Climate and Agriculture (ARC-ISCW), Pretoria. Both geographical and attribute data were then handled by GIS programme to create polygons of soil types over the study area. The





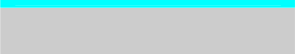


geographical data were related to an attribute database containing two specific attributes, namely CEC and BS. These values were then used to calculate the sensitivity class using the sensitivity allocation described in section 4.2.3 (Figure 4.2).

#### 4.3.4 Determining critical loads from soil sensitivity classes

In this study, critical loads are defined related to the buffering rate of soils ( $\text{meq m}^{-2} \text{ yr}^{-1}$ ) as per method followed. They are therefore highly correlated to the relative classes of sensitivity. Low weathering rates are typical of the most sensitive areas on the map and conversely, the least sensitive areas have high weathering rates. The sensitivity map becomes useful when critical load values are assigned to it in order that it may be compared to deposition estimates or measurements. Based on the obtained higher net acidity levels ( $21 \text{ meq m}^{-2} \text{ yr}^{-1}$  to  $131 \text{ meq m}^{-2} \text{ yr}^{-1}$ ), the following values were assigned to represent the critical loads versus the relevant soil sensitivity classes (Table 4.3). **The critical load for each soil sensitivity class is given at two values; a lower (left column of loads) to higher level (right column of loads) for each class except for the insensitive one** (Table 4.3).

**Table 4.3: Allocated sensitivity classes against critical loads of acidity for use with the regional sensitivity map.**

<b>Sensitivity classes</b>	<b>Critical loads from a lower to a higher sensitivity level (<math>\text{meq m}^{-2} \text{ yr}^{-1}</math>)</b>	<b>Colour code</b>
<b>1 most sensitive</b>	0 – 25	
<b>2</b>	25 – 50	
<b>3</b>	50 – 75	
<b>4</b>	75 – 100	
<b>5 insensitive</b>	>100 (no critical load)	

## 4.4 Results

### 4.4.1 Deposition of acidic compounds over the study region

The two-year mean S and N total deposition rates (cumulative dry and wet) are provided in Section 3.4.6. These were converted from units used in Section 3.4.6, (deposition rate as  $\text{kg ha}^{-1} \text{ yr}^{-1}$ ) into the units suitable for critical loads assessment ( $\text{meq m}^{-2} \text{ yr}^{-1}$ ). For this the appropriate conversion factors were applied where [ $\text{kg ha}^{-1}$  of S] was multiplied by a conversion factor of 62.5; and [ $\text{kg ha}^{-1}$  of N] was multiplied by conversion factor 71.4 to obtain depositions expressed as *chemical equivalent of element X per unit area* [ $\text{eq X ha}^{-1}$ ]. The *eq* units are further converted into *meq* (divided by 1 000) and ha further converted



into  $\text{m}^{-2}$  (divided by 10 000) and thus the final presented units are  $[\text{meq X m}^{-2}]$  (Posch *et al.*, 2001). Detailed tables for deposition of each species are provided in APPENDIX B. Here only the main parameters are given (Table 4.4).

**Table 4.4: The mean and standard deviations of chemical deposition rates for all options used.**

	<i>(meq m<sup>-2</sup> yr<sup>-1</sup>)</i>				
	<i>Acidic anions</i>	<i>Higher base cations</i>	<i>Lower net acidic deposition</i>	<i>Lower base cations</i>	<i>Higher net acidic deposition</i>
<b>Mean</b>	54	84	-30	37	17
<b>Std. dev.</b>	25	11	20	11	20

The results for all sites were interpolated into isopleths through use of a GIS programme for a spatial distribution view of the total (dry and wet) acidic deposition loads (Figure 4.9).

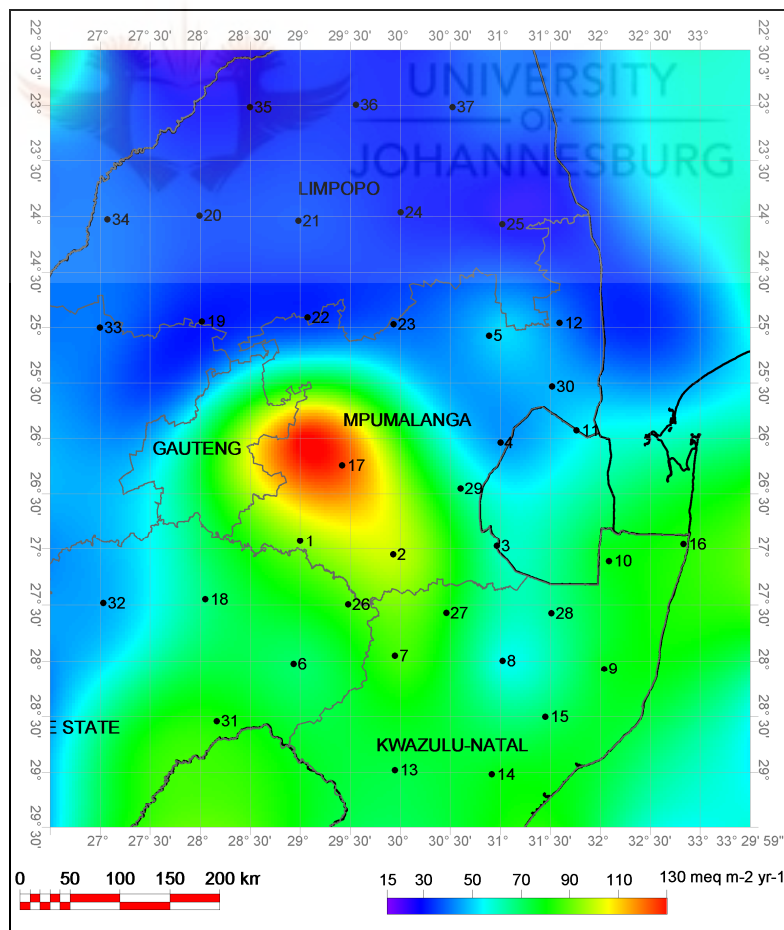


**Figure 4.9: Acidic deposition (total dry and wet) ( $\text{meq m}^{-2} \text{ yr}^{-1}$ ).**





The base cation deposition results (lower and higher options) were subtracted from the mean total (dry and wet) acidic deposition values and so the net acidic deposition values were obtained, a higher option and a lower option. The lower net acidic deposition values were interpolated and plotted into isopleths for a spatial overview (Figure 4.10). For much of the area, except on the central Highveld, the net deposition in this scenario is basic (i.e. *negative* values of net acidic deposition).

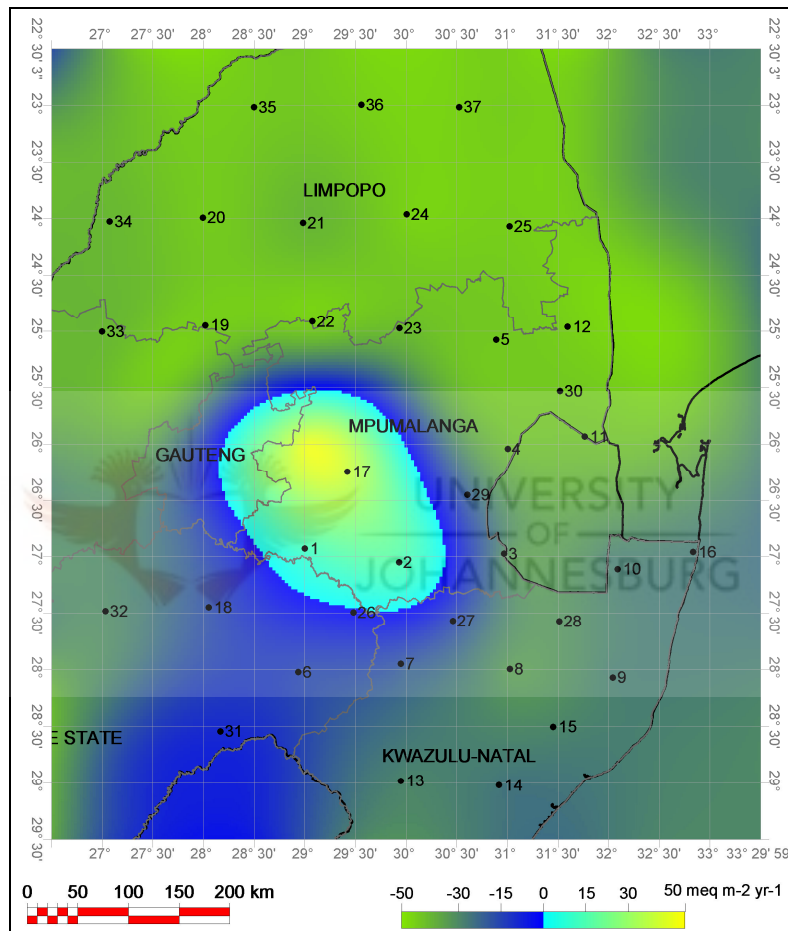


**Figure 4.10:** The lower net acidic deposition (Net Level 1) for the study region (*higher* base cation estimate) ( $\text{meq m}^{-2} \text{yr}^{-1}$ ).

The higher net acidic deposition was plotted and interpolated into isopleths for a spatial overview (Figure 4.11).

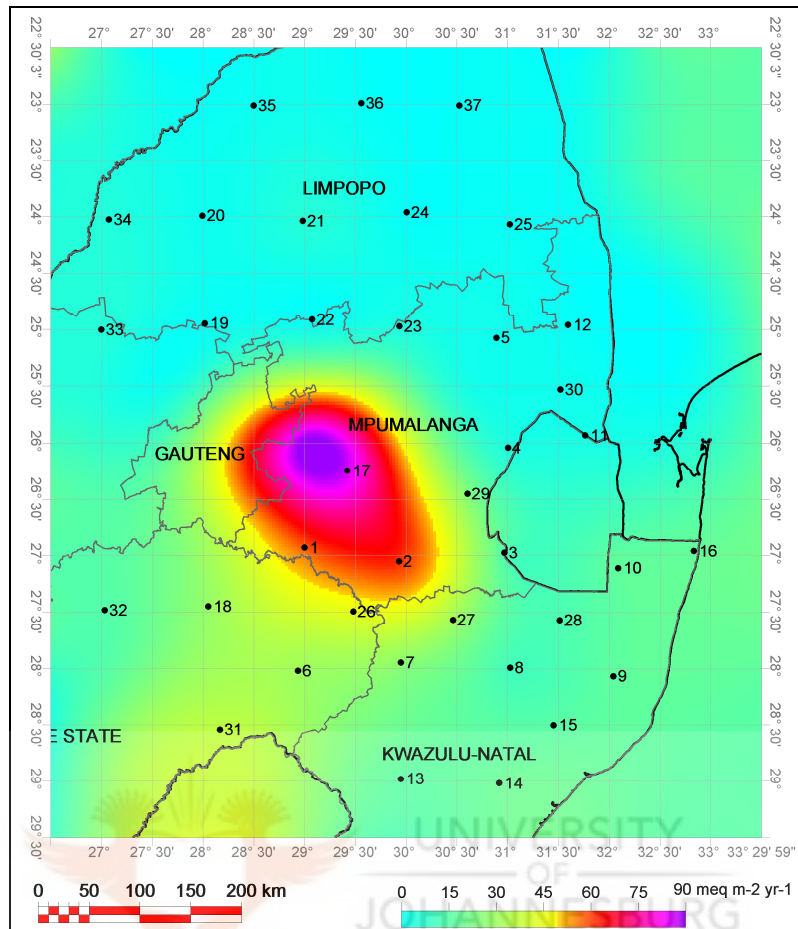


**Figure 4.11:** The higher net acidic deposition (Net Level 2) for the study region (*lower base cation estimate*) ( $\text{meq m}^{-2} \text{yr}^{-1}$ ).

#### 4.4.2 *Soil sensitivity*

The next stage of the analysis is to compare the net acidic deposition with derived critical loads for the soils in the study area. The soil sensitivity polygons are presented in Figure 4.12. These were then assigned critical loads as described above.

Overall most soils fell into the least sensitive class. However, certain areas show the dominance of the most sensitive and second most sensitive classes, 1 and 2 respectively.

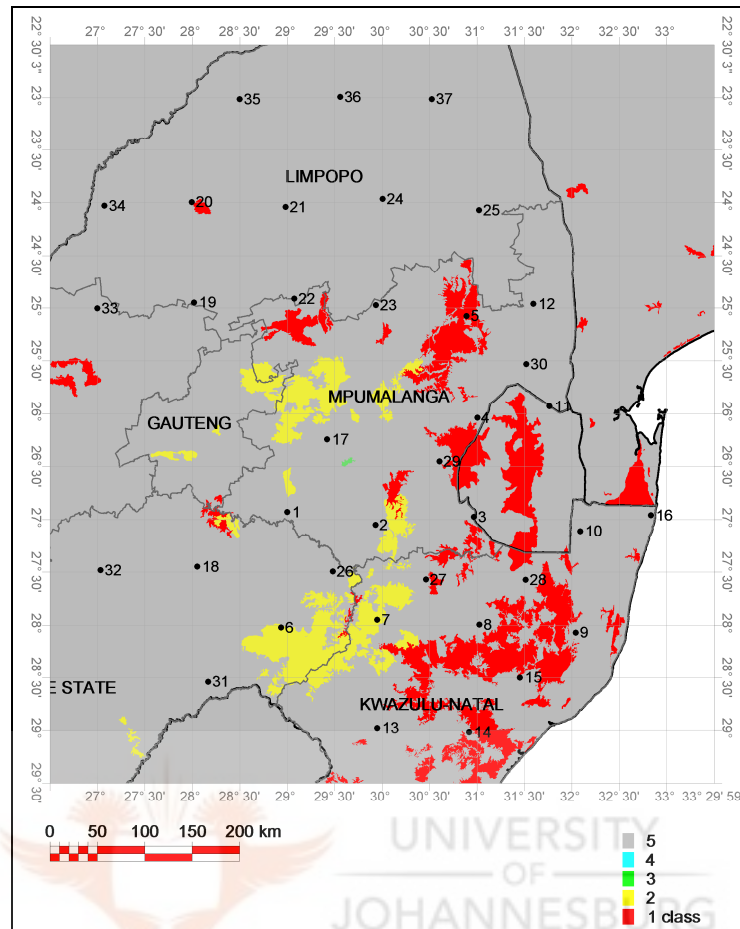


**Figure 4.12:** Sensitivity classes of the soils based on soil attributes, with Class 1 being the most sensitive. (Source: [ISRIC, 2003](#); [Kuylenstierna et al., 2001a](#)).

#### 4.4.3 Acidification risk in the study region

The base cation deposition has been subtracted from the acidic inputs associated with sulphur and nitrogen deposition to derive net acidic load. The lower net acidic deposition map (Net Level 1, Figure 4.10) was not suitable any longer for laying over the sensitivity map, as most of the areas were in *negative* net acidic deposition, with only the central pollution source area showing existence of deposition to a maximum of  $50 \text{ meq m}^{-2} \text{ yr}^{-1}$ . However, the higher net acid inputs map (Net Level 2, Figure 4.11) was suitable for an overlay.

#### 4.4.4 Exceedance of buffering capacity: exceedance of critical loads

The Net Level 2 acid deposition layer was laid over the critical loads maps corresponding to the lower (0-25-50-75) and higher (25-50-75-100) soil sensitivity estimates. The outputs are shown as the exceedances of critical loads in  $[\text{meq m}^{-2} \text{ yr}^{-1}]$  for the two soil sensitivity levels (Figure 4.13 and Figure 4.14).

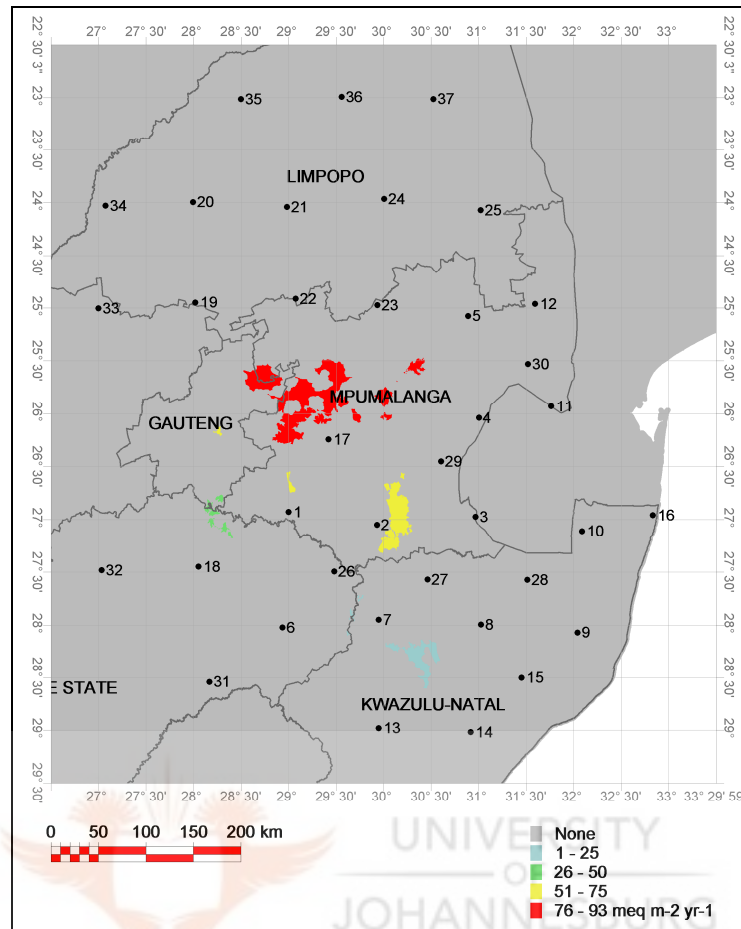


**Figure 4.13:** Exceedance of critical loads, using case of the Net Level 2 acidic deposition and the more critical, lower level of soil sensitivity.

These exceedance maps indicate the areas where and the degree to which net acidic deposition exceeds critical loads. The exceeded areas indicate ecosystems at risk, where acidification and consequent impacts to terrestrial and aquatic ecosystems have occurred or may occur. In contrast, the grey areas indicate areas not at risk from critical load exceedance, according to this study.

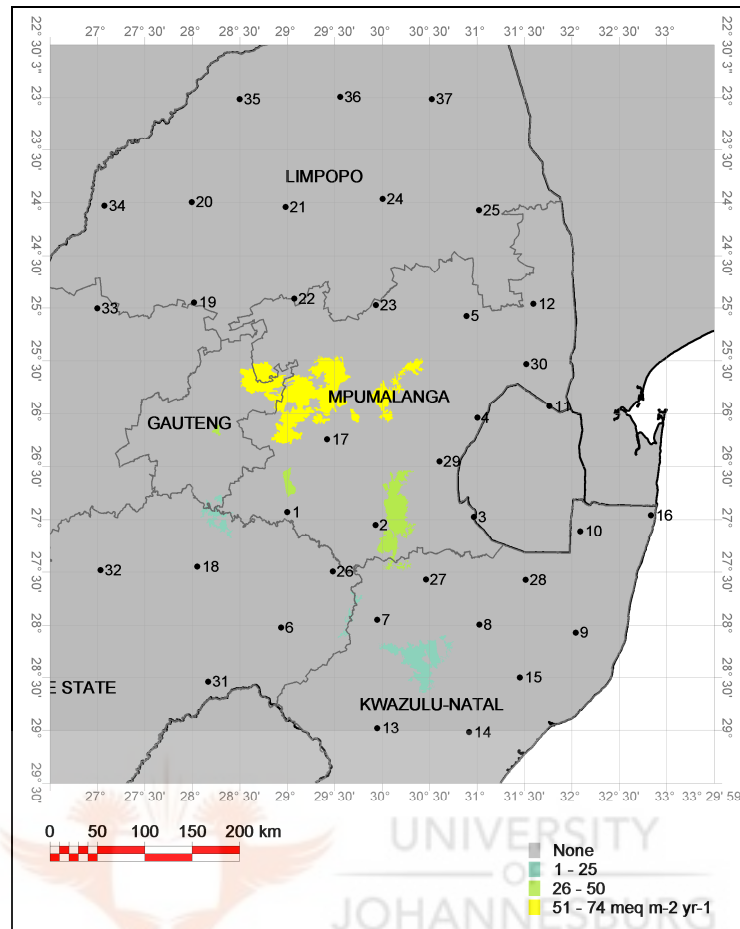


**Figure 4.14:** Exceedance of critical loads, using case of the Net Level 2 acidic deposition and the less critical, higher level of soil sensitivity.

These exceedance maps show that only the central industrial Highveld source area has high values of exceedance. Two smaller areas have exceedances in lower ranges – one just east of Amersfoort and another north of Standerton (range 26 to 50 meq m<sup>-2</sup> yr<sup>-1</sup>). A relatively larger exceedance pocket was established in a lower range (1-25 meq m<sup>-2</sup> yr<sup>-1</sup>) in the Kwa-Zulu Natal Midlands (in a triangle south-east from Newcastle, north east from Escourt and northwest from Kranskop). Several scattered minor pockets of exceedance in this lower range are found: north of Heilbron and northwest of Newcastle but southeast from Memel. However, in none of these secondary areas of exceedance do the values reach the highest ranges observed on the central Highveld (51-75 and 76-93 meq m<sup>-2</sup> yr<sup>-1</sup>).

#### 4.5 Discussion

The results of this study have produced estimates of total acidic deposition on a regional scale, encompassing the entire north-eastern section of country. In addition, estimates of cation deposition were estimated, whereby it was possible using the methodology



developed by the Stockholm Environment Institute (Kuylenstierna *et al.*, 2001a, b) to perform a critical loads assessment of acidity for South Africa.

Contrary to the results of the *critical levels* assessment (section 2.7), a high *critical loads exceedance* was determined in the western and central Highveld industrial region and adjacent area to the north and not, as anticipated, downwind towards the escarpment and the major forestry areas. This was the case for both options applied, one lower range of critical loads (soil sensitivity levels) (0-25-50-75 meq m<sup>-2</sup> yr<sup>-1</sup>) and another higher range (25-50-75-100 meq m<sup>-2</sup> yr<sup>-1</sup>). Several smaller areas, located downwind from major sources, showed exceedances, although the levels of exceedance are not found to be high.

This conclusion challenges the current understanding of the status of acid deposition from Highveld industrial emissions. However, uncertainties in the data, such as base cation deposition level, wet acidic deposition estimates and soil database attributes, limit the confidence of the assessment output. In this respect, the need for measurements of soil dust deposition, with specific attention to base cation content, is emphasised here as one of the least certain sets of input data. There is a further need for direct wet deposition measurements on an extensive spatial and temporal scale. These types of measurement as additional source of data could greatly improve and confirm or deny these findings. Such additional measurements could provide the greater level of confidence needed to justify and implement costly control and mitigation policies and to justify a decision that such mitigation is not justified on ecological grounds. Also, as the critical loads estimate does not give an estimation of future acidification, a time dimension needs to be tested by a use of dynamic models in order to give a better assessment of acidification impact.

#### **4.6 Conclusions**

This study assessment concentrated on the risk of acidification from both sulphur and nitrogen acidifying species, anthropogenic and natural, through the method of critical loads mapping. It follows an axiom that changes in the ecosystem composition and function could occur as deposition continues. The results presented in Section 4.5 indicate that several areas do exceed the critical loads assigned to the local soils. Surprisingly, these areas of exceedance are on the Highveld plateau and not in the Escarpment and forested areas of eastern Mpumalanga. However, the methodology applied did not distinguish different sites and therefore did not account for different surface vegetation in calculation of the deposition. The literature on acidic species deposition to different vegetation types



state that the forested areas have greater deposition (they intercept more pollution) compared to shorter vegetation such as grassland areas (Lowman, 2003) and so deposition to the regional forested areas may be underestimated.

The types of ecosystems (lying within the *savanna* and *grassland* biomes, present in the mapped areas of exceedance) thus need to be investigated for the effects of the acidity exceedance (Figure 4.15). Fieldwork is suggested to test soil acidity and check the effects of possible acidification in the specific ecosystems of the areas that showed exceedance together with several spot-checks in the regional forested areas for a comparison. This would help to ground-truth the methodology, as well soil attributes used as the methodology basis. If the method is indicative of increased acidification, ecologists should test the effects noted and investigate for the mitigation responses.

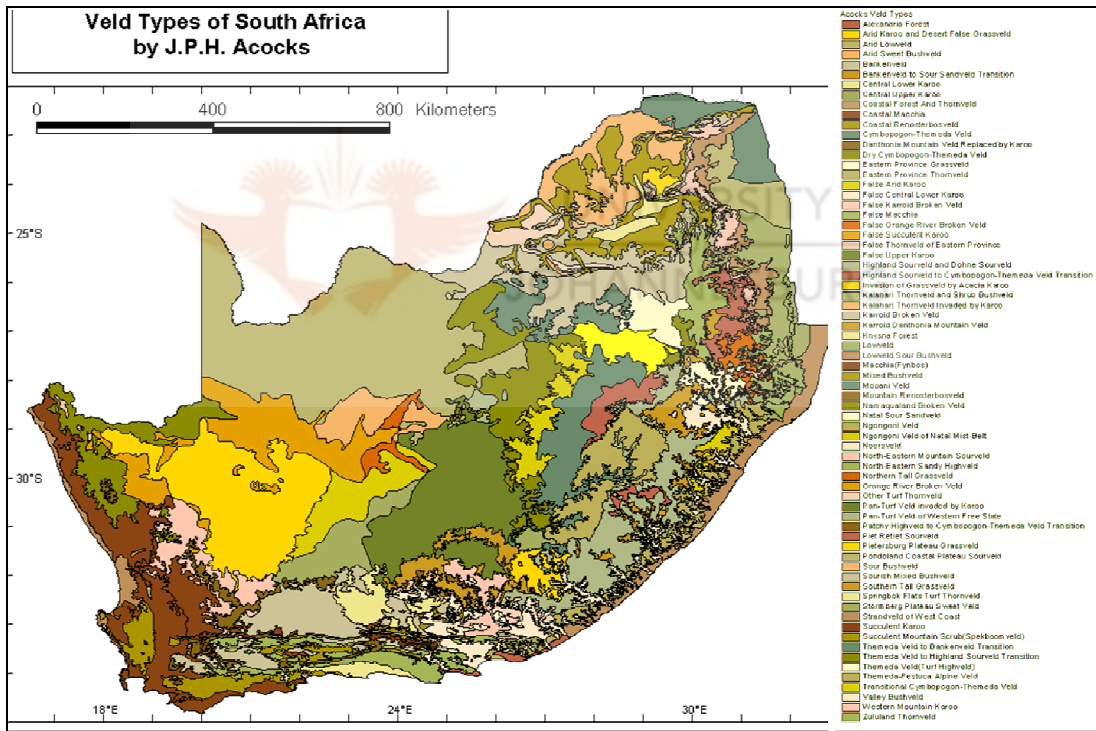


**Figure 4.15** Coarse map of veld types of South Africa (Source: DEAT, 2008).

This, in conjunction with a review of land-cover and land-use, should indicate circumstances of the exceedance areas and needs for possible response measures, if any.

#### 4.6.1 Summary

Although the methodology applied indicates areas where the terrestrial ecosystems may be, or could become acidified, there are uncertainties in most of the data layers and in the methodology. Nevertheless, the critical loads (and levels) represent two indicators for



ecosystem at risk and can aid in pollution monitoring, emission controls and prevention and mitigation policies for the studied region. However, further improvements in input data sets are necessary in order to reduce key uncertainties.

#### **4.6.2**      *Comments*

This study recommends further investigation of soil deposition and base cation content thereof. Also recommended is measurement of wet deposition on a greater spatial and longer temporal scale. These two measures could improve estimated exceedances by reducing the main uncertainties of the critical loads acidification assessment.

While the scientific evidence linking atmospheric acidic deposition with acidification of surface waters and consequent damage to aquatic ecosystems is convincing, the same cannot be said of damage to terrestrial ecosystems, particularly in the context of exceedance of critical load of acidity to soils. Soil acidification is, of course, also a natural process and it is difficult to quantify the extent to which this process is being accelerated by atmospheric acidic deposition. It is also extremely difficult to demonstrate in the field a clear connection between critical load exceedance, declining base cation to aluminium ratios in the soil solution and biological damage resulting from such changes.

Accordingly, there should be a certain degree of caution in acceptance of the critical load exceedance maps method in determining the environmental impact of acidification as the best available method. Of course, this method is not the only method available. Suitability of other methods, particularly direct methods, such as determination of an index of acid neutralising capacity ([Dodds and Fey, 1998](#)) in local circumstances should be explored.





## CHAPTER FIVE

*This chapter uses the database of ground-level trace gas concentrations of SO<sub>2</sub>, NO<sub>x</sub> and O<sub>3</sub> from Chapter Two to compare and validate remote sensing measurements of these pollutants. A method to compare ground-level passive sampling concentrations to remote sensing derived integrated column densities is developed, based on assumptions of a well-mixed boundary layer and on partitioning of the trace gases between layers of the atmosphere. Results are produced that constitute a new angle on utilising remote sensing technologies in regional-scale air pollutant measurements.*

### **5. Comparison of Remote Sensing Tropospheric Trace Gas Measurements with Regional-scale SO<sub>2</sub>, NO<sub>2</sub> and O<sub>3</sub> Ground-level Measurements**

#### **5.1 Comparison of Tropospheric Boundary Layer Concentrations to Ground-level Pollutant Concentrations**

As for air dispersion modelling, it is equally important for remote sensing measurements to be validated through comparison with measured results. In this context, the large spatial and temporally extended monitoring performed for this study and its concentration database has potential for comparison and validation of satellite-borne remote sensing measurements. Satellite-borne remote sensing images of atmospheric trace gases consistently show the study region as one of the world-hotspots of SO<sub>2</sub> and particularly of NO<sub>2</sub> pollution. Thus, an attempt to validate satellite-borne remote sensing observations for the studied region became a desirable and important additional task of this research.

The purpose of this chapter is to present the development of a method and results of tests on the comparability and relative accuracy of RS column density measurements versus the ground-level concentration measurements. The procedure applied tested also the applicability of the conversion process of RS data that are routinely presented as vertical column density (VCD) to volume mixing ratio (VMR). This conversion was necessary to allow direct comparison of RS and PS results.

The procedure for this study was to obtain and compare concurrent tropospheric trace gas mixing ratios from RS and PS techniques. This approach required as an initial step a review of current knowledge on the atmospheric layering over the South African Highveld,



to facilitate estimation of the depth of the boundary layer and the strength of the inversion layer separating it from the mid-troposphere.

An assumption is made that the concentrations of trace gases within the boundary layer represent a distinguishable fraction of the total column density and hence the total column density observed by RS can be converted into an *average volume mixing ratio* (VMR) through the depth of the mixing layer. A second and major assumption is made that the boundary layer is uniformly mixed throughout its depth and hence the ground-level measurement of the VMR by passive sampling is representative of the average VMR throughout the mixing layer. In this way the boundary layer RS results could be further converted for comparison with the ground-level volume mixing ratio results. The procedure used atmospheric pressure difference equations to separate indirectly the boundary layer column from the tropospheric column. Comparisons for all three gaseous species, NO<sub>2</sub>, SO<sub>2</sub> and O<sub>3</sub>, were carried out in a similar manner.

## 5.2 Measurements of Tropospheric Gases from Space

Recent scientific and technological developments allow that many important atmospheric phenomena can be monitored on a global scale and over an extended period. Satellite observations in particular allow monitoring of the temporal and spatial variability of atmospheric trace gases, such as NO<sub>2</sub>, SO<sub>2</sub> and O<sub>3</sub> (Khokhar *et al.*, 2003). For example, global hot-spots of NO<sub>2</sub> on an annual scale have been compiled from the GOME sensor (Figure 5.1) (Wenig *et al.*, 2003).

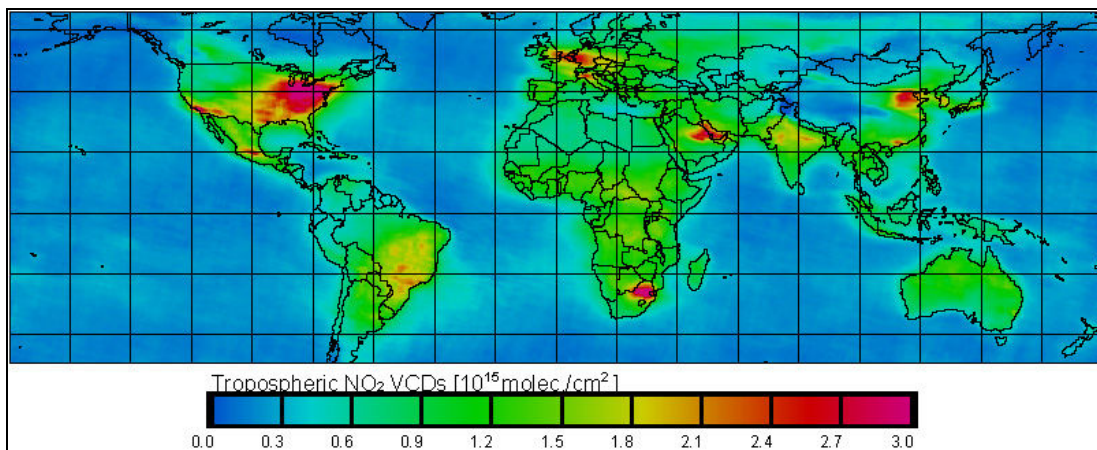


Figure 5.1: Annual tropospheric NO<sub>2</sub> observed by GOME instrument (Source: Wenig *et al.*, 2003).



However, an inherent difficulty with atmospheric satellite measurements is the separation of the tropospheric absorption from reflected sunlight shine, which is measured in a downward-viewing (nadir) configuration from ~800 km altitude through the stratosphere. Some of trace gas species of interest in the troposphere (e.g. O<sub>3</sub>, NO<sub>2</sub>) are also abundant in the stratosphere, while others (e.g. SO<sub>2</sub> or HCNO) are not (Borrell *et al.*, 2004). Thus this type of “remote sensing” result needs to be checked for its suitability for comparison with results obtained by ground-level measurements and vice-versa.

### 5.2.1 *NO<sub>2</sub> remote sensing*

While the main sources and source regions of NO<sub>2</sub> are known, large uncertainties remain on the regional source strengths and their latitudinal and seasonal variations (IPCC, 2001). Interest in the climatic role of tropospheric NO<sub>2</sub>, however, has shown up that a significant radiative forcing (exceeding that of CO<sub>2</sub>) can build up during periods with extremely elevated NO<sub>2</sub> levels in the troposphere (Solomon *et al.*, 1999). This is in addition to and different from the well-known radiation forcing influence of the longer lived *nitrous oxide*, N<sub>2</sub>O. Such pollution events might be underestimated in duration and horizontal extension due to the short lifetime of NO<sub>2</sub> in the boundary layer.

Tropospheric NO<sub>2</sub> hot spots and source strengths and their quantification in time and space can be investigated using modern nadir-looking satellite instruments, such as GOME (the **G**lobal **O**zone **M**onitoring **E**xperiment), SCIAMACHY (the **S**Canning **I**maging **A**bsorption spectro**M**eter for **A**tmospheric **C**Hartograph**Y**), or OMI (the **O**zone **M**onitoring **I**nstrument) (Borell *et al.*, 2004; Levelt *et al.*, 2000). However, it was shown only recently that NO<sub>2</sub>-rich pollution hot spots can spread over large areas for several days (Leue *et al.*, 2001) and that NO<sub>2</sub> transport over large distances is possible (Stohl *et al.*, 2003; Schaub *et al.*, 2005). For example, a vertical column density (VCD) image of NO<sub>2</sub> over Africa on a monthly time-scale is illustrated in Figure 5.2.

Differences exist in measurement precision using RS between the stratospheric, upper tropospheric and planetary boundary layers. Particularly, the precision depth distributions of NO<sub>2</sub> in the boundary layer and on near ground level concentrations are still not good. A monthly average of the measured ground-level concentrations in north-east sector of South Africa (this work) for the same month as depicted in Figure 5.2 is illustrated in Figure 5.3.

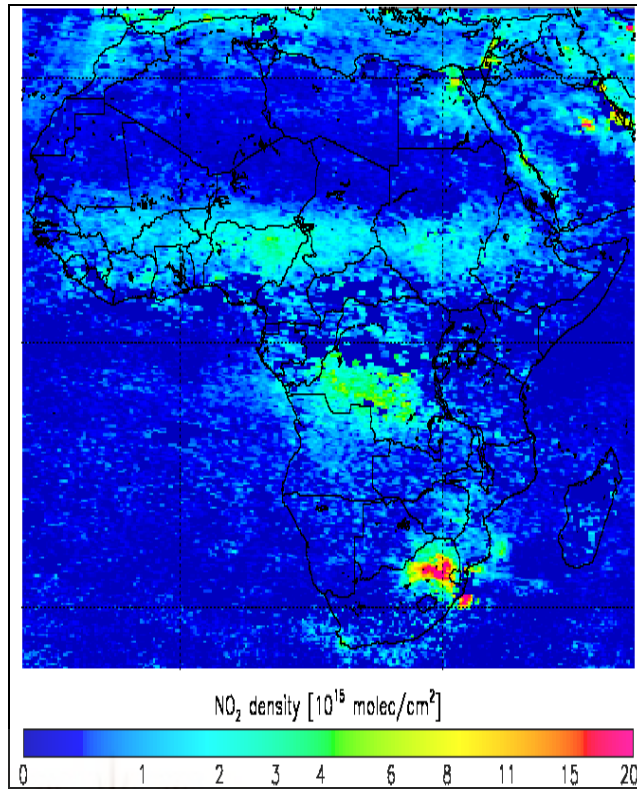


Figure 5.2: NO<sub>2</sub> tropospheric VCD mean for May 2006 (Source: TEMIS, 2008; KNMI/IASB/ESA).

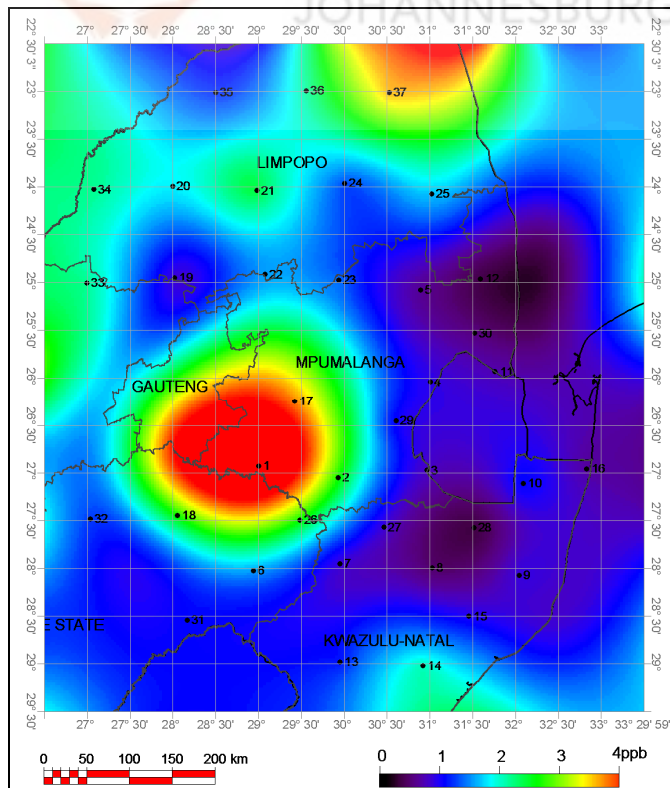


Figure 5.3: Ground level measured NO<sub>2</sub> concentration contours for May 2006.



### 5.2.2 *SO<sub>2</sub> remote sensing*

SO<sub>2</sub> column densities are retrieved from SCIAMACHY measurements in the 315 - 327 nm wavelength range. Because of the large ozone absorption in this spectral region, the intensity of the backscattered radiation is low at these wavelengths and interference by ozone is a problem (IUP, University of Bremen, 2008). However, if signals are large enough or the SO<sub>2</sub> concentrated in the middle or upper troposphere, clear SO<sub>2</sub> signals can be observed in the satellite data. As an example, a part of a global tropospheric sulphur VCD by satellite-borne remote sensing (a 32-month average of SCIAMACHY SO<sub>2</sub>) is shown in the Figure 5.4, highlighting areas of high pollution (e.g. China and the Highveld region of South Africa); volcanic eruptions (e.g. Nyamuragira in the Democratic Republic of Congo); refineries in the Persian Gulf; and smelting in Russia. For calculation of column densities illustrated in Figure 5.4, it was assumed that SO<sub>2</sub> is located in the middle troposphere, which leads to substantial underestimation of SO<sub>2</sub> where it is concentrated in the boundary layer (IUP, University of Bremen, 2008).

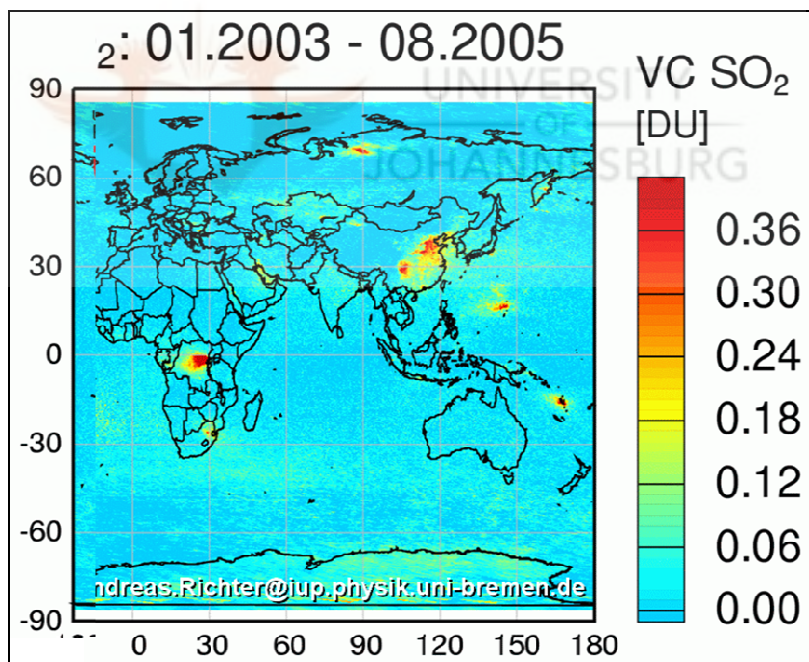
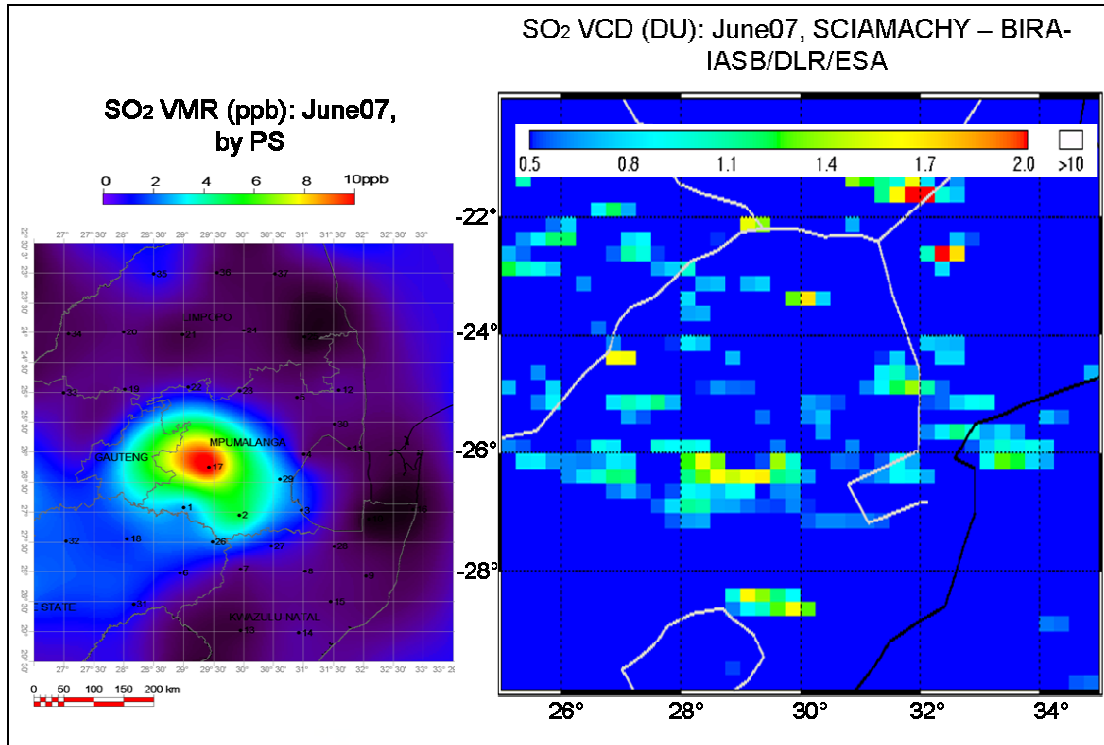


Figure 5.4: A 32-month average of SCIAMACHY SO<sub>2</sub> for a part of the globe. (Source: IUP, University of Bremen, 2008).

A sample of ground level measured SO<sub>2</sub> concentrations results are compared with RS retrievals for visual comparison in Figure 5.5.



**Figure 5.5:** Comparison of a) PS ground-level SO<sub>2</sub> measured (June 2007); and b) RS (SCIAMACHY) VCD at 1 km height over the study region (June 2007) (Source: (a) this work; (b) van Geffen, personal communication, 2008).

### 5.2.3 O<sub>3</sub> remote sensing

Whereas ground-based measurements of tropospheric ozone give limited data in time and space, observations from space platforms offer the possibility to measure the distribution of tropospheric ozone over large areas and to study the large-scale temporal and spatial behaviour (Figure 5.6).

This is of great importance, since ozone formed over source regions, where large amounts of ozone precursors are emitted, can be transported over great distances and affect areas far from the source. The illustration of measured monthly average ozone illustrates relatively higher concentrations outside of the studied main industrial pollution source area (the industrial Mpumalanga Highveld) than within it (Figure 5.7).

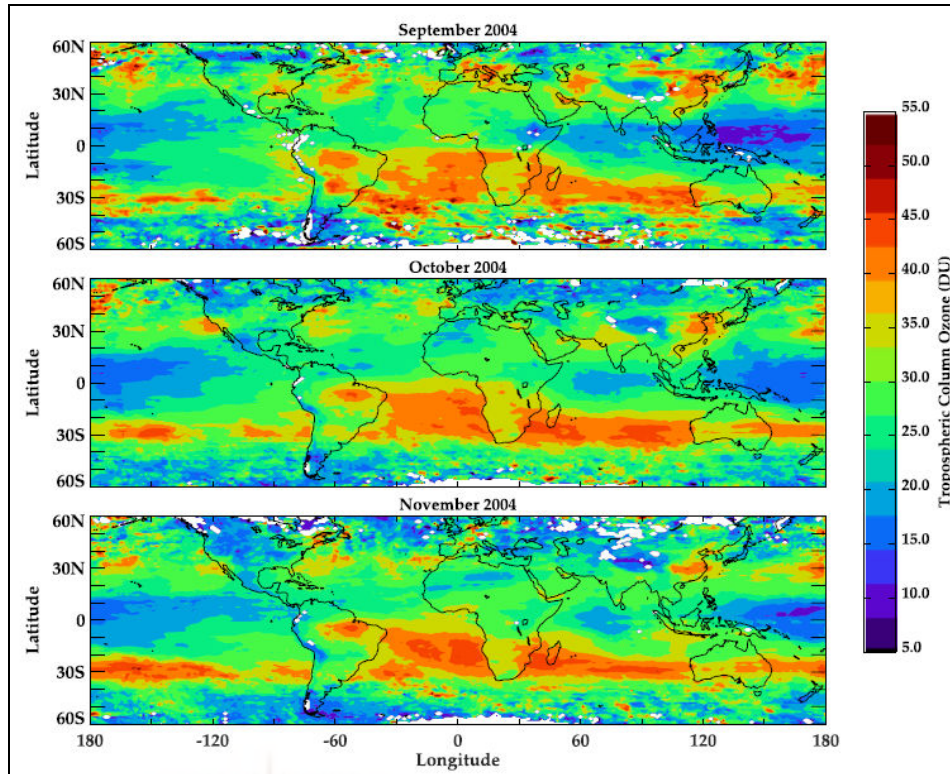


Figure 5.6: Monthly averaged OMI/MLS Tropospheric Column Ozone (DU) for September–November 2004 (Source: Ziemke *et al.*, 2006).

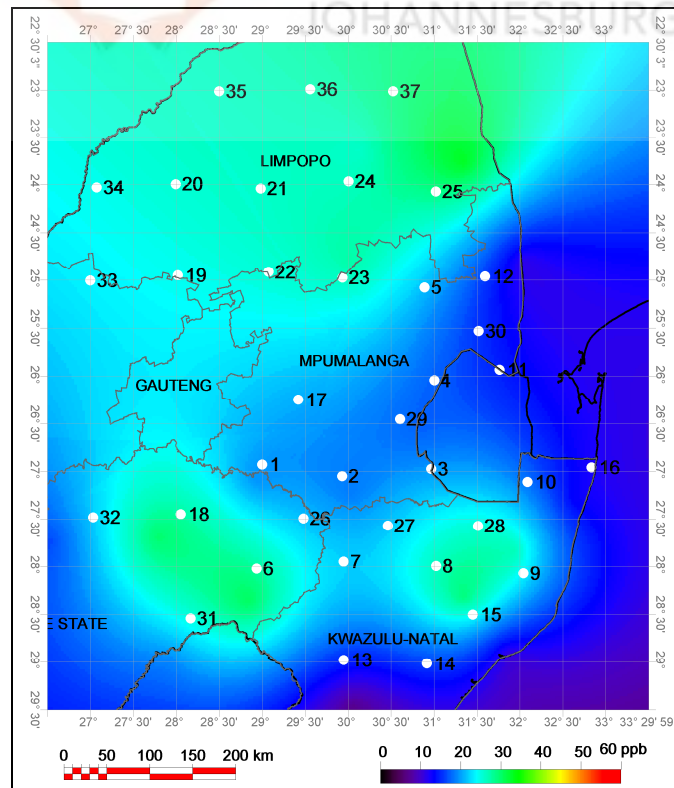


Figure 5.7: Ground-level O<sub>3</sub> measured by passive diffusive sampling and GIS-interpolated for Sep05.



#### 5.2.4 Validation of satellite remote sensing results

The current satellite retrievals of tropospheric trace gases are still of limited accuracy. Error estimates for the satellite data are about 50% for polluted regions and larger in cleaner regions (Richter and Burrows, 2002; Boersma *et al.*, 2004). Therefore, intensive further joint investigations together with ground-based or airborne measurements are required, targeting both validation and synergistic use, i.e. an improved error assessment as well as an improvement of the satellite measurements themselves, by synergistically combining them with the complementary information attainable from in situ measurements.

Currently no specific tropospheric boundary layer data products are available. Although such tropospheric data can be extracted from total vertical tropospheric column, it requires much adjustment of the existing total vertical column data product (von Savigny, personal communication, 2008). The profiles are usually retrieved from the altitude range of 15 to 45 km above the ground (Kuehl, personal communication, 2008) and the corresponding results are thus not suitable for comparison with tropospheric boundary layer (including near ground-level) measurements (Figure 5.8).

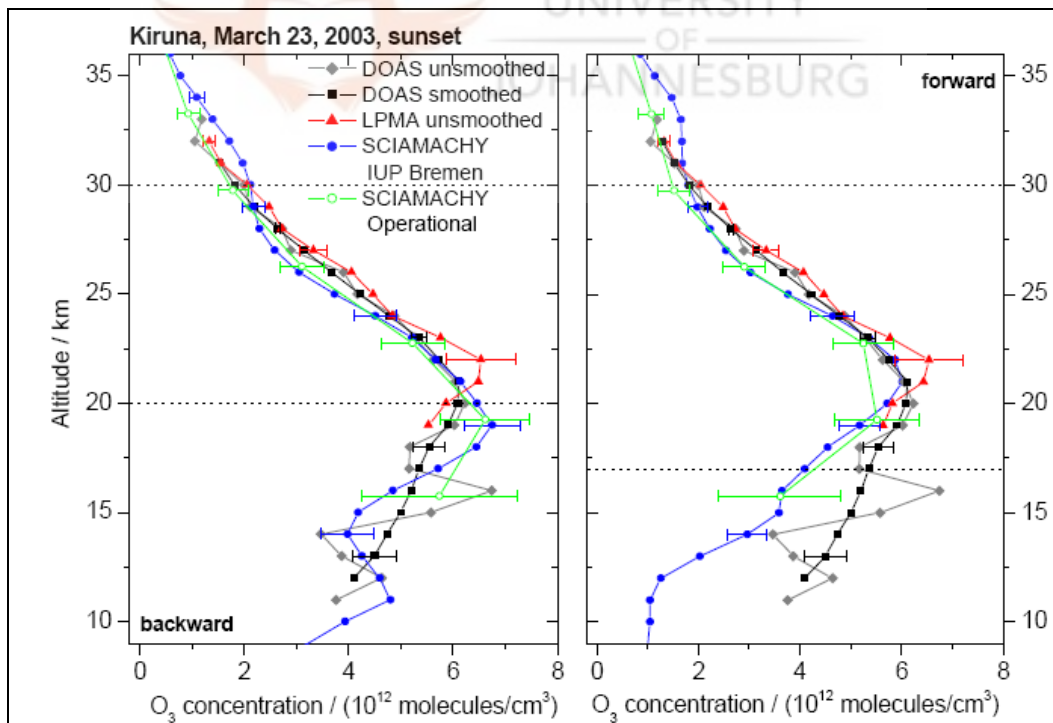
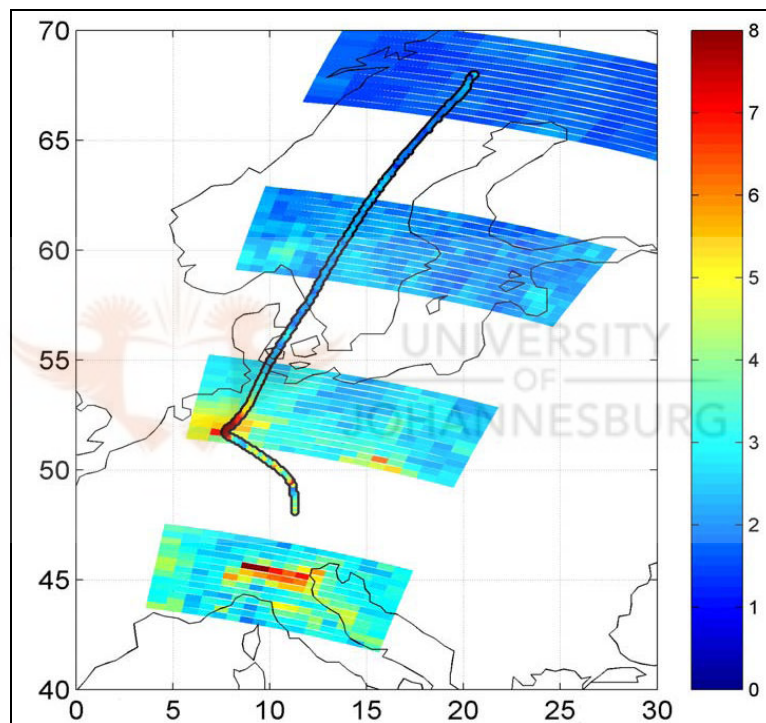


Figure 5.8: Sample of a vertical profile comparison [Comparison of O<sub>3</sub> profiles inferred from SCIAMACHY limb observations with correlative balloon-borne measurements (Source: Pfeilsticker *et al.*, 2007)].





The *in-situ* measurements in this context are the ones resulting in vertical column and vertical profiles derived from air-borne (Figure 5.9) and suitably positioned ground instruments (Figure 5.10). They measure tropospheric columns and profiles (zenith and nadir viewing) for comparisons to satellite-borne measurement for the same area and relatively simultaneously. In the case of an air-borne validation example, measurements have been performed with an Airborne Multi AXis DOAS (AMAXDOAS) instrument that was operated on a Falcon research aircraft (Heue *et al.*, 2004). It flew at 11 km (mid-latitude), thus it can be assumed that zenith-viewing telescope observed the stratosphere and the nadir viewing observed the troposphere.



**Figure 5.9:** Vertical NO<sub>2</sub> column densities [ $10^{15}$  molec cm<sup>2</sup>] observed by SCIAMACHY and AMAXDOAS on 10 March 2003 (Source: Heue *et al.*, 2004).

Validation results taken up until now concentrated on comparison of mid- and upper tropospheric layers and often, given the low accuracy of the satellite-borne results for the lower troposphere, clearly avoided presenting satellite vertical profiles extending to ground level (Figure 5.10).

Despite these current practical limitations, an effort is undertaken in this study to compare and validate available and accessible remote sensing, satellite-borne tropospheric measurements of trace gas column densities with the ground-level measurements from this study.

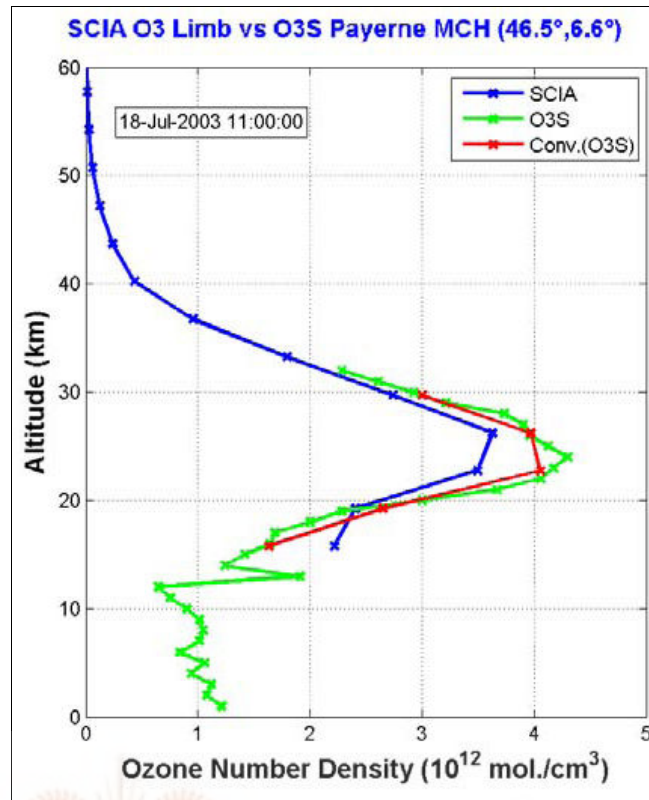


**Figure 5.10:** SCIAMACHY ozone profile plotted versus altitude and coincident ozone sonde profile (O3S) measured at the NDACC/Alpine station of Payerne. Corresponding correlative profile smoothed to the SCIAMACHY vertical perception using averaging kernel matrix and a priori information (Source: [De Clercq et al., 2006](#)).

### 5.3 Methods

#### 5.3.1 *Ground-level measurements by passive diffusive sampling*

The methodology applied to derive a database of ground-level trace gas concentrations for SO<sub>2</sub>, NO<sub>x</sub> and O<sub>3</sub> was as presented in Section 2.2.

#### 5.3.2 *Remote sensing of tropospheric gases and instruments used*

Remote sensing of tropospheric constituents (trace gases, aerosol and cloud) is a relatively new area of research. However, both active and passive techniques have been successfully employed to probe the troposphere.

UV-visible absorption spectroscopy using reflected terrestrial sunlight is a widely used technique for measurement of atmospheric trace gases from various platforms: ground, aircraft, balloon or satellite. Satellite measurements are used in particular for remote sensing of stratospheric species. However, despite the reduced sensitivity towards the troposphere and the more complex radiative transfer, also tropospheric species can be



determined. The GOME and SCIAMACHY sensors measure the solar radiation scattered from the Earth's atmosphere or reflected from its ground. The absorption and emission of photons by molecules changes the energetic state of the molecule by causing electronic, vibrational and rotational transitions. The absorption cross sections are characteristic for the absorbing molecule. In principle, the analysis of absorption spectra allows the retrieval of atmospheric trace gas quantities (Beirle, 2004).

### *Differential Optical Absorption Spectroscopy*

In this technique, data are retrieved by **Differential Optical Absorption Spectroscopy** (DOAS) as applied to satellite observation of up-welling radiation for a selected spectral window (IUP, University of Heidelberg, 2008). The relatively narrow band spectral features of gases are then separated from broadband gas and aerosol absorption as per the schema in Figure 5.11.

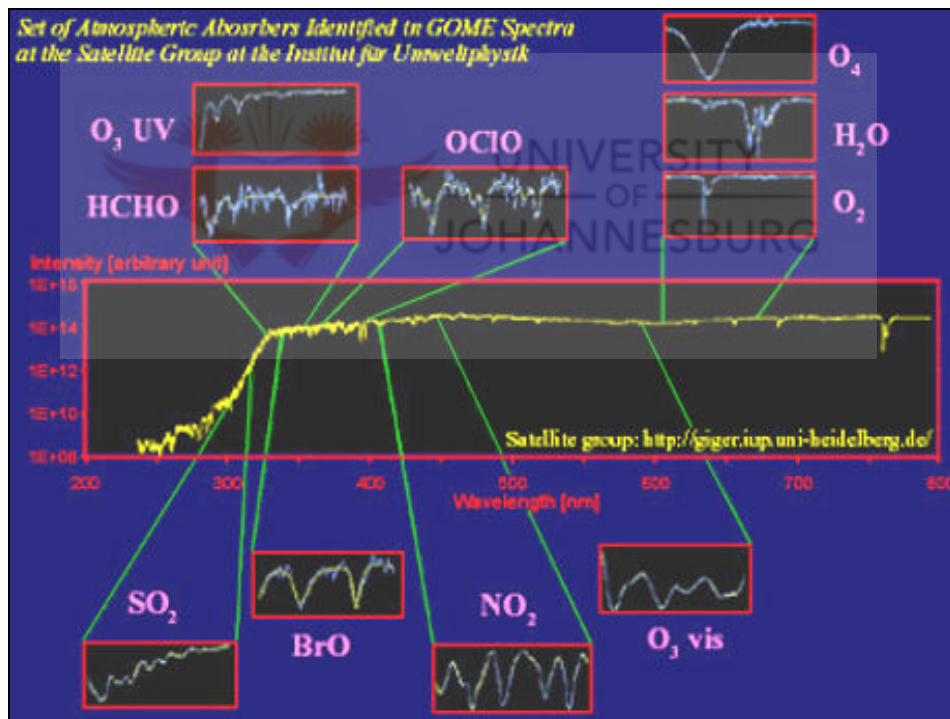


**Figure 5.11: Spectral windows for the various species measured by GOME (Source: IUP, University of Heidelberg, 2008).**

The unique location of South African sources (well separated from any other major regional and global sources) of the trace gases bodes well for the comparison and possibly validation of the trace gases measurement by these satellite instruments (Annegarn, personal communication, 2005). This study utilised SCIAMACHY and OMI/MLS results



for the study region for comparison (and validation) against the ground level concentration measurements obtained in this work.

#### *Satellite-borne instruments*

The first satellite-borne instrument to be used to retrieve a tropospheric amount of a trace gas was the NASA TOMS (Total Ozone Monitoring Spectrometer). This instrument yielded the tropospheric abundance of ozone and aerosol. GOME, since 1995 and SCIAMACHY, since 2002, are European instruments developed to measure scattered solar light from the Earth's atmosphere. Although GOME was designed for about 5 years of operation, some parts of the instrument remained operational after the designed operational time. However, several parts of the instrument degraded and subsequently the measurement of the direct solar spectrum failed from August 2001 until October 2002. Finally, on 22 June 2003, the on-board data recorder failed. Since then, only data that can be received directly by the ground stations are available, effectively covering an area reaching from the North Pole towards Southern Europe (Beirle, 2004). Thus for this study over Africa, only RS data obtained from SCIAMACHY coinciding with the concurrent measurements by passive sampling were available for comparison. Images from GOME-2, the successor to GOME, were not considered for this work.

#### *SCIAMACHY sensor*

SCIAMACHY was launched in March 2002 onboard the ESA satellite ENVISAT. Its general layout and measuring principle are similar to GOME, but in comparison to GOME, SCIAMACHY has been improved widely. It incorporates eight spectral channels that cover also the near infrared. SCIAMACHY provides additional viewing geometries, namely limb and direct occultation of sun, moon and stars. Especially for trace gases that exist in the stratosphere and troposphere (like  $\text{NO}_2$ ), information on the tropospheric burden require first the stripping out of the stratosphere component. Due to the limb-nadir-matching of SCIAMACHY, i.e. the alternation of viewing geometries, information about the stratospheric profile can be used to subtract the stratospheric from total column, resulting in tropospheric column densities. Measurements are made with a ground pixel size of  $15 \times 30 \text{ km}^2$ , but due to the restricted bandwidth for data transmission, usually four observations are integrated on board, leading to a standard retrieved ground pixel size of  $60 \times 30 \text{ km}^2$ . However, due to the alternating viewing geometries, there are gaps along track, leading to a checkerboard pattern. The limb-nadir alternation is timed in such a way



that the areas missed during one scan are covered by the next overpass 3 days later. Thus, SCIAMACHY achieves global coverage at the equator with a 6-day cycle (Beirle, 2004).

#### *OMI and MLS sensors*

The OMI and MLS are two of the sensors on the NASA EOS Aura satellite platform. The OMI is a nadir-viewing, wide-field-imaging spectrometer. The OMI instrument employs hyper-spectral imaging in a push-broom mode to observe solar backscatter radiation in the visible and ultraviolet band. The hyper-spectral capabilities improve the accuracy and precision of the total ozone amounts. It also measures other key air quality components such as NO<sub>2</sub>, SO<sub>2</sub>, BrO, OCIO and aerosol characteristics. It has daily global coverage and it is capable of mapping pollution products on urban-to-super-regional scales.

MLS uses microwave emissions to measure stratospheric temperature and upper tropospheric constituents. The simultaneous MLS measurements of upper tropospheric constituents, under all conditions and with good vertical resolution, are of great value for improving our understanding of processes affecting the distribution of atmospheric constituents, climate variability and tropospheric-stratospheric exchange.

#### **5.3.3 Comparison of passive sampling with satellite remotely sensed data**

Satellite data need to be apportioned into components for the various layers, specifically to isolate the tropospheric column and the boundary layer column. Thereafter data are converted into a mean VMR for the boundary layer. A method was followed to partition the tropospheric column density to obtain the column density for the boundary/mixing layer. Ground level measurements, which are mean values measured over 30-day intervals, are reasonably assumed to represent the mean concentration (VMR) of a well-mixed boundary layer. Once these preparatory steps are completed and with these assumptions, it is possible to make a direct comparison of the two data sets.

The tropospheric (total) column density of a trace gas derived by satellite remote sensing is usually reported in units of [molec cm<sup>-2</sup>] and less often in Dobson Units [DU], representing a thickness of a layer of specific gas contained in a column above the Earth's surface. Dobson Units were originally derived for measurement of ozone concentrations, referring to a specific measurement technique for that gas. As some of the satellite-derived products used in this work were received in [DU], these units have been used in this chapter for SO<sub>2</sub> and O<sub>3</sub> discussions, while acknowledging that the use of [molec cm<sup>-2</sup>] is preferred by other researchers. Such Vertical Column Density (VCD) units (DU or molec cm<sup>-2</sup>) needed to be



converted into a **Volume Mixing Ratio (VMR)** expressed in units of [ppm] or [ppb] in order to compare satellite-derived measurements with ground-level concentrations. For this, the following definitions and equations apply Figure 5.12 (Ziemke *et al.*, 2001; Ziemke *et al.*, 2006).

Definition: 1 Dobson Unit  $\equiv 2.69 \times 10^{20}$  molecules- $m^{-2}$

$$\Delta\Omega(\text{Dobson Units}) \approx 0.79 \int_{P_1(\text{hPa})}^{P_2(\text{hPa})} \chi(\text{ppmv}) \cdot dP_{ATM}(\text{hPa})$$

$$\langle \chi(\text{ppmv}) \rangle \approx 1.27 \cdot \frac{\Delta\Omega(\text{DU})}{P_2(\text{hPa}) - P_1(\text{hPa})}$$

**Figure 5.12: The DU and pressure-averaged mixing ratio (Source: Ziemke, personal communication, 2008; Ziemke *et al.*, 2006).**

In essence, separation and conversion of the tropospheric column from the stratospheric column is also applicable for conversion of boundary layer column from tropospheric column resulting in the following equation:

$$X_{VMR} [\text{ppm}] = 1.27 * \Delta VCD_{(tp-bl)} [\text{DU}] / (P_t [\text{hPa}] - P_{bl} [\text{hPa}]) \quad 5.1$$

where  $X_{VMR}$  is in ppm,  $\Delta VCD$  is the difference in vertical column density [DU] between the tropopause (tp) and the boundary layer (bl) and t, terrain, indicates pressure at Earth's surface. The mean Highveld terrain pressure is 850 hPa (Tyson and Preston-Whyte, 2000) and the mixing layer mean pressure over the Highveld is 700 hPa (Freiman and Tyson, 2000). Thus the above equation becomes:

$$X_{VMR} [\text{ppm}] = 1.27 * VCD_{bl} [\text{DU}] / (850 [\text{hPa}] - 700 [\text{hPa}]) \quad 5.2$$

This equation was then applied with the conversion and column segregation rendering the RS data comparable with the ground-level data for all three gases. However, depending on the source of the remotely sensed products, which used differing units, there are minor differences in determining the  $\Delta VCD_{(tp-bl)}$  for each observed species.

### *SO<sub>2</sub> comparison*

Remote sensing global and regional data products for SO<sub>2</sub> are available from Tropospheric Emission Monitoring Internet Service (TEMIS, 2008) and PROMOTE (PROtocol MO尼Toring for the GMES Service) of the European Space Agency (ESA) (PROMOTE, 2008). However, for this study domain, the tropospheric SO<sub>2</sub> numerical values and



regional plots extractions were provided by Belgian Institute for Space Aeronomy/German Aerospace Centre/European Space Agency (BIRA-IASB/DRL/ESA) (van Geffen, personal communication, 2008). The data originated from their *Air Quality SO<sub>2</sub> – Regions Information* product, representing monthly VCD averages (the monthly means were determined by averaging all available daily data within each month). A sub-set of results were extracted for this study, comprising SO<sub>2</sub> fields at a 0.25° by 0.25° grid cells, corresponding to the 37 passive sampling sites. SO<sub>2</sub> vertical column densities in [DU] were supplied at three different heights above ground level: 1, 6 and 14 km. The RS data received covered the entire passive sampling period from January 2005 to September 2007.

For the purposes of this study, the SO<sub>2</sub> VCD at the height of 1 km above ground, the lowest height for which SO<sub>2</sub> VCD could be extracted, is used, taken to represent the boundary layer. Thus, these values already represent  $\Delta$ VCD in Equations 6.1 and 6.2. Equation 6.2 is applied to separate the boundary layer values and convert VCD (DU) into VMR (ppm and ppb). The 'error' given is the monthly average of the error and serves as an indicator of the error on the monthly average (van Geffen, personal communication, 2008). For several sites and months, negative RS values of SO<sub>2</sub> were reported. These values are assumed to be below detection limit and are omitted from further processing.

#### *NO<sub>2</sub> comparison*

The NO<sub>2</sub> SCIAMACHY RS global and regional data are available from ACCENT-TROPOSAT-2 Programme (ACCENT-TROPOSAT-2, 2008). However, further extraction was needed and regional RS data applicable to the southern African region were obtained from the Max Planck Institute - Chemistry (MPI-C), Mainz (Beirle, personal communication, 2008).

The dataset comprises the monthly mean tropospheric VCDs of NO<sub>2</sub> that are derived assuming a meridionally smooth stratosphere; a ground albedo of 5%; cloud fractions from FRESCO (algorithm) and 80% of the NO<sub>2</sub> profile in the BL. Partly clouded columns are corrected accounting for the radiances of the cloud free/clouded part. The data provided give the NO<sub>2</sub> columns with a resolution of 0.5°, covering the region (20-40°E, 15-35°S, corresponding to 40\*40 pixels with 0.5° resolution) (Beirle, personal communication, 2008). For NO<sub>2</sub> regional data, these were provided in units of [molec 10<sup>13</sup> cm<sup>-2</sup>]. Thus, in order to apply the Equation 6.1 and separate and convert boundary layer NO<sub>2</sub> plume into VMR [ppb] another step was necessary. The molec cm<sup>-2</sup> values were converted into DU as per Figure 5.12.



Another modification of the SO<sub>2</sub> comparison technique was applied for NO<sub>2</sub> comparisons. In contrast to the SO<sub>2</sub>, which was provided in a multiple layered structure, for which only the boundary layer was used, the assumption in the extraction algorithm for NO<sub>2</sub> is that 80% of tropospheric VCD NO<sub>2</sub> is contained in the boundary layer (Beirle, 2008, personal communication). Accordingly, 80% of the RS VCD represented  $\Delta$ VCD and thus was taken as the value for comparison with the PS-derived NO<sub>2</sub> concentrations.

### *O<sub>3</sub> comparison*

Remote sensing ozone results were obtained from the NASA Goddard Space Flight Center website, sub-site for tropospheric ozone (NASA-GSFC, 2008). The Ozone Monitoring Instrument (OMI) and Microwave Limb Sounder (MLS) on the Aura satellite platform measured the concentrations. Tropospheric column ozone retrievals were determined daily by subtracting MLS stratospheric column ozone from OMI total column ozone. Stratospheric column ozone from MLS was spatially interpolated (2D Gaussian/linear latitude-longitude interpolation) each day to fill in between the actual along-track measurements. The monthly means were then determined by averaging all available daily data within each month. The formatting of the data files is at 1.0° latitude by 1.25° longitude resolution. OMI total column ozone was filtered for near clear-sky conditions by including only measurements when coincident OMI reflectivity was less than 0.3 (NASA-GSFC, 2008).

Ozone retrievals were not available for the full period coinciding with the PS ground campaign. One period concurrent with the PS campaign was matched (September 2005 – September 2006). Ozone retrievals were extracted for locations corresponding to grid points of the passive monitoring campaign, using an Interactive Data Language (IDL) script. The ASCII data files were scaled by the RS processing team to maximize information content given three numeric characters per value. The original tropospheric column ozone data (in Dobson Units) were made available increased 10-fold and thus the downloaded data were divided by 10 to reach the measured RS values first. The next step was then taken to determine the apportionment of the boundary-layer component  $\Delta$ VCD<sub>(tp-b)</sub> of the total column density (Equation 5.1), and conversion from vertical column density to volume mixing ratio.

A different approach from that used for SO<sub>2</sub> and NO<sub>2</sub> was necessary for determination of the boundary layer O<sub>3</sub> as a portion of the entire troposphere. A study by Zbinden *et al.*





(2006) was used as a basis. They estimated the various concentrations for the entire troposphere, upper troposphere, mid troposphere and boundary tropospheric layer for four sites on three continents, by use of air-borne instruments. These results were used to estimate an average percentage of the boundary layer VCD within the *total ozone column* (TOC) of the entire tropospheric VCD (Table 5.1). This resultant apportionment was 23%.

**Table 5.1: Annual and seasonal mean of *Total Ozone Column* (DU) and corresponding short-term trends (%/year) for the entire troposphere and for the boundary layer (BL, 0–2 km altitude), mid troposphere (MT, 2–8 km altitude) and upper troposphere (UT, 8 km altitude to the dynamical tropopause DT) over New York, Paris, Frankfurt and Japan (Source: Zbinden *et al.*, 2006).**

		Annual		Spring		Summer		Fall		Winter	
		DU	%/year	DU	%/year	DU	%/year	DU	%/year	DU	%/year
	<i>TOC</i>	30.3	1.1	33.4	1.5	37.8	0.0	26.8	0.8	24.0	1.9
New York 2631 profiles	TOC in BL	7.2	0.4	8.3	1.2	9.4	-1.2	6.2	1.2	5.4	3.9
	TOC in MT	17.9	1.2	20.0	1.2	20.3	0.6	16.2	1.0	15.6	2.0
	TOC in UT	5.5	1.3	5.7	1.6	8.1	0.1	4.8	-0.1	3.8	-0.7
	<i>TOC</i>	29.5	0.9	32.5	0.5	34.3	0.2	26.2	0.4	25.3	2.0
Paris 3308 profiles	TOC in BL	6.8	0.9	7.9	0.3	7.8	0.3	5.8	0.6	5.8	3.1
	TOC in MT	17.7	1.5	19.5	1.4	20.0	0.4	16.0	0.7	15.5	1.8
	TOC in UT	5.2	-0.1	5.5	-0.9	6.6	-0.4	4.6	-0.2	4.2	1.9
	<i>TOC</i>	28.5	0.7	32.0	1.3	34.0	0.0	25.1	0.3	23.9	2.0
Frankfurt 6338 profiles	TOC in BL	6.2	0.3	7.5	0.5	7.7	-0.2	5.1	0.7	5.0	3.3
	TOC in MT	17.7	0.7	19.6	1.5	20.3	0.0	16.0	0.3	15.3	1.7
	TOC in UT	4.9	0.8	5.3	1.2	6.2	0.2	4.2	0.0	4.0	1.7
	<i>TOC</i>	30.2	0.8	36.1	0.9	31.5	0.1	27.5	0.8	26.4	1.0
Japan 1899 profiles	TOC in BL	7.4	-0.1	9.5	0.5	6.4	0.1	6.6	0.3	7.1	0.3
	TOC in MT	17.8	0.8	21.3	1.0	17.8	0.1	16.1	1.0	16.4	1.0
	TOC in UT	5.4	1.0	5.9	-0.4	7.2	0.3	5.0	1.1	3.5	3.7

Assuming  $\Delta\text{VCD}_{(\text{tp-bl})}$  to be 23%, uniform over entire study area, resulted in the Equation 6.3:

$$X_{\text{VMR}} [\text{ppm}] = 1.27 * 0.23 * \text{VCD}_{\text{tp}} [\text{DU}] / (850[\text{hPa}] - 700[\text{hPa}]) \quad 5.3$$

Equation 6.3 was then applied in conversion of O<sub>3</sub> RS VCD data to VMR [ppb] for each of the grid-points that matched PS sites. Clearly, some measurements over higher altitude locations would be desirable to confirm this relationship.

## 5.4 Results

### 5.4.1 SO<sub>2</sub> passive sampling with remote sensing results

A spatial comparison is presented for all sites of the mean SO<sub>2</sub> VMR values from PS and the corresponding RS derived values, for the period January 2005 to September 2007



(Figure 5.13). The PS systematic error bars are set at 25% (Ayers *et al.*, 1998) and RS systematic error values at 50%.

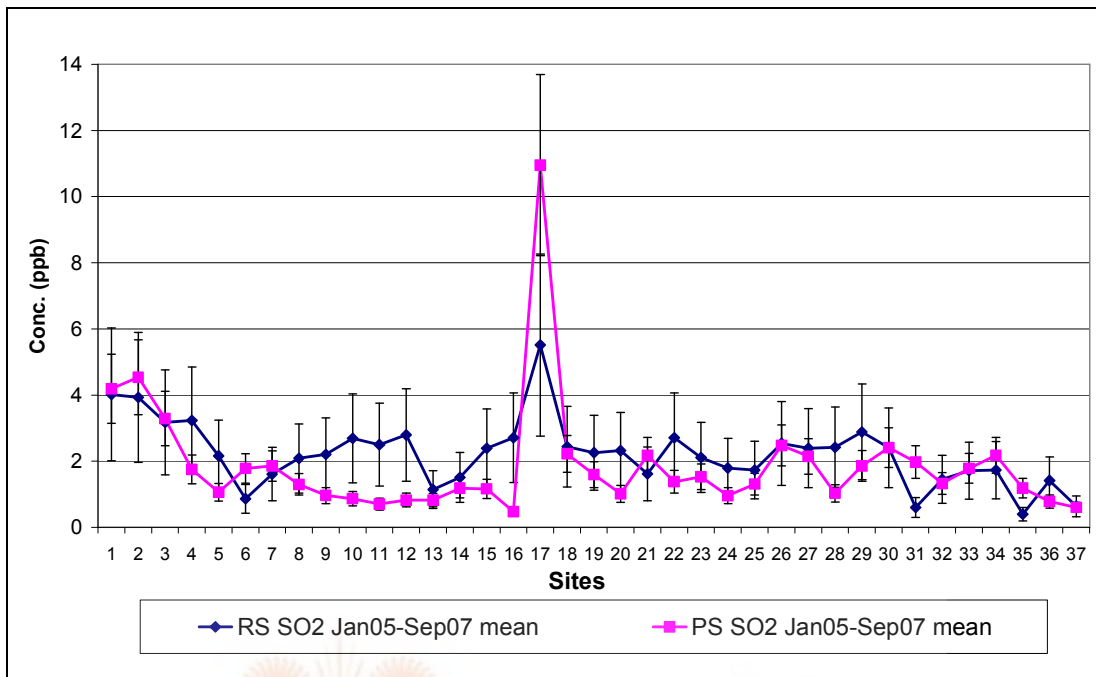


**Figure 5.13: Spatial comparison of SO<sub>2</sub> concentrations by PS and RS measurements for all sites as the means over entire passive sampling period. The systematic error bars for PS are 25% and for RS are 50%.**

In order to check the temporal agreement, comparisons were performed for selected sites on a month-by-month basis. Results for three representative sites are presented in Figure 5.14 to Figure 5.16, for the centre of the industrial Highveld (site 17, Elandsfontein); downwind of the industrial Highveld (site no. 2, Amersfoort); and a remote site (site no. 36, Louis Trichardt).

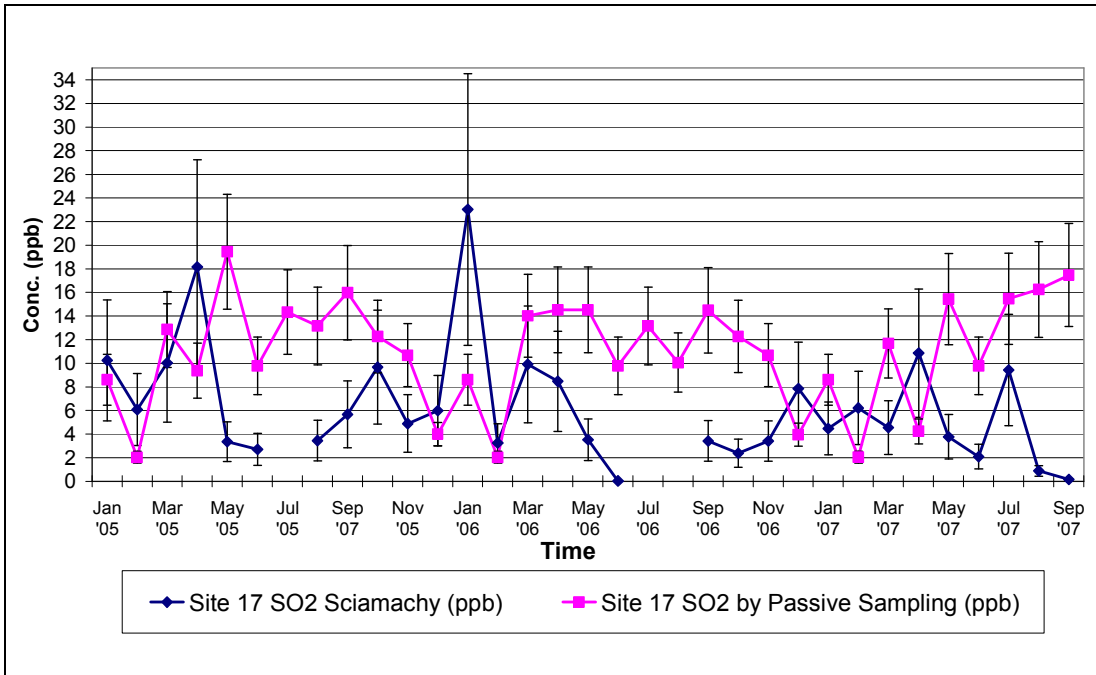


**Figure 5.14: Comparison of SO<sub>2</sub> concentrations by PS and RS at a site in the major pollution emission source-area (Site 17). The systematic error bars for PS are 25% and for RS are 50%.**

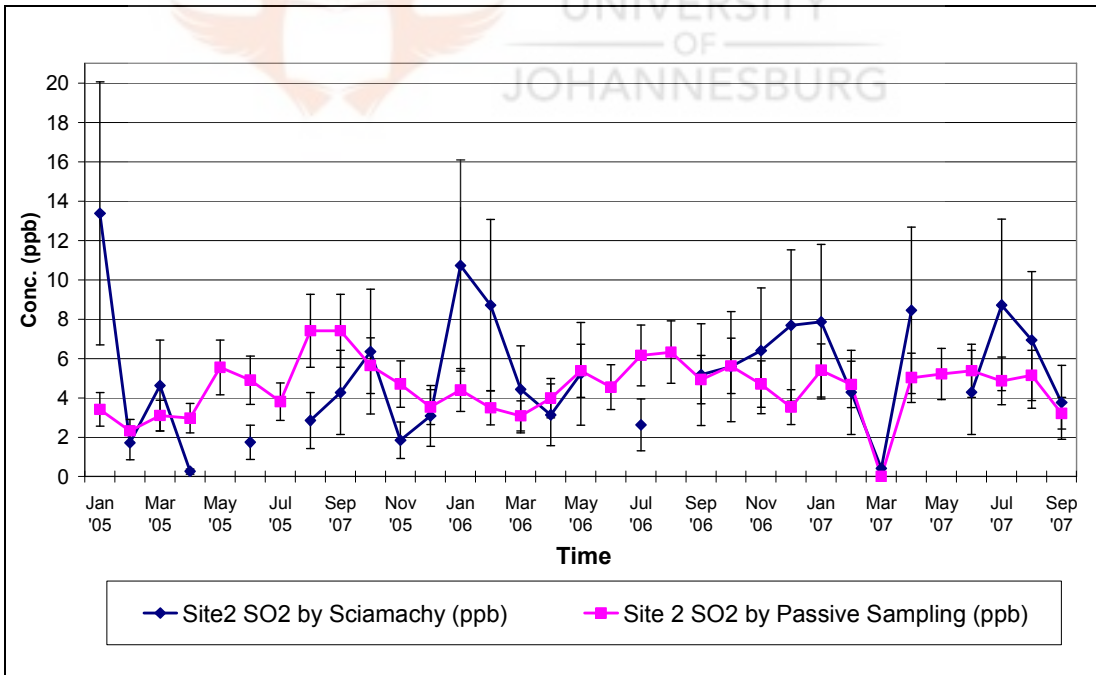


**Figure 5.15: Spatial comparison of SO<sub>2</sub> concentrations by PS and RS for a site downwind from the major pollution emission source-area (Site 2). The systematic error bars for PS are 25% and for RS are 50%.**

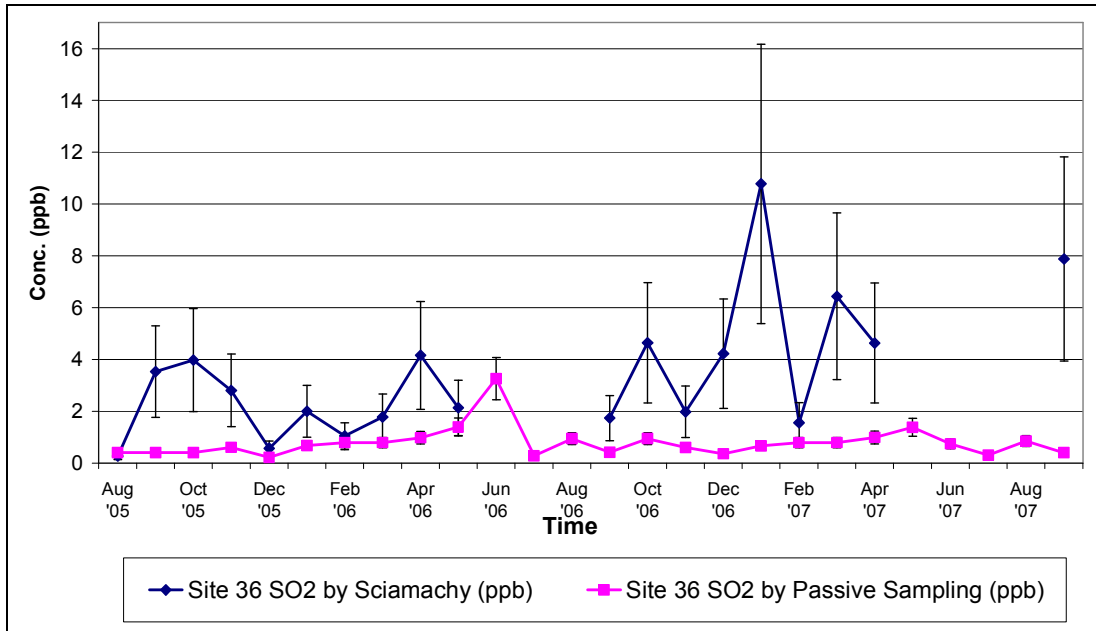


**Figure 5.16: Spatial comparison of SO<sub>2</sub> concentrations by PS and RS for a site remote from the major pollution emission source-area (site 36). The systematic error bars for PS are 25% and for RS are 50%.**

Similarly to the previous sections on the ground-level concentrations and depositions (sections 2.5, 3.4, 3.5 and 3.6), three sites representing industrial, downwind and remote category of sites were compared with each other in a single graph, Figure 5.17.

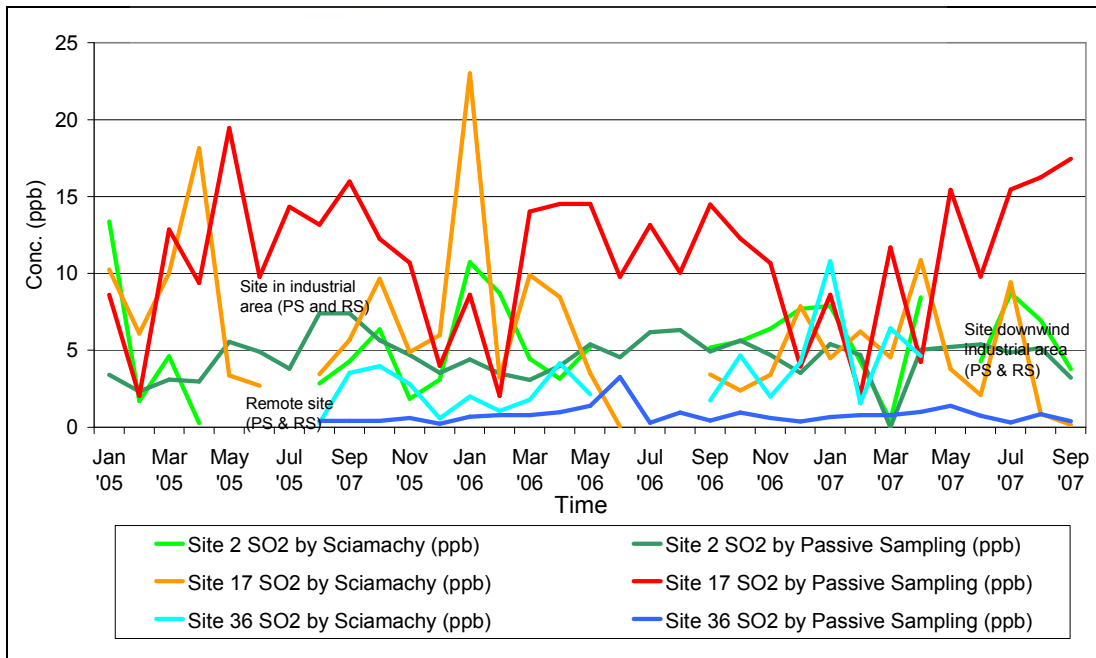


**Figure 5.17: Combined time series comparison of SO<sub>2</sub> concentrations measured by PS and RS for three different site categories (Site 2 – downwind; Site 17 – polluted; Site 36 – remote).**



While the resulting graphs are overlapping in some periods it can be seen that the satellite data also follow the PS data trends, with higher values in the industrial area, dropping significantly downwind and low values at remote locations. However, the variation in the satellite data with many months the measurements being below detection means that while the trend is there, there are as many periods which are not as clear, as there are periods where it is clear that separate categories are *not* clearly distinguished (Figure 5.17).

#### 5.4.2 *NO<sub>2</sub> passive sampling with remote sensing results*

A sample spatial comparison is presented for all sites of the mean NO<sub>2</sub> VMR values from PS and the corresponding RS derived values, for the period January 2006 (Figure 5.18).

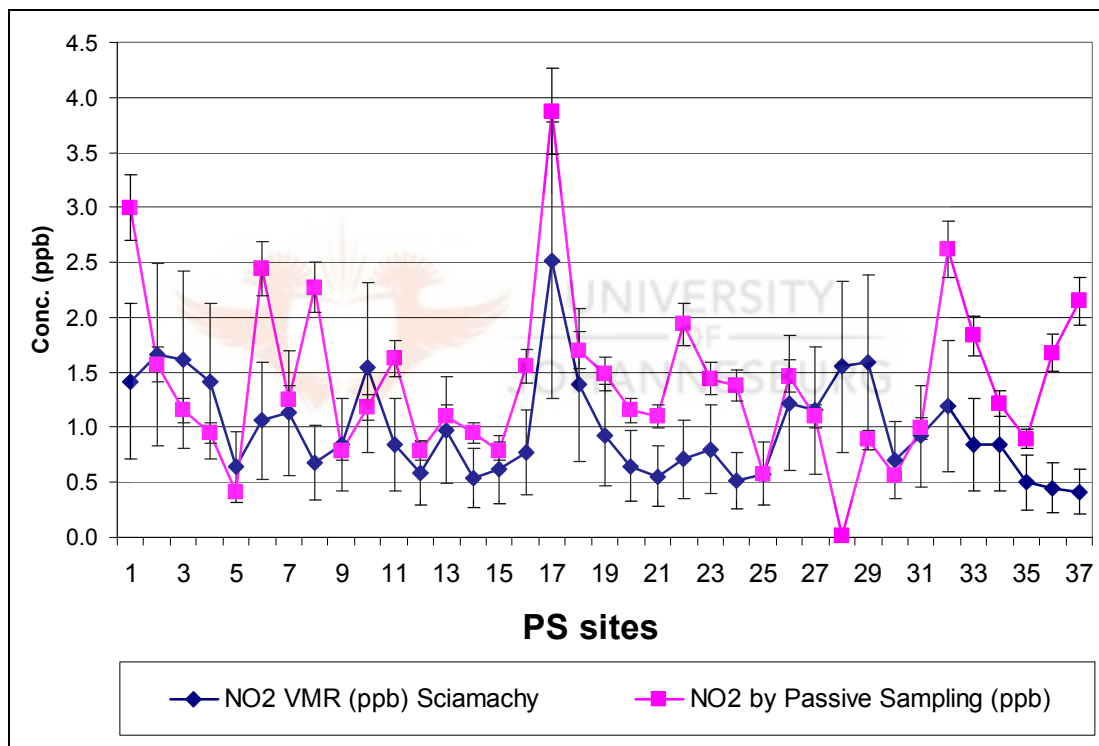


**Figure 5.18: Spatial comparison of NO<sub>2</sub> concentrations by PS and RS for all sites for January 2006 (50% systematic error bars for RS data).**

For the same month, spatial maps of PS and RS measurements can be compared visually for distribution agreement, despite different spatial resolution and different concentrations units used for two maps (Figure 5.19). The hotspot over the industrial Highveld is apparent in both images.

If a temporal comparison is undertaken, then the following diagrams illustrate the similarity of the relative trends for three representative sites (Figure 5.20 to Figure 5.22).



The PS systematic error bars are set at 10% (Ayers *et al.*, 1998) and RS systematic error bars at 50% (Richter and Burrows, 2002; Boersma *et al.*, 2004).

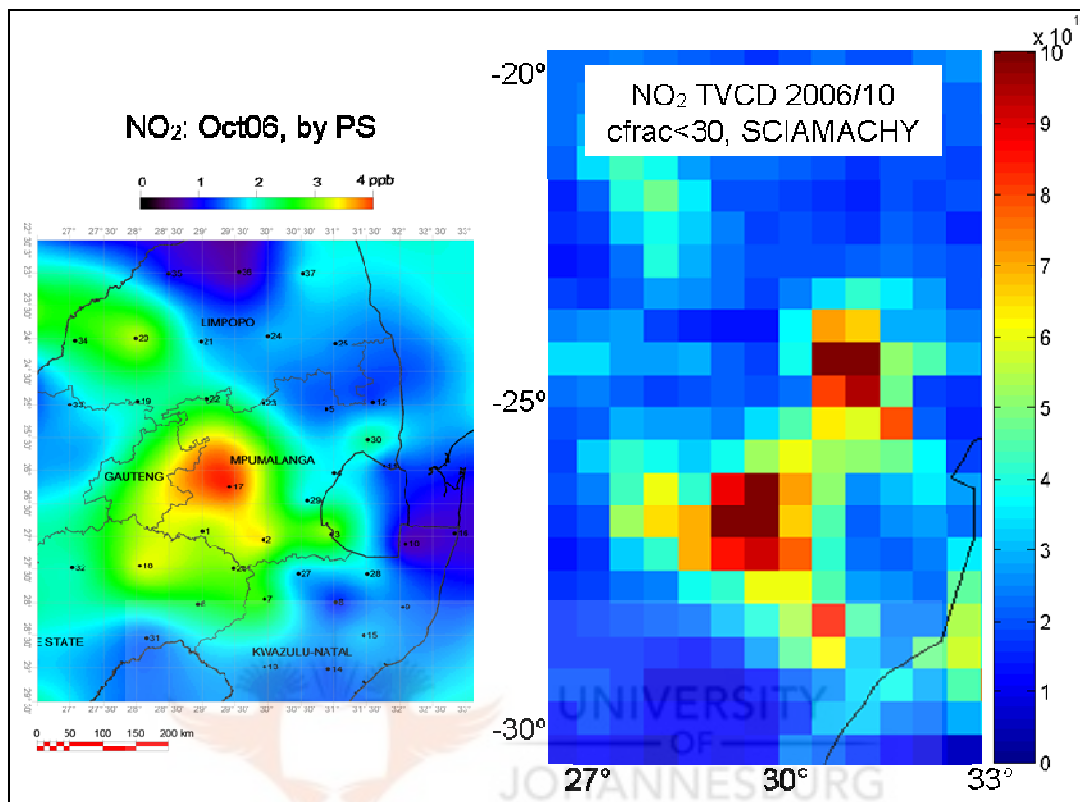


**Figure 5.19:** Comparison of a) ground-level NO<sub>2</sub> measured for October 2007 monthly averaged and b) RS (SCIAMACHY) VCD over the same region for October 2007. (Sources: (a) this work; (b) Beirle, personal communication, 2008).

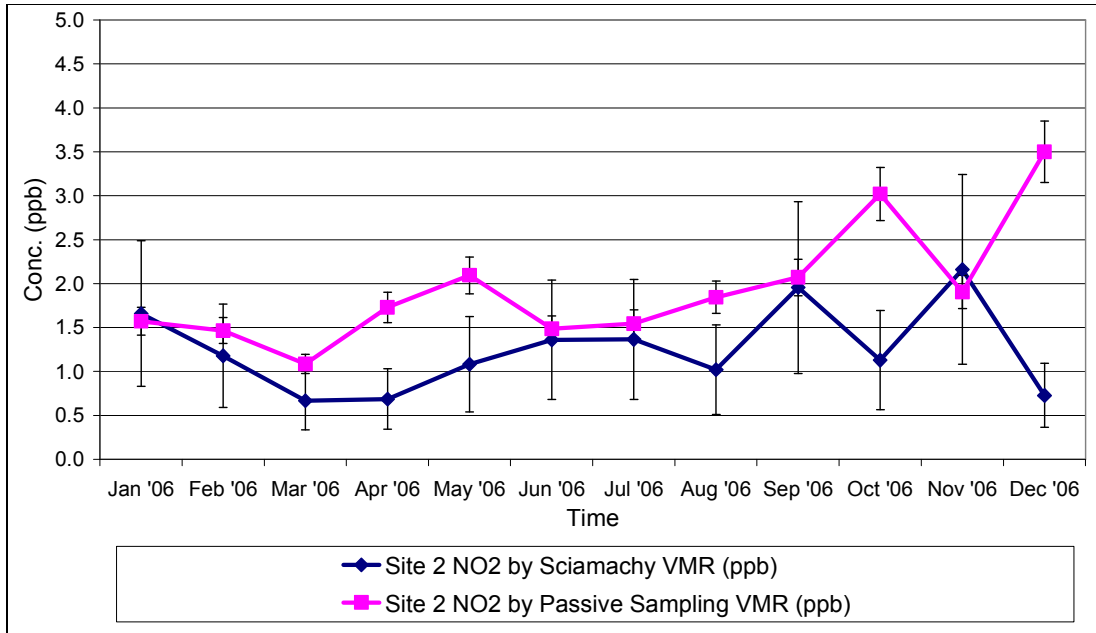


**Figure 5.20: Comparison of NO<sub>2</sub> concentrations by PS and RS for site 2 (Amersfoort, a site down-wind from the major pollution emission source-area). PS systematic error bars at 10% and RS at 50%.**

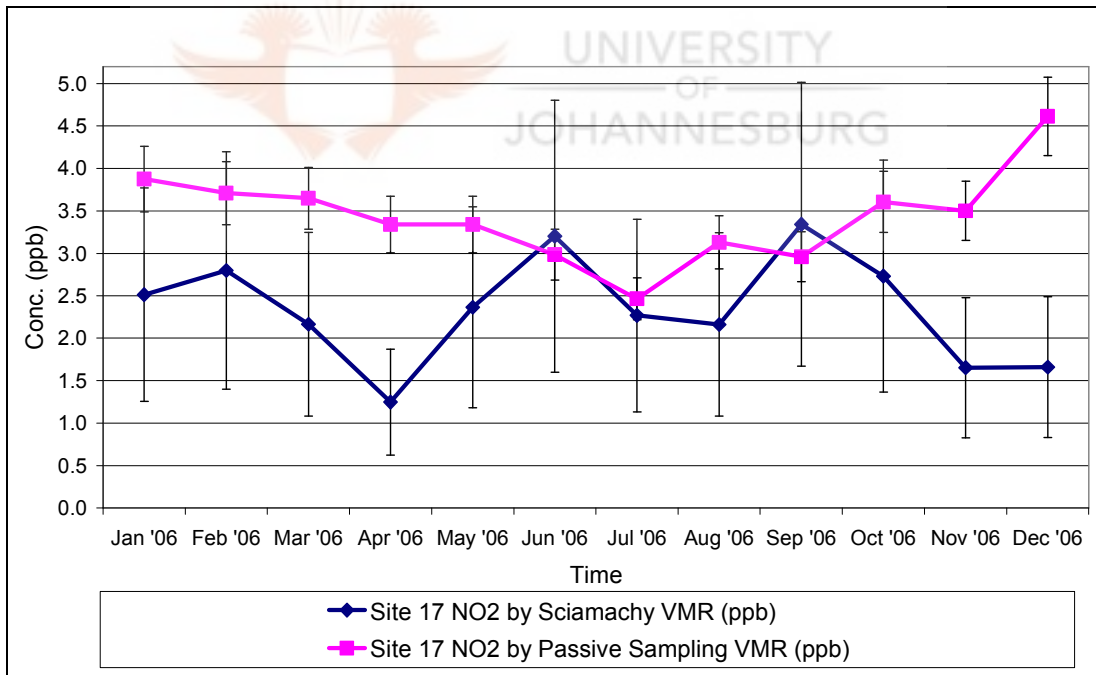


**Figure 5.21: Time series comparison of NO<sub>2</sub> concentrations by PS and RS for site 17 (Elandsfontein, a site in the major pollution emission source-area). PS systematic error bars at 10%, RS at 50%.**

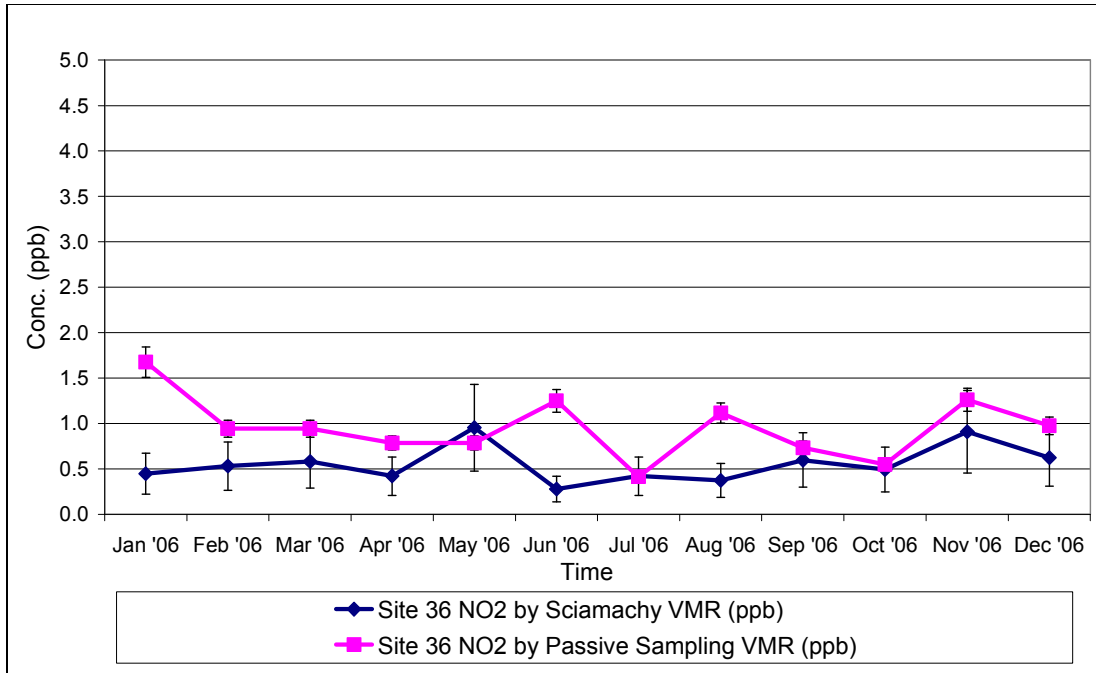


**Figure 5.22: Time series comparison of NO<sub>2</sub> concentrations by PS and RS for site 36 (Louis Trichardt, a remote rural site off the major wind axis from the major pollution emission source-area). PS systematic error bars at 10% and the RS at 50%.**

These comparison illustrations show some pattern agreement. However, the detailed time-series correlation is not strong. Nevertheless, if the cumulative averages of the three representative sites are compared together as different site categories, through a box-whisker plot, then a recognisable differentiation for both PS and RS is seen in addition to overlaps between the RS and PS data (Figure 5.23).



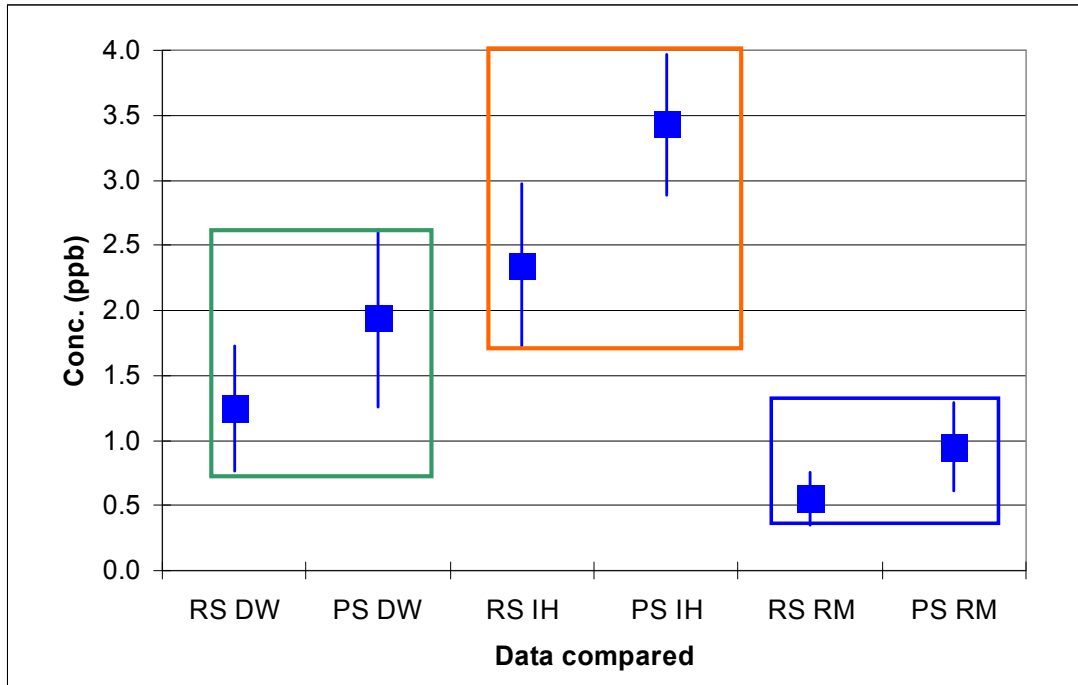


**Figure 5.23: Comparison of three categories of sites for NO<sub>2</sub> measured by PS and RS. NO<sub>2</sub> mean concentrations and standard deviations at sites DW-remote downwind site, IH – industrial Highveld site, RM – remote rural site).**

For both RS and PS, NO<sub>2</sub> concentrations are highest in the industrial Highveld zone, then somewhat reduced downwind from the source area and markedly lower at the remote site (Figure 5.23). This supports the earlier concentration gradient assessment (Section 2.6.2).

Numerical values of the ratio of NO<sub>2</sub> concentrations between RS and PS are presented in (Table 5.2). Values of the ratio that exceeded 2 standard deviations of the mean for over all sites for a given month were excluded and the means recalculated on remaining values. The overall ratio of NO<sub>2</sub> (RS:PS) is **0.77**, a remarkably good agreement, indicating relative reliability of the results, far above that expected considering the uncertainties in deriving RS concentrations of NO<sub>2</sub> for the boundary layer. However the NO<sub>2</sub> RS and PS comparisons result in moderately large standard deviations (Mean Std. Dev. = 0.57).



**Table 5.2: Ratios and standard deviations of ratios between remote sensing and passive sampling measurements for all months.**

<b>Month 2006</b>	<b>Mean Ratio ( <math>NO_{2RS} : NO_{2PS}</math> ) across all sites</b>	<b>Standard Deviation across all sites</b>
<i>Jan</i>	0.78	0.39
<i>Feb</i>	0.87	0.52
<i>Mar</i>	0.75	0.61
<i>Apr</i>	0.66	0.65
<i>May</i>	0.85	0.82
<i>Jun</i>	0.66	0.35
<i>Jul</i>	0.94	0.50
<i>Aug</i>	0.80	0.91
<i>Sep</i>	0.84	0.48
<i>Oct</i>	0.70	0.43
<i>Nov</i>	0.76	0.44
<i>Dec</i>	0.63	0.52
<b>Annual Means across all sites and months</b>	<b>0.77</b>	<b>0.57</b>

#### 5.4.3 *O<sub>3</sub> passive sampling with remote sensing results*

A spatial comparison of ozone by PS and RS, for all sites for one month, is presented in Figure 5.24. The PS systematic error bars are set at 25% (Martins, personal communication, 2006) and for RS at 50% (Richter and Burrows, 2002; Boersma *et al.*, 2004). Other reports give different give error margins of 15%, based on comparisons with continuous ozone analyzers (Tang and Lau, 2000).

The values of ozone for RS and PS are evidently different, as the RS results are systematically lower. Spatial variations are not present in the RS values, which are effectively uniform across the study region. In addition, the RS ozone results do not reflect any local high and low value fluctuations on the 1° grid cells reflected in the PS results. However, these localised anomalies may also be due to sampling anomalies rather than being characteristics of the ozone field over a large scale.

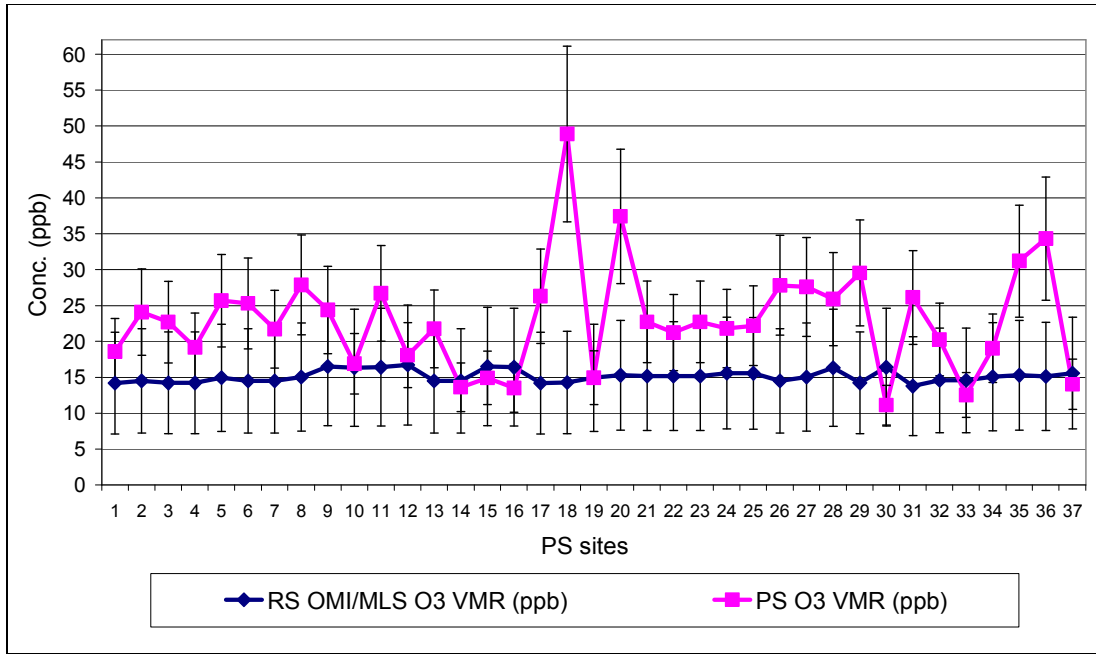


**Figure 5.24: Spatial comparison of O<sub>3</sub> by PS and RS for all study sites during September 2006 (Systematic error bars for RS data are 50% and for PS 25%).**

The same differences between the overall magnitudes of ozone concentrations are apparent in a temporal comparison between PS and RS for the three representative sites of this study (Figure 5.25 to Figure 5.27).

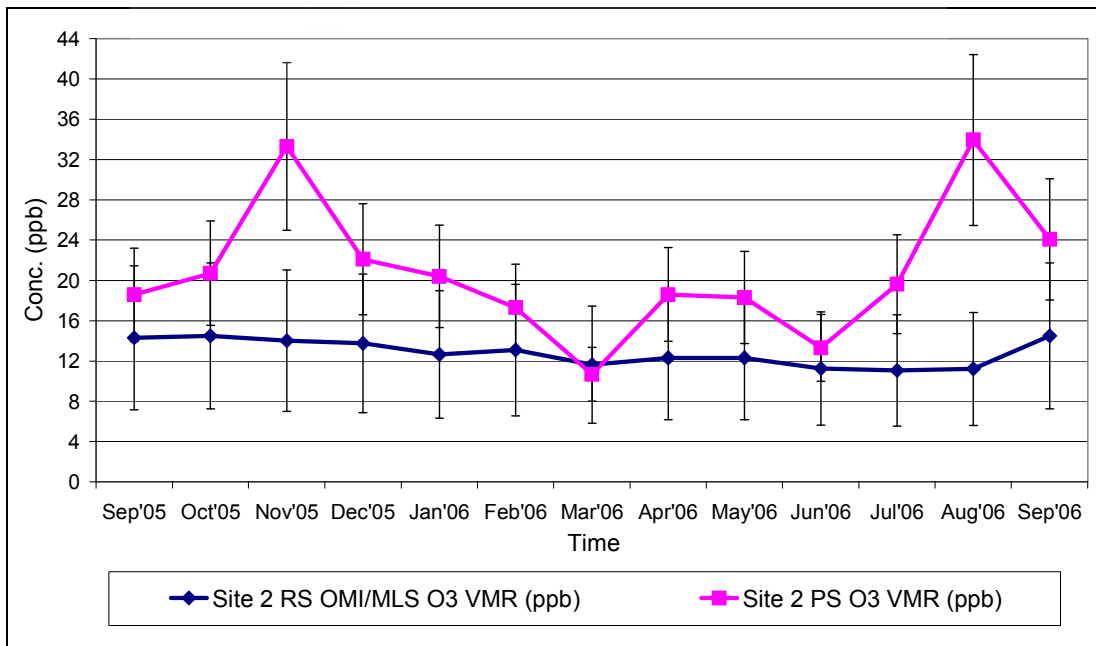


**Figure 5.25: Time series comparison of O<sub>3</sub> by PS and RS at site 2 (Amersfoort) over the period Sep05-Sep06. The systematic error bars for RS data are 50% and for PS are 25%.**

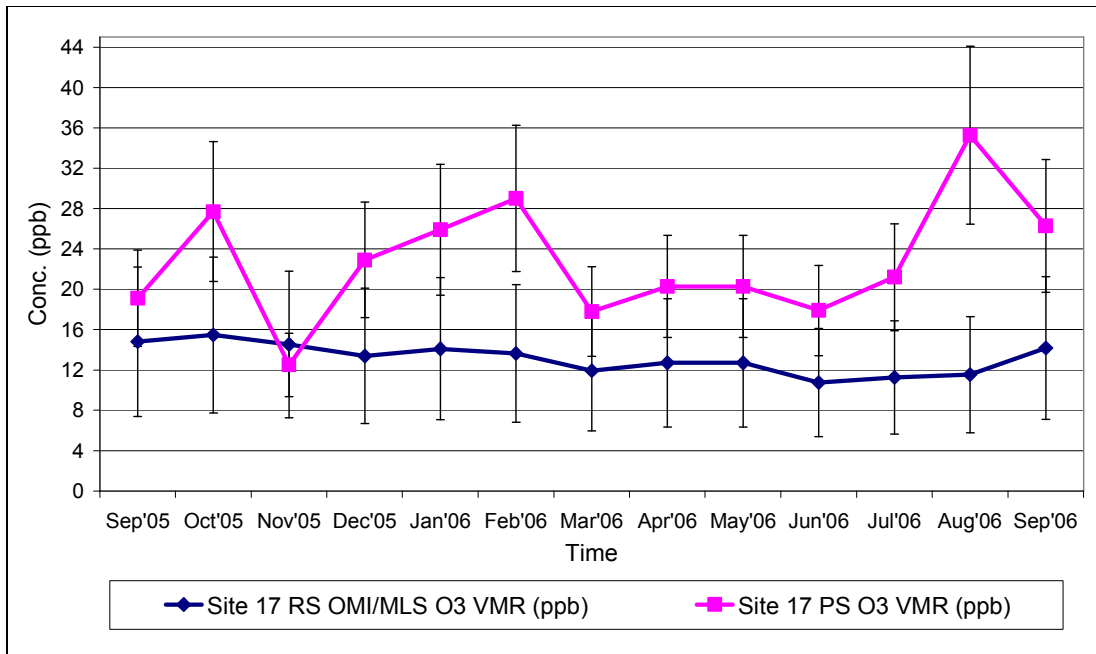


**Figure 5.26:** Time series comparison of O<sub>3</sub> by PS and RS at site 17 (Elandsfontein) over the period Sep05-Sep06. The systematic error bars for RS data are 50% and for PS are 25%.

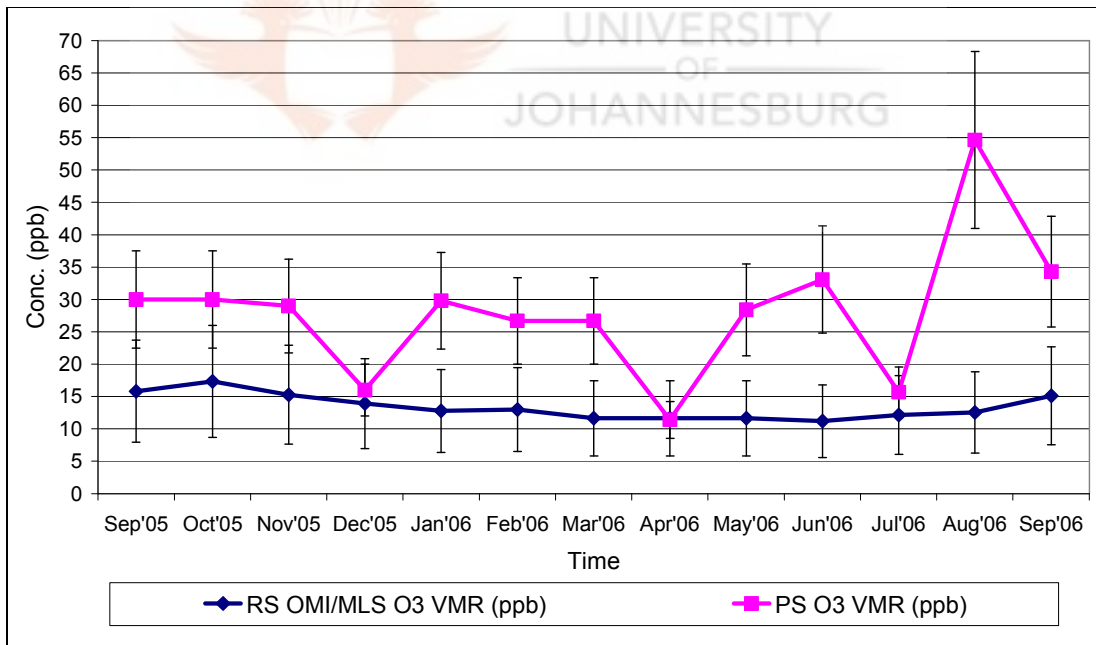


**Figure 5.27:** Time series comparison of O<sub>3</sub> by PS and RS at site 36 (remote rural) over the period Sep05-Sep06. The systematic error bars for RS data are 50% and for PS are 25%.

If all three representative sites are compared together (Figure 5.28), the uniformity of the RS ozone values in space and time are accentuated. In contrast, the PS results for ozone show a much greater variability, with no clear spatial or seasonal variation.

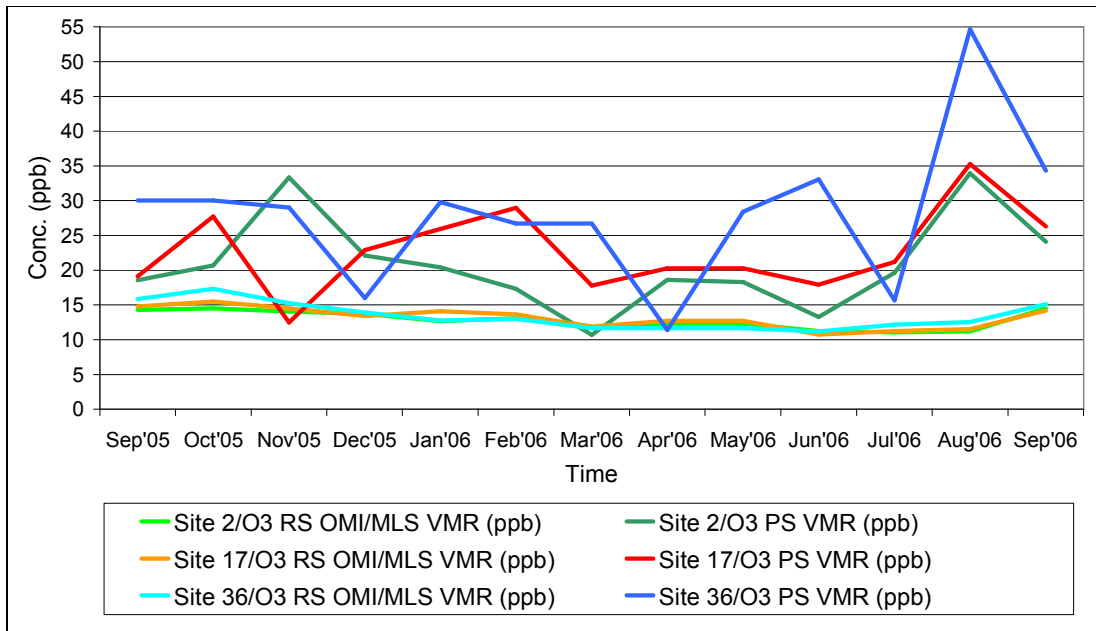


**Figure 5.28: Combined times series comparison of O<sub>3</sub> measured by PS and RS for three site categories.**

The corresponding discussions for all sites and all gas species over their corresponding and concurrent sampled periods are provided in the next section.

## 5.5 Discussion

### 5.5.1 SO<sub>2</sub> by PS and RS comparison

After the assessment of the SO<sub>2</sub> comparison, it can be concluded that besides overall trend, following and some agreement over industrial Highveld RS uncertainties leave many values with large errors resulting in no good correlation. Overall, more work needs to be done on both RS retrieval algorithms and the boundary layer conversion in order to achieve a more robust SO<sub>2</sub> product. Particularly, error margins must be reduced for any improved future validations.

### 5.5.2 NO<sub>2</sub> by PS and RS comparison

The NO<sub>2</sub> measurements compared were found to be in an exceptionally good agreement, spatially and temporally when compared at individual sites and for all sites combined. The RS evidently picked up the category differences from polluted to remote sites and was able to give the same overall trends and pattern of the differences within the region. Overall ratio (0.77) indicates good agreement, however with moderately large standard deviations (0.57). In some cases, due mainly to several rather low PS values, these values had to be



excluded from the data set, in order to exclude such ratios, which pushed cumulative ratio determination over two standard deviations.

The quantitative values did not differ greatly and they were mainly lower than the ground-level values. When spatial plots were compared, the main areas of high concentration are shown in both. Although the distributions were spatially different it has to be noted that the RS plots (Beirle, personal communication, 2008) pictured entire regional tropospheric VCD while PS plots presented concentration interpolation of spotted ground-level measurements, assuming to be also mixing layer as VMR. This then can account for the differences in spatial distribution on different atmospheric levels, where influences of vertical and horizontal atmospheric transport and mixing are reflected, regardless of the strength (and units) measured.

### **5.5.3 $O_3$ by PS and RS comparison**

The numerical ozone comparison of ozone did not indicate obvious spatial patterns, other than a regional uniformity in the RS retrievals. There was substantial difference in mean values across RS results, which fell regularly out the error margins of the sometimes erratic PS measurements, with a few exceptions. In addition, the occasional spikes in local PS measurements were not picked up at all by the RS and this indicates that neither general nor localised temporal and spatial trend could be traced by the satellite instruments. The spatial distribution plots were not compared for ozone as the RS data gave similar readings over a wide zone that covered all of the study area.

## **5.6 Conclusions**

Validation of satellite data is essential if such results are to have full meaning. Much effort has already been undertaken to validate satellite retrievals by different approaches. Efforts using ground-based stations, balloon-sounding, aircrafts and other satellites validation efforts and synergy of combining data from various sources are encouraged. This is not an easy task, as the data from various sources are frequently different in both temporal and spatial coverage and in resolution. The comparison performed in this study contributes towards the broader validation scheme (van Geffen, Beirle, Baier, personal communication, 2008) and might possibly become a part of the norm in the future.

The uncertainties in this task were high and, together with the margin of error from the RS represent a qualitative comparison rather than a quantitative one. Nevertheless, some



progress was achieved. In all cases, the RS and PS results are of the same order of magnitude, indicating that the basic methodology is delivering appropriate numerical results. In the case of  $\text{NO}_2$ , the best agreement was achieved. In the case of ozone, the average spatial and time-averaged results indicate significant disagreement, particularly not being able to account for occasional localised higher amplitudes.  $\text{SO}_2$  RS retrievals are considered the least accurate at the moment and the qualitative agreement achieved is the best that can be expected at this stage.

The comparisons undertaken in this work, supports a compelling case of working towards better vertical stratification of satellite measurements. Undeniably, the timescale of chemical and physical processes in the troposphere is such that a better temporal resolution is required. However, despite the urgent need for a better temporal resolution it is also needed to increase the measurement accuracy throughout entire vertical column. An improved temporal and spatial resolution of the planetary boundary layer would greatly enhance our abilities to monitor and understand the tropospheric processes and fate of its constituents, globally and regionally.

#### **5.6.1 Summary**

Results for  $\text{NO}_2$  are encouraging, while for  $\text{SO}_2$  and  $\text{O}_3$  the RS results are shown to be not yet appropriate for comparison with ground-level measured concentrations. This is to be expected, as precision of RS sensors in the mixing layer of troposphere is limited. Thus, more work on RS advanced measurements, better retrieval algorithms as well as conversion and tropospheric layer profiling is required.

#### **5.6.2 Comments**

Ground concentration measurements are often expensive and time-protracted. The new and combined technologies often need to be employed to achieve quicker yet relatively reliable results. For many regions of the world, absence of local and regional monitoring is the rule. Use of sophisticated technology could fill a gap in understanding of the regional air pollution situation. In this sense, the air-borne and particularly satellite-borne RS could potentially serve well to support ground measurements of the atmospheric constituents.

At this stage of development of satellite remote sensing of tropospheric constituents and data retrieval it is difficult to compare ground-based measurement of ground-level concentrations. Currently the air-borne nadir-viewing measurements as well as ground-located vertical column density zenith-viewing measuring instruments (such as FTIR) are



more reliable than the standard ground level measurements. However, the spatial resolution and time constraints would be a major limiting factor for the larger scale airborne and ground-located measurements. Thus, further investigations and improvements of satellite-borne instruments and techniques still promises better temporal coverage and good spatial resolution.

It should be noted that satellite data can already provide a direct comparison with the chemical transport dispersion models on a global and regional scale as models can provide results at comparative altitudes. So they can be used for more detailed and realistic validation to improve the accuracy and reliability of chemical dispersion models (Scorgie, personal communication, 2007). Satellite data should also be useful in providing real boundary conditions for operational models; in addition, source strengths of trace gas species could be derived. For field campaigns, such as the one being compared here, knowledge of the actual concentrations in the campaign area will be available. In essence, satellite data becomes an essential adjunct to the major activities in atmospheric chemistry in the future (Borrell *et al.*, 2004).

The availability of satellite data for the tropospheric research/observations is promising to become a preferred method for those responsible for environmental policy development and enforcement. Satellite data show promise to be used by the authorities to monitor pollutant concentrations on a regional scale in order to verify the compliance with legislative and control measures. Several studies illustrate the potential of tropospheric satellite measurements for use in environmental management. One of those conducted by the pioneers of the satellite measurements research is the observation of inter-continental plumes of NO<sub>2</sub>, SO<sub>2</sub>, aerosol from high lying South African power plants (Wenig *et al.*, 2003). This all indicates that satellite borne instruments once launched and instruments and data products validated, offer a definite way to achieve very reliable and long-term monitoring from regional to global scales. If used with understanding of the uncertainties, they provide viable information for areas for which there are no air quality measurements available to inform policy and legislation.

This study shows that this will be realised if further improvements are made in developing, validation and integration of remote sensing. It is imperative to explore the required strategies to bring together data produced with different techniques to obtain an overall picture of the atmosphere.





## CHAPTER SIX

*A lightning-generated NO<sub>x</sub> (LNO<sub>x</sub>) budget and the seasonality of this major natural pollutant source are dealt with in this chapter. Intra/inter cloud lightning is estimated and added to previously reported lightning stroke measurements. A range of estimates is calculated into LNO<sub>x</sub> budgets and these are compared with regional anthropogenic NO<sub>x</sub> budgets. A NO<sub>x</sub> budget estimate of the passive sampling measured concentrations is compared with the set of remote sensing measurements within a pre-defined volume in order to challenge the presumed distribution and transport of this particular pollutant.*

### **6. Comparison of Measured Ground-level NO<sub>x</sub> and Lightning-generated NO<sub>x</sub> (LNO<sub>x</sub>) Estimates in the Regional NO<sub>x</sub> Budget**

#### **6.1 LNO<sub>x</sub> as a Component of the Southern African Regional Tropospheric Budget**

In the larger context of this entire study (focusing on critical levels and critical deposition loads of acidic species), an evaluation of lightning contributions to the overall and particularly seasonal NO<sub>x</sub> budgets becomes important. It is important not just to evaluate NO<sub>x</sub> against standards, but also to bring into perspective major emission contributors other than the large power plants.

The purpose of this sub-study was to evaluate the size of LNO<sub>x</sub> contribution as a component of the regional NO<sub>x</sub> budget and hence, as a part of the larger study, evaluate its contribution to South African regional acid deposition. The central question to answer was whether the seasonal nature of LNO<sub>x</sub> production is distinguishable in relation to the uniform anthropogenic generation of the same pollutant.

The procedure followed was to survey recent literature on LNO<sub>x</sub> globally and regionally and then to estimate an LNO<sub>x</sub> budget for the study area. The LNO<sub>x</sub> budget is then compared with published emission (anthropogenic) inventories relevant to the study area in order to bring in perspective the relative relationship of LNO<sub>x</sub> with the anthropogenic NO<sub>x</sub> budgets (including the pyrogenic). Lastly, the measured NO<sub>2</sub> concentrations from this study were reviewed in order to distinguish any evidence of a seasonal component that could be attributable to LNO<sub>x</sub> production over the study area.



The scope of this individual study focused on inferential derivation of an improved regional LNO<sub>x</sub> budget based on recent lightning stroke measurements within the study region. No direct lightning measurements or experiments were performed.

## 6.2 Lightning and NO<sub>x</sub> generation

Observations and laboratory experiments showed increased levels of NO<sub>x</sub> in the atmosphere after the occurrence and in the proximity of lightning flashes (Chameides *et al.*, 1977; Hill, 1979; Price *et al.*, 1997; Skamarock *et al.*, 2003). There is a strong correlation between enhanced tropospheric NO<sub>x</sub> and lightning (Figure 6.1).

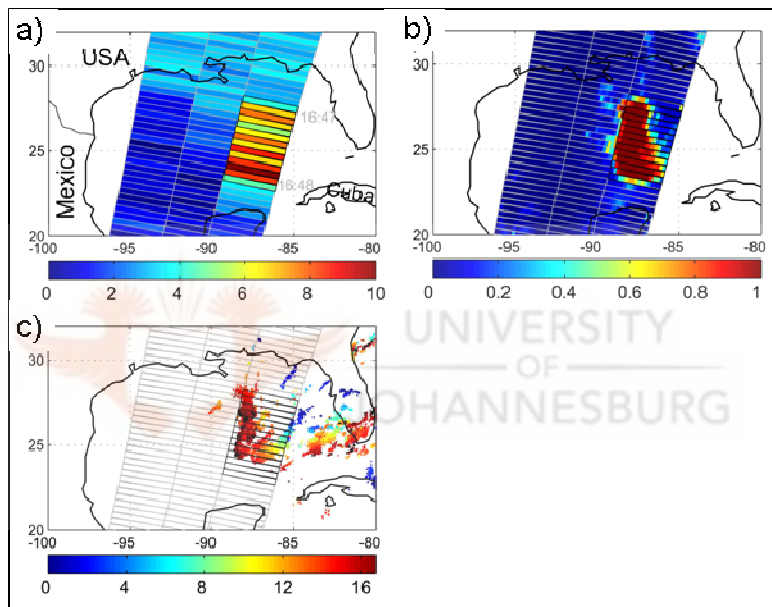


**Figure 6.1:** Co-location of enhanced tropospheric NO<sub>x</sub> and lightning events over Gulf of Mexico: a) GOME tropospheric NO<sub>2</sub> slant column density ( $10^{15}$  molec cm<sup>-2</sup>); b) cloud fraction; c) National (USA) Lightning Detection Network flashes (time of last lightning event) (Source: Beirle *et al.*, 2005).

Research on lightning diverges on numerous issues, for example, the amount of NO<sub>x</sub> produced per flash, the number of flashes occurring per second, the amount of energy released, its distribution, the lightning path length and the number of strokes per flash (Ojelede, 2004).

In the tropics and subtropics, lightning is the dominant contributor of NO<sub>x</sub> in the upper half of the troposphere and adds significantly to that in the lower troposphere over the remote oceans (Levy *et al.*, 1996). Lightning frequencies are highest in the Inter-Tropical



Convergence Zone (ITCZ) over continents. There is far more lightning over landmasses than over oceans (Christian, 2003; Miller and Perkey, 2000).

The photochemical production of ozone depends upon the concentration of  $\text{NO}_x$  (Logan, 1983). Not only does  $\text{NO}_x$  influence the production of ozone, but it also affects the concentration of tropospheric hydroxyl radical (OH) (Holler *et al.*, 1998). Thus,  $\text{NO}_x$  plays an important role in ozone photochemistry and the importance of lightning should not be dismissed in favour of the examination of anthropogenic sources (Biazar and McNider, 1995).

Lightning can be the source of as much as 90% of atmospheric nitrogen oxides in summer, leading to increases of ozone levels by as much as 30% in the free troposphere (Zhang *et al.*, 2003). In agreement with Zhang *et al.*, (2003), Martin *et al.* (2000) found that lightning  $\text{NO}_x$  emissions vary with seasonal solar heating and are highest during the summer months in the southern tropics.

From 1990 onwards a number of large-scale field and laboratory experiments on atmospheric nitrogen fixation by lightning have been conducted, including the Biomass Burning and Lightning Experiment (BIBLE-99), European Lightning Nitrogen Oxide Project (EULINOX-98), Lightning produced  $\text{NO}_x$  (LINOX-96), Subsonic assessment Ozone and Nitrogen Oxide Experiment (SONEX-97) and Tropical Convection Cirrus and Lightning Nitrogen Oxide Experiment [TroCCiNO<sub>x</sub> (2002-2005)]. The EULINOX campaign found that, before industrialisation,  $\text{NO}_x$  from lightning was the major global source of tropospheric ozone and is still the main source in the tropics (Lelieveld and Dentener, 2000). 60% to 70% of the measured  $\text{NO}_x$  was produced by lightning, while in larger EULINOX thunderstorms, the amount of lightning-produced  $\text{NO}_x$  reaches up to 90% of the total (Huntrieser *et al.*, 2000). Lightning activity was found to increase over land, primarily due to increased convection. If lightning produces at least 45 to 50% of the total  $\text{NO}_x$  over southern Africa, it comprises the main natural source of  $\text{NO}_x$  in the region, especially during summer (Lamarque *et al.*, 1996).

Lightning detection technology has improved tremendously over the past years. The characteristics of lightning over both land and sea have been studied using data from space-borne instruments and ground-based networks (Soriano *et al.*, 2005). Earlier investigations of lightning were accomplished using aircraft observations. Space-borne



photography complemented these investigations by providing images from the upper regions of thunderclouds. Following this method of lightning detection and analysis, ground-based detectors were developed. Modern ground-based sensors are able to detect the locations and times of lightning flashes accurately, such as the Lightning Detection Network (LDN) of South African Weather Service (Vaisala Corp, as reported by [Bhika, 2008](#)).

Ground-based lightning measurements are, however, limited in spatial coverage. To eliminate this difficulty, satellite-based sensors have been developed to allow worldwide coverage. Space-borne instruments for measuring lightning consist of sensors that detect light or radio frequency signals emitted in the upward direction by both cloud-to-cloud and cloud-to-ground discharges ([Rakov and Uman, 2003](#)).

Although South Africa is easily surpassed in overall lightning density by regions such as equatorial Africa, it is still considered a relatively lightning-heavy country (Figure 6.2).

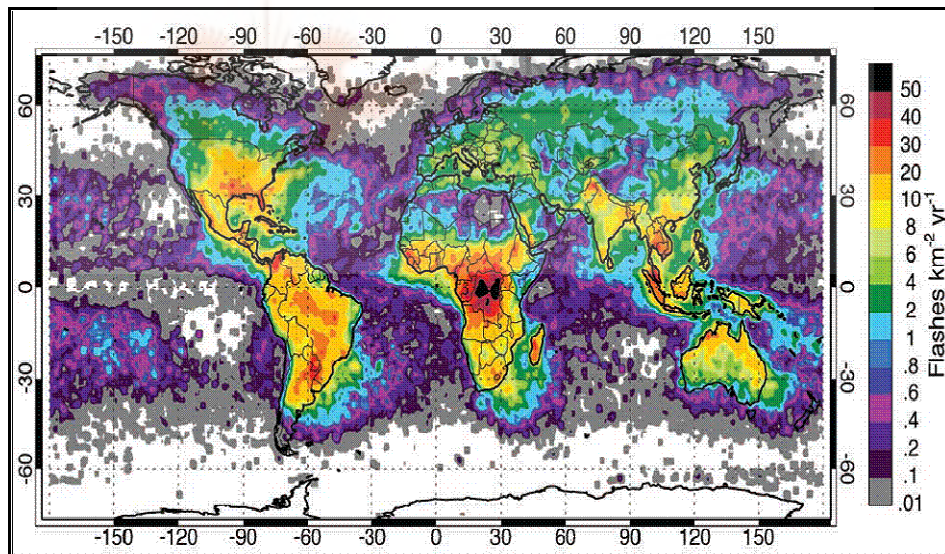


**Figure 6.2:** OTD Global map of total lightning activity from 1995-2000 (Source: [Christian et al., 2003](#)).

It is beneficial for any study of acidic pollution to compare anthropogenic with major natural sources of the same compounds. The results of two recent studies ([Ojelede et al., 2008](#) and [Bhika, 2008](#)) on  $\text{NO}_x$  production by lightning could shed more light on its contribution to overall acidic deposition loads. These are the first quantitative estimates of the natural lightning-produced  $\text{NO}_x$  in Southern Africa. The values obtained indicate that  $\text{LNO}_x$  should be considered a significant source in terms of overall regional inputs, taking into account large inputs from coal-fired power plants on the Mpumalanga Highveld. Thus,



LNO<sub>x</sub> production needs to be characterised and apportioned when assessing the overall acidic compound concentrations and acidic compound deposition loads. These two studies have been used as the basis for a further evaluation of LNO<sub>x</sub> and results compared to recent studies of the regional NO<sub>x</sub> budget and major anthropogenic NO<sub>x</sub> emissions (EDGAR, 2008:32FT2000; Fleming and van der Merwe, 2004; Scorgie *et al.*, 2004b, 2004c).

The first study (Ojelede *et al.*, 2008) focused on producing a quantitative estimate of the lightning-produced NO<sub>x</sub> budget over the (industrial) Highveld region. It compared estimated natural LNO<sub>x</sub> with NO<sub>x</sub> emissions from the major anthropogenic source (power plant coal combustion). A quantitative estimate of the lightning-produced NO<sub>x</sub> for 2002 was obtained using data from the Lightning Positioning and Tracking System (LPATS) set up and run by Eskom (South African electrical generation parastatal utility).

The second study used (Bhika, 2008), aimed, among other things, at evaluating the lightning distribution patterns over South Africa. This study obtained South African Weather Service (SAWS) lightning data from its Lightning Detection Network (LDN) for the first measured annual cycle from February 2006 to January 2007.

### **6.2.1 Lightning-produced nitrogen oxides budget**

Estimates of the rate of NO<sub>x</sub> production from lightning have been reported in literature (Bond *et al.*, 2002; Tie *et al.*, 2002; Lee *et al.*, 1997; Price *et al.*, 1997). These estimates have usually adopted the same approach, assigning a NO<sub>x</sub> emission factor for each lightning flash, calculated as follows:

$$G_N = E * M * C \text{ (g NO}_x \text{ flash}^{-1}\text{)} \quad (6.1)$$

where **E** is the mean energy per flash (J), **M** is the number of NO<sub>x</sub> molecules produced per Joule, **C** is a conversion factor (g molecular mass N<sup>-1</sup>). However, there are widely differing values for flash energy and nitrous oxide (NO) molecules per flash (Lawrence *et al.*, 1995).

For this study the author used the calculation based on Price *et al.* (1997) emission factor for use LNO<sub>x</sub> budget calculations. The reasons for adopting the parameters of Price *et al.* (1997) were strongly supported in Ojelede *et al.* (2008). Bond *et al.* (2002) made use of the production rates suggested by Price *et al.* (1997) after considering results from laboratory investigations, field evaluations and model simulations. Bond *et al.* (2002) also quoted a remark made by Liaw *et al.* (1999) that the values obtained by Price *et al.* (1997) are



consistent with recent field measurements. [Beirle et al. \(2005\)](#) cited the work of [Price et al. \(1997\)](#) as among current best estimates of LNO<sub>x</sub>. Thus, the same emission factor was applied here.

### **6.2.2 Intra-cloud and inter-cloud (IC) to cloud-to-ground (CG) lightning ratios**

Researchers have known for some time that a significant amount of the energy produced by storms is contained in IC lightning flashes. The exact ratio of energy lost to lightning to total energy is very hard to measure. Much of what is known was based on small data sets collected by ground observers and instruments carried by balloons. Recently, satellite measurements were employed to research lightning and help with ratio determination. However, low orbiting sun-synchronous satellite sensors can only be used for limited research because they see only a tiny fraction of the Earth at particular local time.

IC discharges can occur between the charged regions of a cloud. IC flashes differ from CG flashes in that there is no return stroke as in the case of a CG flash, but rather numerous so-called recoil streamers that occur when the continuous leader encounters regions of charge that differ from its own. This produces several bright pulses overlying a continuous low luminosity. Typical IC discharges are 5 to 10 km long and transfer tens of coulombs within the cloud. However, due mainly to the small electric field across which this charge is transported, it has been argued that IC lightning is considered to be two to ten times less energetic than CG lightning ([Turman, 1978](#); [Kowalczyk and Bauer, 1982](#) in [Lawrence et al., 1995](#)), although it is two to six times as frequent. The ratio of IC to CG lightning is considered to be greatest in the lower latitudes and marine regions ([Lawrence et al., 1995](#)). In general, there are some agreements on the latitudinal variance of IC to CG ratios.

The [Boccippio et al. \(2000\)](#) study of IC to CG lightning ratios has been computed over the continental United States using four years of combined remote sensing from an *Optical Transient Detector* (OTD) and ground-based United States *National Lightning Detection Network* (NLDN) data. The particular research represented the first regional (non-point) determination of climatological values of this ratio ever constructed.

### **6.2.3 Soils and vegetation N emissions**

Soils are a large source of NO<sub>x</sub> emissions. It has been found that the largest soil source of NO<sub>x</sub> emissions comes from savanna ecosystems. The estimates of NO<sub>x</sub> emissions from savannas range from 33% to 43% of global NO<sub>x</sub> emissions ([Yienger and Levy 1995](#); [Davidson and Kinglerlee 1997](#); [Scholes et al., 2003](#)). Savannas make up 40% of Africa's



land area (Scholes and Walker 1993); therefore, biogenic emissions from Africa are an important component of the global NO<sub>x</sub> budget (Galloway *et al.*, 2004).

Several publications consider NO emissions from SA savanna/woodland ecosystems. Levine *et al.* (1996) averaged annual budget at 0.7 kg ha<sup>-1</sup> yr<sup>-1</sup> of NO as N for nutrient-poor savanna. However, Scholes *et al.* (1997) estimated that the South African savannah emits on average 2 kg ha<sup>-1</sup> yr<sup>-1</sup> of NO as N. An average between these estimates was used for the N budget from soils calculation for the study region (1.35 kg ha<sup>-1</sup> yr<sup>-1</sup> of NO as N).

After NO is emitted from the soil, it is often rapidly oxidized to NO<sub>2</sub>, which is then readily absorbed onto leaf surfaces if a canopy is present (Bakwin *et al.*, 1990). This process reduces the amount of NO + NO<sub>2</sub> that escapes from the soil-plant system into the atmosphere. Application of the canopy absorption lowers the estimate of net emissions. For this study, the dry and wet depositions were already included and absorption by vegetation and soils is not adjusted for the N budget from soils for the studied area. In addition, the studied area is not entirely savanna and does not cover the entire savanna region in SA. However, the lack of estimations of NO<sub>x</sub> emissions from vegetation prompted the non-reduction of this relatively small overall NO<sub>x</sub> budget contribution. The uptake of N-species by vegetation is complicated due to the existence of a compensation point (Farquhar *et al.*, 1980). It implies that if ambient concentrations are smaller than the compensation point there is an additional biogenic source of N from the vegetation. Observations were documented that there is a NO<sub>2</sub> compensation point of about 0.5-1.0 ppbv (Johansson, 1987; Rondon *et al.*, 1993). Lerdau *et al.* (2000) calculated that based on a compensation point of 1 ppbv, a vegetation emission NO<sub>2</sub> flux of about 2.10<sup>10</sup> molecules cm<sup>-2</sup> s<sup>-1</sup>, which is comparable to the soil NO emission flux (Granier *et al.*, 2004).

## 6.3 Methods

### 6.3.1 Procedural steps

Several different steps were applied in this section.

- Obtaining the lightning data measured by local networks
- Reviewing literature for a suitable LNO<sub>x</sub> budget emission factors and LNO<sub>x</sub> budget calculation
- Reviewing available emission inventories and extracting applicable part to the comparable area for the NO<sub>x</sub> budget comparison



- Reviewing inter- and intra-cloud lightning ratios and choosing one applicable ratio for an adjustment of chosen available lightning counts set.
- Comparing the LNO<sub>x</sub> budget options versus two comprehensive emission inventories
- Determining the vertical column density (VCD) NO<sub>2</sub> budget, over the compared volume in order to determine indirectly the NO<sub>2</sub> (as N) budget of the tropospheric plume.
- Estimating NO<sub>2</sub> budget in the compared volume based on the concentration measurement data and bringing it into a comparable relationship with the vertical column density (VCD) NO<sub>2</sub> budget.

The following subsections will elaborate in more detail the above method steps.

### **6.3.2 *Lightning emission factor and stroke multiplicity***

Data obtained from the Lightning Positioning and Tracking System (LPATS) by [Ojelede \*et al.\* \(2008\)](#) were the lightning stroke data recorded by the LPATS Series III network operated by Eskom. The LPATS sensors detect electromagnetic radiation emitted by lightning strokes. Using the time of arrival from at least four of the sensors, the system data processor calculates the location of a lightning event ([Ndlovu and Evert, 2004](#)). GPS satellites are used to synchronize system clocks to within 100 ns. The sensor is designed to respond primarily to CG strokes and is less sensitive to IC lightning events ([Finke and Hauf, 1996](#); [Ndlovu and Evert, 2004](#)), which were estimated to be three times more frequent than CG strokes ([Price \*et al.\*, 1997](#); [Uman, 1987](#)). Approximately 5% of the lightning events detected by the Eskom LPATS array over the Highveld are estimated to be IC lightning events ([Ndlovu and Evert, 2004](#)). However, for the task of this chapter, literature was searched for recent data including longer time-frame records on IC to CG ratios.

The Eskom LPATS network is composed of six sensors located at the eastern half of South Africa (Figure 6.3), a region with high population and industrial densities and a region of intense lightning activity. The system was set up to provide protection, warnings and fault analysis for the national electrical power distribution system ([Redelinghuys, 1996](#)).

The sensor array has a detection efficiency of 90% over the central zone ([Ndlovu and Evert, 2004](#)). Its efficiency falls rapidly outside this zone (Figure 6.3). In southern Germany, detection efficiencies of 70% have been reported for similar LPATS arrays







and negative strokes (Ojelede *et al.*, 2008). This study used those values obtained by Ojelede *et al.* (2008) to group strokes into flashes and the NO<sub>x</sub> emission factor.

The emission factors and LNO<sub>x</sub> budgets equations used were obtained from Price *et al.* (1997) as used in Ojelede *et al.* (2008).

$$E = \text{mean energy per flash} = 6.7 * 10^9 \text{ J flash}^{-1},$$

$$M = \text{NO production} = 10 * 10^{16} \text{ molecules J}^{-1},$$

$$C = \text{Conversion factor} (46.0 \text{ g NO}_2 \text{ mol}^{-1})$$

$$I (6.02 * 10^{23} \text{ molecules mol}^{-1}) = 7.64 * 10^{-23} \text{ g NO}_2 \text{ molecules}^{-1}.$$

The resultant was a value of  $G_N = 51.2 \text{ kg NO}_2 \text{ flash}^{-1}$  (CG).

### 6.3.3 Lightning counts Data

The Lightning Detection Network of South African Weather Service (SAWS), consists of 19 sensors set over South Africa and has been fully operational since February 2006 (Figure 6.4).

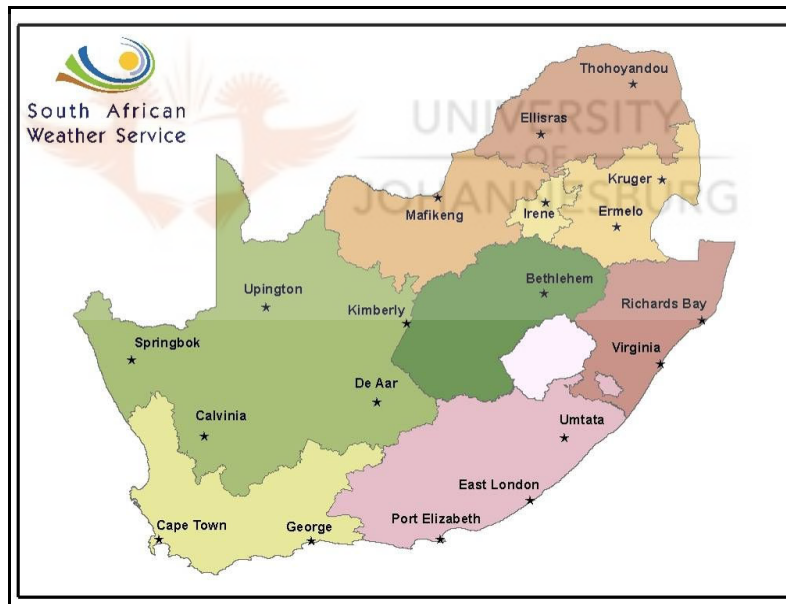


**Figure 6.4:** Location of SAWS lightning detection network sensors in South Africa. (Source: SAWS, as quoted in Bhika, 2008).

This ground-based network manufactured by Vaisala uses the Vaisala Thunderstorm CG Enhanced Lightning Sensor LS7000. This sensor configuration employs low frequency (LF) combined magnetic direction-finding and time-of-arrival technology, which offers high detection efficiency and accurate locations for cloud-to-ground lightning strokes (Vaisala, 2006). The network sensors measure the electromagnetic signatures of a lightning flash using a low frequency bandwidth from 1 kilohertz (kHz) to 350 kHz.



The magnetic direction finder (MDF) senses the electromagnetic field radiated by a lightning flash using two vertical, orthogonal loops with planes oriented NS and EW, each measuring the magnetic field from a given vertical radiator, which can then be used to obtain the direction to the source (Rakov and Uman, 2003). The voltage signals generated by the loops are compared to determine the direction of the flash. The direction finders send data for each registered lightning flash to a centralised position analyser, which triangulates coincident signals from multiple direction finders to locate the position of a lightning flash (SAWS, 2006).

The time of arrival detector consists of four antennas, which sense the electromagnetic field signal from the lightning. Since the lightning signal is dominated by the return stroke (ground to cloud), this locates the ground point of the lightning stroke to within a few hundred metres (Dowden *et al.*, 2002). The location of a lightning stroke is determined from the times of arrival of the signal at two or more antennae. To ensure the accuracy of lightning detection at least three or more sensors are used to detect the same stroke. The location of sensors is important for detection efficiency and a number of criteria were considered when choosing sensor sites.

Based on the above technology and sensor location criteria, the sensors of LDN (SAWS) have been installed across the country to achieve a minimum of 90% network detection efficiency for cloud-to-ground lightning and median location accuracy for cloud-to-ground lightning strokes of 500 m. The SAWS lightning detection network records lightning events chronologically. The attribute information of each lightning stroke is recorded, including latitude and longitude, peak current, polarity, major and minor ellipsoid angle and the number of direction finders that sensed the event. Lightning data from February 2006 to January 2007 were obtained from the South African Weather Services. After data cleaning, ~20.5 million recorded lightning strokes for this period were retained (Bhika, 2008).

#### **6.3.4 *Adjusted SAWS LDN lightning flash statistics***

For this statistic, the 4D Square designated in the study of Ojelede *et al.* (2008) was laid over the lightning (seasonal) density maps of Bhika (2008). The lightning density for the comparative area was reached by determining the average from the legend qualitatively. The method explained above required further preparation of the Bhika (2008) data. This entailed a calculation of the lightning strokes count on the basis of the lightning density per



km<sup>-2</sup> by multiplying the area of the compared region delineated by latitude 25° – 29°S and longitude 27° – 31° E with the seasonal lightning strokes per km<sup>-2</sup> for 92 days (one season) averages. The following sample plot illustrates the seasonal lightning density for the compared region (Figure 6.5).

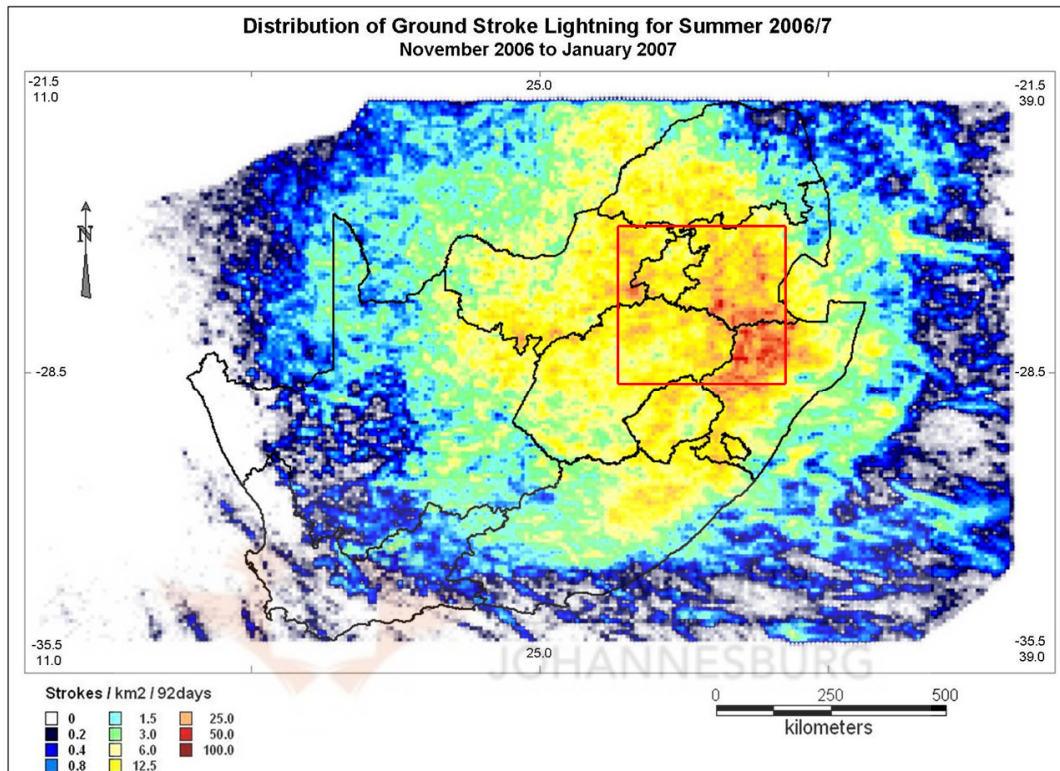


**Figure 6.5: Distribution of groundstroke lightning density for summer 2006/7**  
(Source: [Bhika, 2008](#)).

The next step was to group the lightning strokes into flashes based on the prior determined weighted mean lightning stroke multiplicity data ([Ojelede et al., 2008](#)) for the same studied square (Table 6.1).



**Table 6.1: Determination of lightning flashes from SAWS LDN\* by using stroke multiplicity rates\*\* for the compared study square (4D).**

Season	Mean seasonal lightning densities* (Stroke km <sup>-2</sup> per 92 days)	Lightning strokes (x 10 <sup>6</sup> )	Stroke to flash ** (x 10 <sup>6</sup> )	Flashes (x 10 <sup>6</sup> )
Spring	5.3	0.26.	1.52	0.18
Summer	29.2	1.44	2.43	0.59
Autumn	13.5	0.67	2.26	0.29
Winter	0.2	0.01	1.37	0.0072

\* Off-plots (Bhika, 2008) estimated mean seasonal lightning densities;

\*\* Weighed mean stroke to flash multiplicity (Ojelede *et al.*, 2008).

### 6.3.5 IC lightning ratios and LNO<sub>x</sub> generation strengths

The lightning stroke to flashes factors obtained from Ojelede *et al.* (2008) and Bhika (2008) lightning counts were used as a basis to add additional counts of intra/inter cloud-to-cloud estimates based on applicable published inter/intra cloud-to-cloud ratios (Boccippio *et al.*, 2000). This was carried out to increase the accuracy of counts of lightning strokes towards more realistic natural NO<sub>x</sub> production budget.

Figure 6.6 shows the (smoothed) 0.5° by 0.5° grid point estimates overlaid on the prior results of Pierce (1970), Prentice and Mackerras (1977) and Mackerras *et al.* (1998). The authors noted that the variability in local estimates was comparable to the total equator-to-mid-latitude drop in the IC to CG ratio suggested by these prior estimates (Figure 6.6).

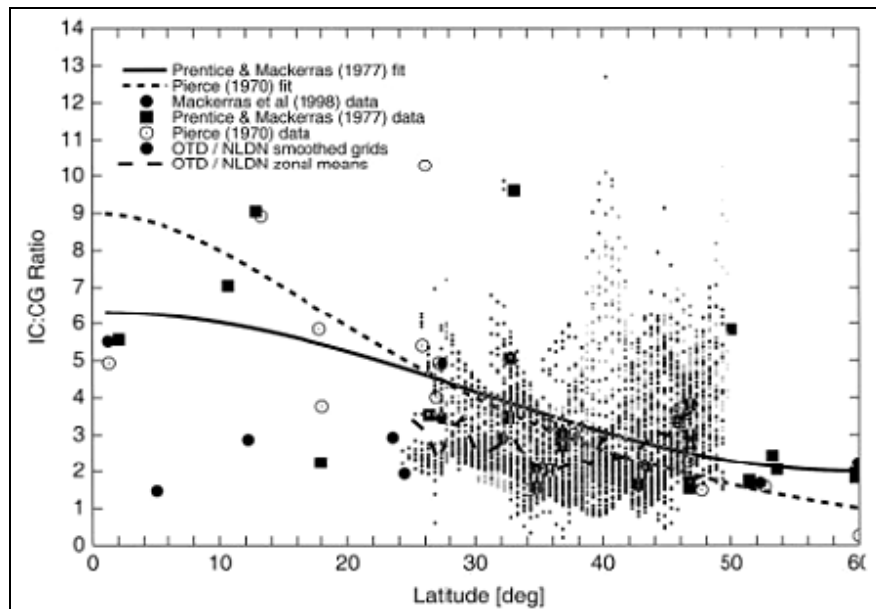


**Figure 6.6: Individual (smoothed) 0.5 ° grid estimates of IC: CG ratio overlaid on prior observations (Source: Boccippio *et al.*, 2000).**



Thus the IC to CG ratio for the adjustment of lightning counts from [Boccippio et al., 2000](#) findings was suitable for this task. Based on the study area latitude (~20° to 30° latitude south), the IC to CG ratio is found to be in the range between 5.5 and 4.5. The mean ratio was then estimated as **5:1** for IC to CG lightning for this 4D study area.

The amount of NO<sub>x</sub> produced by lightning can be estimated by multiplying the NO<sub>x</sub> production rate per flash (NO<sub>x</sub> emission factor) by the total number of flashes. [Price et al. \(1997\)](#) put forward a formula that allows for the calculation of regional and global NO<sub>x</sub> production (G<sub>N</sub>) over a period of time *t*:

$$G_N = (CG E_{CG} + IC * E_{IC}) t * P * C = (CG + 0.1 * IC) * (E_{CG}) * t * P * C \quad (6.2)$$

where CG is the cloud to ground flash frequency (flashes s<sup>-1</sup>); IC is the intra-cloud flash frequency; E<sub>CG</sub> is the mean energy in joule per CG flash; E<sub>IC</sub> is the ratio of energies for IC and CG flashes; *t* is the period in seconds; P is the production rate, taken as 10 x 10<sup>16</sup> NO<sub>x</sub> molecules J<sup>-1</sup>; and C represents the conversion factor (14.006 g N mole<sup>-1</sup>) / (6.02 x 10<sup>23</sup> molecules mole<sup>-1</sup>) = 2.33 x 10<sup>-23</sup> g N (molecules NO)<sup>-1</sup>.

Based on the Equation 5.2 the regional estimates of IC lightning flashes were multiplied by 5.0 to correct for IC to CG counts. In the terms of its energy output per flash, also relying on the referenced works (section 5.2.4), the average IC flash is less energetic than a CG flash by a factor of between 2 and 10. A mean of 6 times less energetic was used. A lower IC adjusted regional LNO<sub>x</sub> budget can then be calculated as follows:

$$G_N = ((CG * E_{CG}) + ((CG * 5) * (E_{CG} / 6)) * t * P * C) \quad (6.3)$$

However, newer literature on the topic brought this widely accepted estimate into question. Findings from the work of [Cooray \(1997\)](#) and [Cooray and Rahman \(2005\)](#) indicate that IC may be equal in energy dissipation and thus likely to have equal potential for producing NO<sub>x</sub>. In addition, relevant modelling suggested equal or slightly higher IC NO<sub>x</sub> production ([Fehr et al., 2004](#)).

If it is assumed that CG and IC flashes are equal in their NO<sub>x</sub> production (and that IC flashes are five times more frequent than CG flashes), the upper budget of G<sub>N</sub> can be calculated as follows:

$$G_N = (((CG * E_{CG}) + (IC * 5) * E_{CG}) * t * P * C) \quad (6.4)$$

After such amendments, the stroke count was adjusted by the seasonal weighted averaged stroke to flashes multiplicity rates determined by [Ojelede et al. \(2008\)](#) to reach an adjusted lightning flashes count. The added IC stroke estimates were set in two different estimates.



One estimate (CG + IC) had less flash energy and therefore a smaller NO<sub>x</sub> generation capacity and the other (CG + IC) had equal energy and NO<sub>x</sub> production capacity to CG. The comparison results are presented for four seasons and one annual cycle in the results section (5.4).

### 6.3.6 *The emission inventories extraction*

Three NO<sub>x</sub> emission inventories were then compared. These were the EDGAR 32FT2000, for year 2000 (EDGAR, 2008), Fleming and van der Merwe SA emission database (year 2000) and the more recent FRIDGE report (Scorgie *et al.*, 2004a, 2004b and 2004c).

For extraction of country-specific database, the Emission Database for Global Atmospheric Research (EDGAR) world emission database was accessed (EDGAR, 2008). The measure unit used in the original inventories (Gg) equals the unit mostly applied in this work (kt) (Table 6.2).

**Table 6.2: Major sources of NO<sub>x</sub> emissions in SA from the EDGAR emission database converted to NO<sub>x</sub> as N (Source: EDGAR, 2008: 32FT2000).**

<i>National NO<sub>x</sub> emissions per source category, Year: 2000.</i>		<i>South Africa NO<sub>2</sub> as N (kt)</i>
B10	Industry	0.7
B20	Power Generation	0.5
B30	Charcoal Production	0.0
B40	RCO: Residential	22.6
B51	Road Transport	0.0
F10	Industrial Sector	28.3
F20	Power Generation	224.8
F30	OTS (All)	3.2
F40	RCO Sector(Res+Com+Oth)	3.9
F51	Road Transp. (Incl. Eva)	125.7
F54	Trans. Land Non-Road	3.4
F57	Air Transport	4.8
F58	International Shipping	57.5
F80	Oil Production	0.3
I10	IRO: Iron & Steel	0.4
I20	NFE: Non-Ferro	1.1
I40	Building Materials	7.2
I50	PAP: Pulp & Paper	0.6
L41	Tropical Forest Fires*	0.0
L42	Savannah And Shrubs Fires*	5.5



<b>National NO<sub>x</sub> emissions per source category, Year: 2000.</b>		<b>South Africa NO<sub>2</sub> as N (kt)</b>
L43	BB-Agric. Waste Burning	2.3
L44	Middle And High Latitude Forest Fires*	2.5
L47	Middle And High Latitude Grassland Fires*	64.2
W40	Waste Incineration (Non-Energy)	0.2
<b>GRAND TOTAL</b>		<b>560</b>

\* Biomass burning: 1997 - 2001 average activity data with EDGAR 32FT2000 emission factors

The above grand total needed to be adjusted for the smaller study region. For this, the publication of Wells *et al.* (1996) was followed, which stated that the Highveld industrial heartland counts for ~90% of the country's industrial NO<sub>x</sub> pollution. Thus, the above budget was reduced by 10% to 90% resulting in **504 kt** of NO<sub>x</sub> as N.

The Fleming and van der Merwe (2004) emission database was also accessed for the overall comparison. This database of anthropogenic sources was compiled in a gridded form. To cover the Highveld industrial heartland, a subset of the results was extracted covering the 4D study area. The result for NO<sub>2</sub> is 2 203 kt, corresponding to **668 kt** NO<sub>2</sub> as N (Figure 6.7).

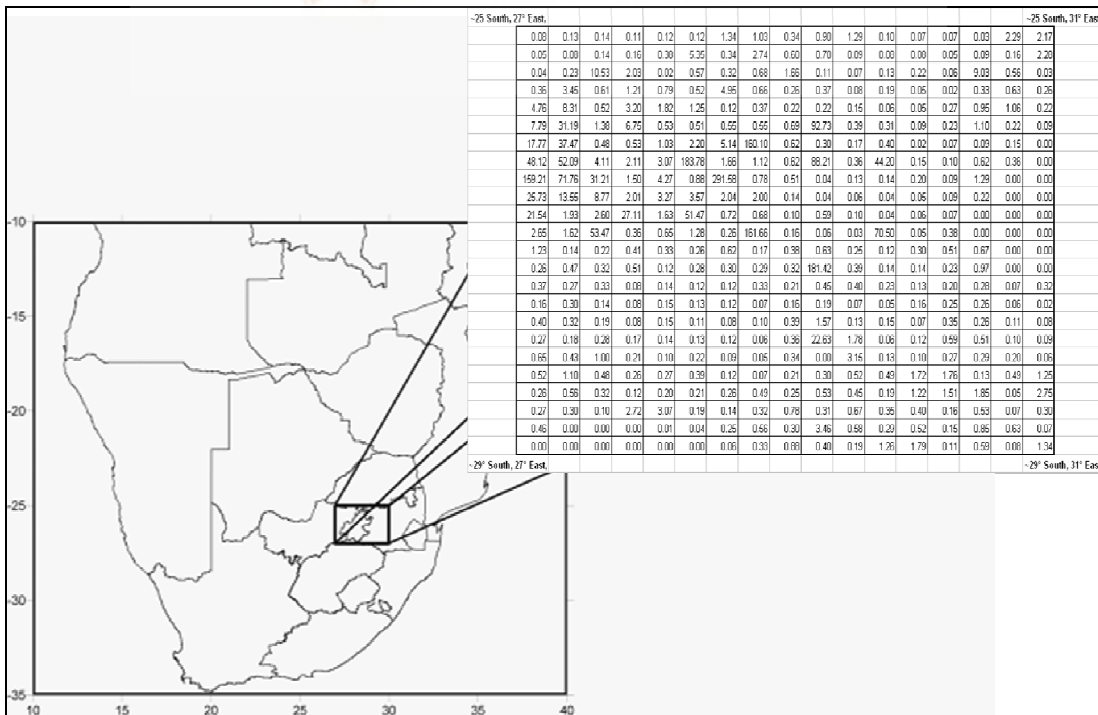


Figure 6.7: 4D extract of Fleming and van der Merwe emission database for NO<sub>2</sub>.





A more recent emission inventory was checked in the form of a study done for the Fund for Research into Industrial Development Growth and Equity (FRIDGE) entitled “Study to Examine the Potential Socio-Economic Impact of Measures to Reduce Air Pollution from Combustion” (Scorgie *et al.*, 2004a, b and c). This study considered the geographical areas of the Mpumalanga Highveld, Vaal Triangle, Johannesburg, Ekurhuleni and Tshwane. The relevant NO<sub>x</sub> emission inventory provided another set of NO<sub>x</sub> emission database covering most of industrial heartland Highveld pollution sources (Figure 1.1).

These areas are essentially equal to the 4D square and the results are compiled together to give a cumulative emission value for comparison with the previous two sets (Table 6.3)

**Table 6.3: Emission inventory extract from the FRIDGE study (t NO<sub>2</sub> yr<sup>-1</sup>)\***

<i>Emission inventory for Highveld sources (FRIDGE sub-area)</i>	<i>Industrial, Commercial &amp; Institutional Fuel Burning (x 10<sup>6</sup>)</i>	<i>Electricity Generation (x 10<sup>6</sup>)</i>	<i>Vehicles (x 10<sup>6</sup>)</i>	<i>Aircraft (x 10<sup>6</sup>)</i>	<i>Biomass Burning (x 10<sup>6</sup>)</i>	<i>Domestic Fuel Burning (x 10<sup>6</sup>)</i>	<i>TOTAL (x 10<sup>6</sup> t NO<sub>2</sub> yr<sup>-1</sup>)</i>
<b>Mpumalanga Highveld</b>	0.15	0.57	0.024	n/a	0.0017	0.00045	0.76
<b>Vaal Triangle</b>	0.099	0.011	0.011	n/a	0.00024	0.00036	0.12
<b>Joburg</b>	0.0009	0.0011	0.046	0.00072	0.00049	0.00041	0.05
<b>Ekurhuleni</b>	0.0047	n/a	0.037	n/a	0.00035	0.00036	0.043
<b>Tshwane</b>	0.0007	0.013	0.03	n/a	0.00043	0.00027	0.044
<b>Totals</b>	0.26	0.59	0.15	0.00072	0.0032	0.0019	1.007

Source: \*Scorgie *et al.*, 2004b.

### 6.3.7 NO<sub>x</sub> budget estimation based on passive sampling measurements

The monthly mean NO<sub>2</sub> concentrations from two annual cycles of passive monitoring were collated. These data gave the mean estimate of the NO<sub>x</sub> (as N) budget over the compared study area. For this budget estimate, the mean concentrations of NO<sub>2</sub> (µg m<sup>-3</sup>) obtained by passive sampling sites falling into the designated 4D study square of Ojelede *et al.* (2008) were used to reach the passive sampling-based NO<sub>x</sub> concentration-budget (Figure 6.8).

The mean concentration values were multiplied by the height of the boundary layer to obtain the total NO<sub>2</sub> mass in the boundary layer column. The planetary boundary layer is taken to average 1500 m for the entire area for the purposes of estimation. The next step was to account for the space around each site, each designed as a part of the sampling network of sites at 1° latitude-longitude spacing (111 km by 111 km). In the initial design



of the network several grid points were left out (the conurbation of Gauteng westwards from site 17 at one and two degrees away) and another westwards from Site 32 at one degree distance. In order to account for the measurements over these grid cells the measurements for Sites 17 (twice) and for Site 31 (once) were added to all others. The results of the prior step were multiplied by the size of area around each site. The results are expressed in kilotons (kt) of NO<sub>2</sub> within this volume (Table 6.4).

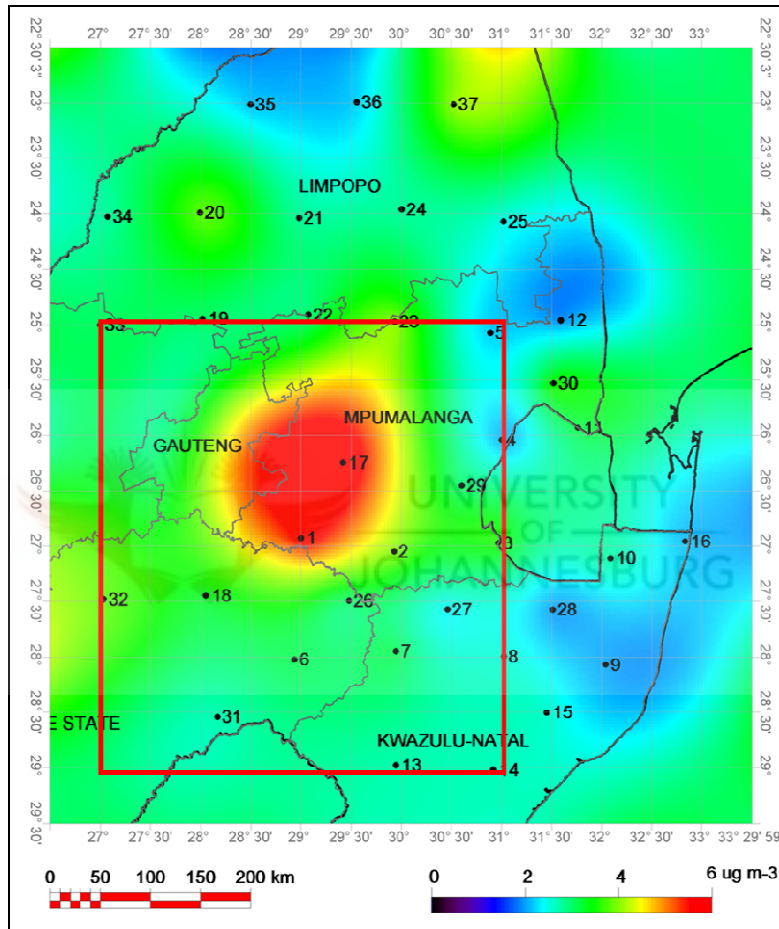


Figure 6.8: NO<sub>2</sub> mean concentrations measured by passive sampling (Sep05-Aug07). Red marking is 4D square.

Table 6.4: Passive sampling (PS) concentration data based estimate of NO<sub>2</sub> mean budget in the study region.

<i>PS sites located within square 4D<sup>1</sup></i>	<i>NO<sub>2</sub> mean concentration<sup>2</sup> (μg m<sup>-3</sup>)</i>	<i>NO<sub>2</sub> column density<sup>3</sup> (μg m<sup>-2</sup>)</i>	<i>NO<sub>2</sub> mass per cell<sup>4</sup> (t 1 500m 12 100 km<sup>-2</sup>)</i>	<i>NO<sub>2</sub> mass per cell<sup>5</sup> (kt)</i>
1	74.1	111124	1369	1.4
2	45.7	68585	845	0.8
4	19.6	29419	362	0.4
5	21.1	31600	389	0.4



<i>PS sites located within square 4D<sup>1</sup></i>	<i>NO<sub>2</sub> mean concentration<sup>2</sup> (µg m<sup>-3</sup>)</i>	<i>NO<sub>2</sub> column density<sup>3</sup> (µg m<sup>-2</sup>)</i>	<i>NO<sub>2</sub> mass per cell<sup>4</sup> (t 1 500m 12 100 km<sup>-2</sup>)</i>	<i>NO<sub>2</sub> mass per cell<sup>5</sup> (kt)</i>
6	35.0	52507	647	0.6
7	34.8	52169	643	0.6
8	26.5	39741	490	0.5
13	29.3	43996	542	0.5
14	28.3	42434	523	0.5
17	79.8	119750	1475	1.5
17	79.8	119750	1475	1.5
17	79.8	119750	1475	1.5
18	35.9	53823	663	0.7
19	33.9	50822	626	0.6
22	33.0	49534	610	0.6
23	49.0	73524	906	0.9
26	33.6	50330	620	0.6
27	24.8	37142	458	0.5
29	34.0	51009	628	0.6
31	29.0	43463	536	0.5
31	29.0	43463	536	0.5
32	45.6	68361	842	0.8
33	32.7	49086	605	0.6

**TOTAL: Mean cumulative NO<sub>2</sub> budget is 17 kt of NO<sub>2</sub> equivalent to 5 kt of NO<sub>2</sub> as N**

<sup>1</sup> Plus 2 sites filling the gap (no. 17 twice and 31 once)

<sup>2</sup> Cumulative annual mean over Sep05-Aug07 period

<sup>3</sup> Concentration above specific site (1.5 km height)

<sup>4</sup> Square over 1° x 1° latitude-longitude and 1.5 km high vertical column

<sup>5</sup> Centred over specific site 1° x 1° lat-lon and 1.5 km height.

### 6.3.8 *NO<sub>x</sub> budget on the basis of remote sensing measurements for the study region*

It is useful to evaluate the remotely sensed measured NO<sub>2</sub> density-budget in relation to the boundary layer passive sampling measured and calculated concentration-budget within the same volume. For this task, use is made of a set of long-term (2003 to 2007) satellite image from the SCIAMACHY sensor with accompanying dataset (Beirle, personal communication, 2008). This image indicates an enlarged spatial presence of NO<sub>x</sub> as NO<sub>2</sub> seen at the tropopause. In comparison with the Figure 6.8 it differs in its spatial distribution while still showing a strong density values contrary to the ground level mean concentrations (Figure 6.9).



It was possible to calculate the mass of the NO<sub>2</sub> plume contained within the vertical column density above the given region and more specifically to extract it for the region compared (4D). The retrieved RS measurements are provided in 10<sup>13</sup> molec cm<sup>-2</sup> and at a resolution of 0.1° latitude-longitude (Beirle, personal communication, 2008). The one degree was assumed to be 111 km and the Table 6.5 is the output of the method used.

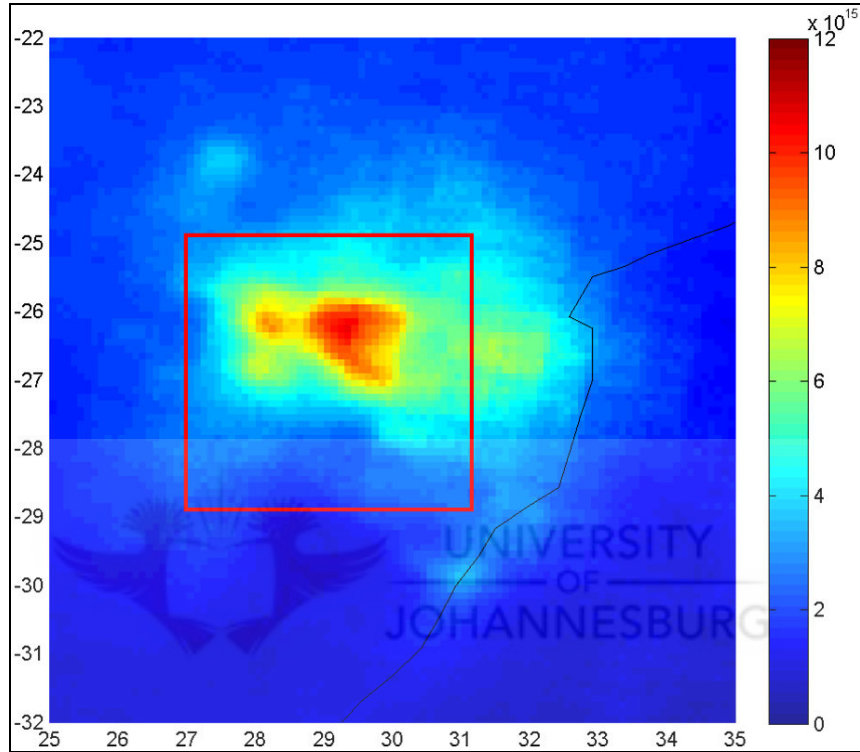


**Figure 6.9:** NO<sub>2</sub> mean RS 4-year (2003 to 2007) tropospheric vertical column density (10<sup>15</sup> molec cm<sup>-2</sup>) by SCIAMACHY for the study area (Source: Beirle, personal communication, 2008). The red square represents 4D compared area.

**Table 6.5:** NO<sub>x</sub> budget within the VCD measured by SCIAMACHY and averaged for 2003-2007<sup>#</sup> over 4D region.

<i>Area measured</i>	<i>Molec/area</i>	<i>NO<sub>2</sub> molar weight</i>	<i>Avogadro Number</i>	<i>Total mass (g)</i>	<i>Total mass (kt)</i>
<b>4D</b>	9.18E+31	46.005	6.02E+23	7.01E+09	<b>7</b>

Source: # Beirle, personal communication, 2008.

The next section compares the above determined and adjusted budgets and analyses differences between them.



## 6.4 Results

The LNO<sub>x</sub> emission factor introduced in section 5.2.3 was used to arrive at two intra-cloud adjusted LNO<sub>x</sub> budgets. Two LNO<sub>x</sub> budgets, one lower estimates and one higher estimate, were calculated for comparison. The LPATS count for the period from January to December 2002 (Ojelede *et al.*, 2008) were not taken into the calculation as the study relied on more recent data measured by more advanced technology. Accordingly, the SAWS Lightning Detection Network count for one annual cycle, February 2006 to January 2007 (Bhika, 2008) was the basis of the LNO<sub>x</sub> budgets estimates.

### 6.4.1 Lower LNO<sub>x</sub> estimate

The new flash count with the inter-cloud flash estimates using the procedure explained in the methods section (section 5.3.4) resulted in two budgets. One presents a set of lower seasonal and annual NO<sub>2</sub> budget estimates (Table 6.6).

**Table 6.6: LNO<sub>x</sub> budget based on flashes detected by the SAWS Lightning Detection Network<sup>#</sup>, adjusted with IC flashes (less energetic option).**

Season	Spring (x 10 <sup>6</sup> )	Summer (x 10 <sup>6</sup> )	Autumn (x 10 <sup>6</sup> )	Winter (x 10 <sup>6</sup> )	Annual (x 10 <sup>6</sup> )
No. of CG flashes recorded (SAWS LDN, Feb06-Jan07)	0.17	0.59	0.29	0.0072	1.07
Estimated IC flashes (CG x 5)	0.86	2.96	1.47	0.036	5.33
CG flashes x 51.2 kg flash <sup>-1</sup> of LNO <sub>x</sub>	8.80	30.32	15.07	0.37	54.56
IC = CG/6 x 51.2 kg flash <sup>-1</sup> of LNO <sub>x</sub>	7.33	25.27	12.56	0.31	45.47
Total = IC + CG (kg LNO <sub>x</sub> )	16.13	55.59	27.63	0.68	100.03
Total (kt LNO <sub>x</sub> )	16	56	28	0.7	100
Total (kt LNO <sub>x</sub> as N)	4.8	17	8.5	0.30	30

<sup>#</sup> Source of lightning counts: Bhika, 2008.

### 6.4.2 Higher LNO<sub>x</sub> estimate

A second estimate was compared here, for which the IC flashes are taken to be as productive (energetic) as CG flashes. This provided a set of higher seasonal and annual estimates (Table 6.7).



**Table 6.7: LNO<sub>x</sub> budget based on flashes detected by the SAWS Lightning Detection Network<sup>#</sup>, adjusted with IC flashes (equally energetic option).**

<b>Season</b>	<b>Spring (x 10<sup>6</sup>)</b>	<b>Summer (x 10<sup>6</sup>)</b>	<b>Autumn (x 10<sup>6</sup>)</b>	<b>Winter (x 10<sup>6</sup>)</b>	<b>Annual (x 10<sup>6</sup>)</b>
<b>No. of CG flashes Recorded (SAWS LDN, Feb06-Jan07)<sup>#</sup></b>	0.17	0.59	0.29	0.0072	1.07
<b>Estimated IC flashes (IC = CG x 5)</b>	0.86	2.96	1.47	0.036	5.33
<b>CG flashes x 51.2 kg flash<sup>-1</sup> of LNO<sub>x</sub></b>	8.80	30.3	15.1	0.37	54.6
<b>IC = CG x 51.2 kg flash<sup>-1</sup> of LNO<sub>x</sub></b>	44.0	151.6	75.4	1.8	272.8
<b>Total = IC + CG (kg LNO<sub>x</sub>)</b>	52.8	181.9	90.4	2.2	327.4
<b>Total (kt LNO<sub>x</sub>)</b>	53	182	90	2	327
<b>Total (kt LNO<sub>x</sub> as N)</b>	<b>16</b>	<b>55</b>	<b>27</b>	<b>0.60</b>	<b>99</b>

<sup>#</sup> Source of lightning counts: [Bhika, 2008](#).

Subsets of the various emissions inventories were extracted corresponding to the 4D region of the central industrial Highveld of South Africa (Figure 6.3). The inventories used were EDGAR 32FT2000 for year 2000 ([EDGAR, 2008](#)); Fleming and van der Merwe SA emission database for year 2000 ([Fleming and van der Merwe, 2004](#)); and more recent FRIDGE reports ([Scorgie et al., 2004a, 2004b and 2004](#)). These anthropogenic emission inventories were then compared with two options of the LNO<sub>x</sub> budget derived from LDN stroke counts ([Bhika, 2008](#)), that were adjusted stroke multiplicity rates ([Ojelede et al., 2008](#)). Two LNO<sub>x</sub> budget estimates were included, one using the less energetic IC option, leading to a lower estimate; and the other using the equally energetic IC and CG option, leading to a higher estimate of NO<sub>x</sub> production (Table 6.8).

#### **6.4.3 LNO<sub>x</sub> and anthropogenic NO<sub>x</sub> budget comparison**

In addition to the compared emission inventories of anthropogenic data with LNO<sub>x</sub> inventory, most pyrogenic emissions in the region were also included. So in order to account for another major natural emission sources, estimates of NO<sub>x</sub> from soils and vegetation needed to be included. Based on the emissions discussed in section 5.2.3 the resultant soil emission of 7 kt encompassing entire South Africa is taken to represent joint soil and vegetation NO<sub>x</sub> as N emissions (3.5 kt + 3.5 kt) in the compared area 4D. All the relevant estimates are compiled for a comparison (Table 6.8).



**Table 6.8: Comparison of NO<sub>x</sub> emissions (kt N yr<sup>-1</sup>) from the major inventories applicable to the Highveld.**

<b>Emission inventory</b>	<b>Anthropogenic (Industrial, commercial &amp; residential)</b>	<b>Pyrogenic (anthropogenic and biogenic)</b>	<b>Lightning NO<sub>x</sub> (LNO<sub>x</sub>)</b>	<b>Soil and plant NO<sub>x</sub></b>	<b>Total (kt N yr<sup>-1</sup>)</b>
<b>EDGAR 32FT<sup>b</sup></b>	437	67	n/a	n/a	<b>504</b>
<b>Fleming &amp; van der Merwe, 2004<sup>c</sup></b>		668	n/a	n/a	<b>668</b>
<b>FRIDGE study<sup>d</sup></b>	304	1	n/a	n/a	<b>305</b>
<b>LNO<sub>x</sub> production - this study</b>	n/a	n/a	99 (upper est.) 30 (lower est.) <sup>a</sup>		<b>99</b> <b>30<sup>a</sup></b>
<b>Soil emission estimates (this study)</b>				7	<b>7</b>

<sup>a</sup> Lower LNO<sub>x</sub> estimate; <sup>b</sup> EDGAR, 2008; <sup>c</sup> Fleming & van der Merwe, 2004; <sup>d</sup> Scorgie *et al.*, 2004c.

In comparison with the anthropogenic emissions, LNO<sub>x</sub> adds substantially to the load of NO<sub>x</sub>. The FRIDGE emissions inventory study, which was based on emission factors derived from consultations with the major industries and is hence regarded as better informed than scanning surveys, was used to estimate high and low estimates of the LNO<sub>x</sub> fraction of the anthropogenic NO<sub>x</sub> budget. The LNO<sub>x</sub> low estimate gave 10% (30 kt: 305 kt), and a high estimate of 32% (99 kt: 305 kt). In either case, the LNO<sub>x</sub> budget represents a significant portion of the overall anthropogenic budget and the higher estimate is essentially within the same order of magnitude with anthropogenic inventories.

#### *LNO<sub>x</sub> seasonality review*

In case of the higher LNO<sub>x</sub> budget estimate (~30%); this contribution is significant enough that it should be recognisable in the seasonal variation of ground level measurements of the NO<sub>x</sub> (NO<sub>2</sub>) concentrations. As summer lightning activity is a factor of over 81 times greater than winter, the LNO<sub>x</sub> production is similarly concentrated in summer (Table 6.6 and Table 6.7). Hence wet season (spring and summer) measured NO<sub>x</sub> should be higher than winter NO<sub>x</sub>. The comparison is made in Figure 6.10, showing that there is no clear indication of seasonal differences.

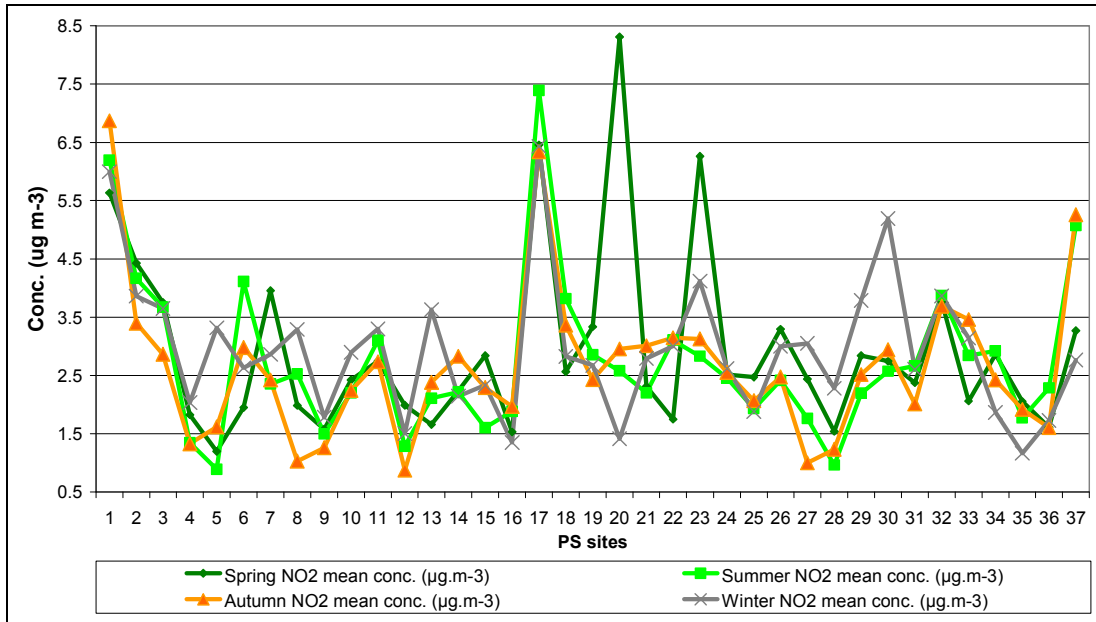


**Figure 6.10: A NO<sub>2</sub> seasonal concentration means (Sep05-Aug07).**

However, Figure 6.10 does not indicate clear high of the summer and or spring mean (when most of the lightning happens on the central industrial Highveld). Relatively highest NO<sub>2</sub> mean is only enhanced for two sites (site 20, near Vaalwater and 23, near Steelpoort) for spring season (located out of the industrial Highveld zone) and despite this; the plot indicates that the anthropogenic emissions dominate the ground-level concentration measurements.

As Figure 6.10 does not confirm a distinguishable lightning season (mainly summer on Highveld) the question still remains whether the seasonality of the LNO<sub>x</sub> is picked up by the ground measurements at all or simply indicates that the major portion of LNO<sub>x</sub> is concentrated above the boundary layer (mixing layer) as subject to both horizontal and vertical fluxes out of zone of the highest generation (Boersma *et al.*, 2005; Beirle 2004, Richter and Burrows, 2002; Zhang *et al.*, 2000). Similarly, with this axiom, possibilities exist that some parts of anthropogenic emissions have similar path and are likely vertically advected out of the boundary layer and horizontally transported over and out of the source area.

## 6.5 Discussion

The NO<sub>x</sub> budget is directly dependant on natural and anthropogenic emissions, the mixing of NO<sub>x</sub> in the atmosphere, horizontal and vertical transport in and out of a particular area,





chemical transformation, its dry deposition and the conversion of NO<sub>x</sub> with wet deposition of species. The budget dependency can be presented schematically (Figure 6.11).

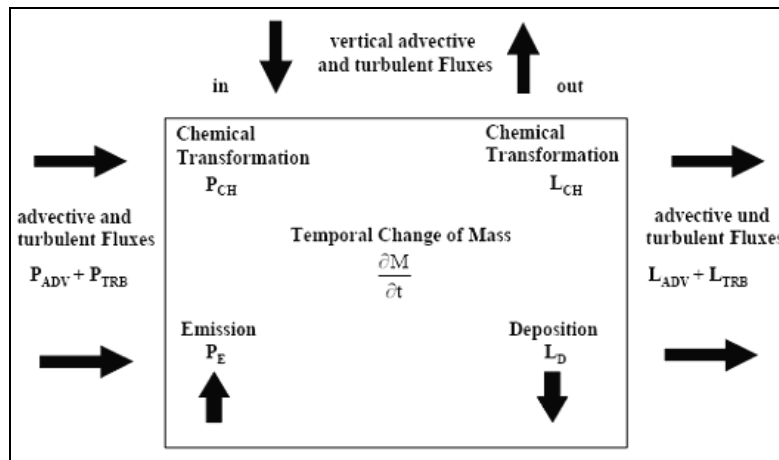


**Figure 6.11: Schematic illustration of a gaseous species mass budget calculation in a predefined volume (Source: Panitz and Nester, 2002).**

The NO<sub>x</sub> budget calculations must take into account real atmospheric processes. The NO<sub>x</sub> budget depends on a number of known and unknown elements and processes. It is important to mention the known elements affecting the fate of trace gas species in question and relate this to the budget totals reached. These processes and their dependencies can be approximated as in Equation 5.5:

$$\begin{aligned} \sim\text{NO}_x \text{ BUDGET} = & \{[(\sum\text{NO}_x\text{Em} - \sum\text{NO}_x\text{EmCt}) + (\sum\text{NO}_x\text{T}_{in} - \sum\text{NO}_x\text{T}_{in}\text{Ct})] \\ & - [\sum\text{NO}_x\text{T}_{out} + (\sum\text{NO}_x\text{D}_d + \sum\text{NO}_x\text{D}_w)]\} \end{aligned} \quad (6.5)$$

where **NO<sub>x</sub>Em** are all NO<sub>x</sub> emissions, **NO<sub>x</sub>EmCt** is NO<sub>x</sub>Em chemically transformed, **NO<sub>x</sub>T<sub>in</sub>** is transported NO<sub>x</sub> (by horizontal and vertical fluxes) into the bounded volume and **NO<sub>x</sub>T<sub>in</sub>Ct** is NO<sub>x</sub>T<sub>in</sub> chemically transformed, **NO<sub>x</sub>T<sub>out</sub>** is NO<sub>x</sub> transported out (exited) from the bounded volume, and **NO<sub>x</sub>D<sub>d</sub>** is NO<sub>x</sub> dry-deposited and **NO<sub>x</sub>D<sub>w</sub>** is NO<sub>x</sub> converted into N-compounds and then wet-deposited.

Natural and anthropogenic emissions of NO<sub>x</sub> may enter and exit the bounded volume, or may be chemically converted within the volume. The vertical mixing of the atmosphere with vertical convection and export to the medium and higher troposphere, as well as the intrusion of gases from the upper tropospheric into lower tropospheric layers, contribute to the quantity of NO<sub>x</sub> in the bounded volume. While it is not possible currently to measure or model all these processes with their various gains and losses of NO<sub>x</sub>, they should not be neglected in a qualitative assessment.



When the remote sensing retrieved measurements of NO<sub>2</sub> column density are transformed into total mass units to coincide with the region 4D, then such a NO<sub>2</sub> budget accounts to 7 kt of NO<sub>2</sub> (or 2 kt of NO<sub>x</sub> as N) as annual average (Table 6.9).

**Table 6.9: NO<sub>2</sub> budget over the 4D volume by passive sampling and by remote sensing.**

<b>Main emission inventories NO<sub>2</sub> as N (kt yr<sup>-1</sup>)</b>	<b>Total NO<sub>x</sub> (kt NO<sub>x</sub>)</b>	<b>Total NO<sub>x</sub> as N (kt N)</b>
<b>NO<sub>2</sub> by PS (4D)</b>	17	5
<b>NO<sub>2</sub> by RS (4D)</b>	7	2

It is useful to evaluate here the remote sensing measured NO<sub>2</sub> budget in relation to the boundary layer passive sampling measured and calculated budget within the same volume (17 kt of NO<sub>2</sub> or 5 kt of NO<sub>2</sub> as N). The results point to a difference of 40% and this is an unexpected, a paradoxical result assuming all other parameters being correct, as the vertical column density includes the entire boundary layer in addition to rest of tropospheric column. Thus, the column NO<sub>2</sub> budget is expected to be higher than estimated boundary layer NO<sub>2</sub> budget.

Upon a spatial inspection of both concentration means, the ground-level measurements show different spatial distribution patterns over essentially the same (central) region (Figure 6.8) in comparison with the RS spatial plot (Figure 6.9). This is especially case over an extended study region beyond 4D rectangular (Figure 6.9). Discussing the possible reasons, one possibility strongly is suspected, that NO<sub>x</sub> has a different distribution above the mixing/boundary layer. The sensitivity of RS sensors is decreased with depth and optical obstacles such as clouds, so there is a possibility that the parts of NO<sub>x</sub> present within the boundary layer are obscured to the sensor instruments. Of course, a precaution has to be taken here as the imagery represent medium to – long term averages for which no chemical conversion and other dynamics were calculated and taken into account. However, the idea behind, to compare averages as transects of particular representative moment in time was considered suitable for the type of comparison undertaken.

It must be noted that a portion of emitted NO<sub>x</sub> is converted during the advective and horizontal transport until it reaches above mixing layer where the life of NO<sub>x</sub> is longer. The lifetime of NO<sub>x</sub> is a very important parameter for tropospheric chemistry in general. Due to high variability of the factors controlling the lifetime of NO<sub>x</sub>, i.e. meteorology, chemical composition and actinic flux, NO<sub>x</sub> lifetime is itself highly variable. Mean values are of the



order of hours for the lower troposphere up to days for the upper troposphere (Jaegle, 1998). This then could support a notion that  $\text{NO}_x$  once advected is present longer over main source region, subject to spread and thus dilution and often transported much further away from its main sources region.

Considering this and having the findings on remote sensing by satellite borne instrument of the trace gases (section 6.4); some more clarity about the regional  $\text{NO}_x$  budget could be in the following hypothesis.

According to the findings of the global and regional RS (satellite-borne) together with their validation efforts, there is a strong indication that a significant portion of emitted  $\text{NO}_x$  is lifted above the mixing boundary layer and then horizontally spread/diluted, generally re-circulated and occasionally exported out of the major source and recirculation areas. Such might be a case for Highveld area of South Africa. A case in point is presented in Figure 6.12. It tracks sequence of distributions of tropospheric  $\text{NO}_2$  columns by the GOME instrument east of South Africa in May 1998 (left column).

As per Wenig *et al.* (2003),  $\text{NO}_x$  emission densities in the Highveld are among the highest in the world. In addition, with an altitude of 1400 to 1700m above sea level the Highveld is one of the most elevated industrial regions worldwide. In addition, buoyant emissions from tall stacks are usually lifted above the ground-based, nocturnal inversions (Held *et al.*, 1996). This reduces chemical losses and dry deposition of  $\text{NO}_x$ . During anticyclones, such as those prevailing during May 1998, several inversion layers were created, pollutants were trapped between them (Tyson *et al.*, 1997) and the pollutant's entrainment within the boundary layer was prevented.

Pollution export occurs effectively only when a low-pressure system sweeps over SA and leads to transport towards the Indian Ocean and Australia (Piketh *et al.*, 1999; Tyson and D'Abreton, 1998). If transported offshore, polluted air masses from the Highveld travel above the marine boundary layer (Tyson and D'Abreton, 1998). Figure 6.12, right column, indicates that the major part of the  $\text{NO}_x$  plume was decoupled from the surface (Wenig *et al.*, 2003).

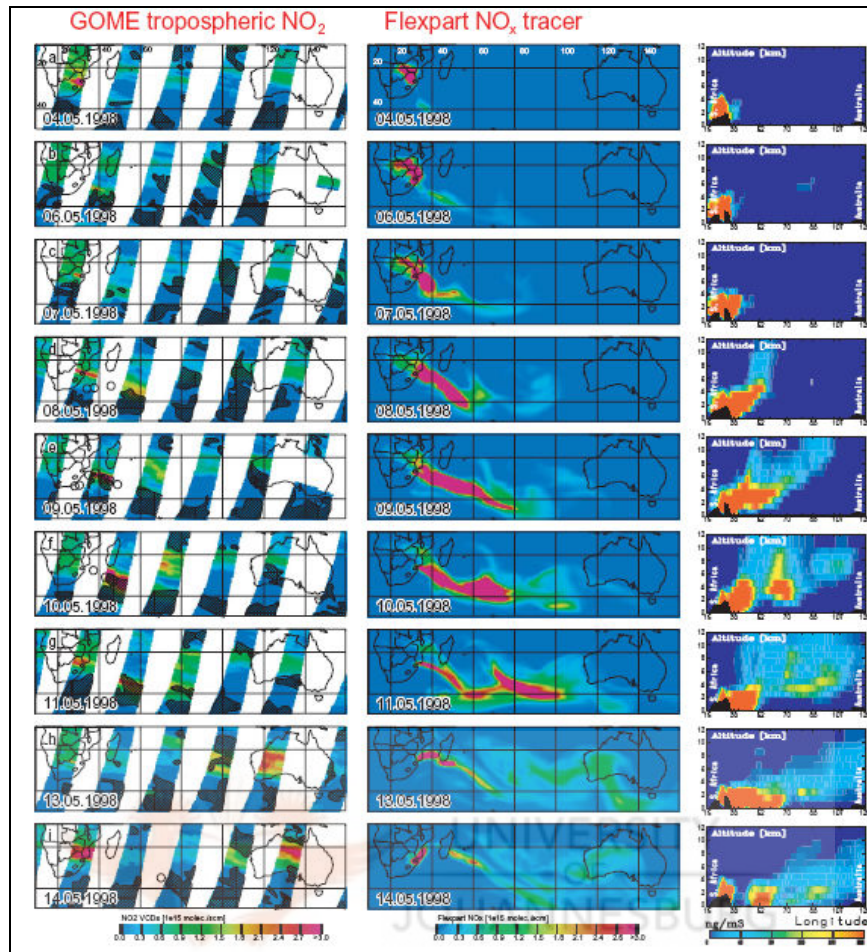


**Figure 6.12:** Sequence of distributions of tropospheric NO<sub>2</sub> columns from the GOME instrument east of SA in May 1998 (left column). Corresponding NO<sub>x</sub> tracer column densities (centre column) and vertical sections of the NO<sub>x</sub> tracer concentrations only for industrial emissions (Wenig *et al.*, 2003).

This study suggests that the NO<sub>x</sub> emissions ascend substantially above the source area, although reduced through the deposition and conversion processes, they are subjected to lift and export away from the wider source area by the prevailing mid to upper air mass movement in dominant directions.

## 6.6 Conclusions

As per the purpose set for this task, improved lightning stroke counts have been applied in estimation of LNO<sub>x</sub> generation. Two options were employed resulting in two LNO<sub>x</sub> budget estimates. These two budget estimates were brought into relationship with several relevant NO<sub>x</sub> emission databases, adjusted to overlay the specific pre-defined volume of the Highveld for a better comparison. The applied methods have confirmed prior knowledge that the regional LNO<sub>x</sub> is a significant contributor to the overall NO<sub>x</sub> budget and could



potentially make a significant addition to the size of the anthropogenic (with pyrogenic)  $\text{NO}_x$  budget.

However, the measurements of the concentrations on the ground level through determination of seasonal variations have not shown evidence of a lightning season component. The remote sensing results suggest that the  $\text{LNO}_x$  is not entirely added to the boundary/mixing layer. And that a large portion of the Highveld region lightning  $\text{NO}_x$  generation is produced and remains above the boundary layer. This makes it part of the upper/mid-tropospheric  $\text{NO}_x$  and its budget but does not essentially contribute to the concentrations level of  $\text{NO}_x$  measured on the ground (lower troposphere). Even more so the same type of evidence (RS) may point out that a substantial portion of anthropogenic  $\text{NO}_x$  is advected above the boundary layer from where it is eventually spread, converted and partly exported. This could go some way to explaining why the areas in vicinity of the source zone do not show a stronger influence of  $\text{LNO}_x$ .

#### **6.6.1 Summary**

The above comparison constitutes a quantitative attempt to determine a budget estimate of a particular pollutant. The budget calculations then confirm that  $\text{LNO}_x$  is a major contributor to the natural  $\text{NO}_x$  emissions and a significant contributor in an overall  $\text{NO}_x$  budget. Although many uncertainties still exist,  $\text{LNO}_x$  budget options estimated here were put into an improved perspective in a comparison with several available and relevant emission inventories. However, the evidence through the RS coupled with modelling of case studies strongly point out that substantial portion of  $\text{NO}_x$  from source region is lifted and diluted above the immediate zone of expected deposition. This might explain in part relatively low concentrations and deposition loads near the source region and no strong pollution gradient out from the pollution zone, as discussed in earlier chapters of this thesis.

#### **6.6.2 Comments**

Estimates of global  $\text{NO}_x$  production by lightning could be enhanced by an improved understanding of the mechanism of  $\text{NO}_x$  production by IC lightning. Of course, this is an ongoing work and improvements in tropospheric remote sensing can further enhance all aspects of  $\text{NO}_x$  research. More should be done to combine the new technologies into improved methodologies with fewer uncertainties, such as remote sensing of gaseous species. Development of methods to analyse and complement enhanced data, such as



vertical profile differentiation in non-steady state by dispersion modelling must be further explored ([Scorgie, personal communication, 2007](#)).





## CHAPTER SEVEN

*In this chapter, summaries are given of the main findings from each individual sub-study. The chapter presents an overall concluding statement addressing the central question of the thesis. The original research contributions of this thesis are highlighted. The final section gives recommendations for future research based on the findings of the study and identified gaps and data limitations.*

### 7. Conclusion

#### 7.1 Summary of Findings

- **Monitoring of concentrations and distribution of SO<sub>2</sub>, NO<sub>2</sub> and O<sub>3</sub>**

The concentrations and spatial distributions for two acidic species SO<sub>2</sub> and NO<sub>2</sub> were measured monthly over two annual cycles at 37 sites across the northern and eastern areas of South Africa. Low concentrations were recorded upwind and in areas remote from the Mpumalanga industrial Highveld. Increased concentrations were recorded in the centre and immediately downwind from Highveld source region. Inter-annual differences for SO<sub>2</sub> and NO<sub>2</sub> (and relationally of their acidifying compounds SO<sub>4</sub><sup>2-</sup>, NO<sub>3</sub><sup>-</sup> and NH<sub>4</sub><sup>+</sup>) were not substantial, although sulphur species showed larger inter-annual variations than nitrogen.

Seasonal trends for SO<sub>2</sub> were apparent, winter having the highest concentrations. Second highest concentrations occurred in spring or autumn, depending on site. For NO<sub>2</sub> the seasonal trends were less obvious. However, summer with late spring and early autumn had slightly elevated levels compared to the remainder of the year.

**Ozone** concentrations had a different space and time distribution patterns. Increased concentrations were recorded outside of the industrial pollution area towards the edges of the study area, both south and north, compared to the central area over the Mpumalanga Highveld. In terms of the inter-annual ozone comparison, the majority of sites did not fluctuate widely from year to year. In terms of seasonal comparisons, late winter and most of spring had elevated ozone concentrations, with summer lower and autumn the lowest concentrations.



- **Determining whether critical levels of SO<sub>2</sub>, NO<sub>2</sub> and O<sub>3</sub>, were exceeded**

Concentrations at upwind, downwind and remote sites were tested against the LRTAP vegetation critical levels for SO<sub>2</sub>, NO<sub>2</sub> and O<sub>3</sub>, in absence of nominal local standards and limits. The only sites at which monthly **critical levels for SO<sub>2</sub>** were exceeded were the centre of the Highveld, at the Elandsfontein site, for three critical SO<sub>2</sub> levels (for sensitive lichen, semi-natural and natural vegetation respectively); and just downwind, at Standerton and Amersfoort (for sensitive lichen only). At the intermediate and remote sites, concentrations were found to be substantially lower than any of the selected critical levels.

**NO<sub>2</sub> critical levels** were not exceeded, even in the industrial Highveld area. It is possible that the design of the network – focusing at sites with more distance from the sources and setting sites one degree apart – contributed to the low reading of the NO<sub>2</sub> in the source area. However, the conclusion that ground levels of NO<sub>2</sub> in the background areas measured by the network are below critical levels even near local industrial sources or roads-has been confirmed by this study. The ground level concentrations are low and unless measured near local industrial sources and or near major roads, are far below prescribed levels. The measurement of other gaseous acidifying nitrogen compounds (such as ammonia and nitric acid) could change the overall nitrogen acidifying potential, in which case all nitrogen species should be adjudged in terms of their synergistic and cumulative critical level.

**Ozone** annual mean concentrations did not exceed the annual thresholds. Ozone exceedance was found for monthly and seasonal exceedances of the 30 ppb concentration threshold at only a few sites, by small amounts. However, here is important to emphasise that monthly averages were used, which conceal possible peaks and thus do not give evidence that occasional exceedances may have occurred over shorter averaging periods. At only two sites for one month each were monthly concentrations above 40 ppb (43 and 41 ppb respectively). The disposition of the increased ozone concentrations is not sufficiently understood, and could not be related to the industrial pollution circulation and re-circulation directly.

Regional and local influences, including bio-, pyro- and anthropogenic contributions play a role. Slightly higher ozone concentrations occurred in the northern regions of South Africa (Limpopo Province). Nonetheless, critical concentration thresholds (related to vegetation) are not exceeded annually or seasonally and relatively increased values in parts of the study region might be typical characteristic of the entire subcontinent and pre-industrial conditions. Thus, the regional ecosystem/s might be well adapted to the prevailing





concentrations (Scholes and Scholes, 1998). In such a case, the remaining concerns would be any substantial increase of the anthropogenic precursor pollution, which might push the prevailing concentrations over the damage thresholds.

- **Computing dry and wet deposition of SO<sub>2</sub> and NO<sub>2</sub>**

The dry deposition computations were performed using an inferential model, with the measured deposition velocities of Mphopya (2002). Measured concentration results of two acidic gas species, SO<sub>2</sub> and NO<sub>2</sub> from the 37 sites were used, for two complete annual cycles. For the dry deposition of sulphur and nitrogen, winter had the lowest deposition rates, followed with autumn or spring. Deposition velocities were highest in summer, influenced strongly by the seasonal air turbulence and other meteorological factors.

The wet deposition of sulphur and nitrogen acidifying compounds (SO<sub>4</sub><sup>2-</sup>, NO<sub>3</sub><sup>-</sup> and NH<sub>4</sub><sup>+</sup>) was linearly related to seasonal precipitation and its resultant volumes. Thus, highest wet deposition rates were recorded mainly in summer, or in spring or autumn for other sites. For wet deposition, a prior long-term measured rainfall chemistry data set was used (Turner and de Beer, 1996). Their mean chemical concentrations in rainfall were combined with precipitation for the target years, to generate wet deposition rate estimates. This enabled a cumulative estimate of total dry and wet (non-organic) acidic deposition for the region to be given. The wet deposition depended strongly on the precipitation and this in turn influenced strongly the total deposition.

Sites with high concentrations and dry deposition in conjunction with relatively high precipitation showed the highest total acidic deposition, while sites with relatively low concentrations, proportionately low dry deposition and with very low precipitation had the lowest total acidic deposition. Nevertheless, the total deposition rates confirmed the general understanding that the background remote sites do not have acidic deposition problems, while the site immediately downwind of the industrial Highveld shows overall total acidic deposition to be as high as for the control site in the centre. Only one site with extreme precipitation and proportional increased wet deposition was the only exception to this conclusion. This site owes its high rate of deposition to an above average mean precipitation during one of the annual cycles.

- **Validation or comparison with regional dispersion modelling results**

A direct validation of the monitored results with modelled results could not be carried out, as available modelling studies dealt with different periods from the monitoring study.



Nevertheless, comparisons were performed with regional modelling carried out using emissions estimates and meteorology pertaining to prior years. Results of the meso-scale monitoring campaign (this work) were compared with two meso-scale to sub-continental modelling studies, for ozone and for SO<sub>2</sub> and NO<sub>2</sub> respectively (Zunckel *et al.*, 2006, Fourie, 2006).

For this task, three monitoring sites were selected for comparison with modelling results. These sites were strategically selected to be representative of the entire region. Site Elandsfontein in the centre of the industrial Highveld, site Amersfoort, downwind from the central pollution source region and site Louis Trichardt, a remote site. Sulphur, nitrogen and ozone comparisons were considered in turn.

In most cases, modelled SO<sub>2</sub> concentrations underestimated the measured values. The modelled S (SO<sub>2</sub> and SO<sub>4</sub><sup>2-</sup>) dry deposition rates were approximately equal to the calculated rates based on measured concentrations. The modelled S wet deposition rate (SO<sub>4</sub><sup>2-</sup>) comparison although varied from site to site overestimated the results based on the measured parameters for all compared sites and seasons. The wet deposition comparison gave a larger range of differences, but most of these disparities could be explained by variations in the precipitation.

NO<sub>2</sub> concentrations were generally overestimated. The NO<sub>2</sub> dry deposition rates overestimated the measurements for the central and close downwind site but underestimated for the remote site. Wet modelled deposition rates (NO<sub>3</sub><sup>-</sup>) overestimated the rates inferred from concentrations from this study (NO<sub>3</sub><sup>-</sup> only) for all compared sites in all compared seasons.

One very interesting finding is that the modelled seasonal trends are less well matched with the evident measured (and calculated on the basis of the measurements) seasonal trends for all three species (S, N and O<sub>3</sub>). It is possible that such differences are a reflection of differences in the meteorological information for the different modelling and measurement years. Ideally, further research would be valuable to establish more accurately reasons for atypical seasonal disparities.

The modelled and measured **ozone** concentrations were compared only for the South African growing seasons, October through April, as this was the only available regional-scale modelling data for ozone. Generally, CAPIA (van Tienhoven *et al.*, 2006, Zunckel *et*



*al.*, 2006,) ozone modelling overestimated the measurements results. However, the absolute and relative differences in ozone were of smaller amplitude in comparison with the differences established for sulphur and nitrogen. The agreement between the modelled and the measured ozone concentrations was closer at the northern background stations. Both modelling and measurements have traced areas of increased ozone concentrations for the northern region of South Africa.

However, modelling could not pick up occasional spikes and drops in values at individual (monitored) spots. Within the south and south-eastern region of the measurement field, several areas of increased concentrations were evident that were not predicted by the modelling findings. Several limiting factors constrain the reliability of the comparison between the modelled and measured ozone. These factors were considered to have increased uncertainties. Modelling took into account only ten daylight hours; the measurements were taken at 1.5 m above surface while the modelling resulted for a block 70 m deep; biogenic emissions in modelling were limited to three VOCs and modelling excluded pyrogenic emissions entirely. Thus future validation is recommended of the same periods with fewer uncertainties.

- **Determining critical deposition loads for SO<sub>2</sub> and NO<sub>2</sub> and their compounds**

Estimates were made of the critical loads for acidic deposition, by calculating soil buffering capacity and neutralising base cation deposition. Comparisons were made between high and low estimates of buffering capacity, with total deposition rates estimated from this work. High *critical loads exceedance* was determined in the western and central Highveld industrial region and adjacent area to the north and not, as anticipated, downwind towards the escarpment and the major forestry areas, bearing in mind all outstanding uncertainties. This was case for both options applied, with lower and higher soil sensitivity levels.

For these sites where exceedances occurred, the methodologies applied in this work indicate that exceeding pollution levels and loads could affect and continue to affect the local scale environment. Although the methodology applied can indicate areas where the terrestrial ecosystems may already be, or could become acidified in future, these results were based on a number of assumptions and thus could have contributed to overestimation/underestimation of acidic deposition and its effects. The coarse spatial resolution/precision of soil chemistry information and poor estimates of neutralising deposition (base cation concentrations in rain and dust-fall, which could either increase or



decrease net acidic loads) are identified as major limitations in locating and quantifying areas vulnerable to critical load exceedance. These uncertainties in the local soil buffering capacity mean that while it is possible that there is a potential acidification problem it is also possible that actual conditions could be less sensitive to acidification. The critical loads (and levels) represent two indicators for ecosystem at risk and can aid in pollution monitoring, emission controls and prevention and mitigation policies in and for the studied region. The locations most likely to be affected have been identified and can now be treated as priority areas for further monitoring and research.

- **Comparison and correlation of NO<sub>x</sub> generation by lightning within the study region**

LNO<sub>x</sub> production within the study region was updated using an improved set of lightning stroke measurements. The revised budget calculations confirm that LNO<sub>x</sub> is a major contributor to the natural NO<sub>x</sub> emissions and a significant contributor to the overall regional NO<sub>x</sub> budget. Depending on alternative high and low options, contributions of LNO<sub>x</sub> vary significantly. If the higher option is taken, LNO<sub>x</sub> amounts to one third of the anthropogenic NO<sub>x</sub> budgets. The anthropogenic (with pyrogenic) budgets were extracted from three relevant emission databases. However, despite this large fractional estimate, the strong seasonality of the LNO<sub>x</sub> production is not clearly recognisable in the measured NO<sub>2</sub> time plots. A possible explanation could be that a large portion of LNO<sub>x</sub> is generated and distributed above the mixing layer, therefore not contributing substantially to the ground level concentrations in regions of high lightning occurrences.

Although many uncertainties still exist, NO<sub>x</sub> budgets were put into another perspective when the results of the passive measurement campaign were recalculated into a budget of a predetermined volume, which was compared with NO<sub>x</sub> budget calculated based on the RS vertical column density measurements within the same volume. An interesting result, where VCD density budget over the entire troposphere calculation gave lower budget in comparison with the budget calculated from PS measurements for the boundary layer only. Although the estimates were conducted based on mean temporal values and did not take the conversion and transport processes into account the findings still leave open questions on advection, transport and strengths of NO<sub>x</sub>, essentially fate of bulk NO<sub>x</sub> generated mainly at the industrial Highveld. One plausible explanation was offered that NO<sub>x</sub> is horizontally spread after is lifted above the mixing boundary layer where the life of NO<sub>x</sub> is extended and allowing spread and transport above an enlarged area in comparison to its hotspot limit as measured on the ground.



- **Comparison and possible validation with spatial investigations of tropospheric trace gas species in boundary layer by remote sensing**

Concentrations of the three gas species in the boundary layer were extracted from various satellite retrievals and compared to measured ground level concentrations, assumed representative of a well-mixed boundary layer. The overall assessment of the  $\text{SO}_2$  comparison is that, besides general agreement in the order of magnitude of the concentrations and some agreement of enhanced concentrations over the industrial Highveld, large uncertainties in the  $\text{SO}_2$  RS extractions preclude quantitative comparisons at this stage, either in spatial or temporal patterns.

The  $\text{NO}_2$  measured and remotely sensed concentrations were found to be in exceptionally good agreement, spatially and temporally when compared for individual and all PS sites. They diverged slightly when spatial plots were compared, as the distributions were different. This could be explained as differing spatial distribution in different atmospheric layers, in which influence of vertical and horizontal atmospheric mixing is reflected in RS results as explained in the findings of the above objective.

The  $\text{O}_3$  comparison did not reveal any agreeable spatial and temporal pattern. Remote sensing values were mainly lower when compared to the passive sampling measured concentrations. The spatial distribution plots were not compared for ozone as the RS data gave similar readings in a wide zone, which covered all of the study area.

## **7.2 Conclusions**

In essence, this study dealt with a perennial problem, to which there has so far been no satisfactory answers in the Southern African context:

*Will the impacts of emitted pollutants and relationally accumulated deposition of acidic air pollutants (sulphur and nitrogen through their acidifying compounds) eventually exceed the carrying capacity of the natural environment? In addition, would the anthropogenic precursors substantially contribute to secondary pollutants, such as ozone, exceeding the levels of tolerance?*

The full thesis has been presented as a series of separate studies. The connection between these studies is an overarching theme of acidification by trace gas pollution. This theme leads to the overall assessment of atmospheric distribution and deposition of acidic species and ozone and evaluation of current and likely environmental impacts of emissions from



the industrial Highveld. The study has taken into account a quantitative, empirical set of measurements, extensive in space and time, to answer the acidification questions in a deterministic fashion.

The central task of this study was to establish a large-scale, medium-term operational air pollutant monitoring network over the northern and eastern portions of South Africa to measure concentration data of SO<sub>2</sub>, NO<sub>2</sub> and O<sub>3</sub> using passive monitors and thereby to provide direct, measured information with which to address the above question. This task was successfully carried out.

The regional study network produced a database of concentrations for each monitored gaseous species over two-annual cycles, which represents the major output of the study. Monitoring on this spatial and temporal extent has not been carried out previously in southern Africa. Based on this concentration database, an assessment of exceedance against critical levels was performed, and hence of the potential risks that acidic depositions pose to the regional ecosystems.

The concentration database enabled determination, by inferential computation, of dry deposition rates of acidic species and this task has been completed successfully. In addition, a wet deposition estimate was carried out to round up total dry and wet deposition rates. Combination of the concentration database, inferential dry deposition and estimated wet deposition rates of acid precursor gases and ozone was then used to compare with two regional-scale photochemical dispersion models as a further delivered output.

In relation to the atmospheric NO<sub>x</sub> budget, this work has used lightning detection records to estimate natural production of LNO<sub>x</sub>, which was found to be smaller by factors in the range 1:3 to 1:22 than anthropogenic NO<sub>x</sub> production, depending on assumptions. It also related the concentration databases to validation of emerging satellite remote sensing retrievals of tropospheric trace gases.

Together with the outputs presented and interpreted in the body of the text but bearing in mind the stated uncertainties – the study results point to the following overall conclusion: acidic pollution originating from the central industrial Highveld is not a current environmental threat to the environment in remote areas of South Africa, specifically the Mpumalanga Escarpment and forestry areas, and, by implication, neither is it a threat to adjacent countries.



However, zones within north-west Mpumalanga and south to south-east of the Witbank industrial area have indicated as areas exceeding critical loads of acidification, due also to local districts of sensitive soils. Although not extensive in spatial distribution, with one area only showing the highest exceedance level, these results indicate that areas in the vicinity of the central industrial zone that have susceptible soils are at risk of exceeding critical loads. Several smaller areas, which showed lesser exceedance and lesser spatial distribution of such exceedance, were located further down-wind. The findings have to be moderated in the light of identified uncertainties, arising either from this work or encountered, but outside the scope. These uncertainties need to be addressed in further research for their elimination and or reduction. These can be listed as follows:

- The cumulative impact of N deposition and its fate in sensitive ecosystems is not fully taken into account.
- Base cation deposition, particularly dry deposition was mostly estimated on the basis of a model and not measured for the studied region thus proportion of the mitigating factor in overall acidic deposition is proportionally uncertain.
- Ozone peaks were not assessed as the hourly data was not measured and critical impacts of ozone remain uncertain.
- Sensitivity of South African vegetation in respect to critical levels of trace gas species is not known and thus applying the European critical levels for vegetation leaves some uncertainty of their appropriateness.
- Troposphere mixing and export of pollutants is not researched sufficiently yet.

Future work should focus on the major uncertainties identified above and confirmation of areas that are particularly vulnerable to the impacts arising from S and N deposition.

### **7.3 Original Contributions and Significance**

This study was designed to measure concentrations of three important trace gas species, SO<sub>2</sub>, NO<sub>2</sub> and O<sub>3</sub> and to calculate their dry and wet deposition on a regional scale for an extensive (two-year) observation period. Monitoring of these gas species has not been carried out on this scale before in southern Africa. The database of near-surface concentrations generated by this study could be used for later analyses related to the entire observed region, for scientific and for air quality management and regulatory purposes.



Remotely sensed satellite-borne regional air quality retrievals were obtained, in the form of vertical column densities, and initial validations were performed by comparison with ground level concentrations from this study. Despite the uncertainties and inherent errors, there is significant benefit in comparing data from different sources on as broad a scale as has been attempted in this study. While there are serious issues with the error ranges and methodologies, this study represents the first substantive effort at combining long-term ground level monitoring and satellite measurements of pollutant trace gases into useful information for regional environmental protection.

The assessment of spatial concentrations and critical levels and loads of acidic gas species has not previously been attempted in South Africa on the scale of this study. Relatively recent modelling of acid precursor gases and ozone were compared with monitoring results from this study. The eco-sensitivity levels were evaluated.

This study has the potential to contribute to regional policies and environmental management planning in both the public and private domain. It may influence mitigation and control measures in the study region in the setting and design of new power generating plants. On the other hand, the relevance and validity of the methods employed for determining critical loads and levels and their applicability locally were scrutinised in a local context.

The remote (satellite-borne) sensing of gaseous pollutant species is a relatively new area of scientific activity. This activity includes appropriately validation of measurements and ongoing development of improved remote sensing technologies and validation measures. Presently, the bulk of efforts for the validation are oriented to validate vertical column densities. Current remote sensing retrievals are sensitive primarily in the mid and upper troposphere and the stratosphere. No similar efforts have been found published on validating the lowest layer of the Vertical Column Density, including mixing layer. This study attempted such a validation. Thus, this work constitutes a pioneering effort in this direction (at least for this study region). The comparison-cum-validation results are encouraging and found desirable by colleagues in remote sensing teams. Further investigations of such validations are supported by the specific teams that collaborated in the effort by providing the region-specific remote sensing data.





#### 7.4 Future Research

In terms of the future forecast, the answer to the central questions of the study depend on further growth of coal-fired energy generation plants and associated emissions, distributed by continental and regional synoptic airflows and influenced by climatic changes. Continued long-term ecological monitoring is recommended at a limited number of sites, (guided by the outcomes of this study) as part of the South African Environmental Observation Network (SAEON, 2008). Possibly the existing long-term monitoring sites of the IGAC/Debits/Africa passive monitoring network (IDAF, 2005) could be confirmed as appropriate and sufficient for this purpose.

More use of advanced technologies such as remote sensing of tropospheric constituents both air and space-borne are encouraged. Particularly more work is necessary on vertical profiling of trace gas concentrations, in support of satellite remote sensing observations, to allow increased precision of these measurements for the boundary layer. The use of regional-scale air dispersion modelling should undergo more validation and constant correlation of modelling should be performed with relevant remote sensing data.

For example, future research should be carried out to clarify a still unexplained distribution disparity between the remotely sensed  $\text{NO}_x$  plume and the ground-level measured concentrations distribution. The remotely sensed  $\text{NO}_x$  vertical column density strength and its spatial distribution is expected to reflect similar concentration distribution to ground based measurements; is highly concentrated over the industrial Highveld with an evident gradient just around and close downwind and this is not a case. The remotely sensed images provided by the remote sensing retrieval teams ubiquitously show enlarged distribution of surprising density. Thus, it is assumed that vertical column density possibly reflects also the columnar  $\text{NO}_x$  concentrations above the mixing layer undergoing different horizontal and vertical advection enabled due prolonged  $\text{NO}_x$  life out of the mixing layer. This disparity still represents an unresolved puzzle that needs further and concentrated scientific attention. Further airborne measurements could be useful in this regard.

An establishment of specific ecosystem-relevant critical limits determined in the local conditions on the local species of both flora and fauna and including water-living species, is recommended. These should be determined through both field and experimental research and should be undertaken in the short, medium and long-term. Future results of deposition



studies for the gaseous species studied should be analysed on a cumulative basis over corresponding periods, at a small number of key sites.

Flux experiments should be undertaken to determine the local air pollutant fluxes (and flux critical limits) in local conditions for the local environment. The current existing South African standards must be researched beyond the primary concern for human and commercial animal health – additional standards for regulating issues of air quality impacts on the wider environment should be added, to include natural ecosystems, commercial forests and agricultural crops.

Ideally, adverse effects on the most sensitive species in an ecosystem should define the levels of concern and guide the definition of critical levels. Sensitivity to these pollutants within local ecosystems needs to be measured so that appropriate levels can be set. The impact on the weakest species should be tested for the most sensitive critical levels because critical impacts on the weakest species constitute impacts on the biodiversity of the affected ecosystem. Possible loss of any species in an ecosystem makes the whole system vulnerable. Adaptation by systems to species losses show chain reactions where biodiversity is adversely affected in permanent ways. Therefore, all efforts towards controlling air pollution among the other environmental changes should strive towards reducing imbalances however small they appear.



## References

- ACCENT-TROPOSAT-2 (AT2), (2008), internet accessed May 2008, <http://troposat.iup.uni-heidelberg.de/index.html>.
- Al Ourabi H. and J. P. Lacaux (1999), Measurement of the Atmospheric Concentrations of NH<sub>3</sub>, NO<sub>2</sub>, HNO<sub>3</sub> in Tropical Africa by Use of Diffusive Samplers, International Global Atmospheric Chemistry (IGAC) Symposium, 13-19 September 1999, Bologna, Italy.
- Almer, B., W. Dickson, C. Ekström and E. Hörnström (1978), Sulphur pollution and the aquatic ecosystems, in J. O. Nriagu (ed.), *Sulphur in the Environment, Part II: Ecological Impacts*, Wiley, New York, pp. 271–311.
- Annegarn, H. J., A. P. S. Terblanche, J. S. Sithole, R. P. Rorich and C. R. Turner (1996a), Residential Air Pollution, in G. Held, B. J. Gore, A. D. SurrIDGE, G. R. Tosen, C. R. Turner and R. D. Walmsley (eds), *Air pollution and Its impacts on the South African Highveld*, Environmental Scientific Association, Cleveland, pp. 47-57.
- Annegarn, H. J., C. R. Turner, G. Helas, G. R. Tosen and R. P. Rorich (1996b), Gaseous Pollutants, in G. Held, B. J. Gore, A. D. SurrIDGE, G. R. Tosen, C. R. Turner and R. D. Walmsley (eds), *Air Pollution and Its Impacts on the South African Highveld*, Environmental Scientific Association, Cleveland, pp. 25-34.
- Annegarn, H. J., M. A., Kneen, S. J., Piketh, A. R., Horne, H. P. S., Hlapolosa and G. A. Kirkman (1993), Evidence for large-scale circulation of anthropogenic sulphur over southern Africa, in Proceedings of the 24<sup>th</sup> National Association for Clean Air Conference, Clean Air Challenges in a Changing South Africa, Brits, October 2003.
- Avila, A., I. Queralt., F. Gallart and J. Martin-Vide (1996), African dust over north-east Spain: mineralogy and source regions, in S. Guerzoni, R. Chester (eds), *The Impact of Desert Dust across the Mediterranean*, Kluwer, Amsterdam, pp. 201-205.
- Ayers, G. P., M. D. Keywood, R. Gillett, P. C. Manins, H. Malfroy and T. Bardsley (1998), Validation of passive diffusion samplers for SO<sub>2</sub> and NO<sub>2</sub>, *Atmospheric Environment*, 32, pp. 3587-3592.
- Bain, D. C. and S. J. Langan (1995a), Weathering rates in catchments calculated by different methods and their relationship to acidic inputs, *Water, Air and Soil Pollution*, 85, pp. 1051-1056.
- Bain, D. C., D. M. L. Duthie and C. M. Thomson (1995b), Rates and processes of mineral weathering in soils developed on Greywackes and Shales in the southern uplands of Scotland, *Water, Air and Soil Pollution*, 85, pp. 1069-1074.
- Bakwin, P S, S. C. Wofsy, S. Fan, M, Keller, S. E. Trumbore and J. M. da Costa (1990), Emission of nitric oxide (NO) from tropical forest soils and exchange of NO between the forest canopy and atmospheric boundary layers, *Journal of Geophysical Research*, 95, pp. 16755-15764
- Barrie, L. A. (1988), Scavenging ratios, wet deposition and in-cloud oxidation: An application to the oxides of sulphur and nitrogen, *Journal of Geophysical Research*, 90, pp. 5789-5799.



- Beirle, S. (2004), Estimating source strengths and lifetime of Nitrogen Oxides from satellite data, Doctor of Science thesis, the Ruperto-Carola University of Heidelberg, Germany
- Beirle, S., N. Spichtinger, A. Stohl, K. L. Cummins, T. Turner, D. Boccippio, O. R. Cooper, M. Wenig, M. Grzegorski, U. Platt, T. Wagner (2005), Estimating the  $\text{NO}_x$  produced by lightning from GOME and NLDN data: a case study in the Gulf of Mexico, *Atmospheric Chemistry and Physics Discussion*, 5, pp. 11295-11329.
- Beirle, S., U. Platt, M. Wenig and T. Wagner (2004),  $\text{NO}_x$  production by lightning estimated with GOME, *Advances in Space Research*, 34, pp. 793-797.
- Bernhard, U. (1983), An Ecosystem oriented hypothesis on the effect of air pollution in forest ecosystems, in *Ecological Effects of Acidic Deposition*, Report PM 1636, National Swedish Environment Protection Board, Solna, Sweden.
- Bhika, B. (2008), The Influence of Terrain Elevation on Lightning Density in South Africa, MSc dissertation, University of Johannesburg, Johannesburg. South Africa.
- Biazar, A. P. and R. T. McNider (1995), Regional estimates of lightning production of nitrogen oxides, *Journal of Geophysical Research*, 101(D11), pp. 22861-22874.
- BIBLE-99 (1999), Biomass Burning and Lightning Experiment 1999, June 2005, <http://www.igac.unh.edu/newsletter/igac20/bible.html>.
- Bishop, K. A. and H. Hultberg (1995), Reversing Acidification in a forest ecosystem: the Gardsjön covered catchment, *Ambio*, 24, pp. 85-91.
- Blair, S. A. (1998), Monitoring Ground level Ozone and Nitrogen Dioxide in Parts of Kwa-Zulu Natal and Mpumalanga (South Africa) by Means of Chemical and Biological Techniques, MSc dissertation, University of Natal, Durban, South Africa.
- Bluff E., C. R. Turner and G. H. De Beer (1991), Rain Chemistry: 1985 to 1990, Eskom Report, TRR/S90/033.
- Boccippio, D. J., K. L. Cummins, H. J. Christian and S. J. Goodman (2000), Combined satellite- and surface-based estimation of the intracloud–cloud-to-ground lightning ratio over the continental United States, *Monthly Weather Review*, 129, pp. 108-122.
- Boersma, K. F., Eskes, H. J., Meijer, E. W. and Kelder, H. M. (2005), Estimates of lightning  $\text{NO}_x$  production from GOME satellite observations, *Atmospheric Chemistry and Physics*, 5, pp. 2311-2331.
- Boersma, K. F., H. J. Eskes and E. J. Brinksma (2004), Error analysis for tropospheric  $\text{NO}_2$  retrieval from space, *Journal of Geophysical Research*, 109, D04311, doi: 10.1029/2003JD003962.
- Bond, D.W., S. Steiger, R. Zhang, X. Tie and R.E. Orville (2002), The importance of  $\text{NO}_x$  production by lightning in the tropics, *Atmospheric Environment*, 36, pp. 1509-1519.
- Borell, P., P. M. Borell, J. P. Burrows and U. Platt (2004), TROPOSAT–Sounding the troposphere from space: a new era for atmospheric chemistry, EUROTRAC-2 Subproject Final Report, ISBN 3-8236-1390-1, Springer-Verlag, Heidelberg, Germany.
- Botha, A. T., L. D. Moore and J. H. Visser (1990), Gladiolus and bean plants as bio-monitors of air pollution impacts in the Cape Town area, the 1<sup>st</sup> IUAPPA Regional Conference on Air Pollution: Towards the 21<sup>st</sup> Century, Pretoria, 24-26 October 1990, South Africa.



- Carlson, C. A. (1994), An Assessment of the Risk Posed by the Gaseous Pollutant Ozone to Commercial Forests in the Eastern Transvaal, Report to the Department of Water Affairs and Forestry, Report FOR-DEA 754, CSIR, Pretoria, South Africa.
- Chameides, W. L., R. R. Stedman, D. W. Dickerson, R. J. Cicerone (1977), NO<sub>x</sub> production in lightning, *Journal of Atmospheric Science*, 34, pp. 143-149.
- Chartres, C. J., C. J. Smith, W. S. McDonald and A. D. Noble (1996), Potential Effects of Acid Deposition on Australian Soils, paper in background documents for a workshop held in Bangkok in 1996 on Validation of Sensitivity Maps to Acidic Deposition, SEI, York, UK.
- Christian, H. J. (2003), Global lightning activity, Proceedings of the 12<sup>th</sup> International Conference on Atmospheric Electricity (ICAE), June 9-13 2003, Versailles, France.
- Christian, H. J., R. J. Blakeslee, D. J. Boccippio, W. L. Boeck, D. E. Buechler, K. T. Driscoll, S. J. Goodman, J. M. Hall, W. J. Koshak, D. M. Mach and M. F. Stewart (2003), Global frequency and distribution of lightning as observed from space by the Optical Transient Detector, *Journal of Geophysical Research*, 108(D1), pp. 1-15, doi: 10.1029/2002JD002347.
- Cooray, V. (1997), Energy dissipation in lightning flashes, *Journal of Geophysical Research*, 102, pp. 21401-21410.
- Cooray, V. and M. Rahman, (2005), Efficiencies for production of NO<sub>x</sub> and O<sub>3</sub> by streamer discharges in air at atmospheric pressure, *Journal of Electrostatics*, 63, 977-983.
- Cowling, E. B. (1982), Acid precipitation in historical perspective, *Environmental Science and Technology*, 16, pp. 110A-122A.
- Cruz, L. P. S, V. P. Campos, A. M.C. Silva and T. M. Tavares (2004), A Field Evaluation Of a SO<sub>2</sub> Passive Sampler in Tropical Industrial And Urban Air, *Atmospheric Environment*, 38, 37, pp. 6425-6429, doi:10.1016/j.atmosenv.2004.07.022
- Davidson, E. A. and W. Kinglerlee (1997), A global inventory of nitric oxide emissions from soils, *Nutrient Cycling in Agroecosystems*, 48, pp. 37-50.
- De Clercq, C., P. Gerard, J. Granville, J-C. Lambert (2006), Geophysical consistency of ENVISAT ozone profiles data with global atmosphere watch pole-to-pole network measurements, Proceedings of the 3<sup>rd</sup> Workshop on the Atmospheric Chemistry Validation of Envisat (ACVE-3) 4-7 December 2006, ESRIN, Frascati, Italy.
- DEAT (2006), Department of Environmental Affairs and Tourism, internet accessed February 2006, <http://www.environment.gov.za/>.
- Dhammapala, R. S. (1996), Use of Diffusive Samplers for the Sampling of Atmospheric Pollutants, MSc dissertation, The Potchefstroom University for Christian Higher Education, Potchefstroom, South Africa.
- Dodds, H. A. and M. V. Fey (1998), Evaluation of some systems for classifying soil sensitivity to acid deposition in the South African Highveld, *Soil Use and Management*, 14, pp. 94-199.
- Dowden, R. L., J. B. Brundell and C. J. Rodger (2002), VLF lightning location by time of group arrival (TOGA) at multiple sites, *Journal of Atmospheric and Solar-Terrestrial Physics*, 64, pp. 817-830.
- Downing, R. J., J.-P. Hettelingh and P. A. M. de Smet (eds) (1993), Calculation and Mapping of Critical Loads in Europe: Status Report 1993, RIVM, Wageningen, The Netherlands.



- EDGAR (2008), EDGAR 32FT2000 Emissions Inventory, internet accessed June 2008, <http://www.mnp.nl/edgar/model/v32ft2000edgar/edgarv32ft-prec/edgv32ft-nox.jsp>.
- Eldar, F. C. and T. Brydges (1983), Effects of Acid Precipitation on Aquatic Regimes of Canada, The Canadian contribution to the Committee on the Challenges of Modern Society, NATO Panel 3 Report.
- Emberson, L. D., M. R. Ashmore, F. Murray (eds) (2003), *Air Pollution Impacts on Crops and Forests: a Global Assessment*, Imperial College Press, London, UK.
- Emberson, L. D., M. R. Ashmore, F. Murray, F., J. C. I. Kuylenstierna, K. E Percy, T. Izuta, Y. Zheng, H. Shimizu, B. H. Sheu, C. P. Liu, M. Agrawal, A. Wahid, N.M. Abdel-Latif, M. A. van Tienhoven, L. I. de Bauer, M. Domingos, (2001), Impacts of air pollutants on vegetation in developing countries, *Water, Air and Soil Pollution*, 130, pp. 107-118.
- Engelbrecht, E. (1987), Effects of Sulphur Dioxide on Bean Cultivar under Greenhouse Conditions, Eskom Report TRR/N870/013, Cleveland, pp. 68, Johannesburg, South Africa.
- ENVIRON, (2003), User's Guide to the Comprehensive Air Quality Model with Extensions (CAMx), ENVIRON International Corporation, 101 Rowland Way, Novato, CA 94945, internet accessed June 2006, <http://www.camx.com>.
- Environment Canada (1987), The potential of soils and bedrock to reduce the acidity of atmospheric deposition in Canada, in *Acid Rain: A National Sensitivity Assessment*, The Inland Waters and Lands Directorate, Environment Ottawa, Ontario, Canada.
- Erisman, J. W. and G. P. J. Draaijers (1995), *Atmospheric deposition in relation to acidification and eutrophication*, Elsevier, Amsterdam, The Netherlands, 405 pp.
- EULINOX-98 (1998), The European Lightning Nitrogen Oxides Project – 1998, internet accessed August 2005, <http://www.pa.op.dlr.de/>.
- FAO (1995), *FAO Digital Soil Map of the World*, Food and Agriculture Organization, Rome, Italy.
- FAO-UNESCO (1977), *Soil Map of the World*, Volumes VI and VIII, VII, UNESCO, Paris, France.
- Farquhar, G. D., S. von Caemmerer and J. A. Berry (1980), A biochemical model of photosynthetic CO<sub>2</sub> assimilation in leaves of C<sub>3</sub> species, *Planta*, 149, pp. 78-90.
- Fehr, T., H. Höller, H. Huntrieser, (2004), Model Study on Production and Transport of Lightning-Produced NO<sub>x</sub> in an EULINOX Supercell Storm, *Journal of Geophysical Research*, 109, S. D09102 -, DOI 10.1029/2003JD003935.
- Ferm M. (1991), A Sensitive Diffusional Sampler, IVL publication B-1020, Swedish Environmental Research Institute, Göteborg, Sweden.
- Ferm M. and H. Rodhe (1997), Measurements of Air Concentrations of SO<sub>2</sub>, NO<sub>2</sub> and NH<sub>3</sub> at Rural and Remote Sites in Asia, *Journal of Atmospheric Chemistry*, 27, pp. 17-29.
- Ferm, M., A. Lindskog, P.-A. Svanberg and C.-A. Boström, (1994), New measurement technique for air pollutants (in Swedish), *Kemisk Tidskrift*, 1, pp. 30-32.
- Finke, U., T. Hauf (1996), The characteristics of lightning occurrence in southern Germany, *Beitrage Zur Physik der Atmosphere*, 69, pp. 361-374.



- Fleming G., M. van der Merwe (2004), Spatial Disaggregation of Greenhouse Gas Emission Inventory Data for Africa South of the Equator, internet accessed, June 2008, <http://gis.esri.com/library/userconf/proc00/professional/papers/PAP896/p896.htm>.
- Fourie, D. G. (2006), Modelling the Long-range Transport and Transformation of Air Pollutants over the Southern African Region, PhD thesis, North-West University, Potchefstroom, South Africa.
- Freiman, M. T. and P. D. Tyson (2000), The thermodynamic structure of the atmosphere over South Africa: Implications for water vapour transport, *Water SA*, 26(2), pp. 153-158.
- Freiman, M. T. and Piketh S. J. (2003), Air Transport into and out of the Industrial Highveld Region of South Africa, *Journal of Applied Meteorology*, 42, pp. 994-1002.
- Galloway, J. N. (1995), Acid deposition: perspectives in time and space. *Water, Air and Soil Pollution*, 85, pp. 15-24.
- Galloway, J. N. M. Bekunda, Z. Cai, J. W. Erisman, J. Freney, R. W. Howarth, L. A. Martinelli, M. C. Scholes and S. P. Seitzinger (2004), A Preliminary assessment of “Changes in the Global Nitrogen Cycle as a Result of Anthropogenic Influences”, Proceedings of the 3<sup>rd</sup> International Nitrogen Conference, October 12-16, 2004 Nanjing, China.
- Galpin, J. S. and C. R. Turner (1999), Trends in rain quality data from the South African interior, *South African Journal Science*, 95, pp. 223-225.
- Garland, J. A. (1978), Dry and wet removal of sulphur from atmosphere, *Atmospheric Environment*, 12, pp. 349-362.
- Garstang, M. and P. D. Tyson (1997), Atmospheric circulation, vertical structure and transport over Southern Africa during the SAFARI-92 campaign, in B. W van Wilgen *et al.* (eds), *FIRE in Southern Savannas: Ecological and Atmospheric Perspectives*, Wits University Press, Johannesburg, South Africa, pp. 57-88.
- Georgii, H-W (1982), Review Of The Chemical Composition of Precipitation as Measured by the WMO BAPMoN, Environmental Pollution Monitoring and Research Programme Report, 8, 40 pp., World Meteorological Organization, Geneva, Switzerland.
- Gomes, L. and D.A. Gillette (1993), A comparison of characteristics of aerosol from dust storms in central Asia with soil-derived dust from other regions, *Atmospheric Environment*, 27A, pp. 2539-2544.
- Hall, J. R., S. M. Wright, T. H. Sparks, J. Ulyett, T. E. H. Allot and M. Hornung (1995), Predicting freshwater critical loads from national data on geology, soils and land use, *Water, Air and Soil Pollution*, 85, pp. 2443-2448.
- Helas, G. and J. J. Pienaar (1996), The influence of vegetation fires on the chemical composition of the atmosphere, *South African Journal of Science*, 92, pp. 132-136.
- Held, G., H. Scheifinger and G. Snyman (1994), Recirculation of pollutants in the atmosphere of the South African Highveld, *South African Journal of Science*, 90, pp. 91-97.
- Held, G., H. Scheifinger, G. Snyman, G. Tosen and M. Zunckel (1996), The climatology and meteorology of the Highveld, in G. Held, B. J. Gore, A. D. Surridge, G. R. Tosen, C. R. Turner and R. D. Walmsley (eds), *Air pollution and its impacts on the South African Highveld*, Environmental Scientific Association, Cleveland, South Africa, pp. 60-71.



- Henriksen, A. (1980), Acidification of freshwaters – a large scale titration, Proceedings of International Conference on Ecological Impact of Acid Precipitation, Norway, SNSF Project, pp. 68-74.
- Hettelingh, J.-P., H. Sverdrup and D. Zhao (1995), Deriving critical loads for Asia, *Water, Air and Soil Pollution*, 85, pp. 2565-2570.
- Heue, K.-P., S. Beirle, M. Bruns, J.P. Burrows, U. Platt, I. Pundt, A. Richter, T. Wagner and P. Wang (2004), SCIAMACHY validation using the AMAXDOAS instrument, Proceedings of the ENVISAT & ERS Symposium, 6-10 September 2004, ESA Publication SP-572, Salzburg, Austria.
- Hicks, B. B., D. D. Baldochi, T. P. Meyers, R. P. Hosker and D. R. Matt (1987), A preliminary multiple resistance routine for deriving dry deposition velocity from measured quantities, *Water, Air and Soil Pollution*, 36, pp. 311-330.
- Hicks, B. B., R. McMillen, R. S. Turner, G. R. Holdren Jr and T. C. Strickland (1993), A national critical loads framework for atmospheric deposition effects assessment: III deposition characterization, *Environmental Management*, 17, pp. 343-353.
- Hicks, B. B., R. P. Hosker, T. P. Meyers and J. D. Womack (1991), Dry deposition inferential measurement technique – I: Design and test of a prototype meteorological and chemical system for determining dry deposition, *Atmospheric Environment*, 10(25A), pp. 2361-2370.
- Hinrichsen, D. (1988), Acid rain and forest decline, in E. Goldsmith, and N. Hylyard (eds), *The Earth Report: The Essential Guide to Global Ecological Issues*, Price Stern Sloan, Los Angeles, USA.
- Holler, H., U. Finke, M. Hagen and H. Huntrieser (1998), Thunderstorm observations during LINOX-combined radar, satellite, lightning and in-situ measurements, European Commission, COST-75 Advance weather radar systems, International Seminar, March 23-27, 1998, Locarno, Switzerland.
- Hörnström, E., C. Eckström and O. Duraini (1984), Effects of pH and different levels of aluminium on lake plankton in the Swedish west coast area, Report No 61, National Swedish Board of Fisheries, Institute of Fresh Water Research Drottingholm, Lund, Sweden, pp. 115-127.
- Hornung, M. and R. A. Skeffington (eds) (1992), Critical Loads: Concepts and Applications, ITE Symposium No. 28, HMSO, London, UK.
- Huntrieser, H., Ch. Feigl, H. Schlaber, F. Schroder, Ch. Gerbig, P. van Velthoven, F. Flatoy, C. Thery, H. Holler and U. Schumann (2000), Contribution of lightning-produced NO<sub>x</sub> to the European and global NO<sub>x</sub> budget: Results and estimates from airborne EULINOX measurements, EULINOX 1998-1999, Final Report, DLR, Oberpfaffenhofen, Germany.
- IDAF (2005), IGAC Debits Africa, internet accessed March 2005, <http://medias.obs-mip.fr/idaf>.
- IPCC Third Assessment on Climate Change (2001), The Scientific Basis, Intergovernmental Panel of Climate Change, Houghton, J.T., Y. Ding, D.J. Griggs, M. Noguer, P.J. van der Linden, X. Dai, K. Maskell, and C.A. Johnson (eds.), Cambridge University Press, Cambridge, U.K., 881 pp.
- Isaksen, I. S. A. and O. Hov (1987), Calculations of trends in tropospheric concentrations of O<sub>3</sub>, OH, CO, CH<sub>4</sub> and NO<sub>x</sub>, *Tellus*, 39, pp. 271-285.





- ISRIC (1995), World Inventory of Soil Emission Potentials, International Soil Reference and Information Centre, Wageningen, The Netherlands.
- ISRIC (2003), internet accessed June 2008, <http://www.isric.org/NR/exeres/BC5BB444-DB94-4FE3-B102-2872B0B1A9F1.htm>.
- IUP, University of Bremen (2008), Institute of Environmental Physics, internet accessed June 2008, [http://www.iup.uni-bremen.de/doas/so2\\_from\\_scia.htm](http://www.iup.uni-bremen.de/doas/so2_from_scia.htm).
- IUP, University of Heidelberg (2005), Institute of Environmental Physics, internet accessed March 2005, <http://satellite.iup.uni-heidelberg.de/index.php/DOAS/doas/0/>.
- Jaegle, L., D. J. Jacob, Y. Wang, A. J. Weinheimer, B. A. Ridley, T. L. Campos, G.W. Sachse and D. Hagen (1998), Sources and chemistry of NO<sub>x</sub> in the upper troposphere over the United States, *Geophysical Research Letters*, 25, pp. 1709-1712.
- Johansson, C., (1987), Pine forests: a negligible sink for atmospheric NO<sub>x</sub> in rural Sweden, *Tellus*, 39B, pp. 426-438.
- Jordan, C. F. (1985), *Nutrient Cycling in Tropical Forest Ecosystems*, John Wiley, Chichester, UK.
- Kanyanga, J. K. (2008), Atmosphere-Biosphere Interactions: El Niño Southern Oscillation (ENSO) and Atmospheric Transport over Southern Africa, PhD thesis, University of Johannesburg, Johannesburg.
- Khokhar, M. F., S. Beirle, C. Frankenberg, C. Friedeburg, J. Holwedel, S. Kraus, S. Kuel, S. Shangavi, U. Platt, W. Wilms-Grabe, T. Wagner (2003), GOME Observations of Atmospheric SO<sub>2</sub>, *Geophysical Research Abstracts*, 5, (Abstract #07383).
- Kowalczyk, M. and E. Bauer (1982), Lightning as a source of NO<sub>x</sub> in the troposphere, Technical Report FAA-EE-82-4, Institute for Defence Analysis, Alexandria, VA, USA, 76 pp.
- Kuylenskierna, J. and K. Hicks (2002), Air Pollution in Asia and Africa: The approach of the RAPIDC Programme, Proceedings of the 1st Open Seminar on the Regional Air Pollution in Developing Countries, Stockholm, Sweden, June 4, 2002, internet accessed February 2006, <http://www.rapidc.org>
- Kuylenskierna, J. C. I. and M. J. Chadwick (1989), in J. Kämäri, D. F. Brakke, A. Jenkins, S. A. Norton and R. F. Wright (eds), *The Relative Sensitivity of Ecosystems in Europe to the Indirect Effects of Acidic Depositions in Regional Acidification Models*, Springer-Verlag, Berlin, Germany, pp. 3-22.
- Kuylenskierna, J. C. I., H. Cambridge, S. Cinderby and M.J. Chadwick (1995), Terrestrial ecosystem sensitivity to acidic deposition in developing countries, *Water, Air and Soil Pollution*, 85, pp. 2319-2324.
- Kuylenskierna, J. C. I., H. Rodhe, S. Cinderby, K. Hicks (2001a), Acidification in developing countries: ecosystem sensitivity and the critical load approach on a global scale, *Ambio*, 30, pp. 20-28.
- Kuylenskierna, J. C. I., H. Rodhe, S. Cinderby, K. Hicks (2001b), Global Assessment of Terrestrial Ecosystem Sensitivity to Acidic Deposition, internet accessed June 2008, <http://www.sei.se/dload/seiy/globalassess.pdf>.



- Lacaux, J. P. (1999), DEBITS Activity in Africa: Atmospheric Deposition in Northern Hemisphere of Tropical Africa, International Global Atmospheric Chemistry (IGAC) Symposium, 13-19 September 1999, Bologna, Italy.
- Lamarque, J. F., G. P. Brasseur, P. G. Hess and J. F. Muller (1996), Three-dimensional study of the relative contributions of the different nitrogen sources in the troposphere, *Journal of Geophysical Research*, 101(D17), pp. 22955-22968.
- Langan, S. J., H. U. Sverdrup and M. Coull (1995a), The calculation of base cation release from the chemical weathering of Scottish soils using the PROFILE model, *Water, Air and Soil Pollution*, 85, pp. 2497-2502.
- Langan, S. J., M. E. Hodson, D. C. Bain, R. A. Skeffington and M. J. Wilson (1995b), A preliminary review of weathering rates in relation to their method of calculation for acid sensitive soil parent materials, *Water, Air and Soil Pollution*, 85, pp. 1075-1081.
- Langner, J., P. Rodhe, P. Crutzen and P. Zimmerman (1992), Anthropogenic influence on the distribution of tropospheric sulphate aerosol, *Nature*, 359, pp. 712-715.
- Lawrence, M. G., W. L. Chameides, P. S. Kasibhatia, H. Levy, I. I. Moxim, W. Moxim (1995), Lightning and atmospheric chemistry: the rate of atmospheric NO production, In: Hans Volland (ed.), *Handbook of Atmospheric Electrodynamics*, 1, pp. 189-202, CRC Press Inc., Boca Raton, Florida, USA.
- Lee, D. S., I. Kohler, E. Grobler, F. Rohler, R. Sausen, L. Gallardo-Klenner, J. G. J. Oliver, F. J. Dentener, A. F. Bouwman (1997), Estimations of global NO<sub>x</sub> emissions and their uncertainties, *Atmospheric Environment*, 31, pp. 1735-1749.
- Lelieveld, J. and F. J. Dentener (2000), What controls tropospheric ozone? *Journal of Geophysical Research*, 105(D3), pp. 3531-3551.
- Lerdau, M. T., J. W. Munger and D. J. Jacob (2000), The NO<sub>2</sub> flux conundrum, *Science*, 289, pp. 2291-2293.
- Leue, C., M. Wenig, T. Wagner, O. Klimm, U. Platt and B. Jahne (2001), Quantitative analysis of NO<sub>x</sub> emissions from Global Ozone Monitoring Experiment satellite image sequences, *Journal of Geophysical Research*, 106, pp. 5493-5505.
- Levelt, P. F., R. van der A. and P. K. Bhartia, (2000), Science Requirements Document for OMI-EOS, ISBN 90-369-2187-2, KNMI publication 193, internet accessed April 2005, <http://www.knmi.nl/omi/documents/science/SRD-Version-2-version-2-of-7-December-2000.pdf>
- Levine J. S., E. L. Winstaed and D. I. Sebacher (1996), Biogenic soil emissions of nitric oxide (NO) and nitrous oxide (N<sub>2</sub>O) from savannas in South Africa, the impact of wetting and burning, *Journal of Geophysical Research*, 101, pp. 23689-23698.
- Levitt, J. (1980), Miscellaneous stresses, in J. Levitt (ed.) *Responses of plants to Environmental Stresses. Volume II: Water, Radiation, Salt and other Stresses*, Academic, New York, USA, Chapter 11, p. 607.
- Levy, H., W. Moxim, A. A. Klonecki and P. S. Kasibhatha (1996), Simulated tropospheric NO<sub>x</sub>: Its evaluation, global distribution and individual source contributions, *Journal of Geophysical Research*, 104(D21), pp. 26279-26306.



- Liaw, Y. P., D. R. Cook, D. L. Sisterson and N. L. Miller (1999), Direct field measurements of NO<sub>x</sub> production by lightning, Fall Meeting of the American Geophysical Union, San Francisco, USA, EOS 80, F195.
- LINOX-96 (1996), Thunderstorm observations during LINOX Combined radar, satellite, lightning and in situ measurements, internet accessed July 2005, <http://www.pa.op.dlr.de/eulinox/publications/cost-75/cost-75/html>.
- Linzon, S. N. (1986), Activities and results of the terrestrial effects program: Acid Precipitation in Ontario Study, *Water, Air, Soil Pollution Journal*, 31, pp. 295-305.
- Logan, A. F. (1983), Nitrogen oxides in the troposphere global and regional budgets. *Journal of Geophysical Research*, 88(C15), pp. 10785-10807.
- Lowman, G. R. P. (2003), Deposition of Nitrogen to Grassland versus Forested Areas in the Vicinity of Sabie, Mpumalanga, South Africa, MSc dissertation, University of the Witwatersrand, Johannesburg, South Africa.
- Lucas, A. E. and D. W. Cowell, (1984), Regional assessment of sensitivity to acidic deposition for eastern Canada, in O. P. Bricker (ed.), *Geological Aspects of Acid Deposition*, Butterworth, Canada.
- Lydén, A. and O. Gratin (1985), Phytoplankton species composition, biomass and production in Lake Gardsjön – an acidified Clearwater lake in SW Sweden, *Ecological Bulletins*, 37, pp. 195-202.
- Mackerras, D., M. Darveniza, R. E. Orville, E. R. Williams and S. J. Goodman (1998), Global lightning: Total, cloud and ground flash estimates, *Journal of Geophysical Research*, 103, pp. 19791-19809.
- Manual on Methodologies and Criteria for Modelling and Mapping Critical Loads & Levels and Air Pollution Effects, Risks and Trends (2004), UNECE Convention on Long-Range Transboundary Air Pollution, internet accessed September 2005, <http://www.icpmapping.org>.
- Marshall, F. M., M. R. Ashmore, J. N. B. Bell and E. Milne (1998), Air pollution impacts on crop yield in developing countries – a serious but poorly recognized problem?, in Proceedings of the 11<sup>th</sup> World Clean Air and Environment Congress, 13-18 September, 1998, Durban, South Africa, 5, 13E-2.
- Martin, R. V., D. J. Jacob, J. A. Logan, J. M. Ziemke and R. Washington (2000), Detection of a lightning influence on tropical tropospheric ozone. *Geophysical Research Letters*, 27, pp. 1639-1642.
- McCormick, J. (1997), *Acid Earth – The politics of Acid pollution, 3rd Edition*, Earthscan, London, UK.
- McDowell, W. H. (1988), Potential effects of acid deposition on tropical terrestrial ecosystems, in H. Rodhe and R. Herrera (eds), *Acidification in Tropical Countries*, John Wiley, New York, USA, Scope, 36, pp. 117-140.
- McFee, W. W. (1980), Sensitivity of Soil Regions to Acid Precipitation, EPA/600/02, Environmental Research Laboratory, US Environmental Protection Agency, Corvallis, USA.



- Miller, J. M. ((1992), Review of the Global precipitation Chemistry programme of BAPMoN, WHO GAW Report 83, 35 pp., World Meteorological Organization, Geneva, Switzerland.
- Miller, T. and D. Perkey (2000), *The Global Hydrology and Climate Centre (GHCC) Forecast*, 6, NASA, Huntsville, Alabama, USA.
- Morling, G. and B. Pejler (1990), Acidification and zooplankton development in some West-Swedish lakes, 1966–1983, *Limnologica*, 20, pp. 307-318.
- Mphepya, N. J. (2002), Atmospheric Deposition Characteristics of Sulphur and Nitrogen Compounds in South Africa, PhD thesis, The Potchefstroom University for Christian Higher Education, Potchefstroom, South Africa.
- Mphepya, N. J. , J. J. Pienaar, C. Galy-Lacaux, G. Held and C. R. Turner (2004), Precipitation Chemistry in Semi-Arid Areas of Southern Africa: A Case Study of a Rural and an Industrial Site, *Journal of Atmospheric Chemistry*, 47, pp. 1573-0662.
- NASA-GSFC (2008), Tropospheric Ozone Data from Aura OMI/MLS, internet accessed June 2008, [http://acdb-ext.gsfc.nasa.gov/Data\\_services/cloud\\_slice/new\\_data.html](http://acdb-ext.gsfc.nasa.gov/Data_services/cloud_slice/new_data.html)
- Ndlovu, N. and C. R. Evert (2004), Statistical analysis of data from an aged LPATS network, 18<sup>th</sup> International Lightning Detection Conference, 7–9 June 2004, Helsinki, Finland.
- NEMA (National Environmental Management Act), No. 107, (1998), Government Gazette No. 19519, Cape Town, 27 November 1998.
- NEMA QA (2004), National Environmental Management: Air Quality Act, No. 39, 2004, Government Gazette 476, Cape Town, 24 February 2005.
- Nihlgard, B. (1985), The ammonium hypothesis – an additional explanation to the forest dieback in Europe, *Ambio*, 14, pp. 2-8.
- Nilsson, J. (ed.) (1986), Critical Loads for Nitrogen and Sulphur - report from a Nordic working group, Report 1986:11, The Nordic Council of Ministers, Copenhagen, Denmark.
- Nilsson, J. and P. Grennfelt (eds) (1988), Critical Loads for Sulphur and Nitrogen in the Environment, Report 1988:15, Nordic Council of Ministers, Copenhagen, Denmark.
- Oden, S. (1968), The Acidification of Air and Precipitation and its Consequences in the Natural Environment, Ecology Committee Bulletin No. 1, Swedish National Science Research Council, Stockholm, Sweden.
- Ojelede, M. E. (2004), NO<sub>x</sub> production by lightning over southern Africa, MSc dissertation, University of the Witwatersrand, Johannesburg, South Africa.
- Ojelede, M. E., H. J. Annegarn, C. Price, M. A. Kneen and P. Goyns (2008), Lightning produced NO<sub>x</sub> budget over the Highveld region of South Africa, *Atmospheric Environment*, 42, pp. 5706-5714, doi:10.1016/j.atmosenv.2007.12.072
- Olbrich, K. A. (1990), The Geographic Distribution of Possible Air Pollution Induced Symptoms in the Needles of *Pinus patula*, CSIR Report FOR-1, Pretoria, South Africa, 39 pp.
- Olbrich, K. A. (1993), Patterns of Shoot Growth, Needle Growth and Foliar Symptom Development in Fertilised and Unfertilised *P. patula*, Report to the Department of Water Affairs and Forestry, Report No. 665, Pretoria, South Africa.



- Olbrich, K. A., R. Skoroszewski, J. Taljaard, M. Zunckel (1994), An acid deposition risk advisory system: a test study of Region F to define actual and critical loads, CSIR Internal Report FOR-I 497, CSIR, Pretoria, South Africa.
- Omernik, J. M. (1982), Total Alkalinity of Surface Waters, 1:7,500,000. Corvallis Environmental Research Laboratory, US EPA, Oregon State University, Oregon, USA.
- Panitz, H-J. and K. Nester (2002), Evaluation of modelled urban NO<sub>x</sub> and CO emissions for the city of Augsburg based on mass budget simulations with the KAMM/DRAIS model, internet accessed April 2008, [http://people.web.psi.ch/keller\\_j/GLOREAM/WS2001/Final/Panitz.pdf](http://people.web.psi.ch/keller_j/GLOREAM/WS2001/Final/Panitz.pdf).
- Pearce, F. (1986), The strange death of Europe's trees, *New Scientist*, pp. 41-45.
- Pfeilsticker, K., H. Bösch, A. Butz, C. Camy-Peyret, M. P. Chipperfield, M. Dorf, K. Grunow, L. Kritten, A. Lindner, S. Payan, A. Rozanov, C. von Savigny, B. Simmes, C. Sioris and F. Weidner (2007), Validation Of Operational Sciamachy Level-2 Products by balloon-Borne-Differential Optical Absorption Spectroscopy (DOAS), Proceedings of the 3rd Workshop on the Atmospheric Chemistry Validation of Envisat (ACVE-3), ESRIN, 4-7 December 2006, Frascati, Italy, (ESA Report SP-642, February 2007).
- Pienaar, J. J., P. Artaxo, C. Galy-Lacaux, L. Chow Peng, R. Bala, "Presentation of the DEBITS' activity: Past, present and future", I LEAPS Conference, 29 September – 3 October 2003, Helsinki, Finland.
- Pierce, E. T. (1970), Latitudinal variation of lightning parameters, *Journal of Applied Meteorology*, 9, pp. 194–195.
- Piketh, S. J. (2000), Transport of Aerosols and Trace Gases over Southern Africa, PhD thesis, University of the Witwatersrand, Johannesburg, South Africa.
- Piketh, S., H. J. Annegarn and P. Tyson (1999), Lower tropospheric aerosol loadings over South Africa: the relative contribution of aeolian dust, industrial emissions and biomass burning, *Journal of Geophysical Research*, 104, pp. 1597-1607.
- Posch, M., P. A. M. de Smet, J.-P. Hettelingh and R. J. Downing (eds) (1995), Calculation and Mapping of Critical Thresholds in Europe, Status Report 1995 of the Coordination Centre for Effects, CCE/RIVM, Bilthoven, The Netherlands.
- Posch, M., P. A. M. de Smet, J.-P. Hettelingh and R.J. Downing (eds) (2001), Modelling and Mapping of Critical Thresholds in Europe: Status Report 2001, RIVM Report No. 259101010, Coordination Centre for Effects, National Institute for Public Health and the Environment, Bilthoven, Netherlands.
- Prentice, S. A. and D. Mackerras (1977), The ratio of cloud to ground lightning flashes in thunderstorms, *Journal of Applied Meteorology*, 16, pp. 545-549.
- Price, C., J. Penner, M. Prather (1997), NO<sub>x</sub> from lightning: 1. Global distribution based on lightning physics, *Journal of Geophysical Research*, 102, pp. 5929-5941.
- PROMOTE website, internet accessed May 2008, <http://www.gse-promote.org/>.
- Rakov, V. A. and M. A. Uman (2003), *Lightning: Physics and Effects*, Cambridge University Press, Cambridge, UK.



- Redelinghuys, M. G. (1996), Consideration of the optimization of transmission lines using data from a lightning positioning and tracking system (LPATS), MSc dissertation, University of the Witwatersrand, Johannesburg, South Africa.
- Richter, A. and J. P. Burrows (2002), Retrieval of tropospheric NO<sub>2</sub> from GOME measurements, *Advanced Space Research*, 29, pp. 1673-1683.
- Rodger, C. J. and N. A. Russell (2002), Lightning flash multiplicity measurements by the US National Lightning Detection Network, in Proceedings of the 27<sup>th</sup> General Assembly of the International Union of Radio Science, 17–24 August 2002, Maastricht, The Netherlands.
- Rodhe, H., E. Cowling, I. Galbally, J. Galloway and R. Herrera (1988), Acidification and regional air pollution in the tropics, in H. Rodhe and R. Herrera (eds), *Acidification in Tropical Countries*, SCOPE 36, John Wiley and Sons, Chichester, UK.
- Rondon, A., C. Johansson and L. Granat (1993), Dry deposition of nitrogen dioxide and ozone to coniferous forest, *Journal of Geophysical Research*, 98, pp. 5159-5172.
- Rorich, R. P. and J. S. Galpin (1998), Air quality in the Mpumalanga Highveld region, South Africa, *South African Journal of Science*, 94, pp. 109-114.
- SAEON (2008), South African Environmental Observation Network, internet accessed June 2008, <http://www.saeon.ac.za/>.
- SANS 1929 (2004), South African National Standard - Ambient Air Quality - Limits for Common Pollutants, Standard Document SANS 1929, South African Bureau of Standards, Pretoria, South Africa.
- SAWS (2006), The South African Weather Service Lightning Detection Network, internet accessed March 2006, <http://www.weathersa.co.za/Pressroom/>.
- Schaub, D., A. K. Weiss, J. W. Kaiser, A. Petritoli, A. Richter, B. Buchmann and J. P. Burrows (2005), A transboundary transport episode of nitrogen dioxide as observed from GOME and its impact in the Alpine region, *Atmospheric Chemistry and Physics*, 5, pp. 23-37.
- Schenone, G. (1993), Impact of air pollutants on plants in hot, dry climates, in M. B. Jackson and C. R. Black (eds), *Interacting Stresses on Plants in a Changing Climate*, NATO ASI Series 1, *Global Environmental Change*, 16, Springer, Berlin, Germany.
- Schmidt, K., H. D. Betz, W. P. Oettinger, M. Wirz, H. Hoeller, Th. Fehr, O. Pinto Jr, K. P. Naccarato and G. Held (2005), A comparative analysis of lightning data during the EU-Brazil TROCCINOX/TroCCiBras campaign, in 8th International Symposium on Lightning Protection, 21-25 November 2005, Sao Paulo, Brazil.
- Scholes, M. C., P. A. Matrai, M. O. Andreae, K. A. Smith and M. R. Manning (2003), Biosphere-Atmosphere Interactions, in G.P. Brasseur, R.G. Prinn and A. A. P. Pszenny (eds), *Atmospheric chemistry in a changing world: An integration and synthesis of a decade of tropospheric chemistry research*, Springer, Berlin, Germany.
- Scholes, M. C., R. J. Scholes, D. Parsons, R. Martin and E. Winstead (1997), NO and N<sub>2</sub>O emissions from savanna soils following the first rains, *Nutritional Cycling Agroecosystems*, 48, pp. 115-122.
- Scholes, R. J. and B. H. Walker (1993), An African Savanna synthesis of the Nylsvley study, Cambridge University Press, Cambridge, UK.



- Scholes, R. J. and M. C. Scholes (1998), Natural and human-related sources of ozone forming trace gases in southern Africa, *South African Journal of Science*, 94, pp. 422-425.
- Schulze, B.R. (1965), Climate of South Africa Part 8, General Survey. South African Weather Bureau, WB28, Pretoria.
- Scorgie Y., L. Burger, H. J. Annegarn and M. A. Kneen (2004a), Study to examine the potential socio-economic impact of measures to reduce air pollution from combustion, Part 1 Report: Definition of Air Pollutants associated with Combustion Processes, Fund for research into Industrial Development Growth and Equity (FRIDGE), Department of Trade and Industry, Pretoria, South Africa.
- Scorgie Y., L. Burger, H. J. Annegarn and M. A. Kneen (2004b), Study to examine the potential socio-economic impact of measures to reduce air pollution from combustion, Part 2 Report: Establishment of Source Inventories and Identification and Prioritisation of Technology Options, Fund for research into Industrial Development Growth and Equity (FRIDGE), Department of Trade and Industry, Pretoria, South Africa.
- Scorgie Y., L. Burger, H. J. Annegarn and M. A. Kneen (2004c), Study to Examine the Potential Socio-economic Impact of Measures to Reduce Air Pollution from Combustion, Part 3 Report: Quantification of Environmental Benefits Associated with Fuel Use Interventions, Fund for research into Industrial Development Growth and Equity (FRIDGE), Department of Trade and Industry, Pretoria, South Africa.
- Scütt, P. and E. Cowling (1985), *Waldsterben*, a general decline of forest in Europe: symptoms, developments and possible causes, *Plant Disease*, 69, pp. 548-558.
- Seinfeld, J. H. and S. N. Pandis (1998), *Atmospheric Chemistry and Physics: From Air Pollution to Climate Change*, John Wiley, New York, USA, 1326 pp.
- Sivertsen, B. C., C. Matala and L. R. M. Pereira (1995), Sulphur emissions and trans-frontier air pollution in southern Africa, SADC Environment and Land Management Sector Coordination Unit, Report 35, 117 pp.
- Skamarock, W. C., J. E. Dye, E. Defer, M. Barth, J. L. Stith, B. A. Ridley, K. Baumann (2003), Observation and modelling based budget of lightning produced NO<sub>x</sub> in a continental thunderstorm, *Journal of Geophysical Research*, 108(D10), pp. 4305.
- Skeffington, R. A. (1999), The use of critical loads in environmental policy making: a critical appraisal, *Environmental Science & Technology – Environmental Policy Analysis*, 33, pp. 245.
- Smith, B., B. Whalley and F. Vasco (1988), Elusive solution to monumental decay, *New Scientist*, pp. 49-53.
- Snyman, G. M., G. Held, C. R. Turner and G. R. Tosen (1991), A feasibility study for the establishment of a co-ordinated wet acid deposition monitoring network covering Transvaal, Natal and Orange Free State, CSIR Rep. EMA-C9197, Pretoria, South Africa, 43 pp.
- Solomon, S., R. W. Portmann, R. W. Sanders, J. S. Daniel, W. Madsen, B. Bartram, and E. G. Dutton (1999), On the role of nitrogen dioxide in the absorption of solar radiation, *Journal of Geophysical Research*, 104, pp. 12047-12058.
- SONEX-97 (1997), Subsonic assessment, ozone and nitrogen oxide experiment -1997, internet accessed June 2005, <http://aoss.engin.umich.edu/SASSarchive/SONEX.htm>.



- Soriano, L. R., F. de Pablo and C. Tomas (2005), Ten-year study of cloud-to-ground lightning activity in the Iberian Peninsula, *Journal of Atmospheric and Solar-Terrestrial Physics*, 67, pp. 1632-1639.
- Stohl, A., H. Huntrieser, A. Richter, S. Beirle, O. R. Cooper, S. Eckhardt, C. Forster, P. James, N. Spichtinger, M. Wenig, T. Wagner, J. P. Burrows and U. Platt (2003), Rapid intercontinental air pollution transport associated with a meteorological bomb, *Atmospheric Chemistry and Physics*, 3, pp. 969-985.
- Summers, P.W. (1992), Role of clouds in the chemistry, transport, transformation and deposition of air pollutants: general concepts, current understanding and future research needs, in WMO WMP Report No. 17, World Meteorological Organization, Geneva, Switzerland, pp. 27-45.
- Sverdrup, H., W. de Vries and A. Henriksen (1989), Mapping Critical Loads: A Guide to the Criteria, Calculations, Data Collection and Mapping of Critical Loads, UN-ECE and Nordic Council of Ministers, Report *Miljörapport 1990:98*, Copenhagen, Denmark.
- Swap, R., H.J. Annegarn, J.T. Suttles, M.D. King, S. Platnick, J.L. Privette, R.J. Scholes (2003), Africa Burning – A thematic analysis of the Southern African Regional Science Initiative (SAFARI 2000), *Journal of Geophysical Research*, 108, D13, 8465, doi:10.1029/2003JD003747
- Tang H. and T. Lau (2000), A New All Season Passive Sampling System for Monitoring Ozone in Air, *Environmental Monitoring and Assessment*, 65, pp. 129-137.
- Tegen, I. and I. Fung (1995), Contribution to the atmospheric mineral aerosol load from land surface modification, *Journal of Geophysical Research*, 100, pp. 18707-18726.
- TEMIS (2008), Tropospheric Emission Monitoring Internet Service website, internet accessed June 2008, <http://www.temis.nl/airpollution/o3global.html>
- Tie, X., R. Zhang, G. Brasseur and W. Lei (2002), Global NO<sub>x</sub> production by lightning, *Journal of Atmospheric Chemistry*, 43, pp. 61-74.
- TroCCiNOx (2002-2005), Tropical Convection, Cirrus and Nitrogen Oxides Experiment, internet accessed July 2005, <http://www.pa.op.dlr.de/troccinox/>
- Troedsson, T. & N. Nykvist (1973), *Marklära och markvård*, Almquist & Wiksell, Stockholm, 402 pp. (In Swedish).
- Turman, B. N. (1978), Analysis of lightning data from the DMSP satellite, *Journal of Geophysical Research*, 83, pp. 5019-5024.
- Turner C. R., G. R. Tosen and S. J. Lennon (1996), Atmospheric pollution in South Africa, in L. Y. Shackleton, S. J. Lennon and G. R. Tosen (eds), *Global Climate Change and South Africa*, Environmental Scientific Association, Cleveland, Johannesburg, South Africa, pp. 135-144.
- Turner, C. R. and G. H. de Beer (1996), A Review of Ten Years' Rain Quality Data from the South African Interior, Report TRR/S96/1341, Eskom, Johannesburg, South Africa.
- Tyson, P. D. and R. A. Preston-Whyte (2000), *The Weather and Climate of Southern Africa*, Oxford University Press, Oxford, UK, 303 pp.
- Tyson, P. D., F. J. Kruger and C. W. Low (1988), Atmospheric Pollution and its implications in the Eastern Transvaal Highveld, NPWCAR Report 150, CSIR, Pretoria, pp. 82-95.





- Tyson, P.D. and P. C. D'Abreton (1998), Transport and recirculation of aerosols off Southern Africa – macroscale plume structure, *Atmospheric Environment*, 32, pp. 1511-1524.
- Ulrich, B. (1985), Interaction of indirect and direct effects of air pollutants in forests, in C. Troyanowski (ed.), *Air Pollution and Plants*, VCH, Weinheim, Switzerland, pp. 149–181, as quoted in J. C. I. Kuylenstierna, H. Rodhe, S. Cinderby, K. Hicks (2001b), Global Assessment of Terrestrial Ecosystem Sensitivity to Acidic Deposition.
- Ulrich, B. and M.E. Sumner (eds) (1991), *Soil Acidity*, Springer, Berlin, Germany.
- Uman, M.A., (1987), *The Lightning Discharge*, Academic, San Diego, USA, 377 pp.
- UN WHO (2005), United Nations World Health Organisation, *Air Quality Guidelines, Global Update 2005: Particulate Matter, Ozone, Nitrogen Dioxide and Sulphur Dioxide*, internet accessed June 2007, [http://www.euro.who.int/InformationSources/Publications/Catalogue/20070323\\_1](http://www.euro.who.int/InformationSources/Publications/Catalogue/20070323_1).
- UN WHO: Air Quality Guidelines for Europe (2000), *WHO Regional Publications, European Series*, 2<sup>nd</sup> edition, No. 91, WHO Regional Office for Europe, Copenhagen, internet accessed September 2007, [http://www.euro.who.int/air/activities/20050223\\_3](http://www.euro.who.int/air/activities/20050223_3).
- UNECE (1988) Conclusions and draft recommendations of the workshops on critical levels for forests, crops and materials and on critical loads for sulphur and nitrogen, Report EB.AIR/R.30, Geneva, Switzerland.
- UNECE (2004), Manual on methodologies and criteria for modelling and mapping critical loads and levels and air pollution effects, risks and trends, UNECE Convention on Long-Range Trans-boundary Air Pollution, internet accessed September 2005, <http://www.icpmapping.org>.
- UNECE (2009), The 1999 Gothenburg Protocol to Abate Acidification, Eutrophication and Ground-level Ozone (1999), internet accessed, April 2009, [http://www.unece.org/env/lrtap/multi\\_h1.htm](http://www.unece.org/env/lrtap/multi_h1.htm)
- UNECE CLRTAP (2005), UNECE Convention on Long-Range Transboundary Air Pollution, internet accessed September 2005, [www.unece.org/env/lrtap](http://www.unece.org/env/lrtap).
- US Navy Office (2007), Astronomical Information Center, Data Service, Day/Night Across the Earth, internet accessed August 2007, <http://aa.usno.navy.mil/data/docs/earthview.php>.
- Vaisala (2006), Vaisala Thunderstorm Information Systems, internet accessed April 2006, <http://www.vaisala.com>.
- Van der Merwe, N. M. (1998), Mesoscale Dispersion Modelling of SO<sub>2</sub> over the South African Highveld, MSc dissertation, Rand Afrikaans University, Johannesburg, South Africa.
- Van Rensburg, E. (1992), Ambient SO<sub>2</sub> Concentrations in the Eastern Transvaal Highveld and Their Potential to Impact on Crop Yields – A Review, Eskom Report TRR/S92/012, Johannesburg, South Africa.
- Van Rensburg, E. (1993), Assessment of Air Pollution on the Natural Grassland of the Eastern Transvaal Highveld, Eskom Report TRR/S93/144, Johannesburg, South Africa.
- Van Tienhoven A.M., M. Zunckel, L. Emberson, A. Koosailee and L. Otter (2006), Preliminary Assessment of Risk of Ozone Impacts to Maize (*Zea Mays*) in southern Africa, *Environmental Pollution* 140, pp. 220-230.



- Van Tienhoven, A. M. and M. C. Scholes (2003), Air pollution impacts on vegetation in South Africa, in L. D. Emberson, M. R. Ashmore, F. Murray (eds), *Air Pollution Impacts on Crops and Forests: a Global Assessment*, Imperial College Press, London, UK, pp. 237-262.
- Van Tienhoven, A. M. and M. Zunckel (2004), Cross-border air pollution in SADC Region, Report No. ENV-D-C 2004-017, Department of Science and Technology, internet accessed January 2006, [http://dbn.csir.co.za/capia/documents/Final\\_Report.pdf](http://dbn.csir.co.za/capia/documents/Final_Report.pdf).
- Van Tienhoven, A. M., K. A. Olbrich, R. Skoroszewski, J. Taljaard and M. Zunckel (1995), Application of the critical loads approach in South Africa. *Water, Air, Soil Pollution*, 85, pp. 2577-2582.
- Wada, H., Y. Iwasa and K. Arimitsu (1983), Map for Assessing Susceptibility of Japanese Soils to Acid Precipitation, Scale 1:2,000,000, Kokudo Mapping Company, Tokyo, Japan.
- Wells, R. B., S. M. Lloyd and C. R. Turner (1996), National air pollution source inventory, in G. Held, B. J. Gore, A. D. Surridge, G. R. Tosen, C. R. Turner and R. D. Walmsley (eds), *Air pollution and Its Impacts on the South African Highveld*, Environmental Scientific Association, Cleveland, Johannesburg, South Africa, pp. 3-9.
- Wenig, M., N. Spichtinger, A. Stohl, G. Held, S. Beirle, T. Wagner, B. Jahne and U. Platt (2003), Intercontinental transport of nitrogen oxide pollution plumes, *Atmospheric Chemistry and Physics Discussions*, 2, pp. 2151-2165.
- Wesely, M. L. and B. B. Hicks (1977), Some factors that affect the deposition rates of sulfur dioxide and similar gases on vegetation, *Journal of Air Pollution Control Association*, 27, pp. 1110-1116.
- Whelpdale, D. M. and M. S. Kaiser (eds) (1996), *Global Acid Deposition Assessment*. WMO Report No. 106, Global Atmosphere Watch, World Meteorological Organization, Genève, Switzerland.
- WMO (1996), *Global Acid Deposition Assessment*, Report No. 106, World Meteorological Organization, Geneva, Switzerland.
- Xie, S. J. Hao, Z. Zhou, L. Qi and H. Yin (1995), Assessment of critical loads in Liuzhou, China using static and dynamic models, *Water, Air and Soil Pollution*, 85, pp. 2401-2406.
- Yienger, J. J. and H. Levy (1995), Empirical models of global soil-biogenic NO<sub>x</sub> emissions, *Journal of Geophysical Research*, 100, pp. 11447-11464.
- Zbinden, R. M., J.-P. Cammas, V. Thouret, P. Nédélec, F. Karcher and P. Simon (2006), Mid-latitude tropospheric ozone columns from the MOZAIC program: climatology and inter-annual variability, *Atmospheric Chemistry and Physics*, 6, pp. 1053-1073.
- Zhang, R., N. T. Sanger, R. E. Orville, X. Tie, W. Randel and E. R. Williams, (2000), Enhanced NO<sub>x</sub> by lightning in the upper troposphere and lower stratosphere inferred from the UARS global NO<sub>2</sub> measurements, *Geophysical Research Letters*, 27, pp. 685-688.
- Zhang, R., X. Tie, D.W. Bond, (2003), Impacts of anthropogenic and natural NO<sub>x</sub> sources over the US on tropospheric chemistry, *Proceedings of the National Academy of Science of the United States of America*, 100, pp. 1505-1509.
- Zhao, D., J. Xiong and J. Mao (1994), Mapping sensitivity, critical loads and exceedance for China, Research Centre for Eco-environmental Sciences, Beijing, China.



- Ziemke, J. R., S. Chandra and P. K. Bhartia (2001), Cloud slicing: A new technique to derive upper tropospheric ozone from satellite measurements, *Journal of Geophysical Research*, 106, pp. 9853– 9867.
- Ziemke, J. R., S. Chandra, B. N. Duncan, L. Froidevaux, P. K. Bhartia, P. F. Levelt and J. W. Waters (2006), Tropospheric ozone determined from Aura OMI and MLS: Evaluation of measurements and comparison with the Global Modeling Initiative's Chemical Transport Model, *Journal of Geophysical Research*., 111(D19303), doi:10.1029/2006JD00708.
- Zunckel, M. (1999), Dry deposition of sulphur over eastern South Africa, *Atmospheric Environment*, 33, pp. 3515-3529.
- Zunckel, M., A. Koosailee, G. Yarwood, G. Maure, K. Venjonoka, A. M. van Tienhoven and L. Otter (2006), Modelled surface ozone over southern Africa during the Cross Border Air Pollution Impact Assessment Project, *Environmental Modelling & Software*, 21, pp. 911-924.
- Zunckel, M., L. Robertson, P. D. Tyson and H. Rodhe (2000), Modelled transport and deposition of sulphur over Southern Africa, *Atmospheric Environment*, 34, pp. 2797-2808.
- Zunckel, M., S. Piketh and T. Freiman (1999), Dry deposition of sulphur at high-altitude background station in South Africa, *Water, Air and Soil Pollution*, 115, pp. 445-463.





**APPENDIX A: EXAMPLE OF DRY AND WET DEPOSITION CALCULATIONS FOR A SITE**

**Table A1: Site # 01 (Weyden Vaalbank Farm, near Standerton) dry SO<sub>2</sub> deposition calculation for the period Sep05-Aug06.**

Site No.	South	-26.93°	Average between Palmer and Elands (means for 1996/97/98)	Monthly seconds of light	Average between Palmer and Elands (means for 1996/97/98)	Monthly seconds of darkness	Deposition values	
	East	29.00°	Deposition velocity (daytime) cm <sup>-1</sup>		Deposition velocity (nighttime) cm <sup>-1</sup>			
Concentration in µg m <sup>-3</sup>	SO <sub>2</sub> sep05	14.56	Spring	0.23	1289400	0.115	1302600	6.50
	SO <sub>2</sub> oct05	9.82		0.23	1421160	0.115	1170840	4.53
	SO <sub>2</sub> nov05	11.58		0.23	1451340	0.115	1140660	5.39
	SO <sub>2</sub> dec05	11.58	Summer	0.36	1540380	0.15	1051620	8.25
	SO <sub>2</sub> jan06	16.57		0.36	1519200	0.15	1072800	11.73
	SO <sub>2</sub> feb06	16.57		0.36	1311120	0.15	1280880	11.01
	SO <sub>2</sub> mar06	18.38	Autumn	0.26	1365780	0.12	1226220	9.23
	SO <sub>2</sub> apr06	18.38		0.26	1236360	0.12	1355640	8.90
	SO <sub>2</sub> may06	18.38		0.26	1204860	0.12	1387140	8.82
	SO <sub>2</sub> jun06	11.58	Winter	0.145	1131240	0.10	1460760	3.59
	SO <sub>2</sub> jul06	11.58		0.145	1186260	0.10	1405740	3.62
	SO <sub>2</sub> aug06	11.58		0.145	1248360	0.10	1343640	3.65
<b>Average SO<sub>2</sub> Jan05-Apr07</b>	<b>11.58</b>						<b>mg cm<sup>-2</sup> yr<sup>-1</sup></b>	<b>85.22</b>
							µg m <sup>-2</sup> yr <sup>-1</sup>	0.852*10 <sup>6</sup>
							µg ha <sup>-1</sup> yr <sup>-1</sup>	8.52*10 <sup>9</sup>
							kg ha <sup>-1</sup> yr <sup>-1</sup>	8.52
							<b>SO<sub>2</sub> as S (kg ha<sup>-1</sup> yr<sup>-1</sup>)</b>	<b>4.26</b>



**Table A2: Site # 01 (Weyden Vaalbank Farm, near Standerton) dry NO<sub>2</sub> deposition calculation, deposition velocities (Mpheya, 2002) for the period Sep05-Aug06.**

Site No.	South	-26.93°	The average between Palmer and Elands (means for 1996/ 97/ 98)		Monthly seconds of light	The average between Palmer and Elands (means for 1996/97/98)		Monthly seconds of darkness	Deposition values
	East		29.00°	Deposition velocity (day-time) cm <sup>-1</sup>		Deposition velocity (night-time) cm <sup>-1</sup>			
Concentration ( µg m <sup>-3</sup> )	NO <sub>2</sub> sep05	4.04	Spring	0.115	1289400	0.045	1302600	0.21	
	NO <sub>2</sub> oct05	6.08		0.115	1421160	0.045	1170840	0.87	
	NO <sub>2</sub> nov05	6.44		0.115	1451340	0.045	1140660	1.33	
	NO <sub>2</sub> dec05	6.44	Summer	0.250	1540380	0.080	1051620	3.02	
	NO <sub>2</sub> jan06	5.72		0.250	1519200	0.080	1072800	3.00	
	NO <sub>2</sub> feb06	5.72		0.250	1311120	0.080	1280880	2.46	
	NO <sub>2</sub> mar06	8.47	Autumn	0.135	1365780	0.070	1226220	1.55	
	NO <sub>2</sub> apr06	8.47		0.135	1236360	0.070	1355640	2.22	
	NO <sub>2</sub> may06	8.47		0.135	1204860	0.070	1387140	2.20	
	NO <sub>2</sub> jun06	6.44	Winter	0.050	1131240	0.040	1460760	0.97	
	NO <sub>2</sub> jul06	6.44		0.050	1186260	0.040	1405740	0.74	
	NO <sub>2</sub> aug06	6.44		0.050	1248360	0.040	1343640	0.75	
								mg cm <sup>-2</sup> yr <sup>-1</sup>	19.3
								µg m <sup>-2</sup> yr <sup>-1</sup>	0.193*10 <sup>6</sup>
								µg ha <sup>-1</sup> yr <sup>-1</sup>	1.93*10 <sup>9</sup>
								kg ha <sup>-1</sup> yr <sup>-1</sup>	1.93
								<b>NO<sub>2</sub> as N (kg ha<sup>-1</sup> yr<sup>-1</sup>)</b>	<b>0.59</b>



**Table A3: Wet deposition of sulphate (SO<sub>4</sub><sup>2-</sup>) estimate for site #1 (Weyden Vaalbank Farm, near Standerton) for the period Sep05-Aug06.**

South	-26.93°
East	29.00°
Site Number	1
Nearby Town	Standerton
The pivot site - basis for this site (wider area)	Amersfoort
10-year volume weighted mean in $\mu\text{eq l}^{-1}$ for the pivot sites	57.2
Rainfall ( $\text{mm m}^{-2}$ ) Sep05-Aug06	667.5
Step 1: concentration divided by the valence of the SO <sub>4</sub> <sup>2-</sup>	28.6
Step 2: Step 1 values multiplied by precipitation (mm)	19090.
Step 3: conversion to $\text{mmol m}^{-2} \text{yr}^{-1}$	19.10
Step 4: $\text{mmol m}^{-2} \text{yr}^{-1}$ conversion to $\text{mol m}^{-2} \text{yr}^{-1}$	0.02
Step 5: conversion to $\text{g m}^{-2} \text{yr}^{-1}$	1.83
Step 6: SO <sub>4</sub> <sup>2-</sup> as S ( $\text{g m}^{-2} \text{yr}^{-1}$ )	0.61
Step 7: SO <sub>4</sub> <sup>2-</sup> as S conversion to $\text{kg ha}^{-1} \text{yr}^{-1}$	<b>6.11</b>

**Table A4: Wet deposition of nitrate (NO<sub>3</sub><sup>-</sup>) estimate for site #1(Weyden Vaalbank Farm, near Standerton) for the period Sep05-Aug06.**

South	-26.93°
East	29.00°
Site Number	1
Nearby Town	Standerton
The pivot site - basis for this site (wider area)	Amersfoort
10-year volume weighted mean in $\mu\text{eq l}^{-1}$ for the pivot sites	24.6
Rainfall ( $\text{mm m}^{-2}$ ) Sep05-Aug06	667.5
Step 1: concentration divided by the valence of the NO <sub>3</sub> <sup>-</sup>	24.6
Step 2: Step 1 values multiplied by precipitation (mm)	16421.
Step 3: conversion to $\text{mmol m}^{-2} \text{yr}^{-1}$	16.42
Step 4: $\text{mmol m}^{-2} \text{yr}^{-1}$ conversion to $\text{mol m}^{-2} \text{yr}^{-1}$	0.02
Step 5: conversion to $\text{g m}^{-2} \text{yr}^{-1}$	1.02
Step 6: NO <sub>3</sub> <sup>-</sup> as N ( $\text{g m}^{-2} \text{yr}^{-1}$ )	0.23
Step 7: conversion to $\text{kg ha}^{-1} \text{yr}^{-1}$ of NO <sub>3</sub> <sup>-</sup> as N	<b>2.30</b>



**Table A5: Wet deposition of ammonium (NH<sub>4</sub><sup>+</sup>) estimate for site #1(Weyden Vaalbank Farm, near Standerton) for the period Sep05-Aug06.**

South	-26.93°
East	29.00°
Site Number	1
Nearby Town	Standerton
The pivot site - basis for this site (wider area)	Amersfoort
10-year volume weighted mean in (µeq l <sup>-1</sup> ) for the pivot sites	25
Rainfall (mm m <sup>-2</sup> ) Sep05-Aug06	667.5
Step 1: concentration divided by the valence of the NH <sub>4</sub> <sup>+</sup>	25
Step 2: Step 1 values multiplied by precipitation (mm)	16688.
Step 3: conversion to mmol m <sup>-2</sup> yr <sup>-1</sup>	16.69
Step 4: mmol m <sup>-2</sup> yr <sup>-1</sup> conversion to mol m <sup>-2</sup> yr <sup>-1</sup>	0.02
Step 5: conversion to g m <sup>-2</sup> yr <sup>-1</sup>	0.30
Step 6: NH <sub>4</sub> <sup>+</sup> as N (g m <sup>-2</sup> yr <sup>-1</sup> )	0.23
Step 7: conversion to kg ha <sup>-1</sup> yr <sup>-1</sup> of NH <sub>4</sub> <sup>+</sup> as N	<b>2.33</b>





## APPENDIX B: ACIDITY LOADS AND BASE CATION DEPOSITION

Table B1: Total S and N deposition per site over the study region.

Site Number	Acidic deposition ( $\text{meq m}^{-2} \text{ yr}^{-1}$ )		
	Sep05-Aug06*	Sep06-Aug07*	Mean Sep05-Aug07
1	102.36	74.62	88.5
2	126.01	68.15	97.1
3	66.85	45.27	56.1
4	39.36	39.40	39.4
5	55.40	37.57	46.5
6	71.66	60.09	65.9
7	97.70	68.68	83.2
8	46.87	56.15	51.5
9	69.36	76.42	72.9
10	71.30	77.20	74.2
11	58.32	48.24	53.3
12	34.06	24.01	29.0
13	77.42	61.17	69.3
14	81.80	69.82	75.8
15	62.07	60.24	61.2
16	72.74	91.38	82.1
17	159.48	102.17	130.8
18	86.03	46.59	66.3
19	28.66	21.80	25.2
20	34.76	26.12	30.4
21	31.13	31.06	31.1
22	31.72	28.68	30.2
23	34.61	35.07	34.8
24	26.92	24.14	25.5
25	23.10	19.19	21.1
26	95.00	60.18	77.6
27	69.61	64.03	66.8
28	32.68	42.34	37.5
29	40.39	45.53	43.0
30	63.11	37.19	50.2
31	98.94	67.45	83.2
32	61.54	23.25	42.4
33	35.54	35.63	35.6
34	45.67	24.87	35.3
35	24.12	22.33	23.2
36	26.70	24.82	25.8
37	38.31	30.65	34.5





**Table B2: The lower net S and N (total cumulative dry and wet S and N minus total dry and wet estimated BC) deposition for the study region (*higher BC estimate*).**

<b>Site Number</b>	<b>Total dry and wet deposition (meq m<sup>-2</sup> yr<sup>-1</sup>)</b>		
	<b>Acidic anions</b>	<b>Base cations</b>	<b>Net acidic deposition</b>
1	88.5	79	9.5
2	97.1	83.4	13.7
3	56.1	88.7	-32.7
4	39.4	80.4	-41
5	46.5	90	-43.5
6	65.9	81.7	-15.9
7	83.2	104.7	-21.5
8	51.5	85	-33.5
9	72.9	100.8	-27.9
10	74.2	102.3	-28
11	53.3	94.9	-41.6
12	29	75.7	-46.7
13	69.3	98.6	-29.3
14	75.8	101.1	-25.3
15	61.2	91.5	-30.4
16	82.1	108	-26
17	130.8	84.4	46.5
18	66.3	81.7	-15.4
19	25.2	69.5	-44.3
20	30.4	74.6	-44.2
21	31.1	70.5	-39.4
22	30.2	73.2	-43
23	34.8	75.3	-40.5
24	25.5	71.4	-45.9
25	21.1	66	-44.9
26	77.6	86.2	-8.6
27	66.8	93	-26.1
28	37.5	76.7	-39.2
29	43	80.8	-37.9
30	50.2	89	-38.9
31	83.2	90.7	-7.5
32	42.4	72.1	-29.7
33	35.6	75.5	-39.9
34	35.3	75.2	-39.9
35	23.2	67.9	-44.7
36	25.8	72.1	-46.3
37	34.5	79	-44.5



**Table B3: The higher net acidic (total cumulative dry and wet S and N minus total dry and wet estimated BC) deposition for the study region (*lower BC estimate*).**

<b>Site Number</b>	<b>Total dry and wet deposition (meq m<sup>-2</sup> yr<sup>-1</sup>)</b>		
	<b>Acidic anions</b>	<b>Base cations</b>	<b>Net acidic deposition</b>
1	88.5	32.3	56.2
2	97.1	36.6	60.5
3	56.1	42	14.1
4	39.4	33.6	5.7
5	46.5	43.2	3.3
6	65.9	35	30.9
7	83.2	58	25.2
8	51.5	38.3	13.2
9	72.9	54.1	18.8
10	74.2	55.5	18.7
11	53.3	48.1	5.1
12	29	29	0.1
13	69.3	51.9	17.4
14	75.8	54.3	21.5
15	61.2	44.8	16.4
16	82.1	61.3	20.8
17	130.8	37.6	93.2
18	66.3	34.9	31.4
19	25.2	22.8	2.4
20	30.4	27.8	2.6
21	31.1	23.7	7.4
22	30.2	26.5	3.7
23	34.8	28.6	6.3
24	25.5	24.7	0.9
25	21.1	19.3	1.9
26	77.6	39.4	38.2
27	66.8	46.2	20.6
28	37.5	29.9	7.6
29	43	34.1	8.9
30	50.2	42.3	7.9
31	83.2	44	39.2
32	42.4	25.3	17.1
33	35.6	28.7	6.9
34	35.3	28.5	6.8
35	23.2	21.2	2
36	25.8	25.4	0.4
37	34.5	32.2	2.3



## APPENDIX C: REMOTE SENSING SAMPLE DATA AND CONVERSION EXAMPLES

**Table C1: Example of conversion of SO<sub>2</sub> VCD\* [DU] to VMR\*\* [ppb] with boundary layer separation for PS site 1 (near Standerton).**

<i>Year</i>	<i>Month</i>	<i>SO<sub>2</sub> VCD at 1 km value (DU)</i>	<i>RS error (DU)</i>	<i>SO<sub>2</sub> VMR Sciamachy (ppb)</i>
2005	1	0.910	0.777	7.7
2005	2	0.329	0.793	2.8
2005	3	0.768	0.933	6.5
2005	4	0.894	0.975	7.6
2005	5	-0.150	1.32	omitted
2005	6	0.512	1.33	4.3
2005	7	-0.319	1.39	omitted
2005	8	0.195	1.31	1.7
2005	9	0.230	1.23	1.9
2005	10	0.295	1.13	2.5
2005	11	0.555	0.90	4.7
2005	12	0.283	0.93	2.4
2006	1	1.277	0.99	10.8
2006	2	0.969	0.92	8.2
2006	3	0.555	1.12	4.7
2006	4	0.186	0.99	1.6
2006	5	0.624	1.32	5.3
2006	6	0.027	1.26	0.2
2006	7	0.082	1.86	0.7
2006	8	-0.317	1.30	omitted
2006	9	0.234	1.14	2.0
2006	10	0.726	1.010	6.1
2006	11	1.395	2.10	11.8
2006	12	1.007	1.04	8.5
2007	1	0.575	0.96	4.9
2007	2	0.064	1.14	0.5
2007	3	0.281	1.09	2.4
2007	4	0.922	1.23	7.8
2007	5	-0.692	1.57	omitted
2007	6	0.539	1.81	4.6
2007	7	0.873	1.75	7.4
2007	8	0.968	1.59	8.2
2007	9	0.872	1.51	7.4

\* Vertical Column Density, \*\* Volume Mixing Ratio.



**Table C2: Example of conversion of NO<sub>2</sub> VCD\* [DU] to VMR\*\* [ppb] with boundary layer separation for all PS sites for January 2006.**

<i>Site numbers</i>	<i>(molecules cm<sup>-2</sup>)</i>	<i>Dobson unit (DU) = 2.6868e+16 molecules cm<sup>-2</sup></i>	<i>80% of TS VCD in BL</i>	<i>NO<sub>2</sub> VMR Sciamachy (ppb)</i>
site 01	3.54E+15	0.20917	0.167	1.4
site 02	6.58E+15	0.2449	0.196	1.7
site 03	6.41E+15	0.23858	0.191	1.6
site 04	5.62E+15	0.20917	0.167	1.4
site 05	2.53E+15	9.42E-02	0.075	0.6
site 06	4.20E+15	1.56E-01	0.125	1.1
site 07	4.49E+15	0.16711	0.134	1.1
site 08	2.70E+15	0.10049	0.080	0.7
site 09	3.33E+15	0.12394	0.099	0.8
site 10	6.12E+15	0.22778	0.182	1.5
site 11	3.35E+15	0.12468	0.100	0.8
site 12	2.33E+15	8.67E-02	0.069	0.6
site 13	3.85E+15	0.14329	0.115	1.0
site 14	2.14E+15	7.96E-02	0.064	0.5
site 15	2.44E+15	9.08E-02	0.073	0.6
site 16	3.07E+15	0.11426	0.091	0.8
site 17	9.97E+15	0.37108	0.297	2.5
site 18	5.51E+15	0.20508	0.164	1.4
site 19	3.68E+15	0.13697	0.110	0.9
site 20	2.56E+15	9.53E-02	0.076	0.6
site 21	2.20E+15	8.19E-02	0.066	0.6
site 22	2.82E+15	0.10496	0.084	0.7
site 23	3.17E+15	0.11799	0.094	0.8
site 24	2.03E+15	7.56E-02	0.060	0.5
site 25	2.28E+15	8.49E-02	0.068	0.6
site 26	4.84E+15	0.18014	0.144	1.2
site 27	4.58E+15	0.17046	0.136	1.2
site 28	6.16E+15	0.22927	0.183	1.6
site 29	6.30E+15	0.23448	0.188	1.6
site 30	2.78E+15	0.10347	0.083	0.7
site 31	3.64E+15	0.13548	0.108	0.9
site 32	4.74E+15	0.17642	0.141	1.2
site 33	3.34E+15	0.12431	0.099	0.8
site 34	3.35E+15	0.12468	0.100	0.8
site 35	1.99E+15	7.41E-02	0.059	0.5
site 36	1.78E+15	6.63E-02	0.053	0.4
site 37	1.64E+15	6.10E-02	0.049	0.4

\* Vertical Column Density, \*\* Volume Mixing Ratio.



**Table C3: Example of conversion of O<sub>3</sub> VCD\* [DU] to VMR\*\* [ppb] with boundary layer separation for PS site 36 (near Louis Trichardt).**

<i>Period</i>	<i>Corresponding PS Site</i>	<i>O<sub>3</sub> RS OMI/MLS value (x10<sup>-1</sup> ppb)</i>	<i>O<sub>3</sub> RS OMI/MLS re-scaled d/b (/10) *0.23 values (DU)</i>	<i>O<sub>3</sub> RS OMI/MLS VMR (ppb)</i>
Sep 2005	36	81.2	1.87	15.8
Oct 2005	36	89	2.05	17.3
Nov 2005	36	78.4	1.80	15.3
Dec 2005	36	71.4	1.64	13.9
Jan 2006	36	65.6	1.51	12.8
Feb 2006	36	66.6	1.53	13.0
Mar 2006	36	59.8	1.38	11.6
Apr 2006	36	59.8	1.38	11.6
May 2006	36	59.8	1.38	11.6
Jun 2006	36	57.4	1.32	11.2
Jul 2006	36	62.4	1.44	12.2
Aug 2006	36	64.4	1.48	12.5
Sep 2006	36	77.6	1.78	15.1

\* Vertical Column Density, \*\* Volume Mixing Ratio.



## APPENDIX D: PUBLICATIONS, TECHNICAL REPORTS AND PRESENTATIONS

### List D1: Publications

Josipovic, M., H. J. Annegarn, M. A. Kneen, S. J. Piketh and J. J. Pienaar (2007), A Regional-Scale Passive Monitoring Study of SO<sub>2</sub>, NO<sub>2</sub> and Ozone in South Africa, *IGACtivities (International Global Atmospheric Chemistry) Newsletter 36*, July 2007, accessible at internet <http://www.igac.noaa.gov/newsletter/>.

### List D2: Technical reports

Annegarn, H. J., M. Josipovic, M. A. Kneen, S. J. Piketh and J. J. Pienaar (2005), Characterisation and Monitoring of Air Pollutant Emissions - A Regional-Scale Passive Monitoring Study, 1<sup>st</sup> Progress Report to Anglo American.

Annegarn, H. J., M. Josipovic, M. A. Kneen, S. J. Piketh and J. J. Pienaar (2006a), Characterisation and Monitoring of Air Pollutant Emissions - A Regional-Scale Passive Monitoring Study, 1<sup>st</sup> Annual Report (and 2<sup>nd</sup> interim progress report) to Anglo American.

Annegarn, H. J., M. Josipovic, M. A. Kneen, S. J. Piketh and J. J. Pienaar (2006b), Characterisation and Monitoring of Air Pollutant Emissions - A Regional-Scale Passive Monitoring Study, 2<sup>nd</sup> Progress Report (3<sup>rd</sup> interim progress report) to Anglo American.

Annegarn, H. J., M. Josipovic and M. A. Kneen (2007a), Characterisation and Monitoring of Air Pollutant Emissions - A Regional-Scale Passive Monitoring Study, 2<sup>nd</sup> Annual Report (RES/RR/06/28502) to Eskom.

Annegarn, H. J., M. Josipovic and M. A. Kneen (2007b), Characterisation and Monitoring of Air Pollutant Emissions - A Regional-Scale Passive Monitoring Study, 3<sup>rd</sup> Progress Report (RES/RR/07/29010) to Eskom.

Annegarn, H. J., M. Josipovic and M. A. Kneen (2008a), Characterisation and Monitoring of Air Pollutant Emissions - A Regional-Scale Passive Monitoring Study, Final Comprehensive Data Report (RES/RR/07/29011) to Eskom.

Annegarn, H. J., M. Josipovic and M. A. Kneen (2008b), Characterisation and Monitoring of Air Pollutant Emissions - A Regional-Scale Passive Monitoring Study, Final Report (RES/RR/07/29012) to Eskom.

### List D3: Presentations

Josipovic M., M. Zunckel, H. J. Annegarn, M. A. Kneen, S. J. Piketh and J. J. Pienaar (2007), Passive monitoring of acid precursor gases over South African interior – a critical levels and loads assessment, presentation to the DEAT Highveld Priority Area Scientific Research Presentation Workshop, 19-20 January 2009, Ekurhuleni.

Josipovic, M., H. J. Annegarn, M. A. Kneen, S. J. Piketh and J. J. Pienaar (2006a), A regional-scale passive monitoring study of SO<sub>2</sub>, NO<sub>2</sub> and O<sub>3</sub>, poster presentation to the Joint CACGP (Commission on Atmospheric Chemistry and Global Pollution)/IGAC (International Global Atmospheric Chemistry)/WMO (World Meteorological Organization) Symposium, 17-22 September 2006, Cape Town, South Africa.



- Josipovic, M., H. J. Annegarn, M. A. Kneen, S. J. Piketh and J. J. Pienaar (2006b), A regional-scale passive monitoring study of SO<sub>2</sub>, NO<sub>2</sub> and O<sub>3</sub> – Interim results of ground level ozone measurements, an oral presentation to the Tropospheric Ozone Workshop – Networking African Scientists International Workshop, 15-17 September 2006, Franschoek Inn, Franschoek, South Africa.
- Josipovic, M., H. J. Annegarn, M. A. Kneen, S. J. Piketh and J. J. Pienaar (2007a), A regional-scale passive monitoring study of SO<sub>2</sub>, NO<sub>x</sub> and ozone – annual observation report, presentation in the Industry-Academia Consortium Acidic Deposition Workshop, 05 April 2007, Eskom Heritage Centre, Heriotdale, Germiston, South Africa.
- Josipovic, M., H. J. Annegarn, M. A. Kneen, S. J. Piketh and J. J. Pienaar (2006c), A regional-scale passive monitoring study of SO<sub>2</sub>, NO<sub>2</sub> and O<sub>3</sub>, poster presentation at SAEON (South African Environmental Observation Network) Summit, 26-28 March 2006, Leriba Lodge, Centurion, South Africa.
- Josipovic, M., H. J. Annegarn, M. A. Kneen, S. J. Piketh and J. J. Pienaar (2006d), A regional-scale passive monitoring study of SO<sub>2</sub>, NO<sub>2</sub> and O<sub>3</sub> – interim results, oral presentation to the SASAS (South African Society for Atmospheric Sciences) 2006 Annual Conference, 04-06 October 2006, Maselspoort Resort, Bloemfontein, South Africa.
- Josipovic, M., H. J. Annegarn, M. A. Kneen, S. J. Piketh and J. J. Pienaar (2007b), Comparison of modelled and passive sampling ozone concentrations over southern Africa, SASAS 2007 Annual Conference, 13-14 September 2007, Origins Centre, University of the Witwatersrand, Johannesburg.
- Josipovic, M., H. J. Annegarn, M. A. Kneen, S. J. Piketh and J. J. Pienaar (2007c), Comparison of the measured and modelled ozone concentrations over north-east of South Africa, NACA (National Association for Clean Air) 2007 Annual Conference, 12-14 October 2007, Champagne Sports Resort, Drakensberg.
- Josipovic, M., H. J. Annegarn, M. A. Kneen, S. J. Piketh and J. J. Pienaar (2005), A regional-scale passive monitoring study of SO<sub>2</sub>, NO<sub>2</sub> and O<sub>3</sub>, SASAS 2005 Annual Conference, 26-27 September 2005, Invubu Lodge, Richards Bay, South Africa.